RECONSTRUCTION OF EL NIÑO – SOUTHERN OSCILLATION VARIABILITY
DURING THE HOLOCENE

Timme Henrik Donders

LPP Foundation 2005

Timme Donders
Laboratory of Palaeobotany and Palynology
Utrecht University
Budapestlaan 4
3584 CD Utrecht
The Netherlands

t.h.donders@bio.uu.nl

RECONSTRUCTION OF EL NIÑO – SOUTHERN OSCILLATION VARIABILITY
DURING THE HOLOCENE

RECONSTRUCTIE VAN 'EL NIÑO – SOUTHERN OSCILLATION'
VARIABILITEIT GEDURENDE HET HOLOCEEN

(Met een samenvatting in het Nederlands, het Italiaans en het Duits)

Proefschrift

Ter verkrijging van de graad van doctor aan de Universiteit Utrecht
op gezag van de Rector Magnificus, Prof. Dr. W.H. Gispen,
involge het besluit van het College voor Promoties
in het openbaar te verdedigen
op donderdag 1 december 2005 des ochtends te 10:30 uur

door

Timme Henrik Donders
Geboren op 18 september 1977, te Nieuwegein

"*If we knew what we were doing it wouldn't be called Science, would it?*"

Albert Einstein

Voor Francesca en "El Niño"

This thesis is based on the following publications:

CHAPTER 1   A novel approach for developing high-resolution sub-fossil peat
             chronologies with ^{14}C dating
             With F. Wagner, K. van der Borg, A.F.M. de Jong and
             H. Visscher, Radiocarbon 2004, 46 (1): 455-463

CHAPTER 2   Quantification strategies for human-induced and natural hydrological
             changes in wetland vegetation, southern Florida, USA
             With F. Wagner, and H. Visscher, Quaternary Research 2005, in
             press

CHAPTER 3   Synchronous documentation of atmospheric CO_2 and precipitation
             signatures in fossil leaf remains
             With F. Wagner and H. Visscher, to be submitted

CHAPTER 4   Botanical proxy time-series indicate stability of the ENSO
             teleconnection to Florida during the 20th century
             With F. Wagner and H. Visscher, to be submitted

CHAPTER 5   Mid- to late-Holocene El Niño-Southern Oscillation dynamics reflected
             in the subtropical terrestrial realm
             With F. Wagner, D.L. Dilcher and H. Visscher, Proceedings of
             the National Academy of Sciences, USA 2005, 102 (31): 10904-10908

CHAPTER 6   Late Pleistocene and Holocene subtropical vegetation dynamics
             recorded in perched lake deposits on Fraser Island, Queensland,
             Australia
             With F. Wagner and H. Visscher, to be submitted

CHAPTER 7   Transition of the eastern Australian climate system from the
             post-glacial to the present-day ENSO mode
             With S. Haberle, G. Hope, F. Wagner and H. Visscher, to be
             submitted

CHAPTER 8   Integration of paleoclimatic and model scenarios for the Holocene onset
             of modern El Niño - Southern Oscillation
             With F. Wagner and H. Visscher, to be submitted

Contents

General introduction and synopsis

The El Niño – Southern Oscillation (ENSO) in the tropical Pacific constitutes the largest source of global climate variability on interannual timescales. The El Niño phenomenon is a periodical reduction of coastal upwelling and increase in sea-surface temperature (SST) along the western coast of tropical South America. The Southern Oscillation, defined by the pressure difference between Tahiti and Darwin, is the atmospheric component of the ENSO system. The anomalous SSTs in the eastern Pacific enhance atmospheric convection along the western coast of South America, while the usual uplift of warm moisture-laden air is relocated from Indonesia to the central Pacific. As a result of this displacement, rainfall patterns in the tropical Pacific are altered and the strength of the zonal Pacific atmospheric circulation is reduced.

An altered Pacific circulation causes precipitation deficits and surpluses in geographically widespread areas through atmospheric teleconnections. The climate disruptions caused by ENSO recur every 2-7 year and have a strong societal and economical impact. Therefore, ENSO is presently one of the best-studied climate systems and much effort is directed at improving the prediction of El Niño and its counterpart La Niña. However, the exact mechanisms and causes of El Niño / La Niña events are still poorly understood and especially the expected behavior of ENSO dynamics in a greenhouse world under increased radiative forcing is heavily debated. It is unclear whether future warming will alter the recurrence, duration, and intensity of El Niño / La Niña events and what the worldwide effects of possible changes in ENSO dynamics will be.

To understand the mechanisms and long-term dynamics of ENSO, it is important to study the past behavior of this large-scale coupled ocean / atmosphere system. A detailed reconstruction of past ENSO activity can provide insight into the spatial and temporal climate variability caused by the ENSO system on centennial to millennial time scales and, at the same time, help assessing the potential role of changes in radiative forcing (e.g. insolation or Milankovitch) as driving mechanism for ENSO dynamics. Documentation of the causes and consequences of changing ENSO dynamics is of prime importance to improve the predictability of extreme precipitation anomalies associated with ENSO.

Investigation of terrestrial systems is essential, since the societal and economic impacts of ENSO are most prominent on the continents. Botanical proxy records of environmental change are increasingly being used for climate reconstructions since plants are highly sensitive to the surrounding conditions and respond immediately to changes in their habitat such as drought or precipitation surplus. Plant remains buried in peat and lake deposits, such as leaves and pollen, preserve adaptations to environmental signals from individual plant to ecological community level. These natural environmental archives provide the source material utilized in proxy-based climate reconstructions.

In this thesis, plant-based proxies are introduced, tested, and applied to reconstruct past hydrological conditions in ENSO key-areas. The first section of this thesis focuses on southern Florida, a region where a strong ENSO teleconnection is well documented in numerous long instrumental time series that can be used for calibration of environmental proxies.

In addition to detailed instrumental data, accurate dating and sound chronologies of the natural archives are a prerequisite for successful proxy development and validation. Improved AMS-radiocarbon chronologies for 20th century organic material are developed in **Chapter 1** and applied to two young peat sequences from the Fakahatchee Strand Preserve State Park (FSPSP, Florida, U.S.A.), a subtropical Florida wetland. The ^{14}C datings are calibrated using a combined wiggle-match and ^{14}C bomb-pulse approach. Reproducible results are obtained and assessment of the different errors involved provides extremely accurate age models with a precision of 3–5 yr. Based on this strategy, the shortcore FAK I98 dates back to 1912 AD while the second, slightly deeper core FAK I02 covers the past 125 years. The dating results allow direct calibration of paleo-environmental proxies with meteorological data and extend the time frame in which ^{14}C dating is commonly applied to the 20th century.

In **Chapter 2**, high-resolution pollen and spore analyses are used to for detect recent hydrological conditions in the accurately dated peat profile FAK I98 from the FSPSP. The mixed cypress swamp gradually shifts from a wet to a relatively dry vegetation assemblage during the past 100 years. Timing of drainage activities in the region is accurately reflected by the onset and duration of vegetation change in the swamp. Numerical comparison of the (sub-) fossil with surface-sediment pollen samples allows determination of the response range of the FSPSP wetland to hydrological perturbations, revealing both the naturally occurring vegetation changes and the response to human impact on Florida wetlands.

Superimposed near-annual variation in the record suggests a positive correlation between winter-precipitation and pollen productivity of the dominant tree taxa. The documented response range of the FSPSP wetland to disturbance on both annual and decadal scales allows recognition and quantification of natural hydrological changes in older deposits from southwestern Florida.

The impact of annual winter precipitation changes on Florida wetland vegetation is further investigated in **Chapter 3**. A newly developed leaf-morphological precipitation proxy based on the analysis of structural xeromorphic features in *Quercus laurifolia* is introduced. It is demonstrated that epidermal cell densities (ED) of both herbarium material and accumulations of annual leaf-shedding in the FSPSP peat sequences FAK I98 and FAK I02 show a consistent inverse relation with the amount of winter precipitation in southern Florida. Moreover, parallel stomatal frequency analysis performed on the fossil *Q. laurifolia* leaves furthermore reveals a distinct CO_2 sensitivity of this species. Combined analysis of CO_2 and drought stress signals in fossil leaf remains from southern Florida provides a unique method to synchronously document changing ENSO-tied precipitation patterns and atmospheric CO_2 concentrations beyond the period of instrumental measurements.

The pollen and ED proxies introduced in Chapters 2 & 3, indicative for moisture availability during the growing season in Florida, are tested for ENSO sensitivity in **Chapter 4**. The high-frequency changes seen in the FAK I98 pollen record in Chapter 2 are investigated at higher resolution in peat section FAK I02. Spectral analysis of the near-annually resolved pollen and ED record of FAK I02 reveals statistically significant variability within the 2-7 year bandwidth, highly comparable to the ENSO periodicity. Band pass filtering of the

data indicates a consistent ENSO signature within the proxy time-series from FAK I02 during the past 125 years. These results show that the ENSO signature can also be detected in non annually-laminated sediments and allow direct testing of past ENSO dynamics in high-accumulation sediment sequences.

High resolution pollen analysis of middle to late Holocene peat deposits from southwest Florida in **Chapter 5** reveals a step-wise increase in wetland vegetation that points to an increased precipitation-driven fresh-water flow during the past 5, 000 years. The tight coupling between winter precipitation patterns in Florida and the strength of the ENSO as described in Chapter 2 strongly suggests that the paleo-hydrology record reflects changes in past ENSO intensity. The subtropical record documents ecosystem response to the onset of modern-day ENSO periodicities between ~7, 000 and 5, 000 years BP, known from tropical marine and terrestrial records, and subsequent ENSO intensification after 3, 500 years BP. The observed increases in 'wetness' are sustained by a gradual rise in relative sea level that prevents a return to drier vegetation through natural succession.

Concepts of Holocene ENSO dynamics outlined on the basis of studies in Florida are further evaluated by focusing on eastern Australia, a region with strong ENSO teleconnections that are anti-correlated with the ENSO impacts in Florida.

At the tropical-subtropical ecotone in Queensland, Australia, occur numerous perched lakes on the Fraser Island dune system. These lakes are strongly influenced by precipitation and act as natural rainfall gauges, which makes them highly sensitive to environmental changes. In **Chapter 6,** relevant paleoecological and paleoclimatological information is discussed on the basis of a high-resolution pollen record obtained from organic-rich sediments that accumulated in Lake Allom from ~56 ^{14}C ky BP to the present, with a major hiatus during the Last Glacial Maximum. Pronounced changes between open woodland and rainforest vegetation occurred at the Glacial-Interglacial transition. The Holocene section reveals a stepwise vegetation development, from dry conditions in the early Holocene, to high lake levels and forest succession between 5.5-3 cal ky BP. At 3-2 cal ky BP, a large diversification occurred towards the present-day heterogeneous subtropical rainforest vegetation, followed by a small rainforest decline at 0.45 cal ky BP.

Since forest succession, dune formation, sea-level rise, and human-impact are insufficient to explain the observed variability, climate dynamics are considered to be the prime driving force for vegetation changes on Fraser Island.

In **Chapter 7**, the results from Fraser Island are incorporated into a review of Holocene climate patterns in eastern Australia, based on a series of high-resolution pollen records across a North-to-South transect. Previously published radiocarbon data are calibrated into calendar years and incorporated into revised age-depth models. The resulting chronologies are used to compare past environmental changes and describe patterns of climate change on a calendar-age time-scale. Based on the present-day Australian climate patterns and impact of the ENSO, the palynological data are interpreted and the prevalent climate mode throughout the Holocene is reconstructed. Results show that early Holocene changes are strongly divergent and asynchronous between sites, while middle to late

Holocene conditions are characterized by more arid and variable conditions. During the middle to late Holocene northern and southern sites show increased coupling, which is in agreement with an increasing influence of ENSO.

Finally, in **Chapter 8** an integrated overview of a variety of marine and terrestrial paleoclimatic data relevant to the detection of ENSO variability is presented, focusing on two time-windows, 6-5 ky BP and 4.5-3.5 ky BP. Analysis of proxy climate data indicate that, after a climate-state change at ~5 ky BP towards active ENSO cyclicity in the equatorial Pacific, ENSO-teleconnected regions are characterized by an increased amplitude of ENSO events around 3 ky BP. Comparison with climate model scenarios shows that the generally accepted view that ENSO intensification results from summer Pacific trade wind reduction cannot completely explain the observed Holocene changes. An additional mechanism is proposed, involving increased Indo-Pacific Warm Pool (IPWP) heat charging, which could have resulted in an increase of ENSO amplitude.

N.B. The chapters of this thesis are or will be published as separate papers in scientific journals. As a consequence, some repetition of statement cannot be avoided.

A novel approach for developing high-resolution sub-fossil peat chronologies with ^{14}C dating.

Abstract

Sub-fossil sections from a Florida wetland are accelerator mass spectrometry (AMS) dated and the sedimentological conditions are determined. ^{14}C data are calibrated using a combined wiggle-match and ^{14}C bomb-pulse approach. Reproducible results are obtained providing accurate peat chronologies for the last ~130 calendar yr. Assessment of the different errors involved leads to age models with 3–5 yr precision. This allows direct calibration of paleoenvironmental proxies with meteorological data. The time frame in which ^{14}C dating is commonly applied can possibly be extended to include the 20th century.

1.1. Introduction

Modern paleoclimatology focuses on the development and validation of biological proxies, which are indicative for climate parameters rapidly changing under ongoing greenhouse gas forcing. The ability to understand the dynamics of major weather determining systems such as the El Niño - Southern Oscillation (ENSO) is a basic requirement to predict the consequences of human interference with the global system. Although increasing amounts of instrumental precipitation and temperature records are available, the relatively short timespan covered in these records generally does not encompass the total range of natural variability.

On this background, the development of proxies able to detect high-frequency changes on near-annual to sub-decadal scale is needed. To test the applicability of any potential proxy, it is essential to first assess the natural range of variability within a single site and compare changes to meteorological data.

Among the available proxies for paleoclimatological reconstructions, pollen and plant macroremain analysis have been demonstrated to be highly indicative for fast changes in their growth environments (Birks and Birks, 2003). Peat-accumulating systems provide well-preserved organic-rich sediments and are, thus, a suitable source for paleobotanical investigations.

Validation and application of these proxies, for studies involving climatological changes occurring on multi-annual to sub-decadal scale, requires meticulous calibration of paleo-records with modern meteorological data series. The proxy quality thereby strongly depends on an extremely accurate age assessment of young sediment cores. Contrary to lake sediments, peat is generally not (annually) laminated. Consequently, radiometric dating is required to obtain a reliable core chronology.

Commonly used ^{137}Cs and ^{210}Pb dating methods depend on analysis of particles that potentially migrate in the sediment due to changing water levels, and the results are not always satisfactory (Jensen *et al.*, 2002) or in mutual agreement (Cohen *et al.*, 1999). Errors in determination of water content and dry bulk densities and the estimation of initial concentrations provide further uncertainties in ^{210}Pb dating (Appleby, 2001). In this study, we assess the applicability of radiocarbon dating in creating high-precision peat chronologies for the 20th century and into the time frame where ^{14}C dating is commonly applied. Furthermore, we consider the different errors involved and provide some recommendations for future application.

1.1.1. Site description

Extensive peat-accumulating wetlands exist in southern Florida (USA). This area is highly suitable for high-resolution studies on climate variability because of the distinct linkage of precipitation and temperature to the ENSO system (Cronin *et al.*, 2002). High-quality ecological and meteorological data for the region are abundant. The site studied is located in a relatively undisturbed wetland ecosystem, part of the Fakahatchee Strand Preserve State Park (25°95' N, 81°49' W, hereafter FSPSP, see Fig. 1.1).

Although widespread in Florida, human impacts by lumbering and drainage activities have not directly affected the area studied; old-growth forest is still dominant (Burns, 1984). Swamp conditions persist within the wide and shallow 40-km-long karst structure or 'strand' where a peat layer seals off the underlying limestone. This organic-rich layer retains water which extends the local hydroperiod. These continuous moist conditions create anoxia that inhibits organic degradation and bioturbation. The strong seasonality, however, creates large fluctuations in water level throughout the year, which allows small inorganic particles to migrate within the sediment column. The wetland forest ecosystem and general low topography of the terrain (Watts and Hansen, 1994) act together as a water capacitor, resulting in a wide sheet flow that deposits no clastic material and creates stable high sedimentation rates. These factors combined make the FSPSP highly suitable for collecting organic-rich undisturbed sediments for both ^{14}C dating and subsequent paleoecological reconstructions.
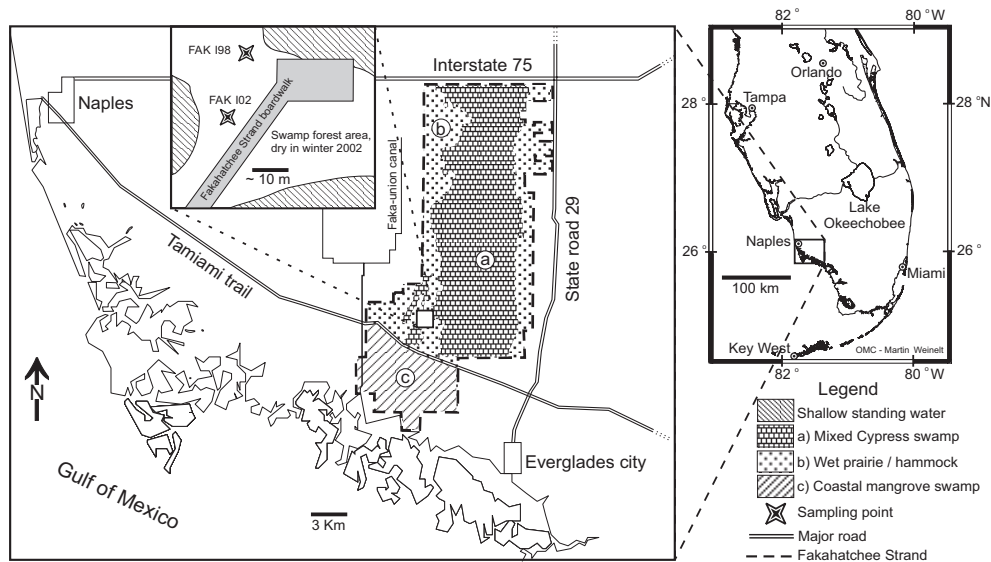
Figure 1.1 Location and environmental setting of the Fakahatchee Strand Preserve State Park (FSPSP) in south-central Florida

1.2. Material and methods
1.2.1. Coring and sampling procedures
Two peat cores were taken in the FSPSP for palynological/paleobotanical studies. The first peat core was taken in 1998 (FAK I98) from the end of a 300-m FSPSP boardwalk that penetrates into an undisturbed mixed cypress forest (Fig. 1.1). The 43-cm-long core was frozen and cut into 1-cm slices for further analysis. A second core (FAK I02) was collected in 2002 at approximately 50 m from FAK I98 in a slightly deeper and wetter section of the swamp.

This 84-cm core was cut in 0.5-cm slices for more detailed analysis. Both cores were taken with a manual 21-cm-diameter peat corer designed for minimal sediment disturbance (Clymo, 1988).The obtained peat sequences consist of dark, organic-rich, non-laminated peat with abundant leaf and plant fragments. Tops were not consolidated and contained the best-preserved plant remains. The peat slices were sub-sampled for AMS ^{14}C dating, plant macrofossil-analysis, pollen analysis, and loss-on-ignition (LOI, FAK I02 only).

For AMS ^{14}C dating, leaf samples from 9 slices of core FAK I98 and 10 slices of core FAK I02 were picked out and determined to highest possible taxonomic level (see Table 1.1 for details). Material from tall canopy trees (*Quercus* and *Taxodium*) was used exclusively to eliminate reservoir effects from any old carbon outgassing and subsequent uptake by low-growing vegetation. The remains were cleaned from any rootlet material that might contaminate the samples, dried for 12 hr at 60 °C, and stored in dry and cool conditions.

1.2.2. ^{14}C analysis
Plant remains were visually inspected using a binocular microscope, and attached allochthonous organic material was removed. The samples were pretreated according to an acid-alkali-acid procedure (Mook and Streurman, 1983) to remove contaminating humic acids. The prepared material was combusted and the carbon dioxide formed was subsequently converted into graphite. The graphite targets were analyzed by the AMS facility of Utrecht University (Van der Borg *et al.*, 1997). The δ^{13}C values were obtained from analysis by the gas mass spectrometer at the Earth Sciences Department of Utrecht University, the Netherlands.

1.2.3. Pollen and loss-on-ignition (LOI)
Pollen from a weighed volumetric sediment sample was counted under the light microscope. A known amount of marker grains (*Lycopodium clavatum*) was added to the sample before standard palynological processing (Faegri and Iversen, 1989) to allow for calculation of pollen concentration (grains cm^{-3}) per sample. At a constant pollen influx on a decadal timescale (Middeldorp, 1982; Hicks, 2001), stability of sedimentation rates can be assessed.

Sediment samples for loss-on-ignition (LOI) were dried for 12 hr at 100 °C, and combusted at 550 °C and 1000 °C. Percent weight loss after each step is a measure of organic and carbonate fractions, respectively. Results of Dean (1974) show that organic material begins combustion at 200 °C and is completely ignited when temperature reaches 550 °C.

1.3. Results
Results of the AMS ^{14}C analysis are given in Table 1.1, represented as ^{14}C ages. The obtained δ^{13}C values are between –32.6 and –25.0‰ , in agreement with the characteristic range of δ^{13}C values in leaves and wood of canopy trees (Lockheart *et al.*, 1998; Loader *et al.*, 2003). Results of the LOI and pollen counts are presented in Fig. 1.2. As Australian pine (*Casuarina equisetifolia*) was introduced to Florida only after AD 1900 (Alexander and Crook, 1974), the deepest occurrence of *C. equisetifolia* pollen in FAK I02 at 52.5 cm depth provides a maximum age of 100 calendar yr for the upper part of the core.

LOI at 550 ºC (Fig. 1.2) reveals a down-core decrease of the organic fraction, pointing to gradual decomposition of organic material. No sudden large influxes of clastic material were observed. Pollen concentrations show significant annual variability but no long-term trend; an apparent small decrease within the top 20 cm is in line with the expected low compaction at this level.

1.3.1. Calibration and age models

Twentieth century nuclear bomb testing created a distinct high-amplitude profile of elevated atmospheric ^{14}C levels, which can be used to calibrate recent samples into calendar yr. For better comparability with our ^{14}C ages, the ^{14}C data were converted into ^{14}C ages. This conversion creates a post-AD 1950 calibration curve with negative ^{14}C ages (Fig. 1.3A, atmospheric and tree-ring ^{14}C data from Northern Hemisphere rural areas, adapted from Cain and Suess, 1976; Levin *et al.*, 1994; Stuiver *et al.*, 1998).

Table 1.1 Samples and results of AMS radiocarbon dating

Depth [a] (cm)	UtC # [b]	Material	Dry weight (mg)	δ^{13}C (‰)	^{14}C age ± 1σ yr BP	Calibrated ages (cal AD ± 1σ)	Total error [c] (yr)
Core FAK I98							
4	11709	leaf (*Quercus / Acer*)	2.17	-30.7	-1018 ± 34	1993 ± 3 [d]	5
6	11710	leaf (*Quercus / Acer*)	1.31	-32.6	-877 ± 27	1995 ± 3 [d]	5
9	11711	leaf (*Quercus / Acer*)	2.08	-29.8	-1476 ± 27	1985.5 ± 2.5 [d]	4.5
12	11712	leaf (*Quercus / Acer*)	0.59	-29.7	-1522 ± 31	1985 ± 2 [d]	4
15	11713	leaf (*Quercus / Acer*)	0.45	-29.9	-1671 ± 32	1983 ± 2 [d]	4
20	11714	leaf (*Quercus / Acer*)	0.2	-28.1	-1507 ± 70	1960.5 ± 1.5 [d]	3.5
23	11715	seed (cf. *Quercus*)	2.29	-26.7	-353 ± 29	1955 ± 1 [e]	3
26	11716	leaflets (*Taxodium d.*)	1.01	-28.9	-100 ± 70	1954 ± 1 [e]	3
39	11717	leaflets (*Taxodium d.*)	1.35	-28.1	170 ± 29	1937 ± 17 [e]	19
Core FAK I02 [f]							
6	12080	leaflets / buds	14	-28.9	-756 ± 34	1998.5 ± 3.5 [d]	5.5
15	12081	leaflets / buds	9	-29.1	-840 ± 40	1995.5 ± 2.5 [d]	4.5
20	12082	leaflets / buds	9.9	-29.2	-825 ± 33	1996 ± 2 [d]	4
30	12083	leaflets / buds	7.4	-29.5	-1851 ± 49	1981.5 ± 1.5 [d]	3.5
40	12084	leaflets / buds	12.4	-27.9	-976 ± 34	1957.5 ± 1 [e]	3
50.5	12085	leaflets / buds	8.6	-28.7	146 ± 45	1937 ± 18 [g]	18
60	12114	leaflets / buds	9	-25.0	124 ± 33	1919 ± 15 [g]	15
70	12086	leaflets / buds	8.7	-28.0	-131 ± 32	1954.5 ± 0.5 [e, h]	2.5
75	12087	leaflets / buds	10.8	-27.9	66 ± 47	1890 ± 15 [g]	15
80.5	12088	leaflets / buds	8.9	-28.3	121 ± 32	1881 ± 10 [g]	10

[a] Depths measured from core top, value is for underside of sample. Sample thickness is 1.0 cm (FAK I98) and 0.5 cm (FAK I02).
[b] Laboratory code: R.J. Van de Graaff laboratorium, Utrecht University.
[c] Total error consists of ^{14}C calibration error plus a 2-year error factor covering sample thickness and transport/coring inaccuracies in samples calibrated with the bomb-pulse.
[d] Calibrated with bomb-peak, data from Levin *et al.* (1994).
[e] Calibrated with Cain and Suess (1974).
[f] All meterial for core FAK I02 is *Taxodium distichum*
[g] Wiggle-match with UWSY98, Stuiver *et al.* (1998).
[h] Sample identified as outlier, not used in construction of age-depth model.

In case of multiple curve intercepts, stratigraphic information (order and depth of samples) was used to either assign data to the up- or down-slope of the bomb pulse (Fig. 1.3A). Assuming stratigraphic order represents a true chronology in FAK I98 and I02, all ages below -100 BP could be accurately calibrated (Table 1.1). ^{14}C data calibrated in this manner have very small 1σ errors (1–2 yr) as a result of the well-determined ^{14}C bomb pulse. Especially evident is the fourfold better precision of the ^{14}C dates calibrated post-AD 1950 in comparison with the single pre-AD 1950 date in core FAK I98 (Fig. 1.3B).
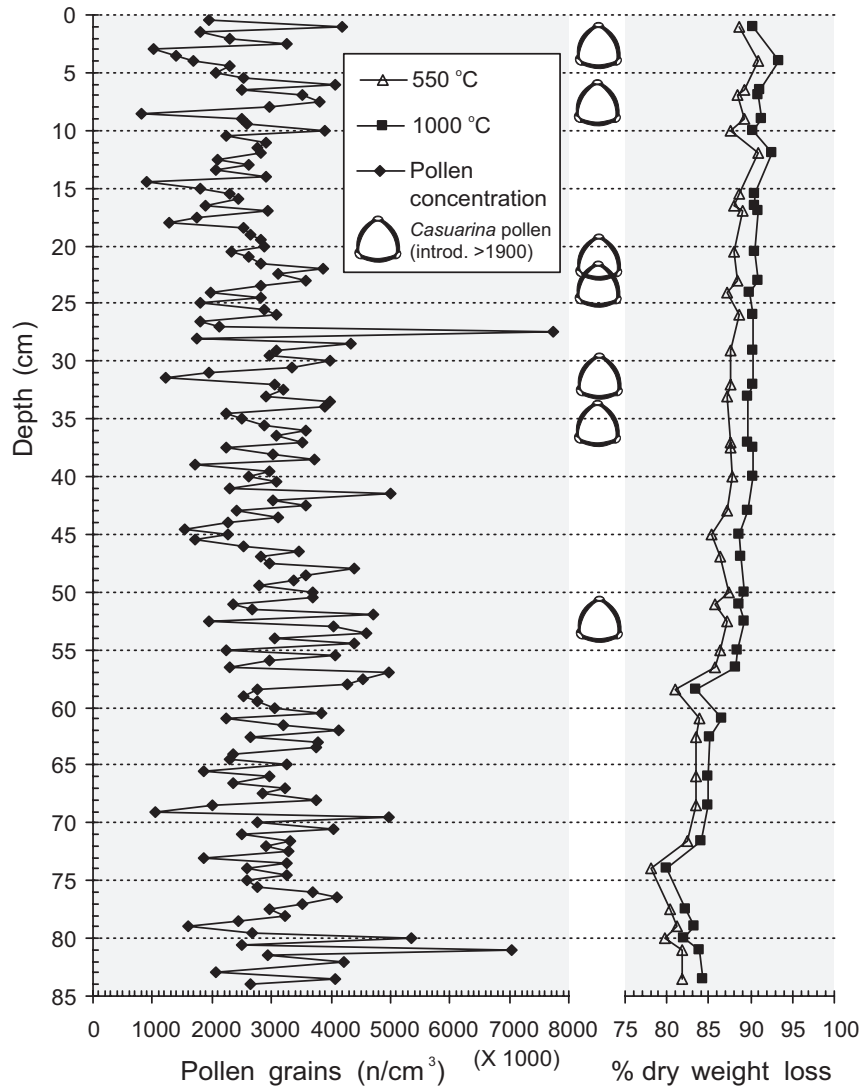
Figure 1.2 Loss-on-ignition (LOI) and pollen concentrations of core FAK I02. Occurrences of *Casuarina equisetifolia* pollen indicate post-AD 1900 sediment deposition.

A smooth transition could be obtained between the pre- and post-AD 1950 sections of core FAK I02 (Fig. 1.4A) by wiggle-matching the pre-bomb ^{14}C dates. The core was well compacted below 25 cm (taking pollen concentration and LOI data into account, Fig. 1.2), thus, a linear accumulation rate could be expected below this level. Four ^{14}C data were calibrated by wiggle-matching with the high-resolution UWSY98 curve (Stuiver *et al.*, 1998). The best fit was obtained visually by varying the slope between and position of the ^{14}C dates relative to the calibration data. The accumulation rate thus found is a
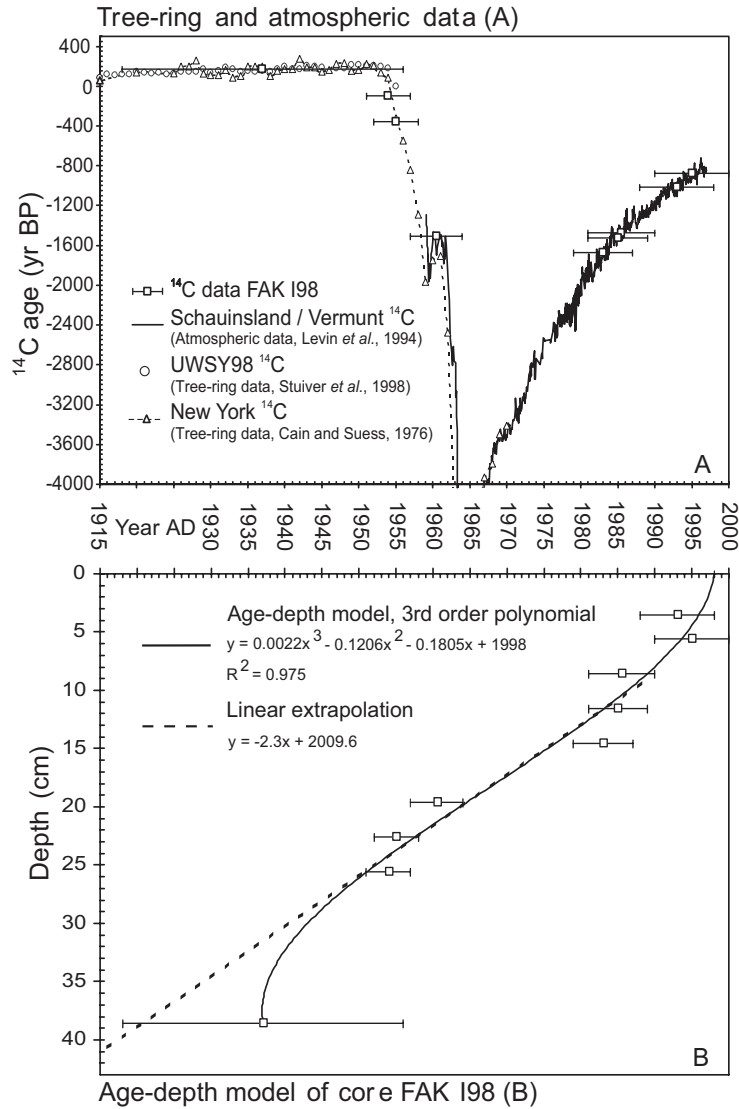
Figure 1.3 Modern ^{14}C bomb-peak anomaly used for calibrating recent samples of core FAK I98. (A) Calibrated samples are used to construct an age-depth model (B). x = depth in cm, y = age in yr AD (axes inverted for comparison between Figures A and B). Errors shown contain an additional 2-yr factor for coring/sampling inaccuracies.

continuation of values encountered in the upper half of core FAK I02 (0.53 cm/yr, Fig. 1.4B), in agreement with the stable sedimentation conditions below the top 25 cm and generally undisturbed setting of the site. Since no intercept is determined with wiggle-matching, error ranges were obtained by calculating the minimum value at which the ^{14}C measurement would fall outside the UWSY98 curve when shifted along the calendar axis.

Chapter 1
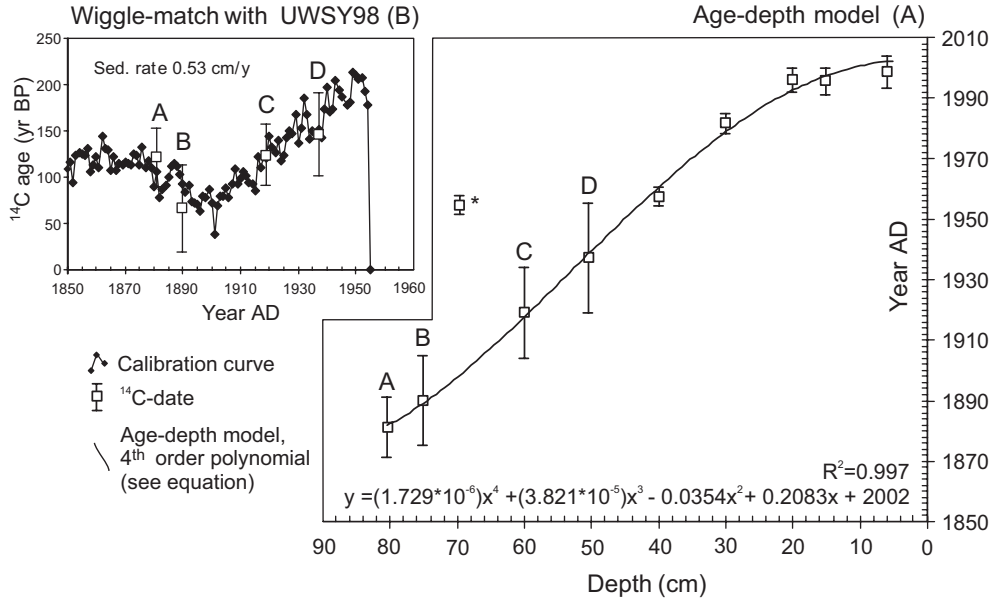
Figure 1.4 Age-depth model of core FAK I02 (A) containing data calibrated with bomb-peak and wiggle-matching approaches (Figure B, samples indicated A–D), x = depth in cm, y = age in yr AD. Errors shown contain an additional 2-yr factor for coring/sampling inaccuracies when calibrated with the bomb-peak. The sample marked with an asterisk (*) was considered an outlier and was not used for constructing the age-depth model (see discussion).

Age models for both cores were obtained by fitting polynomial curves through the calibrated ^{14}C data, while fixing the core top at the year of collection (Figs. 1.3B and 1.4B). In FAK I02, 1 data point was excluded from the age model since it most likely represents an outlier. The resulting age determination range is ~90 calendar yr for FAK I98 and ~130 calendar yr for FAK I02 (see discussion).

1.4. Discussion
1.4.1. Error factors
Since ^{14}C data calibrated with the bomb pulse anomaly have very small 1σ accuracy of coring and sampling contributes significantly to the total error of the date. To account for these effects in the cores studied, a 2-yr error factor was added to the 1σ interval of ^{14}C data calibrated by this method (Table 1.1). Possible artifacts of coring procedure, transport, sampling precision, and resolution are accounted for in this additional factor. The improvement by higher sampling resolution and precision of FAK I02 compared to FAK I98 (with 0.5-cm and 1-cm sampling intervals, respectively) is apparent from a better fit of the age-depth model in FAK I02.

Since in core FAK I98 only 1 data point is present in the pre-AD 1950 period, the lower limit of the age-depth curve cannot be accurately determined. Hence, an unrealistic age-reversal is present that cannot be explained from the ^{14}C and LOI data of the nearby core FAK I02. A linear extrapolation of the polynomial function was, therefore, used below 27

22

cm. Based on the local sedimentation regime, this is considered the most realistic age model available for core FAK I98.

The outlier identified in FAK I02 is possibly due to down-sliding of individual leaves during coring. However, it most likely presents an isolated case since the outside of the core was removed during sample preparation.

The compaction difference between the unconsolidated top and lower sediment section is very apparent in the age models of both cores (Figs. 1.3B and 1.4A). This change is less obvious from the pollen concentrations in the FAK I02 core top (Fig. 1.2). The pollen sub-sampling method used (small volumetric punch core) most likely caused some additional compaction, not fully reflecting the loose non-decomposed nature of the youngest sediment. The lower pollen concentration in the top is apparent, however, and therefore, in agreement with the core descriptions and the depth-models obtained.

Pre-bomb samples from areas with more than average fossil fuel combustion (i.e. cities, industries) can show a locally enhanced Suess effect (Cain and Suess, 1976). For the early 20th century, these local effects could create additional uncertainty that cannot be resolved with high precision unless a calibration data set from the same area is present or industrial areas are avoided.

1.4.2. Use of method

Although southern Florida is known to be highly sensitive to changes in the ENSO system, systematic paleoecological and paleoclimatological investigations on very high temporal resolution was hampered until now by the insufficient accuracy of age assessments for the peat deposits by conventional dating methods as ^{137}Cs and ^{210}Pb (Cohen *et al.*, 1999). By following the approach presented here, the homogenous organic-rich peat accumulations from this key area can be dated with far greater accuracy. The combined wiggle-match and bomb-pulse calibration of ^{14}C data of the peat deposits from South Florida has resulted in extremely accurate age models, especially for core FAK I02. Despite uncertainties about the different error factors mentioned above, the precision is still very high with maximum errors of 5 yr for the post-AD 1950 period. The quality of the age assessments improves both the validation procedure for new proxies and their applicability.

Paleoecological proxies are commonly calibrated by comparison with surface samples as modern analogues. However, this modern analogue approach often suffers from error factors that arise from geographically widespread data sets. The high dating precision obtained here provides the opportunity for direct comparison of proxy data with measured historical meteorological records, thus enabling secure proxy validation and calibration in a restricted geographical area.

The high accumulation rates in both cores studied, with approximately 0.5 cm/yr in the main part of the sections, allows the build-up of proxy records for the time beyond the range of instrumental measurements, with a temporal resolution high enough to detect changes occurring on multi-annual to sub-decadal scale. In addition, we have obtained a smooth transition between samples calibrated by the bomb pulse and the UWSY98 data

set. Therefore, the time frame where ^{14}C dating is commonly applied can be extended to include the 20th century.

The dating strategy outlined above thus meets the requirements for sound proxy validation and application, which is of prime importance in actualizing research fields dealing with dynamic climate systems that vary on multi-annual to centennial timescales, such as ENSO.

Quantification strategies for human-induced and natural hydrological changes in southern Florida wetland vegetation

Abstract

An accurately dated peat profile from a mixed cypress swamp in the Fakahatchee Strand Preserve State Park (FSPSP, Florida, U.S.A.) is examined for pollen and spores. The near-annual resolved pollen record shows a gradual shift from a wet to a relatively dry assemblage during the past 100 years. Timing of drainage activities in the region is accurately reflected by the onset and duration of vegetation change in the swamp. Subsequently, the reconstructed vegetation record is statistically related to pollen assemblages from surface sediment samples. The response range of the FSPSP wetland to environmental perturbations can thus be determined and this allows better understanding of naturally occurring vegetation changes. In addition, the human impact on Florida wetlands becomes increasingly apparent.

Superimposed high-frequency variation in the record suggests a positive correlation between winter-precipitation and pollen productivity of the dominant tree taxa. However, further high-resolution analysis is needed to confirm this relation.

The response range of the FSPSP wetland to environmental perturbations on both annual- and decadal-scales documented in this study, allows recognition and quantification of natural hydrological changes in older deposits from southwest Florida. The strong link between local hydrology and the El Niño - Southern Oscillation makes the palynological record from FSPSP highly relevant for studying past El Niño-variability, magnitude and persistence.

2.1. Introduction

The Florida peninsula is situated at the transition zone between the wet-subtropical and tropical rainy realms (Thomas, 1974). Apart from being broadly determined by this North-to-South temperature gradient, South-Florida wetland ecosystems are strongly controlled by the precipitation-driven surface sheet flow originating from Lake Okeechobee (Burns, 1984; Duever *et al.*, 1986).

Small altitude variations in the generally flat subsurface around Lake Okeechobee create distinctive patterns in local hydroperiod and water depth, which are the two main parameters determining the nature of local plant communities (Kushlan, 1990; Willard *et al.*, 2001a). Hence, local vegetation composition directly reflects water availability and, when reconstructed through time, vegetation changes provide a valuable archive of past hydrologic conditions for the entire region. In South Florida, the strength of the El Niño - Southern Oscillation (ENSO) accounts for over 50% of the precipitation available to the vegetation during the growing season (data available on: http://climexp.knmi.nl/ and http://www.cpc.ncep.noaa.gov, NOAA Climate Prediction Center; Cronin *et al.*, 2002). A record of past hydrologic conditions will thus provide important clues about past El Niño-variability, magnitude and persistence. Although South-Florida swamp ecosystems are in general very sensitive to changes in water availability, the exact extent of vegetation response to changing hydrology needs to be determined in order to enable quantification of observed vegetation changes in the past.

Pollen analysis is the principle technique available for determining vegetation response to past terrestrial environmental change (Bennett and Willis, 2001). Traditionally, vegetation reconstructions based on pollen analysis have focused on long-term, (sub-)centennial to millennial timescales. Pollen records from Florida are no exception to this practice (Watts, 1980; Delcourt and Delcourt, 1985; Watts and Hansen, 1994). However, the potential of high-resolution studies that focus on annual to decadal climate variability, as present in ENSO, has not been fully utilized (Green *et al.*, 1988). Pollen production rates have been shown to depend on annual temperature (Hicks, 2001) and precipitation levels (Willard *et al.*, 2003). Pollen analysis on very high temporal resolution can likely be used as a proxy for annual-scale climate variability, besides general long-term vegetation reconstructions.

This paper presents a well-dated 20th century pollen record at near-annual resolution from a South-Florida wetland. The response of local vegetation to known changes in environmental conditions is determined and the fossil data are compared to a surface-sample dataset previously published by Willard *et al.* (2001b), supplemented with new surface sample data from southwest Florida. Thereby the magnitude of change in the pollen record and the wetland ecosystem sensitivity can be established. In addition, the relation between high-frequency variation in the pollen record and annual precipitation changes is investigated, the latter being strongly influenced by the ENSO climate system. Together, these approaches bridge the gap between present-day ecology and paleoecological reconstructions, and provide a solid framework for interpreting further pollen records from this locality.
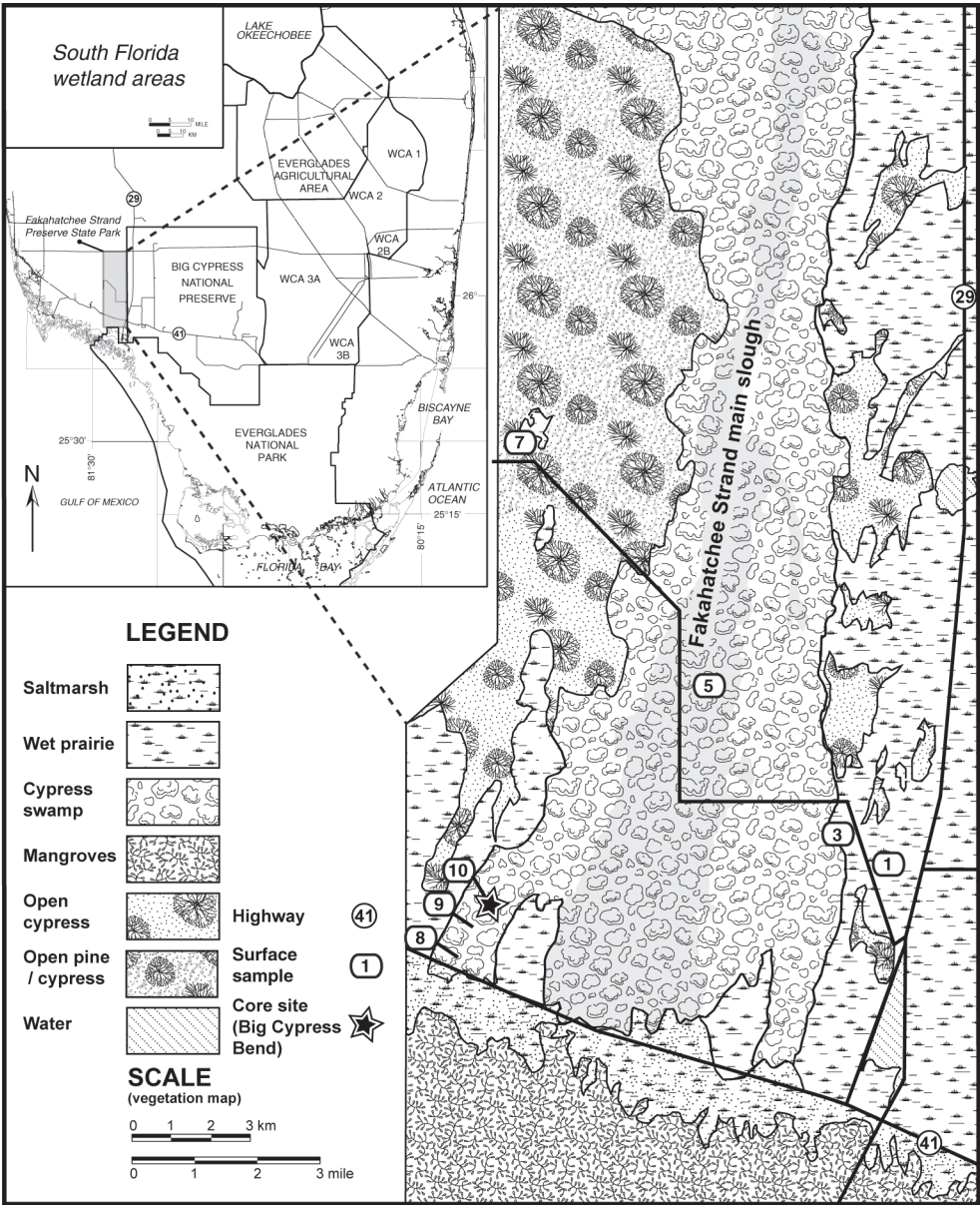
Figure 2.1 Location and natural communities map of the Fakahatchee Strand Preserve State Park (FSPSP), Florida, USA. Coring site (FAK I98, ①) and surface samples sites (⭐) are indicated. Regional map adapted from Willard *et al.* (2001b).

2.2. Site description

2.2.1. Regional and local

The site studied is located in a relatively undisturbed section of the Fakahatchee Strand Preserve State Park (FSPSP) wetland (25°95'N, 81°49'W, Fig. 2.1). The FSPSP is part of the larger 'Big Cypress National Forest' in South-Central Florida, and its central 'strand' is an elongated karst structure forming a wide and shallow channel or slough. A peat layer seals off the underlying limestone deposits of the early Pleistocene Tamiami Formation (Gleason and Stone, 1994). The sheet flow through the 40-km long strand is slow due to high flow-resistance of the forest and generally low topography of the terrain (Watts and Hansen, 1994), where the maximum height difference is 2 m. This creates a stable low-energy depositional environment with undisturbed peat accumulation in the slough.

On the peaty soils bald cypress (*Taxodium distichum*) dominates the central swamp forest, which is surrounded by prairie and pinelands and bordered by mangrove vegetation towards the coastal area in the south. Between 1947 and 1952 a network of tramways and borrows for logging was constructed in the adjacent area, but this did not directly affect the coring site itself (Burns, 1984), which is still dominated by a significant stand of old-growth *Taxodium*.

2.2.2. Hydrology and vegetation

Annual precipitation in Southern-Florida has a bi-modal distribution, and the main precipitation is received during summer and an additional, frequently occurring, wet period in winter (Duever *et al.*, 1986). The swamp forest largely depends on the water storage capacity of the peat to retain the water from winter precipitation into the spring growing season (Burns, 1984). The typical hydroperiod of the cypress swamp ecosystem is 6-9 months / year and it has a moderate fire frequency (5 times / century), which allows extensive organic matter accumulation (peat thickness >1 m.). To thrive in these conditions, *Taxodium* is highly tolerant to long hydroperiods, often associated with low oxygen levels, and is very fire-resistant (Myers and Ewel, 1990). Fires burn through the prairies and pinelands every 2-7 years (Austin *et al.*, 1990), but they seldom penetrate the watterlogged, peaty cypress strands. Fire-frequency is a factor of ~4 lower in swamps than in the surrounding marshes and wet-prairie grasslands, and actual peat burns only occur during extreme droughts (Duever *et al.*, 1986). *Taxodium* are deep-rooting trees and they usually resprout after fires, and only in case of extreme fire events the root system is consumed and tree recovery is no longer possible (Alexander and Crook, 1974).

Vegetation in the FSPSP is very diverse and considered a rare mix of tropical and temperate plants. At least 477 vascular plant species have been identified, of which the major part is tropical (69% of trees and 87% of orchids, epiphytes and ferns, Austin *et al.*, 1990).

In the wet central slough the dominant *Taxodium distichum* is complemented by canopy species typical for swamp soils in Florida (Davis, 1943). At relatively dry sites these are primarily: palms (*Roystonea elata* and *Sabal palmetto*), *Quercus virginiana*, *Q. laurifolia*, *Acer rubrum*, *Pinus elliotii*, *Persea palustris*, *Magnolia virginiana*, *Chrysobalanus icaco*, *Ficus aurea*, *Ilex cassine*, *Rapanea punctata* and *Myrica cerifera*. Ferns (37 species, including

epiphytic forms) constitute the predominant undergrowth in these moist areas that are not inundated for very long periods. At wetter sites where water is relatively deep and hydroperiods are long (>9 months / year) *Salix caroliniana*, *Cephalanthus occidentalis*, *Fraxinus caroliniana* and *Annona glabra* are more abundant.

Table 2.1: Location of surface samples from FSPSP with local vegetation at time of collection (February 2004)

Number & name	Dominant vegetation In order of importance	Sec. vegetation In order of importance	Tert. vegetation In order of importance	Hydrology At time of collection
1 Wet prairie "Fak1 prairie"	*Muhlenbergia capillaris* *Cladium jamaicense* *Spartina bakeri*	*Lobelia feayana* *Phragmites australis*	*Sagittaria graminea* *Crinum americanum*	5-10 cm standing water
3 Pine prairie "Fak3 pine"	*Pinus elliottii* *Taxodium distichum* *Eupatorium capillifolium* *Cladium jamaicense*	*Sabal palmetto* *Rapanea punctata* *Persea palustris* *Serenoa repens* cf. *Baccharis halimifolia*	*Quercus virginiana* *Psychotria nervosa*	Moist soil
5 Ballard's pond "Fak5 pond"	*Taxodium distichum* *Quercus laurifolia* *Fraxinus caroliniana* *Rapanea punctata* *Roystonea regia* *Itea virginica*	*Ilex cassine* *Annona glabra* *Psychotria nervosa* *Fern* indet. *Persea palustris* cf. *Baccharis halimifolia*		10-20 cm Standing water
7 Palm prairie "Fak7 palm"	*Cladium jamaicense* *Myrica cerifera* *Ilex cassine* *Pinus elliottii* *Sideroxylon* sp. *Muhlenbergia capillaris* *Spartina bakeri*	*(Dominant continued)* *Berchemia scandens* cf. *Baccharis glomeruliflora* *(Sec. Vegetation)* *Taxodium distichum* *Sabal palmetto*		Very moist, waterlogged soil
8 Begin boardwalk "Fak8 beginB"	*Acer rubrum* *Quercus laurifolia* *Sabal palmetto* *Roystonea regia*	*Rapanea punctata* *Taxodium distichum* *Acrostichum danaeifolium* *Thelypteris* sp.		20 cm Standing water
9 Mid of boardwalk "Fak9 midB"	*Taxodium distichum* *Fraxinus caroliniana* *Rapanea punctata* *Ilex cassine*	*Sabal palmetto* *Quercus laurifolia*		30 cm Standing water
10 End boardwalk "Fak10endB"	*Taxodium distichum* *Fraxinus caroliniana* *Acer rubrum*	*Ficus aurea* *Quercus laurifolia* *Rapanea punctata* *Thelypteris* sp.	*Saururus cernuus* *Sabal palmetto*	>50 cm Standing water
Tree island tail * "97-10-09-3" (Willard et al 2001a)	*Magnolia* sp. *Smilax* sp. *Ficus* sp.	*Thalia* sp. *Mikania scandens* *Peltandra virginica*	*Cladium jamaicense*	No standing water Note: not from FSPSP

* This sample is identified as a close analogue to core samples from zone FIII in Fig. 2.4B. Location is WCA 3A, see map Fig. 2.1

The central slough is surrounded by wet prairie with numerous tree island stands (Fig. 2.1). The prairie consists mainly of grasses (*Muhlenbergia capillaris*, *Phragmites australis*), sedges (*Cladium jamaicense*, *Cyperus* sp.), Amaranthaceae and Asteraceae (typical of fluctuating water levels) as well as aquatic plants (*Sagittaria graminea*, *Nymphea* sp.) in somewhat wetter areas. With respect to the wet prairie, tree islands are slightly elevated areas dominated by trees and ferns. Their vegetation varies between mixed-temperate and tropical species, even exclusively palms. Wet prairies have a moderate and fluctuating water depth (<0.5 m) and hydroperiod (<6 months / year, Willard *et al.*, 2001b).

Cypress are generally stressed by dewatering and, unlike most other trees, they can survive permanent inundation, although new saplings do need a dry season to germinate (Alexander and Crook, 1974). As a result of this limitation to reproduction, cypress regeneration is generally low (Visser and Sasser, 1994). A study to detect forest stress in response to increased river flow has revealed that increasing water level has a stressing effect in *Q. laurifolia* and to a lesser extent in *F. caroliniana* (Ford and Brooks, 2002). Trees were shown to suffer from trunk rot, increased parasitism, crown thinning, branch mortality and even death. However, no such effects were observed in *Taxodium* trees present in the studied area. *F. caroliniana* is generally considered a wet-tolerant species (Austin *et al.*, 1990; Dunson, W.A., Florida Water Resource Management Department, pers. comm., 2002), although the study by Ford and Brooks (2002) shows there are certain limits to this tolerance. Presently, *F. caroliniana* occurs together with *A. glabra* in the deepest areas of the FSPSP slough but the slow-growing *Taxodium* will most likely replace these trees since the area was logged only 50 years ago (Burns, 1984).

2.3. Material and methods

2.3.1. Coring and processing

A peat core was taken in 1998 from the end of a 300-m boardwalk, which penetrates into old-growth mixed cypress forest. A large-diameter (20-cm) manual surface corer (Clymo, 1988) was used to obtain a 43-cm sediment column (FAK I98), consisting of dark peat with abundant leaf fragments in the uppermost 20 cm. It was sliced and sub-sampled at 1-cm intervals for pollen analysis with a small volumetric peat drill. In addition, seven surface sediment samples from different vegetation units within the FSPSP were collected using a small 4-cm-diameter push core (Fig. 2.1, Table 2.1). These samples were homogenized before sub-sampling for pollen analysis.

Pollen and spores were isolated from samples following standard palynological peat processing techniques adapted from Faegri *et al.* (1989) now in use at the Laboratory of Palaeobotany and Palynology (LPP), Utrecht University, the Netherlands. *Eucalyptus* sp. pollen tablets were added prior to processing to determine pollen concentrations in sediment. *Eucalyptus* was used instead of standard *Lycopodium clavatum,* which occurs naturally in the FSPSP. Processing included carbonate and silicate removal with HCl and HF, sieving over 7-μm and 120-μm mesh to remove fine and coarse fractions, respectively, boiling in KOH to remove organic fractions and acetolysis for removal of polysaccharides and coloring of the pollen. Residues were mounted in silicon oil on microscopic slides for analysis by light-microscopy at 400x magnification.

2.3.2. Chronology

Core chronology is described in detail in Chapter 1. Dating is based on high-resolution AMS ^{14}C dating of leaf macrofossils from nine horizons. Data were calibrated with the ^{14}C-anomaly caused by nuclear testing during the 20th century. An accurate age-depth model was thus obtained, especially for the top half of the core. The base of the core was dated at 1912 AD, in accordance with dates from a core nearby (Chapter 1). Apart from a compaction effect, sedimentation rates are stable, as confirmed by loss-on-ignition (LOI) analysis of a parallel core.

2.3.3. Pollen analysis and data-handling

A minimum of 300 pollen and spores were identified to calculate percent abundances. Pollen and spore identification was based on Jones *et al.* (1995; 1999), Kapp *et al.* (2000) and the reference collections of the United States Geological Survey (Reston, VA), and LPP Utrecht, the Netherlands. To delimit pollen assemblage zones in the record, samples were numerically zoned using optimal sum-of-squares partitioning of Birks and Gordon (1985) as implemented in the program ZONE (Lotter and Juggins, 1991). The significant number of stratigraphic zones was assessed using the broken stick model (Bennett, 1996). With the Tilia/TiliaGraph 2.0.b.5 and TGView 1.3.1.1. computer programs (Grimm, 1991-2001) pollen percentages were calculated and plotted. Taxa with a maximum abundance lower than 2% and/or with less than five occurrences were omitted.

A summary of the data was made using PCA (Principal Component Analysis) ordination methods with the program Canoco 4.0 (ter Braak and Smilauer, 1998). A linear model was used because the gradient length of the pollen data did not exceed 1.5 SD (standard deviations).

The fossil and surface sample pollen data were compared in a Correspondence Analysis (CA) to establish the magnitude of change recorded in the core. The extensive dataset published by Willard *et al.* (2001b) covers a broad range of South-Florida wetland ecosystems. However, most were collected in the Everglades National Park and adjacent natural areas and do not fully encompass the FSPSP ecosystem. Surface samples collected for this study are used to supplement this dataset with samples from cypress forest and other vegetation units dominating the FSPSP. In this manner, pollen 'fingerprints' of modern environments can be used to find similar sedimentary environments in cores, irrelevant of taxa that might be over- or underrepresented compared to their actual abundance (Cohen, 1975). Although deposition rates can vary strongly between sites (Willard *et al.*, 2001a), the low-relief Florida wetland areas are not an erosive setting. Therefore the surface samples are considered to represent recent sedimentary conditions.

2.4. Results

2.4.1. Pollen record, general description and zonation

A total of 42 core samples were analyzed for pollen and spores. Results are plotted as percentages in Fig. 2.2A. Pollen and spore preservation was good although abundant organic matter complicated the analysis. Since the material is recent no large shifts are present in the record. Any changes are limited to trends within the mixed cypress swamp vegetation-unit. No charcoal particles or other indications of fire events (e.g., peaks of fern abundance) were found, corroborating the dating results (Chapter 1).

The numerical zonation indicates two significant splits (95% confidence level), which results in three distinct pollen zones (Fig. 2.2A). Zone FI has the highest amount of *Taxodium* pollen, varying between 70% and 90% (lowermost sample clearly lower, around 60%). Herbs average around 10%, and consist mainly of Amaranthaceae-type pollen although many different species occur in small peaks or as single grains, reflecting the large species diversity. Trees and shrubs, other than *Taxodium*, are not very abundant but slightly increase in the top half of the zone.
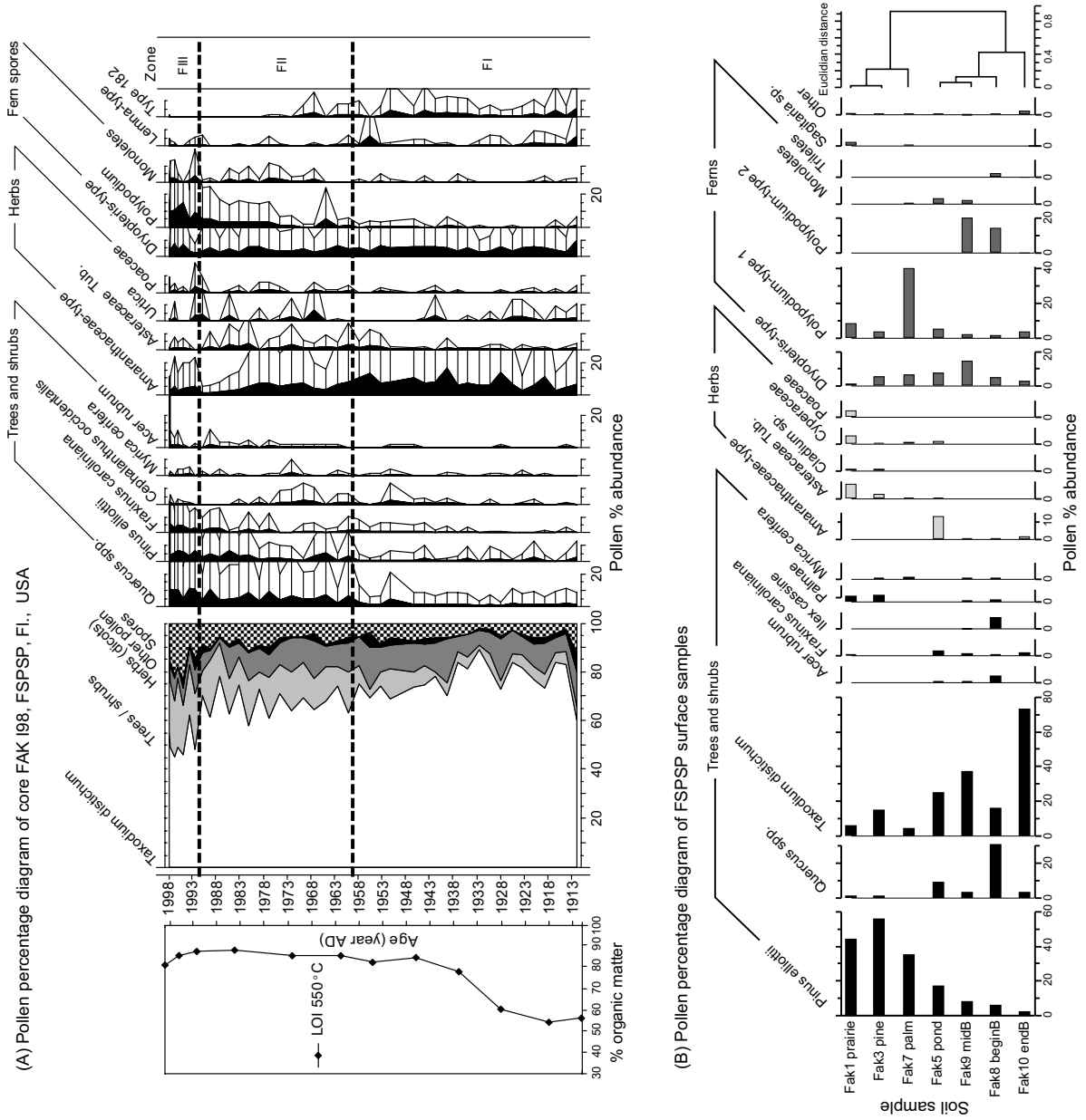
Figure 2.2 Pollen percentage diagrams of core FAK I98 (A) and FSPSP surface sample counts (B). Pollen are grouped according to their ecological characteristics, rare types are omitted. Note that *Taxodium* sp. is only presented in the grouped diagram. Loss-on-ignition (LOI) was measured on a parallel core to quantify organic content, following methods outlined by (Dean, 1974).

Zone FII marks a clear increase of temperate trees and shrubs (mainly *Quercus* and *Pinus*) from 5% in zone FI to approximately 15% in FII. The total number of herbs remains constant but shifts towards a more mixed assemblage with Asteraceae and Poaceae. Ferns become more abundant and diverse, notably *Polypodium* sp. that grows on trunks of *Quercus* trees.

Zone FIII shows a further (recent) increase of temperate trees such as *A. rubrum*, *M. cerifera* and notably *F. caroliniana*. Although the latter occurs in the deepest parts of the swamp it is also a fast-growing opportunistic species. Here it concurs with the rise in less wet-tolerant species, such as *Quercus* sp. and *P. elliottii*.

Although the site is largely inundated, true aquatic plants (*Utricularia* sp., *Myriophyllum aquaticum* and *Typha* sp.) occur infrequently since the swamp experiences seasonal drying and little light penetrates the canopy. The presence of *Lemna*-type pollen and Type 182 spores, described by Van Geel *et al.* (1983) to occur in marshland, indicate a wet environment in zones I and (part of) II. The major trends are also present in the concentration data. However, detailed reliable interpretation is hampered by low exotic counts per sample.

Results of the surface sample counts from FSPSP yield distinctly different pollen assemblages (Fig. 2.2B). Evident is the clear separation between pine-pollen dominated prairie environments and cypress/oak dominated long-hydroperiod swamp forest. The mixed hardwood pollen assemblage in sample 'Fak8 beginB' reflects well the transition zone between short-hydroperiod wet prairie and long-hydroperiod cypress swamp present at the site (Table 2.1). The samples were considered suitable for comparison with fossil data and the available surface sample data of Willard *et al.* (2001b). To combine and compare our data with the results of Willard *et al.* (2001b), the taxa grouping used in that study was followed. Consequently, some loss of information is inevitable.

2.4.2. Ordination results and high-frequency changes
The PCA ordination diagram shows a clear spread of fossil samples and taxa (Fig. 2.3A). The 1st axis of the plot is in concurrence with a hydrological gradient of taxa as described in the 'Hydrology and vegetation' section. Therefore, the value of the 1st PCA axis, explaining 35% of total variance, can be interpreted as a relative measure of the dry/wet species-index of a pollen assemblage. Plotted on a timescale, a trend from stable wet towards drier conditions becomes apparent (Fig. 2.3B). Continuously wet conditions are followed by an initially subtle drying trend around 1930. The drying accelerates after 1955 with a brief interruption by wetter conditions around 1970.

The CA results of all data (surface and fossil samples) show two distinct clusters, each with a separate gradient (Fig. 2.4A). Cluster A is represented by high abundances of mangrove taxa on the upper right (high salt/deepwater tolerant *Rhizophora mangle*, *Avicennia germinans* and *Laguncularia racemosa* and brackish water tolerant *Conocarpus erectus*) and salt-to-fresh marsh taxa on the opposite side (Spackman *et al.*, 1966; Willard *et al.*, 2001b). Thus the gradient is mainly an indication of salinity, which is a prime parameter for Florida coastal wetlands (e.g., O'Neal *et al.*, 2001). However, a water-depth
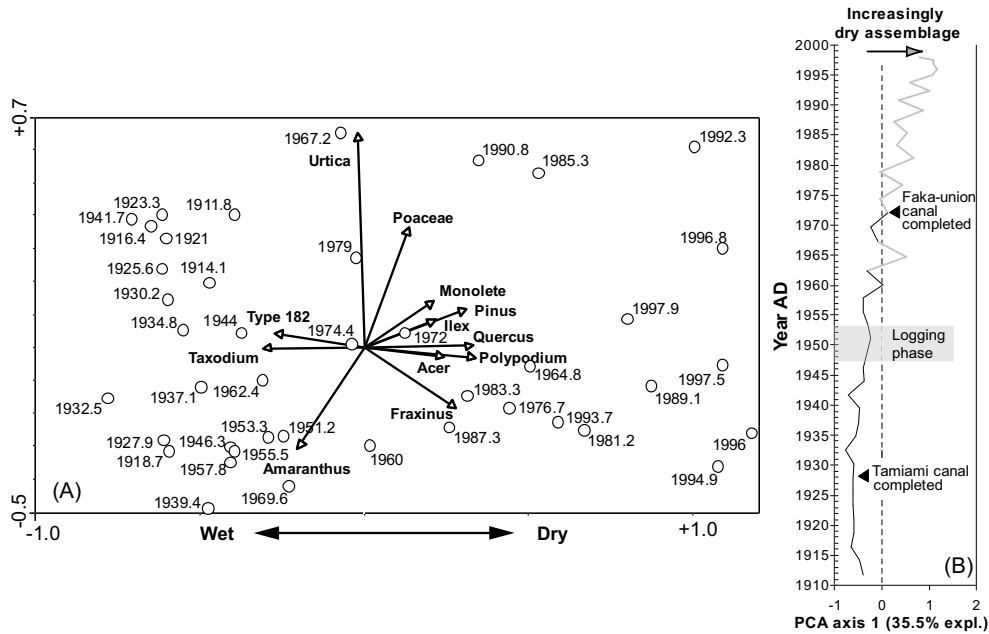
Figure 2.3 Principal component analysis (PCA) diagram of samples and major species in core FAK I98 (A). First axis of the PCA diagram explains 35% of total variance in the dataset and is concurrent with a hydrological gradient. The value of the 1st axis is plotted on a timescale (B) and is interpreted as a measure of wet/dry species-index of each assemblage.

factor is clearly influencing the distribution as well, since mangroves, in contrast to salt marshes, do not experience seasonal drying and can grow in relatively deep water.

Cluster B displays insignificant variation along the x-axis, effectively excluding salinity as a factor of influence. Cluster B includes all the fossil data and is mainly spread along the y-axis, which, analogous to Fig. 2.3A, represents the gradient of relatively dry towards wet-tolerant taxa (Ewel, 1990; Kushlan, 1990; Willard *et al.*, 2001b). The fossil samples overlap with the range of surface samples (Fig. 2.4B), although samples from zone FI with the highest abundances of *Taxodium* have no modern analogue. However, the upper samples plot close to surface samples representing intermediate water depth ('9 Mid Boardwalk' and '97-10-09-3', Table 2.1), which confirms the vegetation development seen in Fig. 2.3B.

Superimposed on the general trend, high-frequency variation is observed, in particular between AD 1950-1998. Comparison with a precipitation record from nearby Tampa reveals an in-phase correlation between the dry/wet pollen index (the PCA 1st axis) and winter precipitation for the period AD 1970-1998 (Fig. 2.5). This is in marked contrast to the pre-AD 1970 data points in which only few peaks show a positive correlation. Pre-AD 1950 data were not included in this comparison since little variability is present there and larger dating uncertainties hamper a year-to-year correlation in the lower part of the core (Chapter 1).

(A) Correspondence Analysis of all data

(B) Correspondence Analysis of all data, detail
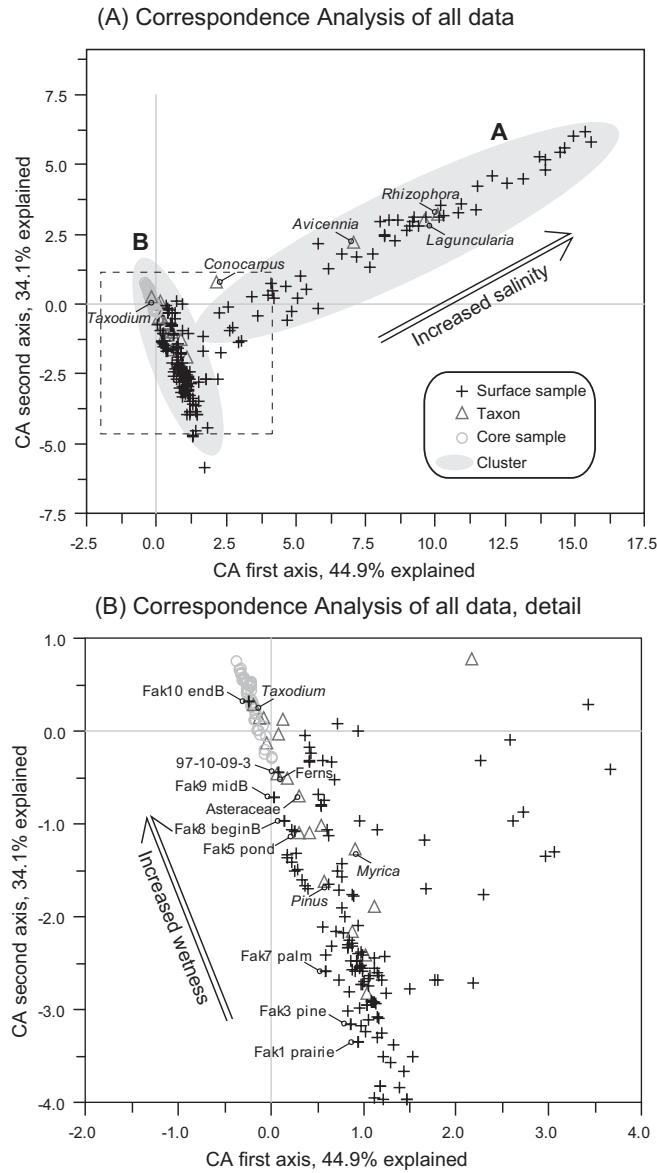
Figure 2.4 The relation of surface sample data from Willard *et al.* (2001b) to surface and fossil samples from the FSPSP based on a Correspondence Analysis of all data (A). The dashed area is given in detail (B), which shows that the fossil samples are distributed between the deep-water site 'Fak10 endB' and shallow water sites '97-10-09-3' and 'Fak9 midB' (Table 2.1). Important taxa are indicated and the gradients (arrows) within the clusters (A, B) are based on ecological descriptions of these taxa.
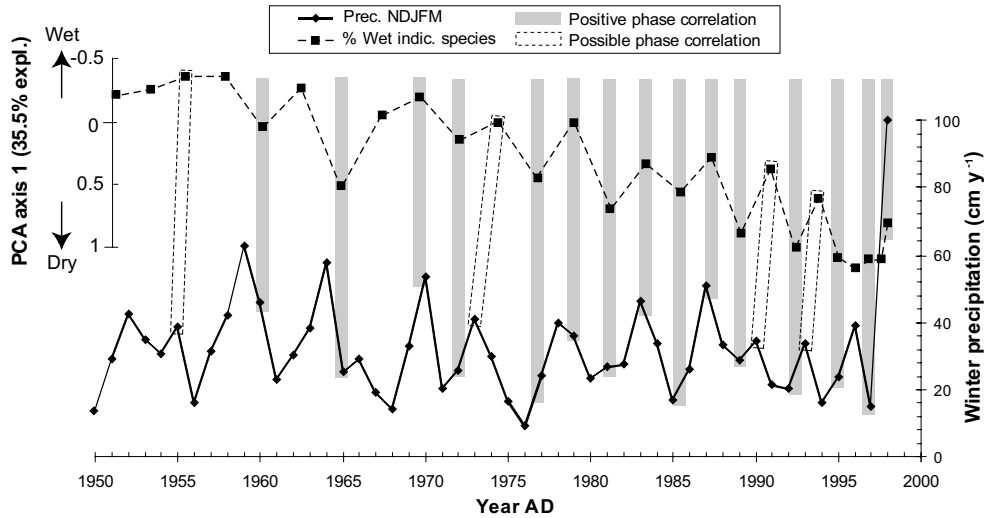
Figure 2.5 Comparison between wet/dry pollen index (PCA 1st axis) of core FAK I98 and annual winter precipitation recorded in nearby Tampa, Fl. Shaded bands indicate a positive phase relation between peaks of precipitation and shifts in the pollen assemblage. Dating uncertainties are about 2-3 years (Chapter 1).

2.5. Discussion

The core top sample contains 60% *Taxodium* pollen, and though it is a dominant feature of the FSPSP vegetation, only approximately 50% of trees are *Taxodium*. The over-representation can partly be explained by the high abundance of tropical plants in the assemblages, which are known to produce low amounts of pollen (Kershaw and Hyland, 1975). *Taxodium* pollen do not disperse very far (Riegel, W.L., pers. comm. 2003) and the relatively closed canopy settings and slow water flow at the site prevent pollen influx from large distances (Birks and Birks, 1980). Consequently, the presented record is predominantly local and must not be compared directly to regional pollen diagrams from large-catchment sites, which present a signal from a much broader, open area (Janssen, 1973). Local effects are normally considered disadvantageous for the interpretation of pollen records. However, since the local water level directly depends on the regional sheet-flow, the observed local vegetation changes can represent a large-scale signal by responding to changes in sheet-flow intensity. The natural drainage pattern has been altered substantially since the early 20th century by construction of levees, canals, the development of the Everglades Agricultural Area, and progressive urbanization (Light and Dineen, 1994). Thus, the drying trend in the pollen data can likely be explained by comparing the timing of the observed changes with man-made alterations of the sheet flow through South-Florida.

The drying in the pollen record starts shortly after the construction and the Tamiami Canal in 1928 (Duever *et al.*, 1986) (Fig. 2.1), which drains large areas in South Florida

and thus increases run off. Construction of the Barron Collier Canal along State Road 29 in 1926 might also have had an impact, however, the canal is shallow and dug in a low-permeable surface. The drying trend accelerates after logging burrows and tramways were constructed between 1947 and 1952 (Burns, 1984). Finally, the completion of the Faka-Union canal in 1972 clearly had an impact by further drying the swamp (Fig. 2.3B). This canal drains the west side of the FSPSP, and lowered the water table from 0.90 to 0.30 m a.m.s.l. (Swayze and McPherson, 1977), although this decrease was in part temporarily. These canals are located within the southwest Florida aquifer and therefore have a direct impact on the FSPSP hydrology (Duever *et al.*, 1986). The water management is obvious from the decrease in Amaranthaceae-type pollen (Fig. 2.2A). Though they occur in dry periods, these annual weeds are characteristic for strongly fluctuating water levels (Willard *et al.*, 2001a), which have been suppressed by the installation of water-control structures.

An 1882 land survey carried out by Florida prospectors describes the area that is now the mangrove-dominated seashore of the FSPSP as:

> '*left unsurveyed, consist*(s) *of salt marsh with a heavy growth of grass, cut up by saltwater layer*(s) *& mangrove*' (Data available on http://www.labins.org).

The area that was surveyed in more detail does not refer to mangrove anywhere else, and only hammocks (tree islands), prairies and swamp are mentioned. Presently, the section of the FSPSP south of Tamiami Trail is dominated by mangrove forest (Fig. 2.1). These changes are consistent with more saltwater intrusion in recent years due to the before-mentioned reduced sheet flow. The historical record thus independently corroborates the changes caused by the water-control structures, and gives additional insight into the original state of the FSPSP wetland.

Within the FSPSP, reconstructed local vegetation appears to accurately reflect variations in regional hydrology. In both Figs. 2.3B and 2.4B the zone FIII samples are consistently related to drier conditions. In the first approach, historical information directly relates the pollen assemblages to past hydrological conditions. The second method compares pollen assemblages with surface samples along environmental gradients, and thus relates the upper samples to a surface sample with intermediate water depth (sites 'Fak9 midB' and '97-10-09-3', Table 2.1). Results of both methods point to a permanent lowering of the water table of between 0.2 and 0.5 m during the second half of the 20th century. Although the human impact in FSPSP is relatively small compared to changes in southeast Florida (Willard *et al.*, 2001a), the ecological information available allows the reconstruction of even these moderate shifts within a fairly accurate range. An entirely quantitative reconstruction is not yet possible, since hydroperiod data are difficult to obtain, but the statistical analysis (CA) of surface and core samples is a valid approach to interpret past vegetation changes in this type of setting.

The high-frequency correlation between the dry/wet index and the winter precipitation shown in Fig. 2.5 indicates a sensitivity of pollen production rates to annual climate

variability. Winter precipitation is the main water supply for the growing season (Burns, 1984), and thus an important parameter. A positive correlation between *Pinus* pollen deposition and precipitation has been observed from pollen trap counts (Willard *et al.*, 2003). *Taxodium,* the main component of the pollen record, favors long hydroperiods for optimal growth conditions (Keeland *et al.*, 1997), likely leading to increased flowering intensity. This relation can offer a mechanism for the observed correlation in Fig. 2.5, analogous to the response seen in *Pinus* (Willard *et al.*, 2003). The observed response can serve as a proxy to detect short periods in increased winter precipitation, which is crucial for ENSO climate reconstruction studies.

The pollen assemblage before AD 1970 is dominated to such a degree by wet-indicating *Taxodium* pollen that short increases in precipitation cannot further change the assemblage (Figs. 2.2A, 2.3A). Therefore, the correlation between winter precipitation and pollen assemblage composition is not visible here. Accurate analysis of single-taxa pollen concentrations might solve this percentage effect. Additionally, slight dating inaccuracies may inhibit the analysis in the early part of the record and although sampling resolution is high, samples contain slightly more sediment than a single year. Generally, the pattern observed from the high-resolution analysis agrees well with a similar study performed by Green *et al.* (1988) on peat material and pollen traps from South-Eastern Australia, which implied that short-term changes in rainfall effect ecological change and are reflected in the pollen record.

2.6 Conclusions

The pattern observed in the pollen data from the Fakahatchee Strand Preserve State Park is consistent with the alterations of water flow in southwest Florida, and thus the local effects of drainage activities and lumbering on Florida wetlands can be clearly defined. The annual variability and decadal trends can be distinguished in palynological analysis on high-resolution, although this can be further improved by using concentration-based pollen data. Such records are crucial for bridging the gap between present-day ecology and paleoecological reconstructions.

The response range of the FSPSP wetland to environmental perturbations on both annual- and decadal-scale documented in this study, allows recognition of natural hydrological changes in older deposits from southwest Florida. Spatial patterns of the vegetation (Spackman *et al.*, 1969; Duever *et al.*, 1986; Myers and Ewel, 1990; Dennis, 1988), and water regime (Gleason, 1974; Burns, 1984) are well studied and, combined with the surface sample data now available (Willard *et al.*, 2001b; this study), variations in past precipitation and sheet flow intensity can be reconstructed and quantified. Since the strength of ENSO accounts for over 50% of the winter precipitation in Florida, the palynological record from FSPSP is highly relevant for studying past El Niño-variability, magnitude and persistence.

Synchronous documentation of atmospheric CO_2 and precipitation signatures in fossil leaf remains

Abstract

It is likely that increased greenhouse forcing has intensified the global hydrological cycle in the second half of the 20th century. The nature and persistence of the link between increasing CO_2 concentrations and climatic extremes are difficult to corroborate in absence of coupled long-term precipitation - CO_2 documentation beyond the range of instrumental measurements. Here a new leaf-morphological paleo-precipitation proxy is introduced, which is based on the analysis of structural xeromorphic features in *Quercus laurifolia* leaves. Lateral leaf epidermal cell expansion is strongly depending on the water availability during the growing season and absolute cell numbers / mm^2 provide a measure of drought stress. Analysis of herbarium material from sites in Florida, were the amount of winter / spring precipitation is depending on the El Niño – Southern Oscillation activity, reveals a significant correlation between the epidermal cell densities and winter precipitation. Continuous time-series from *Q. laurifolia* leafs preserved in peat sequences covering the past 125 years show that epidermal cell densities reflect annual precipitation variability and follow decadal trends in changing winter precipitation.

Furthermore, stomatal frequency analysis performed on the same fossil leaves reveals a distinct CO_2 sensitivity in *Q. laurifolia*. For the first time, combined analyses of CO_2 and drought stress signals in fossil leafs from southern Florida synchronously document changing ENSO-tied precipitation patterns and atmospheric CO_2 concentrations beyond the periodof instrumental measurements.

3.1. Introduction

Continuing greenhouse forcing has intensified the global hydrological cycle in the second half of the 20th century and global average precipitation is expected to increase during the 21st century. By the second half of the 21st century it is likely that precipitation will have increased over northern mid to high latitudes. At low latitudes there are both regional surpluses and deficits over land areas and larger interannual variations in precipitation are very likely over most areas where an increase is projected (IPCC, 2001). One of the major issues in relating observed and projected precipitation anomalies to global warming, however, is the unpredictable response of regional precipitation patterns (Kerr, 2003). To date, the nature and persistence of the link between increasing CO_2 concentrations and climatic extremes are difficult to corroborate in the absence of coupled long-term precipitation - CO_2 data beyond the range of instrumental measurements. The uncertainties in predicting large scale weather situations and the deficiencies in forecasting regional rainfall during specific modes of the main driving weather systems such as the El Niño - Southern Oscillation (ENSO) accentuate the urgent need for long-term documentation of their natural dynamics. Long-term records of past ENSO dynamics are predominantly available from the marine realm and, to a lesser extend, from continental settings (Chapter 8). Despite the high socio-economic importance, detailed records of (paleo-) precipitation, the prime driving force for present and past vegetation dynamics, are still sparse.

Established biological methods utilized so far for precipitation reconstructions include tree-ring and / or pollen analyses. Both proxies, however, are tainted with uncertainties that do not allow unambiguous interpretation of the results in terms of past precipitation changes. While wood-growth is generally a function of multiple environmental parameters (precipitation, temperature), pollen analysis is mainly indicative for changes in vegetation units, a process that reflects longer term trends in hydrological changes rather than high-frequency variability. In exceptional cases, where annual pollen productivity data are available, hydrological conditions can be inferred on a near-annual scale, but quantification of such subtle changes is difficult (Chapter 2).

The general ability of plants, however, to adapt to changes in their environment, including hydrological conditions is well known. Water stress induced occurrence of structural xeromorphic characteristics including thickened leaves, decreased stomatal dimensions and epidermal cells size, is firmly established for a wide variety of plants (Ristic and Cass, 1991; Kürschner *et al.*, 1998; Nevo *et al.*, 2000). Systematic analysis of these anatomical - thus preservable features - from fossil leaf accumulations has the potential to establish a novel paleobotanical approach for recognition of water deficits during the growing season. This drought-stress signal may consequently be interpreted in terms of precipitation fluctuations in geographical areas where hydrological conditions are depending on seasonal rainfall levels.

The distinct leaf morphological adjustment by means of stomatal frequency changes to the human induced atmospheric CO_2 increase is evident for a wide variety of plants and is increasingly used to establish calibration data sets that serve as CO_2 inference models for stomatal frequency data derived from fossil leaf remains (Wagner *et al.*, 2005). High-resolution stomatal frequency based CO_2 reconstructions reveal significant natural

fluctuations during the pre-industrial period of the past millennium (Wagner *et al.*, 2004; Kouwenberg *et al.*, 2005; Van Hoof *et al.*, 2005) which was so far regarded to be relatively stable in terms of atmospheric CO_2 levels (e.g. Etheridge *et al.*, 1996; Indermühle *et al.*, 1999).

Here, initial results are presented of leaf morphological analyses performed on *Quercus laurifolia* from herbarium collections and two near-annually dated peat sequences in the Fakahatchee Strand Preserve State Park (FSPSP) in southern Florida. The oldest section dates back to 1880 (Chapter 1) and thus ranges from the pre-industrial period to the present-day human induced atmospheric CO_2 maximum. The (sub-) tropical southern Florida everglades wetland system is furthermore strongly influenced by ENSO variability, which particularly affects the winter precipitation (Cronin *et al.*, 2002). The precipitation-driven surface sheet-flow across South Florida regulates the hydrological conditions during winter / spring and thus determines the water availability for the vegetation during the growing season (Chapter 2).
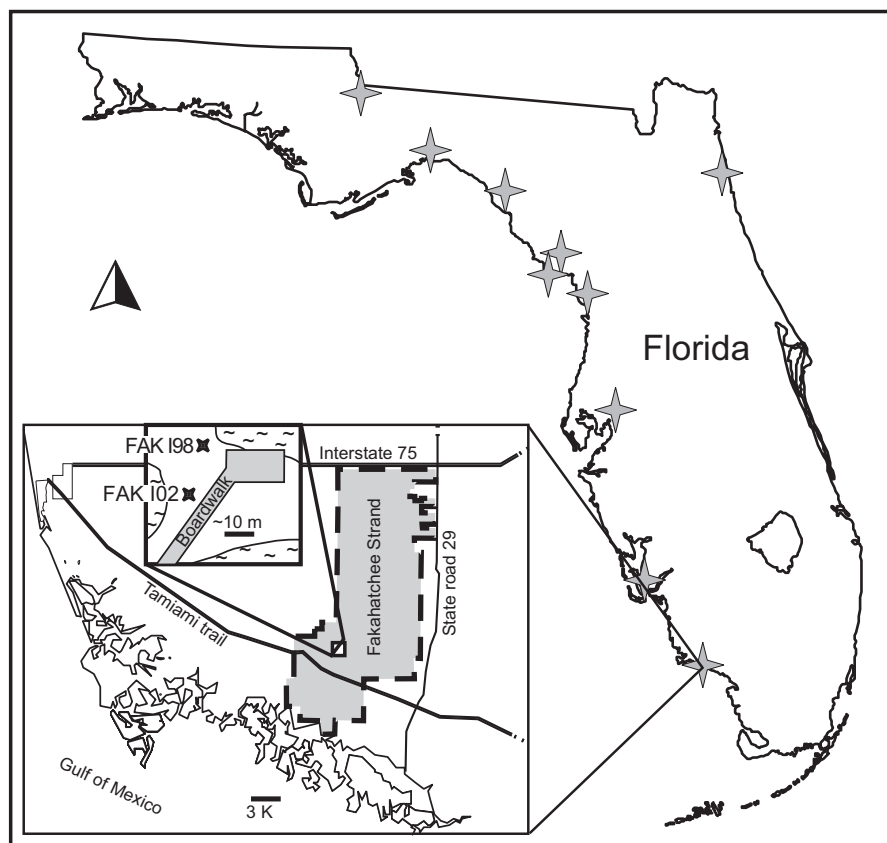
Figure 3.1 Location of the herbarium sample locations and (inset) Fakahatchee Strand Preserve State Park (FSPSP) coring sites in southwestern Florida.

The well-preserved and abundant leaf remains of *Q. laurifolia* in the peat sections are highly suitable to serve as a test case, since a distinct CO_2 responsiveness has already been demonstrated for several other European and N-American oak species (Kürschner *et al.*, 1997; Van Hoof *et al.*, 2005; Wagner *et al.*, 2005). In-situ field studies have furthermore revealed a significant correlation between leaf size in the N-American species *Q. undulata* and precipitation-deficit induced drought stress (Fair and Breshears, 2005). The sensitivity of oaks to both environmental parameters of interest provides the prerequisites needed for analyzing the signatures of drought stress and changing CO_2 concentrations in a single species through time. This study accordingly aims at testing a) the potential CO_2 responsiveness of *Q. laurifolia* and b) to corroborate the concept that precipitation deficits imprint detectable signatures in leaf records. Combined analysis of CO_2 and drought stress signals in fossil leaf remains from southern Florida would provide the first method to synchronously document changing ENSO-tied precipitation patterns and atmospheric CO_2 concentrations.

3.2. Material and methods

A total of 627 herbarium and sub-fossil leaf samples from *Quercus laurifolia* (Laurel oak) were studied for their epidermal properties. The material includes 58 *Q. laurifolia* herbarium leaf samples from the University of Florida Herbarium (FLAS) collection, where 12 years between 1937 and 1998 were available from various locations in Florida (Fig. 3.1). Collection dates of all herbarium samples are later than June to ensure that only fully mature leaves are included in the data set.

The sub-fossil leaf material is derived from two peat cores taken in the Fakahatchee Strand Preserve State Park (FSPSP), south-eastern Florida (25°95'N, 81°49'W, Fig. 3.1) in 1998 (FAK I98; 128 leaf fragments in total) and 2002 (FAK I02; 441 leaf fragments in total). The cores (top 20 cm FAK I98 and total 84 cm FAK I02) were largely composed of accumulated leaf litter. Core FAK I98 was sampled at 1-cm intervals. The age assessment for the sediment core is based on wiggle-match dating with nine AMS ^{14}C dates, providing an age of 1960 AD for the leaf bearing top part of the core (Chapter 1). The improved calibration technique applied to the peat section results in very accurate age-estimates with total errors of maximum 5 calendar years for the post-1950 period (Chapter 1).

Core FAK I02 was sampled in 0.5 cm intervals, ten AMS ^{14}C datings date the base of the core back to 1878 AD (Chapter 1). In this section the combined wiggle-match and ^{14}C bomb-pulse dating approach resulted in an age assessment with accuracies of 5 years in the post-1950 period, and maximum errors of 18 years down-core (Chapter 1).

For microscopic analysis, leaf fragments of approximately 0.5 x 0.5 cm were bleached in 4% sodium hypochlorite solution for a period of between a few minutes and up to 12 h. From the bleached samples the lower cuticles were removed, stained in safranin O, and mounted in glycerin jelly.

Standardized, computer-aided determinations of epidermal parameters were performed on a Leica Quantimet 500C/500+ (Rijswijk, The Netherlands) and an AnalySIS image analysis system (Münster, Germany). Between 3 and 15 leaf remains were analyzed per
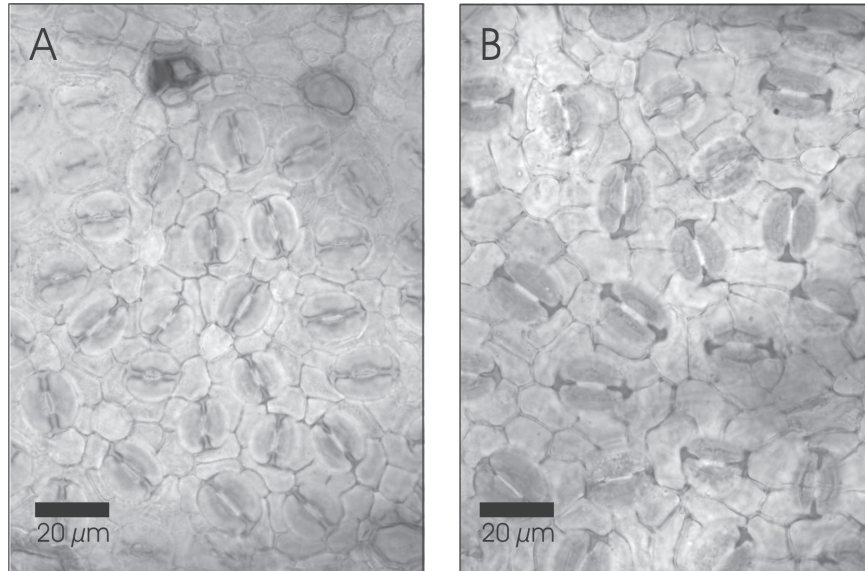
Figure 3.2 Microphotographs of representative *Quercus laurifolia*, Michx. cuticles. A) Cuticle with mean ED = 3995/mm^2 and mean SD = 990/mm^2 (SI % = 19.86) from FAK I02 at 31 cm depth corresponding to the dry year 1976 with 89 mm cumulative NDJFM precipitation. Note single trichomes in upper left and lower left corner; trichomes sparse to moderate on lower cuticles, occurring on veins only. B) Cuticle with mean ED = 2484/mm^2 and mean SD = 603/mm^2 (SI % = 19.53) from FAK I02 at 17 cm depth, corresponding to the wet year 1995 with 297 mm cumulative NDJFM precipitation.

horizon. The following epidermal parameters were determined on 7–10 stomata-bearing alveoles per leaf fragment: epidermal cell density (ED [n/mm²]) and stomatal density (SD [n/mm²]). From SD and ED, the area-independent stomatal index was calculated as percentage stomatal index, SI = [stomatal density/(stomatal density + epidermal cell density)] x 100 (Salisbury, 1927). Historical atmospheric CO_2 concentrations used for calibration are annual means as measured on Mauna Loa since 1952 (Keeling and Whorf, 2003), supplemented by CO_2 measurements from Antarctic ice cores (Siple Station; Neftel *et al.*, 1994). For calibration with precipitation data, instrumental measurements from Fort Myers are used for the sub-fossil material. The herbarium material is compared to the local measurements from the closest meteorological station to the sites the herbarium material originates from. Photographs of representative *Q. laurifolia* cuticles grown under contrasting water availabilities and CO_2 concentrations are depicted in Fig. 3.2.

3.3. Results
3.3.1. Precipitation signal
3.3.1.1. Herbarium leaves
Measured mean epidermal cell densities of the 12 herbarium samples studied are plotted against three different precipitation ranges in Fig. 3.3. No significant correlation was observed between mean ED values and cumulative annual precipitation (Annual: $r = -0.019$; $p = 0.9$) or cumulative summer precipitation (JJAS: $r = -0.247$; $r^2 = 0.06$; $p = 0.4$). A significant negative correlation was observed between mean ED and cumulative winter precipitation with $r = -0.708$, $r^2 = 0.5$ ($p = 0.01$).
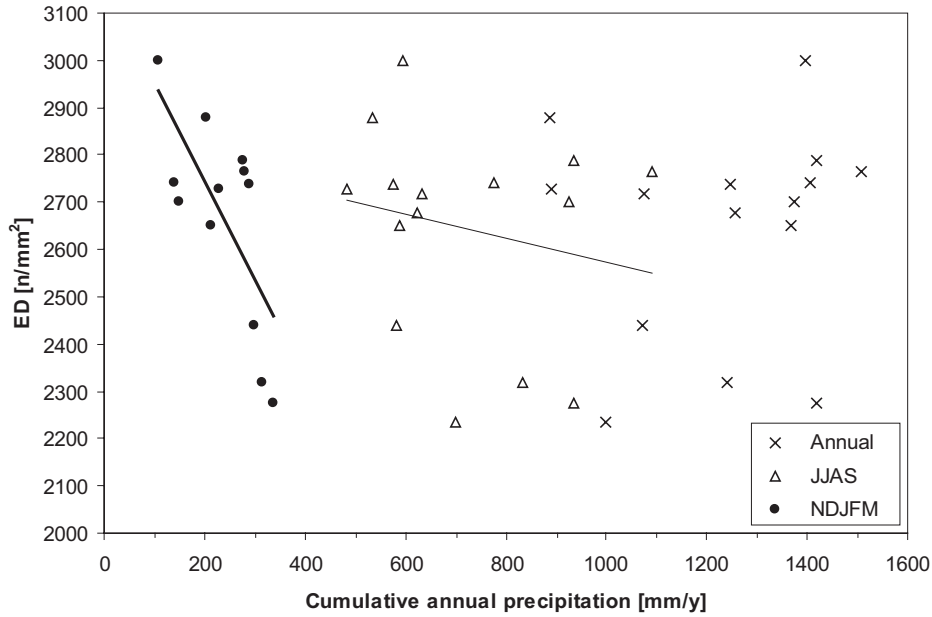
Figure 3.3 Mean ED of *Q. laurifolia* herbarium samples plotted against cumulative precipitation (mm). Crosses are ED against cumulative annual precipitation, triangles are ED against cumulative summer (JJAS) precipitation and black dots are ED against cumulative winter precipitation (NDJFM).
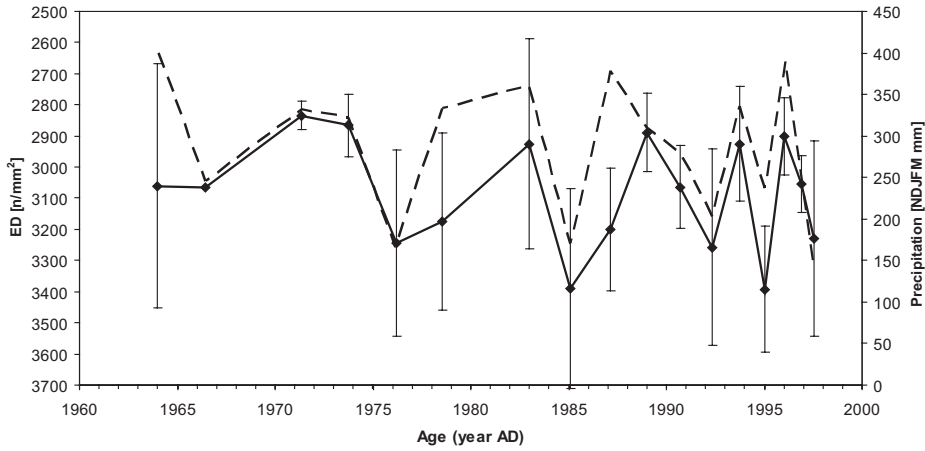
Figure 3.4 ED and cumulative winter precipitation plotted against age of analyzed samples from core FAK I98. Black dots are mean ED±1σ on reversed primary y-axis. Dotted line is cumulative winter precipitation (NDJFM) measured between 1965 and 1998 at Fort Myers, FL (secondary y-axis).

3.3.1.2. Sub-fossil leaves

ED from sub-fossil *Q. laurifolia* leaves preserved in core FAK I98 was measured on up to 12 leaf fragments each in 17 horizons. The ED values are significantly correlated to the cumulative winter precipitation with r = -0.72 (p = 0.001) (Fig. 3.4). ED from sub-fossil *Q. laurifolia* leaves preserved in core FAK I02 was measured on up to 15 leaf fragments per sample from 81 horizons (Fig. 3.5). Age of the sampled horizons from FAK I02 and mean ED±1σ values are given in Table 3.1.
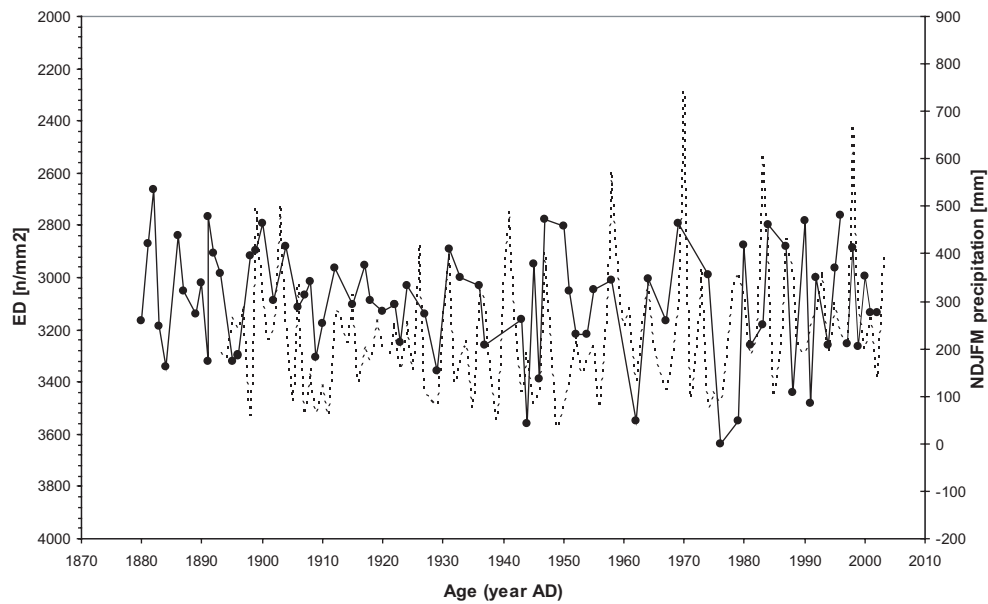
Figure 3.5 ED and cumulative winter precipitation plotted against age of analyzed samples from core FAK I02. Black dots are mean ED on reversed primary y-axis; dotted line is cumulative winter precipitation (NDJFM) measured between 1893 and 2002 at Fort Myers, FL (secondary y-axis).

Table 3.1 Mean ED values and standard deviations for the sampled horizons of core FAK I02. Sample ages are based on the ^{14}C AMS dating of core FAK I02 (Chapter 1).

Age FAKI02	mean ED	±1σ	Age FAKI02	mean ED	±1σ	Age FAKI02	mean ED	±1σ	Age FAKI02	mean ED	±1σ
2002	3132	107	1974	2990	118	1927	3141	101	1896	3300	99
2001	3137	115	1969	2794	99	1924	3031	118	1896	3297	127
2000	2994	126	1967	3167	134	1923	3251	107	1895	3321	82
1999	3263	132	1964	3006	128	1922	3102	103	1893	2983	125
1998	2887	122	1962	3551	131	1922	3102	103	1892	2906	98
1997	3254	106	1958	3012	117	1920	3130	81	1891	2769	97
1996	2761	86	1955	3049	99	1918	3090	140	1891	3323	127
1995	2964	117	1954	3219	123	1917	2954	131	1890	3020	123
1994	3257	101	1952	3218	156	1915	3106	139	1889	3140	105
1992	3001	100	1951	3054	74	1912	2965	121	1887	3054	93
1991	3484	134	1950	2805	122	1910	3178	112	1886	2840	107
1990	2783	144	1947	2778	92	1909	3307	102	1884	3341	118
1988	3440	115	1946	3388	128	1908	3014	118	1883	3187	96
1987	2880	97	1945	2949	107	1907	3066	106	1882	2665	121
1984	2796	93	1944	3561	163	1906	3113	110	1881	2871	107
1983	3182	155	1943	3161	118	1904	2880	109	1880	3163	105
1981	3260	142	1937	3257	111	1902	3088	84			
1980	2876	197	1936	3031	111	1900	2792	80			
1979	3551	133	1933	3002	110	1899	2899	121			
1976	3636	113	1929	3358	111	1898	2919	100			

3.3.2. CO$_2$ response

Atmospheric CO$_2$ responsiveness of *Q. laurifolia* is tested for the sub-fossil leaf material preserved in cores FAK I98 and FAK I02. Fig. 3.6 shows the relationship between SI values of the sub-fossil leaf samples and measured historical CO$_2$ concentrations at the year of growth according to the age assessments of the cores. To account for the non-linear response of SI to changing atmospheric CO$_2$ concentrations, both the SI data and historical CO$_2$ values are log-transformed before fitting a linear response curve through the data set (Wagner *et al.*, 2005). This results in a relation, which can serve as CO$_2$ inference-model for fossil SI values, of CO$_2$ = 10$^{3.7478}$- [0.9598 * log (SI$_{fossil}$)] with r^2 = 0.58 and a root mean square error (RMSE) of 25.21 ppmv CO$_2$.
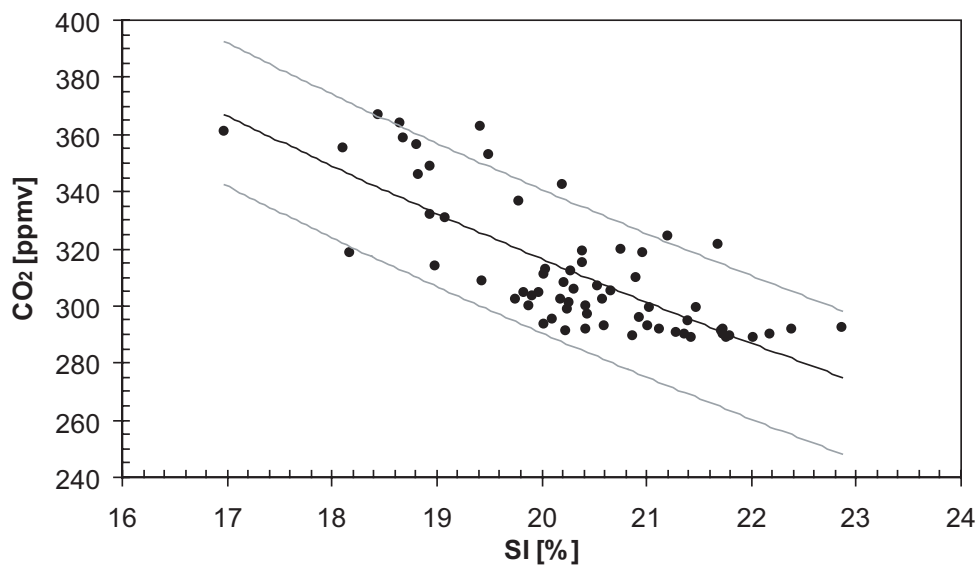
Figure 3.6 Stomatal index response of *Q. laurifolia* from FAK I98 and FAK I02 to changing atmospheric CO$_2$ concentrations over the historical CO$_2$ increase from 295 ppmv to 370 ppmv CO$_2$.

3.4. Discussion
3.4.1. Precipitation signal
3.4.1.1. Herbarium leaves

Quercus laurifolia shows a significant correlation of the leaf epidermal cell numbers with NDJFM precipitation, while no significant correlations are detected between cell numbers and summer or annual precipitation. In warm-temperate to subtropical Florida, the growing season starts between February and March (Vince *et al.*, 1989), and leaf growth in *Q. laurifolia* is completed approximately eight weeks after budburst well before the beginning of the summer wet season. The herbarium data thus strongly support the hypothesis that leaf expansion is depending on the water availablity during the leaf growth period.

Leaf area is a result of initial leaf epidermal cell division and continuing lateral epidermal cell expansion after the cell numbers are fixed in the early stage of leaf growth (Tichá, 1982). Early studies performed on cultivated or annual plants such as *Zea mays*, *Helianthus*, *Polygonum* and *Phaseolus*, have shown that morphological features such as reduced lateral cell expansion and associated stomatal density changes are xeromorphic characteristics associated with the ability of plants to survive under dry conditions (e.g. Penfound, 1931, Oppenheimer, 1960, Ristic and Cass, 1991). Systematic leaf morphological analysis of tree genera important for land-use in arid environments such as olives (*Olea*) or eucalypts have moreover demonstrated in controlled environment experiments that reduced lateral cell expansion, resulting in small epidermal cells, is a typical and well developed response to drought stress in a variety of trees (Bosabalidis and Kofidis, 2002; Li and Wang, 2003). Recent field-studies of morphological responses to precipitation deficit induced drought conditions in leaves of *Quercus undulata*, a deciduous oak widely distributed in south-western North America have shown that leaf area was more than two times larger in water-supplemented plots compared to dry-plots (Fair and Breshears, 2005); although no epidermal cell size measurements are available. Supported by these consistent findings, the significant negative correlation between the number of epidermal cells / mm^2 (used as the reciprocal of absolute cell size) and winter precipitation in *Q. laurifolia* can consequently be interpreted as the development of structural xeromorphic adaptation to limited water supply during the leaf growth season.

3.4.1.2. Sub-fossil leaves

Leaf material from high sediment-accumulation sites in southern Florida was used to test whether the observed responsiveness of *Q. laurifolia* has the potential to serve as a proxy for water availability. In southern Florida laurel oak is an abundant element of the middle canopy layer and leaf fragments are well preserved in the peaty substrate. Determination to species level is possible by cuticle analysis, because the distinct morphological features of the leaf epidermis allow secure identification of even small fragments.

The relationship between ED and cumulative winter precipitation plotted in Fig. 3.4 for the period from 1964 to 1998 shows that the cell frequency, and thus cells size, is closely following the amount of winter precipitation. In this continuous leaf accumulation the correlation between cell numbers and water availability is even slightly exceeds the herbarium study, with r = -0.72 (p = 0.001) compared to r = -0.70 (p = 0.01). However, for

most of the samples relatively high standard deviations are observed. Since sample sizes are large, with up to 15 measured single leaf-fragments, the error source should not be a result of the sampling treatment.

A well known environmental factor influencing lateral epidermal cell growth, is variation in light conditions (e.g. Schürmann, 1959). A distinct development of sun and shade leaf morphotypes has been described for European oaks which show increasing cell size and cell wall undulation under low light intensities (Kürschner, 1997). In the *Q. laurifolia* leaf material studied, no distinct undulation of the cell walls was observed. The majority of leaf fragments possessed epidermal cells with straight walls, which vary in cell size only (Fig. 3.2). Occasionally occurring fragments with significant cell undulation that usually was restricted to the venation, had in advance been excluded from the data set. Although the presence of sun and shade leaf morphotypes in the herbarium training set can not be excluded, the light regime the oaks in the Fakahatchee Strand were exposed to can be considered relatively stable. *Q. laurifolia* is a typical middle storey element and is completely shaded during the growth season by the dense canopy of the *Taxodium distichum* old-growth stand at the sampling site. In suchsettings the development of extreme light related morphotypes is very unlikely.

A clear factor affecting the within-sample variability is the time-span covered per horizon studied. The FAK I98 section has been sampled in 1 cm intervals, which a priory leads to a mixture of at least two consecutive years, since the estimated accumulation rate at this site is 0.5 cm/yr (Chapter 1). Further inaccuracies introduced during the cutting and sampling procedure may lead to even larger pooling of sampled years, and consequently, to the amalgamation of consecutive years with different precipitation levels into one sample. Although the ^{14}C dating-based age-assessment is very accurate and the good fit between ED values and precipitation levels support the reliability of the chronology, the absolute errors prevent to tie the age of the leaf material to single years. Despite the uncertainties, the drought responsiveness first detected in the herbarium material of *Q. laurifolia* is strongly supported by the results of the study on subfossil leaves. Analysis of continuous accumulations of annual leaf shedding from restricted numbers of individual trees has earlier been demonstrated to be a useful approach in proxy validation. Systematic analysis of stomatal frequency in birch leaves preserved in peat deposits from the Netherlands have demonstrated that certain plants possess the ability to adjust the leaf morphology to even small changes in their environment - such as interannual variations atmospheric CO_2 concentrations - with every new leaf generation formed (Wagner *et al.*, 1996). The high value of young sediment accumulations as appropriate test material in proxy-validation is confirmed in the present study.

The assumptions made on the basis of the results from the short FAK I98 core have further been tested on the longer peat section FAK I02, taken only a few meters apart from the FAK I98 sampling point. In order to increase the temporal resolution of the data set, this core has been sampled in 0.5 cm slices, which corresponds to the mean annual accumulation rate of the deposits (Chapter 1). Differences in the compaction of the sediment, especially in the unconsolidated top 15 cm of the core, however, did not allow to analyze leaf fragments on an annual scale. The FAK I02 core moreover was less rich in

Q. laurifolia leaf fragments in the 40 – 25 cm section, which corresponds to the period from 1960 to 1985. Nonetheless, ED frequencies measured in this core again clearly follow the winter precipitation levels and thus replicate the results obtained from core FAK I98. The longer time-span covered in this section, dating back to 1878, furthermore shows that not only discrete events are recorded by the epidermal cell signal, but also decadal trends are clearly reflected.

The precipitation history since 1893 (the period for which instrumental measurements are available) is characterized by considerable annual variability in winter precipitation until 1908, when winter precipitation became very stable for the following 20 years. After 1928, variability increased again and extremely wet years, with cumulative winter precipitation reaching levels of 600 – 750 mm, are known from the instrumental record only from 1960 onwards. ED frequencies closely follow these decadal trends in winter precipitation, where the highest variability, with the most pronounced differences in ED mean values are occurring in the recent decades, while ED remains nearly constant in the core section corresponding to the period between 1908 and 1928. High frequency and magnitude shifts in the period before 1908 parallel the higher precipitation variability measured by instruments and indicate significant annual winter precipitation differences predating the available instrumental record. Instrumental records from the Florida Keys, which are available from 1830 onwards, indeed show highly variable winter precipitation for the late 19th century and thus support the observations based on the ED values measured in FAK I02.

3.4.2. CO_2 response

The capacity to adapt to changing atmospheric CO_2 concentrations via adjustment of the stomatal frequency has extensively been demonstrated for the deciduous European oak species *Quercus robur* and *Quercus petraea* (Van der Burgh *et al.*, 1993; Kürschner, 1996; Van Hoof *et al.*, 2005). In Florida, stomatal frequency analysis of *Quercus nigra* has recently shown that oaks also respond in warm-temperate to sub-tropical areas to changes in atmospheric CO_2 (Wagner *et al.*, 2005). The stomatal index determinations performed on the leaf fragments from the Fakahatchee peat sections confirm that also *Q. laurifolia* adapts to the continuously increasing atmospheric CO_2 concentration by adjusting the number of stomata on the leaf surface. The combined SI data sets from FAK I98 and FAK I02 cover the period from 1880 to 2002 and, thus, the human induced CO_2 increase from 290 ppmv to 370 ppmv.

Although the data set is subject to considerable scatter, 58 % of the variance in the measured SI mean values is explained by the CO_2. The relatively low r^2 value of 0.58 for the CO_2 inference model based on the training set can be explained by a combination of factors. First of all, the CO_2 response in European oaks has been demonstrated to level off at approximately 320 - 330 ppmv CO_2 (Kürschner *et al.*, 1997; Van Hoof *et al.*, 2005). In the data set presented here 25% of the included mean SI values are above this response limit, which is most likely common to not only European oaks but also to North American *Quercus* species since a comparable weak response above 320 ppmv has already been observed in *Q. nigra* data from northern Florida (Wagner *et al.*, 2005). This potential explanation for the scatter occurring in the upper range of CO_2 values, however, does not

sufficiently explain the high variability of SI values in the CO_2 range between 290 ppmv and 330 ppmv.

The potential effects of water availability on the SI are difficult to determine. In the herbarium data no significant correlation with winter precipitation and SI variability (r = 0.02; p = 0.46) is found, while in the sub-fossil material the correlation between ED and precipitation is weak but significant (r = 0.27; p = 0.000). Studies on the effects of different hydrological conditions on the SI in European oaks have not revealed any significant influence of extremely wet and average growing sites in *Q. robur* (Van Hoof *et al.*, 2004). Controlled growth experiments under ambient and high (air) humidity conditions did also not reveal any significant effect on the SI of *Quercus petraea* (Kürschner *et al.*, 1998). Whether the statistical differences between the two *Q. laurifolia* data sets are caused by the better precipitation control in the single site profiles compared to the herbarium data set, or if the effects of water availability on stomatal initiation are on the limits of significance and become only evident in the larger data sets, remains unclear. The effects of interactions between changing CO_2 concentrations and water availability on the SI should be further evaluated in controlled growth experiments.

3.5. Concluding remarks

The results of our study demonstrate that lateral epidermal cell expansion in *Q. laurifolia* is strongly depending on the water availability during the growing season. This structural xeromorphic feature is well preserved and easy to quantify in fossil leaf remains.

The ED signal is sensitive to distinct precipitation anomalies, and thus follows annual deviations in the water availability but also documents trends on decadal time-scales. Analysis of epidermal cell densities in continuous records may provide insight in short-term as well as longer-term dynamics of precipitation changes through time. Although the general trends are well signaled, quantification in terms of absolute precipitation amounts is not yet possible. Controlled growth experiments under various levels of water stress are needed to establish reliable calibration data sets to identify the exact response rates and ranges of the drought sensitivity in *Q. laurifolia*.

The detected CO_2 responsiveness of *Q. laurifolia* is in good agreement with existing stomatal frequency studies performed on other *Quercus* species and provides further evidence that the CO_2 sensitivity is a common feature within this widespread genus. Before used for paleoatmospheric CO_2 estimates, however, the proposed CO_2 inference model needs to be significantly improved by adding modern SI data from alternative sites to evaluate the potential effects of water stress on the SI suggested by the data from the Fakahatchee Strand.

Despite the remaining uncertainties, the approach to jointly detect precipitation changes and time-equivalent atmospheric CO_2 levels on the basis of fossil leaves has the potential to reconstruct pre-industrial precipitation - CO_2 relations far beyond instrumental records.

Botanical proxy time-series indicate stability of the ENSO teleconnection to Florida during the 20th century

Abstract

Two complementary botanical proxies – leaf epidermal cell density and pollen frequencies – analyzed from peat deposits in the wetlands of southern Florida are indicative for changes in the amount of winter precipitation. Because in Florida the El Niño – Southern Oscillation (ENSO) exerts significant control over winter precipitation, the proxy time-series are tested for ENSO sensitivity. The near-annually resolved peat record contains significant variability within the 2-7 year ENSO bandwidth. Bandpass filtering of the data reveals a consistent ENSO signature for the past 125 years.

4.1. Introduction

Land-based paleo-environmental records are essential for understanding the impact of past climate change on the continents. A particular field of interest is the El Niño - Southern Oscillation (ENSO), which has a global impact on terrestrial systems (Van Oldenborgh and Burgers, 2005; Ropelewski and Halpert, 1987). Detailed understanding of past ENSO dynamics is required in order to improve forecasting scenarios and to reconcile paleoclimate data with model output. The ENSO variability is most prominent on inter-annual timescales (McPhaden, 2003), and thus climatic proxy data need to be analyzed with near-annual resolution to detect the 2-7 year ENSO frequency band (Allan, 2000). The main impact of ENSO on terrestrial systems concerns precipitation deficits and surpluses across all continents (Ropelewski and Halpert, 1987). Regions with the most prominent ENSO impact are located within the Indo Pacific Warm Pool (IPWP) (Dai and Wigley, 2000), while most major teleconnections are confined to low-latitude (sub)tropical areas, such as the southern USA (Vega *et al.*, 1998). Terrestrial low-latitude paleoclimate records with sufficient temporal resolution, particularly tree-ring data, are scarce and often obscured by reduced seasonality. Consequently, despite the fact that much work has been done to expand the tropical tree-ring record of ENSO events (Cook *et al.*, 2000), the construction of dendroclimatological records that exceed the period of instrumental observation of ENSO activity is still a challenge (Worbes, 2002).

Apart from variation in tree-ring width, the ability of plants to adapt their leaf-anatomical features to changes in growth environment, including changes in atmospheric CO_2 levels and hydrological conditions, is a powerful trait for documenting past environmental change. It was recently found that precipitation deficits in southern Florida imprint detectable signatures in developing leaves (Chapter 3). In this region water availability for plant growth during spring is largely determined by winter precipitation (Chapter 2). Analysis of herbarium material collected in Florida over the past ~60 years demonstrated that the epidermal cell density (ED) on leaves of *Quercus laurifolia* increases linearly with decreasing winter precipitation. As a corollary of this relationship, fine-resolution ED analysis of *Q. laurifolia* leaves buried in peat deposits formed in the extensive wetlands of southern Florida enables detection of past fluctuations in winter precipitation, including both discrete interannual fluctuations and decadal trends (Chapter 3).

At present, winter precipitation in southern Florida is significantly correlated to the intensity of ENSO (El Niño, La Niña) events (Fig. 4.1A) (Ropelewski and Halpert, 1987; Vega *et al.*, 1998; Cronin *et al.*, 2002). Consequently, ED time-series data may be tested for ENSO sensitivity, thus contributing to accurate reconstruction of the Florida teleconnection.

Complementary botanical evidence of past ENSO activity in southern Florida is provided by pollen records reflecting vegetation responsiveness to changes in water availability. In successive pollen spectra, notably the ratio between pollen types indicative of relatively dry and relatively wet habitats can be used for recognizing changes in ENSO intensity (Chapter 2). In order to assess the stability of the ENSO teleconnection to Florida, the present study investigates the imprint of ENSO variability on near-annually resolved

time-series data of both ED values and pollen ratios obtained from the analysis of a peat core covering the past 125 years (Fig. 4.2B).
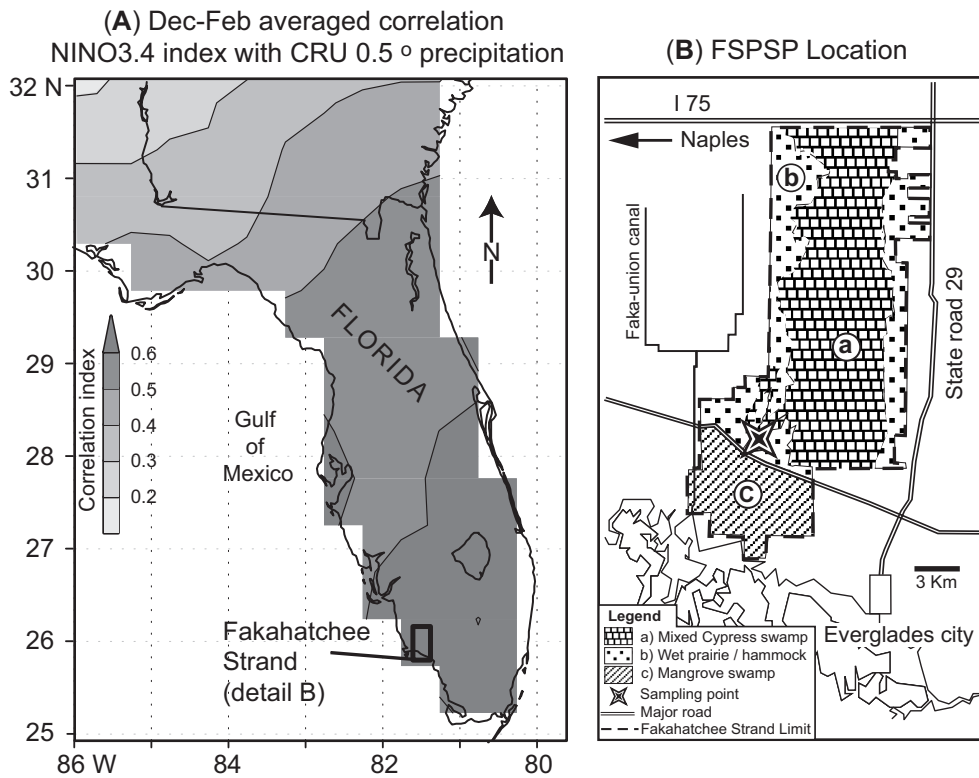
Figure 4.1 (color version on page 132) (A) Location of the Fakahatchee Strand in Florida. Gridded overlay shows average winter (DJF) correlation between precipitation and the NINO3.4 index (performed by KNMI climate explorer, after Van Oldenborgh and Burgers, 2005), based on station data containing >50 years. Note the high correlation in southern Florida (r>0.6, P<0.0001), a region which contains extensive wetland ecosystems. (B) Coring location and the extent and composition of the Fakahatchee wetland.

4.2. Methods

ED analysis of leaf cuticles of *Quercus laurifolia,* and pollen analysis was performed on a peat section from the Fakahatchee Strand Preserve State Park (FSPSP), southwestern Florida (Fig 4.1B). A series of tenaccelerator mass spectrometry (AMS) ^{14}C data was obtained from the 84-cm profile. An accurate chronology was acquired for the past 125 years by performing a combined wiggle-match and ^{14}C bomb-pulse calibration, with an estimated maximum error of ~5 years (Chapter 1). Pollen assemblages were analyzed at 0.5-cm intervals (~1 sample year[-1]); results are displayed as the sample scores of the first axis of a Principal Component Analysis (PCA), which here represents a ratio between pollen types indicative of relatively dry and relatively wet conditions at this locality (Chapter 2). ED analysis was based on leaf fragments collected at ~1-cm intervals (Chapter 3).

59
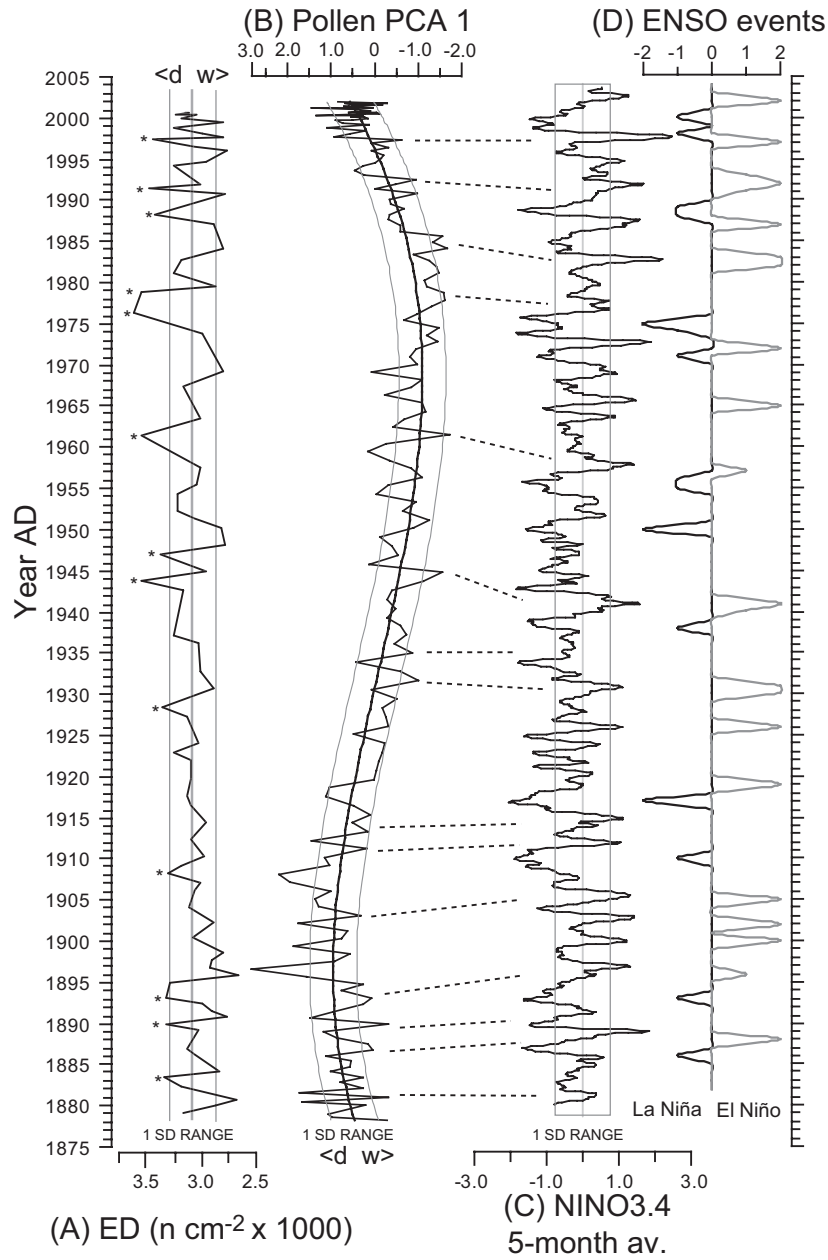
Figure 4.2 Botanical proxy data from the FSPSP peat core compared to ENSO indices. (A) Epidermal density (ED) data from sub-fossil *Quercus laurifolia* leaf remains, expressed as n cells mm^{-2} (Chapter 3). (B) First PCA axis derived from pollen assemblage data (77.5% of total variance explained). SD range envelop calculated on detrended data by fitting 4th order polynomial. Positive anomalies of both curves (A, B) indicate drier conditions during growing season (d=dry, w=wet) (Chapters 2, 3). (C) Five-month running average of NINO3.4 index (Kaplan *et al.*, 1998). (D) ENSO events defined by both the NINO3.4 and SOI indices exceeding the lower (SOI: upper) tercile (± 1) or, during a strong event, exceeding the 20th percentile (± 2) for >4 consecutive months (Smith and Sardeshmukh, 2000). Dashed lines indicate possible correlation of B with C within the age-uncertainty of the proxy data. Y-axis is absolute for C, D and based on an age-depth model (Chapter 1) for A, B.

Proxy environmental data are compared with the NINO3.4 index of SST along the equator in the eastern Pacific, as well as the Southern Oscillation Index (SOI) (Diaz and Kiladis, 1992), the normalized pressure difference between northern Australia and Tahiti. However, small dating uncertainties may impede direct correlation between proxy data and standard ENSO indices. Therefore, ENSO forcing was also assessed by means of Blackman-Tukey spectral analysis and bandpass filtering of the time-series data (Blackman and Tukey, 1959; Paillard *et al.*, 1996).

4.3. Results and discussion

Limited by the availability of leaf material, ED analysis on 82 samples shows 13 ED peaks above the 1σ range between 1879-2001 (Fig. 4.2A), which is equivalent to ~19 years at annual resolution (Table 4.1). In this period 16 La Niña years have actually occurred, defined by both the NINO3.4 (Fig. 4.2C) and SOI indices exceeding the lower (SOI: upper) tercile for >4 consecutive months (Fig. 4.2D) (Smith and Sardeshmukh, 2000). Also the pollen record (Fig. 4.2B) over-estimates La Niña occurrence, while El Niño phases remain slightly under-represented (Table 4.1). Most likely la Niña-induced dry periods have a greater impact on the wetland ecosystem in Florida.

# Samples	# La Niña	# El Niño	Years > ENSO def.
82	13	13	Leaf ED
167	29	27	Pollen PCA 1
122	16	22	NINO3.4 + SOI
Corrected for sample spacing:			
122	19	19	Leaf ED
122	21	20	Pollen PCA 1
122	16	22	NINO3.4 + SOI

Table 4.1 Top panel shows the amount of La Niña / El Niño years recorded by the proxies (value exceeding 1ό) and the actual occurrence ENSO anomalies between 1879-2001 (see Fig 4.2). Lower panel shows expected number of events corrected for differential sample spacing between the proxies and instrumental time-series data.

NINO3.4 time-series power spectra (Fig. 4.3A) show the prominent ENSO variability between 2-7 years, with a triplet of sharp peaks between 2-4.5 years, and a wide peak around ~5.5 years. Spectral analysis of the proxy environmental data (Figs. 4.3B, C) reveals highly similar variability within the ENSO-band. Especially the pollen data contain the prominent ENSO pattern, although the periods do not exactly match the NINO3.4 spectrum. The ED series has a lower data resolution and, therefore, does not contain the 2-3 year signal, but the remaining periods match the ENSO signature very well. Bandpass filtering of the most significant spectral peaks reveals the temporal distribution of the signal (Figs. 4.3D-F). Both the NINO3.4 and the pollen data show a continuous signal of ~5.5 years throughout the entire record. However, the ~2.7 cycle in the pollen data is not always present with the ~2.8 cycle NINO3.4. Besides lowering the water levels, extensive water-control structures implemented after 1930 have resulted in less variable water levels in the Florida wetlands (Chapter 2). The water management may have dampened the high-frequency variability in the proxy datat on bi-annual timescales. A moderate increase of the signal after 1990 reflects the recent restoration efforts that partly restored the dynamic water regime of the pre-drainage period (Sutula *et al.*, 2003).

The filtered ED data demonstrate prominent ~5.5 year-cyclicity. Although somewhat reduced in the lower-resolution middle part of the record, the cycles show amplitude variability very similar to the NINO3.4 'input' signal. Unlike the ED data, the periods from the pollen-spectra slightly deviate from the NINO3.4 signal. The lagged response of
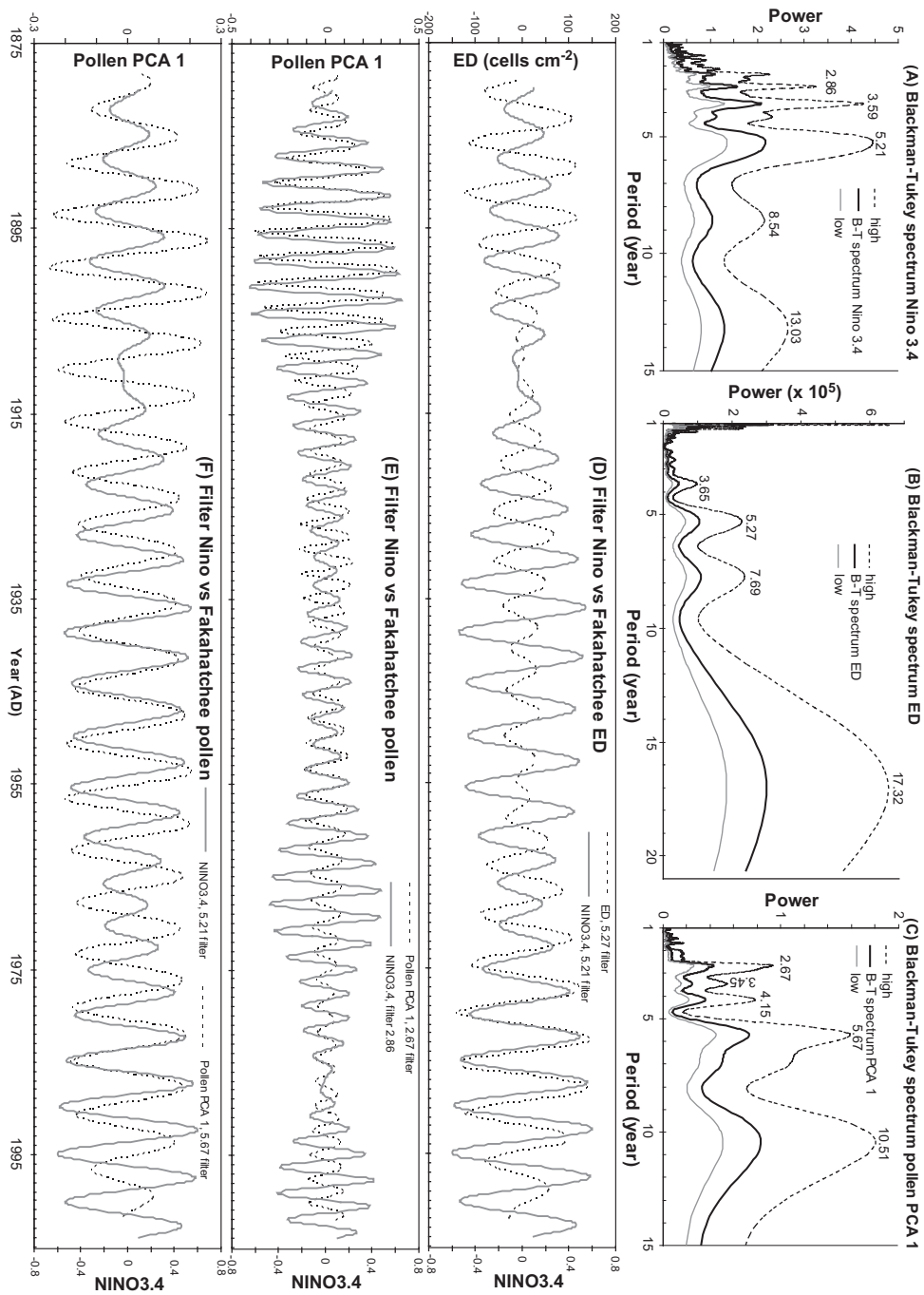
Figure 4.3 Blackman-Tukey spectra from the NINO3.4 index (C) and proxy time-series data (A, B) calculated with Analyseries 1.1 (Paillard *et al.*, 1996). Envelop shows 80% confidence interval. Based on these spectra, the most prominent peaks were bandpass-filtered data at ~5.5 years (NINO3.4 with ED [D] and NINO3.4 with pollen [E]), and ~2.7 years (NINO3.4 with pollen [F]). Prior to spectral analysis, all data were detrended and re-sampled at a constant interval.

pollen productivity to climate variations (Willard *et al.*, 2003) might cause these offsets. Alternatively, offsets can be explained by the dating uncertainties, but the effect is likely limited since the main ED and NINO3.4 periods match very closely.

Periodicity >7 years seems stronger in the proxy data than in the NINO3.4 and has periods that deviate considerably. Consequently, the associated variability is most likely not related to ENSO forcing. Instead, other climate factors, such as the Pacific Decadal Oscillation (PDO) (Cronin *et al.*, 2002) or species-dependent growth dynamics may have been responsible for these patterns.

The presented record confirms the sensitivity of botanical proxies to high-frequency climate variability. As shown by spectral analysis, time-series data reveal the cyclic ENSO signature in remarkable detail, even though a peat sample cannot be regarded as a discrete layer corresponding to a single-year. The ENSO system seems to exert strong control on the Florida wetland vegetation, even though mainly the winter precipitation is affected (Ropelewski and Halpert, 1987; Vega *et al.*, 1998). Since ENSO-modulated winter precipitation is relatively reduced with respect to abundant summer rain, it is likely to be a controlling factor, extending or reducing the annual hydroperiod (inundation length), which is a highly important parameter for plant growth (Chapter 2). The atmospheric teleconnection between the tropical Pacific and the southern USA, which responsible for the influence of ENSO in that region (Vega *et al*, 1998), is apparently a stable feature of the Florida climate during the past 125 years, even though some decadal signal is present (Figs, 4.2B, C) that possibly modulates the ENSO teleconnection strength (Cane, 2005).

4.4. Concluding remarks

The present results provide a method to detect the high-resolution ENSO signal in natural environmental archives, which, unlike tree-ring studies, can also be applied in tropical regions. This allows the detailed reconstruction of ENSO variability in periods for which no instrumental data are available. Spectral analysis of high-resolution ED and / or pollen records with sufficient time-control, would allow direct testing of the reduced mid-Holocene ENSO hypothesis (Clement *et al.*, 2000, Chapter 5) in geographically widely separated regions. In non-varved sediments, wiggle-match dating and micro-tephra chronology (Blaauw *et al.*, 2003; 2004, Blockley *et al.*, 2005) may provide the chronological control needed to implement such studies.

Furthermore, this method can help to resolve the long-term effects of decadal fluctuations in Pacific pressure (PDO) (Deser *et al.*, 2004), which may have a similar environmental impact as ENSO and apparently modulates ENSO teleconnection strength (Cane, 2005).

Middle to late Holocene
El Niño - Southern Oscillation dynamics
reflected in the subtropical terrestrial realm

Abstract

High resolution pollen analysis of middle to late Holocene peat deposits from southwest Florida reveals a stepwise increase in wetland vegetation that points to an increased precipitation-driven fresh water flow during the past 5, 000 years. The tight coupling between winter precipitation patterns in Florida and the strength of the El Niño - Southern Oscillation (ENSO) strongly suggests that the paleo-hydrology record reflects changes in ENSO intensity. A terrestrial subtropical record outside the Indo-Pacific

Warm Pool both documents ecosystem response to the known onset of modern-day ENSO periodicities, between ~7, 000 and 5, 000 years BP, and subsequent ENSO intensification after 3, 500 years BP. The observed increases in 'wetness' are sustained by a gradual rise in relative sea level that prevents a return to drier vegetation through natural succession.

5.1. Introduction

Intensification of the El Niño - Southern Oscillation (ENSO) in the mid-Holocene, between ~7 and 5 thousand years (ky) BP (ages in calendar years unless stated otherwise) (Rodbell *et al*, 1999; Koutavas *et al.*, 2002), is thought to mark the onset of modern-day precipitation patterns in low-latitude regions. Proxy records of climate change indicate that the increased amplitude of ENSO variability had a clear impact on regional hydrological budgets of tropical parts of the Indo-Pacific region, South-America, and Africa (Shulmeister and Lees, 1995; Gagan *et al.*, 2004; Marchant and Hooghiemstra, 2004). Because the mode and intensity of ENSO varied with the orbital precession during the Holocene (Clement *et al.*, 1999; 2000), the solar radiation budget is likely to have influenced global hydrological patterns. However, data on extra-tropical ENSO variability are still limited. Yet, the existent modern ENSO teleconnections imply that Holocene changes in precipitation must have had an impact on a much larger scale. As human-induced global warming progresses, it is crucial to understand to what extent the hydrological cycle has been altered by prominent climate systems such as ENSO. Here, the middle to late Holocene development in hydrological conditions is documented in South Florida, a subtropical area characterized by a strong ENSO teleconnection, to recognize changing precipitation patterns that can be used as indicators of long-term ENSO dynamics outside the tropical Pacific.

The Florida peninsula is strongly influenced by ENSO variability, which particularly affects the winter precipitation (Ropelewski and Halpert, 1987; Cronin *et al.*, 2002; Viles and Goudie, 2003). Precipitation-driven surface sheet flow across South Florida determines water availability during winter/spring, which largely controls the composition and growth conditions of the vegetation (Burns, 1984; Duever *et al.*, 1986). Because of the dependence of local plant growth on the ENSO system, identification of past changes in local wetland vegetation can elucidate past ENSO activity. This study presents a detailed record of vegetation change based on pollen analysis of a radiocarbon-dated peat core from a forested wetland in Southwest Florida.

Wetland areas extremely sensitive to hydrological perturbations have expanded vastly since ~5 ky BP across subtropical South Florida (Gleason and Stone, 1994). The expanse has partly been attributed to continuing relative sea level rise, which reduced the gradient from the Florida aquifer to the coast and, thus, caused wetter soil conditions toward the sea. However, peatland formation in slightly elevated inland areas has likely been caused by increased precipitation (Gleason and Stone, 1994; Winkler *et al.*, 2001). So far, vegetation and climate history studies in southern Florida have been restricted to the Lake Wales Ridge region in south-central Florida, the Everglades, and adjacent water conservation areas (Spackman *et al.*, 1966; Grimm *et al.*, 1993; Watts and Hansen, 1994; O'Neal *et al.*, 2001; Willard *et al.*, 2001a) (Fig. 5.1). Holocene Lake Wales Ridge pollen records display small centennial variations during the past 5,000 radiocarbon years (Watts, 1975; Grimm *et al*, 1993) and do not show a large response to ENSO forcing. However, these records are derived from a relatively dry upland area on permeable carbonate soil, which does not retain the winter precipitation (Myers, 1990). Thus, water is not stored and cannot influence plant growth during the growing season. In contrast, the organic wetland soils south of Lake Wales Ridge support vegetation adapted to continuous moist

conditions, which is therefore strongly controlled by winter precipitation. Hence, South-Florida wetlands provide an ideal setting for reconstructing past ENSO dynamics.
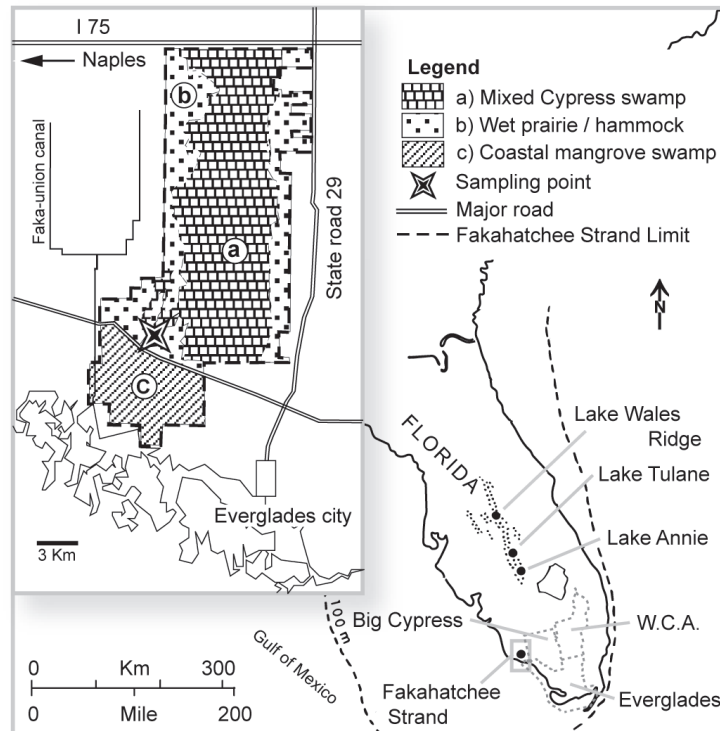
Figure 5.1 Location of the Fakahatchee Strand State Preserve Park (FSPSP, *Inset*) in southwest Florida. Main vegetation units and coring location are indicated in relation to previously studied sites in Florida.

The Big Cypress Swamp ecosystem, an extended forested wetland in southwestern Florida, was selected as study area. A section of this wetland, the Fakahatchee Strand Preserve State Park (FSPSP, 25°95'N, 81°49'W, Fig. 5.1), contains an elongated, wide, and shallow dissolution structure (slough) underlain by the more impermeable, slightly elevated Tamiami Formation (Spackman *et al*, 1966). The low-energy, moist conditions in the slough allow peat formation. The FSPSP present-day ecology has been well studied, and it has been demonstrated that the wetland vegetation is highly sensitive to hydrological changes (Chapter 2, 3). For this study, an undisturbed deposit from the FSPSP *Taxodium* (cypress) swamp has been subjected to palynological investigation (Fig. 5.1). A surface sample data set that covers environmental gradients (Chapter 2; Willard *et al.*, 2001b), water depth/hydroperiod, salinity, and bedrock type, is used here to interpret changes in the FSPSP pollen record.

The FSPSP record will clarify whether pronounced variation in winter rainfall occurred during the middle to late Holocene and help to further elucidate past ENSO variability and its impact on areas outside the tropical Pacific.

5.2. Materials and methods

The FSPSP consists of a forested *Taxodium distichum* (bald cypress) swamp with a long hydroperiod, surrounded by more seasonally inundated hardwood-hammock and wet-prairie vegetation. The peat deposit located in the main slough of the FSPSP was cored in the winter of 1998 with a modified Livingstone corer (Fig. 5.1). The lowermost 5 cm of the 195-cm sequence consists of coarse sand containing some peat fragments, gradually becoming sandy peat and finally dark, organic rich, homogenous fine peat. The top ~25 cm was not consolidated and contained identifiable plant remains. The core sections were subsampled every 4 cm for both pollen analysis and loss-on-ignition (LOI). Pollen samples were prepared by following standard palynological peat processing techniques (Faegri *et al.*, 1989). Pollen and spore identification (~300 grains per sample with a maximum of five slides) was based on the reference collections of the U.S. Geological Survey (Reston, VA), and the Laboratory of Palaeobotany and Palynology, Utrecht, The Netherlands, and reference works by Jones *et al* (1995; 1999) and Kapp *et al* (2000).

All pollen diagrams were made with Tilia/Tiliagraph 2.0.b.5 (Grimm, 1991–2001). Due to closed-canopy setting of the site, all taxa are inside the pollen sum because the local changes are used to reconstruct the hydrology of the area. To identify pollen zones in the record, a stratigraphically constrained cluster analysis was performed. The samples were numerically zoned by using optimal sum-of-squares partitioning (Birks and Gordon, 1985) as implemented in the program zone (Lotter and Juggins, 1991). The significant number of stratigraphic zones was assessed by using the broken stick model (Bennett, 1996).

Peat material from 14 horizons was radiocarbon dated by accelerator mass spectrometry (AMS). To assess possible contamination by younger rootlets, one horizon (at 9 cm depth) was AMS-dated by using both bulk peat and macro leaf remains (Table 5.1). Radiocarbon data were calibrated with OXCAL 3.9 calibration software (Bronk-Ramsey, 1995; 2001), which uses the INTCAL98 calibration curve (Stuiver *et al.*, 1998) and provides output as a probability density function (PDF). With the prior assumption that samples are ordered

Table 5.1 AMS ^{14}C-dated horizons in FAK III98, FSPSP, Florida. All samples are bulk peat, except sample 9.5 a (*Taxodium* sp. leaflet) to assess reservoir effect between peat and macrofossils. Calibration performed with Oxcal 3.9 with prior assumption of chronologically ordered samples. [*] Samples calibrated with 20th century bomb carbon anomaly (Chapter 1). [†] Considered to be an outlier, excluded from age-depth model. UtC = R.J. Van de Graaff laboratory, Utrecht University.

UtC #	Depth (cm)	$\delta^{13}C$ (‰)	[14]C age ± 1σ (year BP)	Cal age ± 1σ (year BP)
12258	9.5 a	-30	-1729 ± 29	-29.5 ± 6 [*]
12257	9.5 b	-28.1	-1703 ± 29	Excluded
12256	18	-28.4	-1062 ± 30	-10.5 ± 6 [*]
12255	31	-27.9	104 ± 33	150 ± 120
12254	45	-28.3	447 ± 31	502 ± 20
12253	56	-29	936 ± 33	805 ± 65
12252	70	-28.2	850 ± 35	860 ± 50
12251	80	-27.8	650 ± 35	608 ± 48 [†]
12250	90	-28.2	1792 ± 45	1720 ± 100
12249	100	-28	2729 ± 37	2813 ± 38
12248	110	-27.8	3468 ± 37	3740 ± 90
12109	119	-28.5	3719 ± 36	4010 ± 80
12247	140	-28.1	3719 ± 38	4085 ± 65
12246	160	-28.4	4169 ± 38	4700 ± 120
12110	180	-28	4290 ± 60	4850 ± 120

chronologically, a Bayesian statistical function within the program reduces the PDFs of overlapping radiocarbon data (Bronk-Ramsey, 2000). Subsequently, the reduced 1σ intervals were used for construction of the age-depth model (Table 5.1 and Fig. 5.2).

Age-depth FAK III98
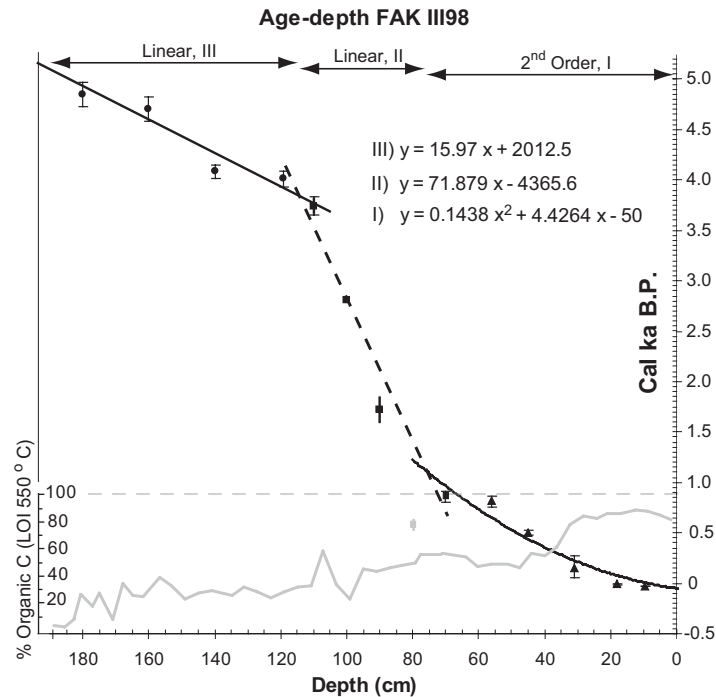
Figure 5.2 Age-depth relationship and Loss-On-Ignition (LOI) results for the FSPSP sediments. Arrows indicate where different models were applied. ▲, radiocarbon ages used in model I; ■, ages in model II; ● ages in model III. Date at 80 cm depth (in gray) has been excluded from models (see Table 5.1).

A semiquantitative technique is available for reconstructing paleohydrology by identifying the closest modern analogue from different vegetation units across hydrological and salinity gradients (Willard *et al.*, 2001a). To describe the main trend and interpret observed changes within the fossil samples, the data were compared with the surface samples by means of a correspondence analysis (CA, Fig. 5.5), thereby closely related samples could be identified. A study on subfossil peat from the FSPSP showed that the technique accurately detects documented hydrology changes that occurred in the 20th century (Chapter 2).

5.3. Results
5.3.1. Chronology
The trend in organic matter content indicates several stages of peat decomposition and, consequently, some changes in apparent sedimentation rate are expected. The prior assumption of chronologically ordered samples in the OxCal calibration procedure significantly reduced several calibrated age ranges (Table 5.1). One sample was considered an outlier and was excluded from the set. Its position on the end of a core section might indicate contamination with younger material during coring.

The ^{14}C ages on both bulk peat and macro remains are effectively identical (Table 5.1), which indicates that the use of bulk peat for dating is justified. However, contamination with small rootlets cannot completely be excluded for the lowermost ^{14}C data (Fig. 5.2), but this conclusion has to be confirmed. Based on the radiocarbon data, an age-depth curve was constructed by plotting a different (simple) models through three data subsets (Fig. 5.2). The lower two sections are described well by a linear model. A second-order model is used for the uppermost part, because gradual decomposition clearly influenced the compaction rate, which is in accordance with earlier radiocarbon data from the site (Chapter 1).

The basal age of the profile is ~5.2 ky BP, which is the base of the peat. The second (II) model clearly shows a reduced accumulation rate between 1.2 and 3.8 ky BP, roughly equivalent to pollen zone FII (Fig. 5.3, see below). Models I and III have a broadly comparable high accumulation rate, which is promising for further high-resolution studies on selected time windows during the mid-Holocene.

5.3.2. Vegetation development.

Both the major pollen groups and associated vegetation units indicate significant change over the past 5 ky (Fig. 5.3). The pollen assemblages were divided into three zones based on the output of optimal sum-of-squares partitioning (Birks and Gordon, 1985). The prime feature of the pollen diagram is the turnover between *Pinus cf. elliottii* (slash pine, presently the only naturally occurring *Pinus* in southeast Florida, Little, 1971) and *Taxodium* sp. (bald cypress). *Pinus cf. elliottii* prevails in zone FI but is gradually replaced during zone FII by *Taxodium* sp., which eventually dominates in zone FIII. Second, significant change of dynamics between zones characterizes the succession. The *Pinus* phase is characterized by large fluctuations from low (20%) to high (70%) values in alternation with *Salix caroliniana*-type (Carolina willow), whereas the *Taxodium* sp. high phase is far more stable.

These changes are the most pronounced features of composition shifts in entire plant communities. In zone FI, *Pinus-Salix* phases occur with low, but significant, abundances of wet prairie vegetation elements, notably Asteraceae and Amaranthaceae-type, *Ambrosia* sp., *Sagittaria* sp., and Poaceae and Cyperaceae (grass and sedge) pollen (Fig. 5.3). In zones FII and FIII, the wet prairie elements gradually decrease in favor of hardwood trees associated with *Taxodium* swamps (*Fraxinus caroliniana*-type, *Acer rubrum*, *Quercus* spp.) and fern understory elements. Additionally, abundant 'Type 182' spores in zone FIII are indicative of wet conditions (Van Geel *et al.*, 1983).

The apparent *Taxodium* sp. peak at 181 cm is not considered representative because the sample counting sum is very low, resulting in underestimation of large pollen types like *Pinus* (Birks and Birks, 1980). The lowermost samples appear to be slightly different, with above-background levels of *Quercus* spp. and nearly 20% Asteraceae followed by short peaks of fern abundance.

Figure 5.3 (Right page, color version on page 133) Pollen percentage diagram of FAK III98 displaying taxa with a minimum abundance of 2% and/or five occurrences. White bars represent exaggeration (factor 5) to visualize variations in low-abundance taxa.

Pollen percentage diagram FAK III98, selected species
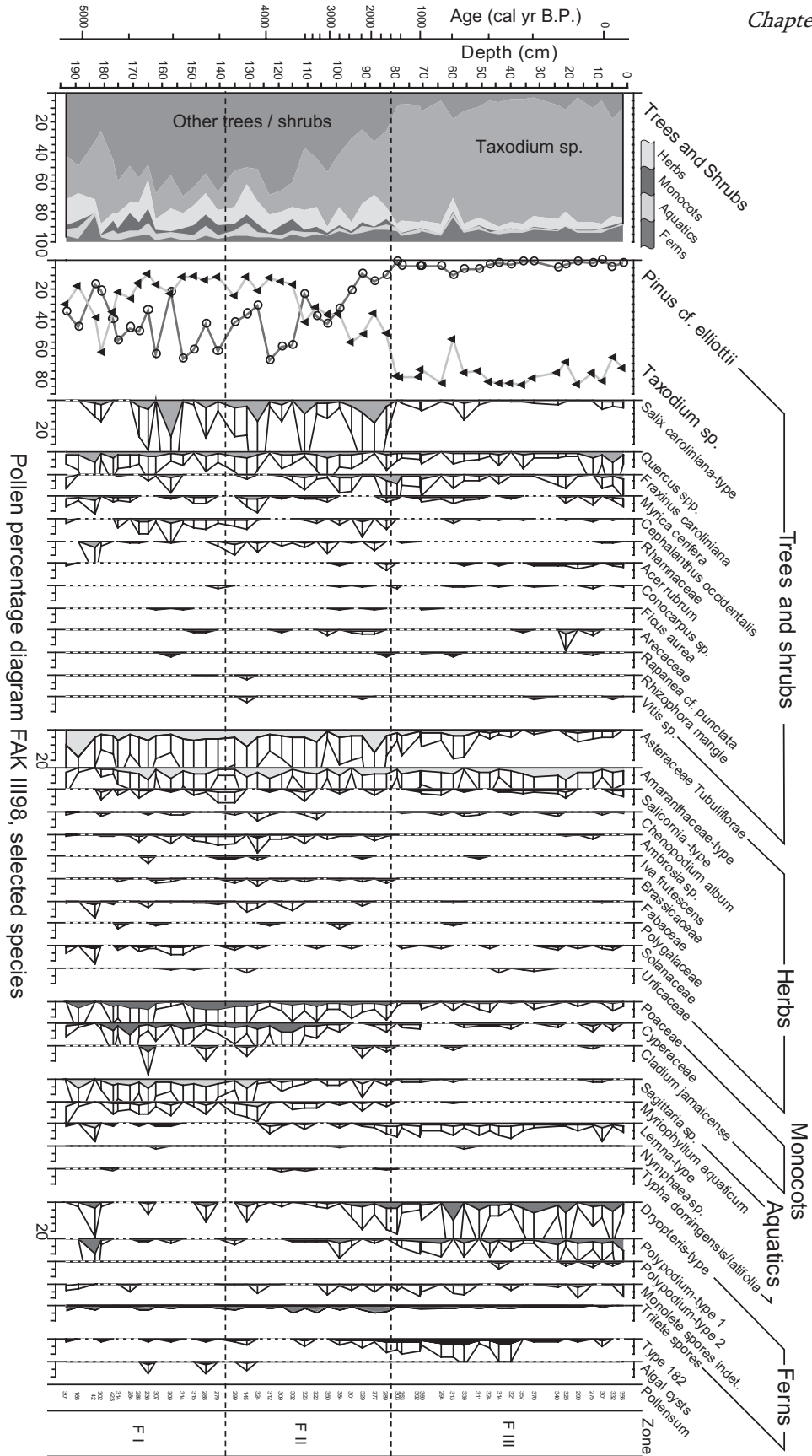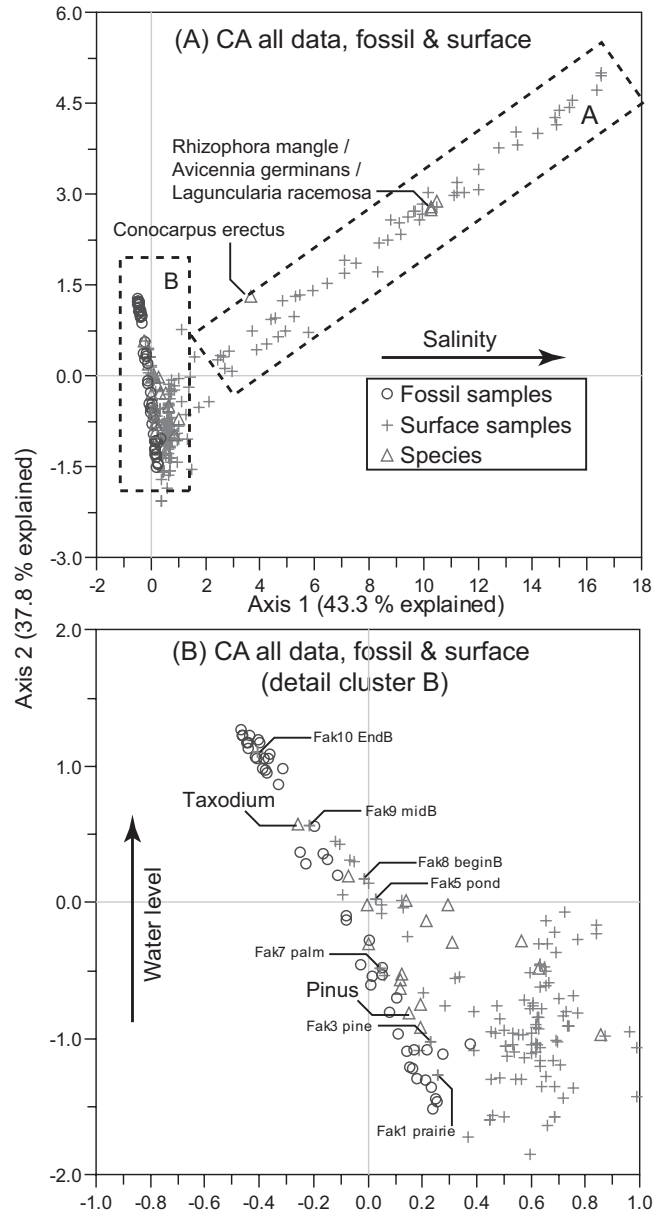
Figure 5.4 The relation of surface sample data (Willard *et al.*, 2001b, Chapter 2) to fossil samples from the FSPSP based on a correspondence analysis of all data (**A**), carried out with C[2] 1.3 software (Juggins, 2003). The dashed areas represent the main gradients within the data. Cluster B in detail (**B**) shows that the fossil samples are distributed along a shallow- to deep-water transect (Fak1–10, Chapter 2). The gradients (arrows) have been interpreted by using ecological descriptions of the different taxa, the main elements of which are indicated.

Clearly, short fluctuations are present but there is no long-term change within zone FI. The assemblage change within zone FII is not unidirectional but exhibits stepwise increases interrupted by stable and regressive phases. The peaks of wet-tolerant *Salix* of up to 20% are mostly short, and no further succession occurs. Only at the FII/FIII zone boundary ~1.3 ky BP, *Salix* is followed by relatively high abundance of *F. caroliniana*-type (~5%) after which *Taxodium* sp. pollen fully dominates the assemblage.

5.3.2. Trends and vegetation units

Both fossil and all available surface samples are plotted together in a CA biplot (Fig. 5.4A). Samples in close proximity are interpreted as similar in composition. In particular, the FSPSP surface samples (marked 'Fak1–10') (Chapter 2) clearly overlap the entire range of the 'fossil' cluster (Fig 5.4B).

Based on the distribution of taxa, a relative environmental gradient can be assigned to both axes. Cluster A is characterized by high abundances of mangrove taxa at one end (high salt/deepwater tolerant *Rhizophora mangle*, *Avicennia germinans*, and *Laguncularia racemosa* and brackish water tolerant *Conocarpus erectus*) and salt to fresh marsh taxa on the other (Spackman *et al.*, 1966, Willard *et al.*, 2001b). The gradient is mainly an indication of salinity (O'Neal *et al.*, 2001), which is a very important parameter in Florida coastal wetlands. However, a water-depth factor is clearly influencing the distribution as well, because mangroves, in contrast to wet prairies, do not experience seasonal drying and can grow in relatively deep water.

The fossil samples in cluster B are spread around a gradient of relatively dry toward wet-tolerant taxa (Chapter 2; Ewel, 1990; Kushlan, 1990; Willard *et al.*, 2001b). Little variation is present along the x-axis, indicating salinity among the fossil samples is not a major influencing factor. Spread of taxa along the CA axes allows interpretation of the trend curve, even for samples with no clear modern analogue, and, therefore, it is a good index of hydrological conditions.

In the calculation of the trend curve (Fig. 5.5B), cluster A was eliminated because it does not represent the conditions in the fossil samples. Consequently, the wet-to-dry gradient in Fig. 5.5B is the first axis from the CA analysis of the reduced data set. Apart from a sign switch, this reduction does not alter the CA results.

Based on the identification of similar surface samples, each phase in the pollen record is coupled to a vegetation unit, which confirms a stepwise development from wet prairie to swamp forest (Fig. 5.5C). The main variability occurs in zones FI and FII. However, in zone FIII a short decrease in *Taxodium* sp. is evident ~750 yr BP, and values are clearly reduced in the 20th century, which is in accordance with recent drainage activities (Chapter 2).

Although fire is an important factor in Florida ecosystems (Duever *et al.*, 1986), no fire events (indicated by charcoal particles or sudden peaks of fern abundance) have been recorded. Possibly, the site was moist enough to prevent fire to penetrate, yet it remains

unclear how fire can seem virtually absent throughout the entire record, in particular during periods with prairie vegetation.
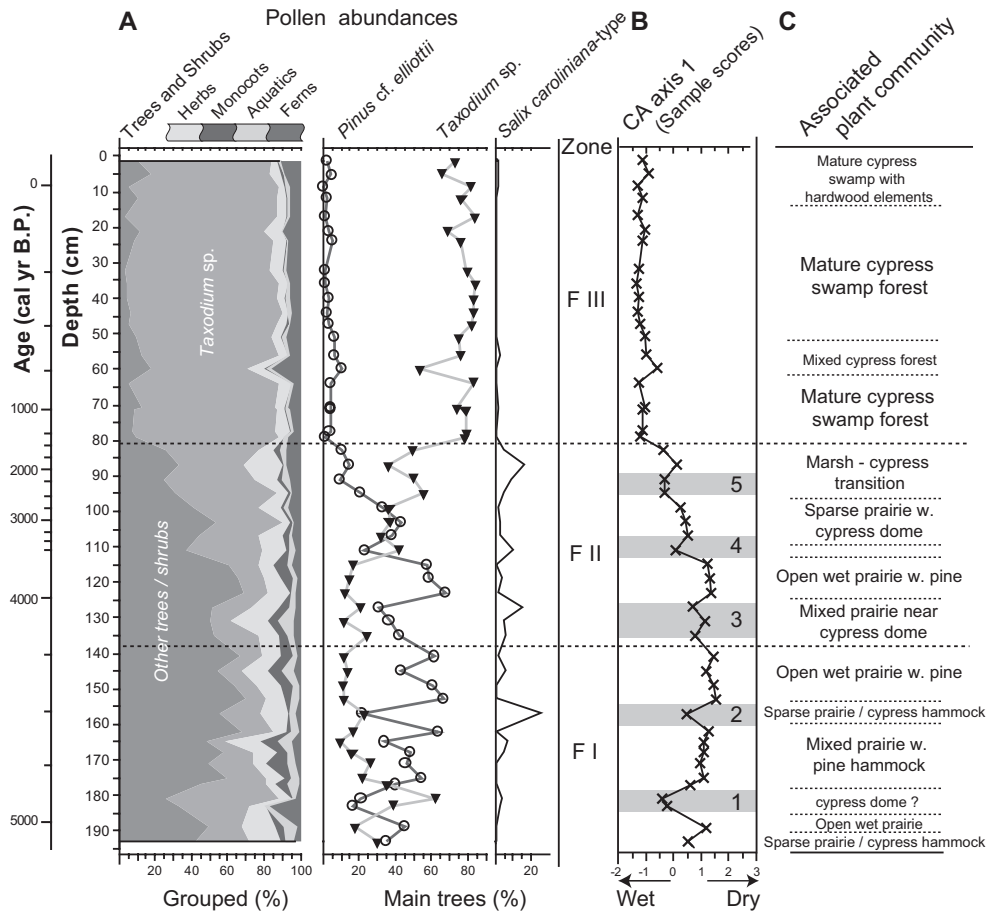
Figure 5.5 (color version on page 134) Summary pollen percentage diagram and reconstructed past vegetation from the FSPSP wetland in Florida. Major pollen curves (A) and general trend between dry and wet assemblages (B) and the associated vegetation units (C). *Pinus* represents relatively dry conditions in contrast to wet *Taxodium* phases. Numbers 1–5 represent short wet pulses characterized by high *Salix* and increased *Taxodium* as referred to in the text.

5.4. Interpretation of shifts and mechanisms
5.4.1. Moisture and ENSO change
The pollen assemblages and derived vegetation units are reconstructions of the local environment and do not represent average regional vegetation cover. However, the local environment depends on a precipitation-driven surface sheet flow across South Florida (Burns, 1984; Duever *et al.*, 1986). And because the reconstructed vegetation changes are primarily shifts between vegetation types adapted to different hydroperiods, they are a measure for the intensity of surface sheet flow across South Florida (Chapter 2).

The onset of peat formation is the first key feature of the record. The basal age of ~5.2 ky BP needs to be confirmed by additional dating, preferably on macrofossil remains, but seems evident from the extrapolation of the age-depth model below 180 cm (Fig. 5.2). Second, the main transition phase between 3.5 and 2 ky BP from wet prairie to swamp forest environments is important (Fig 5.5B, C). Both events are clear increases in water availability, the first indicates the onset of conditions moist enough for peat accumulation, whereas the second prolonged the annual inundation period from ~3 to 9 months (Willard *et al.*, 2001a; Chapter 2).

The start of the peat record confirms earlier dates for the main expansion phase of the Everglades (Gleason and Stone, 1994) and is in marked concurrence with the transition to modern ENSO periodicities reported by Rodbell *et al.* (1999), Koutavas *et al.* (2002), and Sandweiss *et al.* (2001). Furthermore, ENSO intensification after ~3.5 to ~3.1 ky BP shown from records centered around the Indo-Pacific Warm Pool (Rodbell *et al.*, 1999; Sandweiss *et al.*, 2001; Haberle and Ledru, 2001; Riedinger *et al.*, 2002) are coincident with the initial transition to long hydroperiod vegetation during zone FII in our record. A more indirect runoff record from ODP site 1002 in the Cariaco Basin offshore Venezuela confirms ENSO intensification starting ~3.8 ky B.P (Haug *et al.*, 2001). Although these records do not agree on the exact timing, the evidence for the two-stepped ENSO intensification is clear and, as shown here, not limited to the Indo-Pacific Warm Pool.

5.4.2 Sea level fluctuations

An alternative explanation for the increase in moisture involves the contribution of relative sea level (RSL) rise to wetland conditions in Florida. Although no agreement exists about the exact RSL development in the Gulf of Mexico. Several high-resolution reconstructions of relative sea level (RSL) have recently been published for the U.S. Gulf Coast. Reconstructions by Morton *et al.* (2000) and Blum *et al.* (2001) have focused on the western part of the Gulf, in Texas and Alabama. The Texas coast is a particularly tectonically stable area, which could potentially provide good records of RSL. Recent results point to a mid-Holocene highstand based on microfossil assemblages and sedimentological characteristics (Blum *et al.*, 2001) and coastal landforms (Blum *et al.*, 2002). The mid-Holocene highstand, followed by a RSL drop, would cause drier conditions onshore. However, an increase in wetness is actually recorded ~3 ky BP in our record.

However, a validation attempt from the Louisiana coast by using basal peat dates from the Mississippi Delta yielded a more continuous, gradual rise in sea level, with no indication of high-frequency changes (Törnqvist *et al.*, 2004). Even after correcting for local subsidence, the results did not confirm the mid-Holocene highstand from the western Gulf Coast. Although the Louisiana record is detailed and more continuous, uncertainties in the subsidence rate remain and complicate the comparison. An added difficulty is the possible effect of El Niño-Southern Oscillation (ENSO) on river dynamics within these areas. The entire Gulf Coast region is influenced by the ENSO cycle, where moist anomalies are caused by El Niño events (Ropelewski and Halpert, 1987; Vega *et al.*, 1998). Consequently, RSL reconstructions from Gulf Coast river deltas are not entirely independent of the hydrology reconstructions from Florida.

The regional RSL reconstruction by Toscano and Macintyre (2003), based on coral and basal peat dates is an average for the western Atlantic, and is therefore the most suitable for comparison with the FSPSP record. The record is used as the basis of comparison in this article. Qualitatively, the results largely reflect the results from Louisiana (Törnqvist *et al.*, 2004) and point to no sudden increases in RSL during the Holocene. The main increase in RSL occurs before 5 ky BP, after which sea level rise is much reduced. A slowly declining gradient between the Florida aquifer and the coast during the late Holocene would most likely be balanced by the rate of peat accumulation (~2 m since 5 ky BP), because peat accumulation ultimately develops into drier hammock formation filling up the slough (Duever *et al.*, 2002). However, a significant change to wetter, long hydroperiod systems is actually observed, whereas a stepwise increase in RSL ~3 ky BP is not obvious from the sea-level reconstructions. Possibly the start of the peat record is a combination of factors, because the main rise in Holocene RSL occurred before 5 ky BP, and the rate of change in the FSPSP record before that period is not known. A primary RSL cause for all of the observed changes in our record is considered unlikely. Additionally, a climatic cause is supported by moisture increase recorded in 'upland' Florida records (Grimm *et al.*, 1993; Watts and Hansen, 1994), although much reduced because of a lesser dependence on winter precipitation in these ecosystems.

5.4.3 Centennial shifts
During zones FI and FII, superimposed centennial shifts between short and moderate hydroperiod vegetation units indicate subtle shifts resulting from water availability fluctuations. These phases of *Salix* abundance and increased *Taxodium* sp. indicate wetter periods, relative to the prairie. They are likely caused by short periods of increased ENSO intensity as described from beach ridge deposits (Martin *et al.*, 2003). However, comparing timing and duration of these events with other records is, given the limitations on the available chronologies, difficult and a likely source of confusion. A better approach would be to establish and compare event frequencies for available records and, thus, create an integrated paleo-ENSO record through time. In our record, five clear wet pulses occur between 5 and 2 ky BP, which points to an existent, but fairly limited, ENSO activity or weakened teleconnections. Short wetter phases after 2 ky BP are probably not reflected because the *Taxodium* swamp is the region's ecosystem most adapted to wet conditions and can survive, but not reproduce, in permanent flooding (Alexander and Crook, 1974).

5.5 Conclusions
Although earlier records from Florida show increased wet conditions in the mid-Holocene (Watts, 1975; Grimm *et al.*, 1993), the two-stepped increase is not very clear. Changes are concurrent, especially for the Lake Annie pollen record (Watts, 1973), but much suppressed, and a clear link with the ENSO system was therefore not perceived. However, the great dependence of the FSPSP vegetation on ENSO-tied winter precipitation implies an enhanced response and, thus, a clear record of paleo-ENSO conditions outside the Indo-Pacific Warm Pool. Clearly, the FSPSP pollen record displays significant shifts in hydrology during the middle to late Holocene, in agreement with an existent ENSO between 5.2 and 3.5 ky BP, which intensified to resemble modern conditions after 3.5 ky BP. A definite answer to the exact contribution of ENSO dynamics to the hydrological change in Florida, especially in relation to past sea level change, might come from highly

detailed analysis of selected time windows in peat records. Recent high resolution palynological studies indicate that pollen productivity responds to annual climatic variability (Chapters 2, 4; Hicks, 2001), and can therefore potentially reflect 2- to 7-year ENSO dynamics. Periods indicative of reduced ENSO activity can thus be tested in terrestrial ecosystems, analogous to coral studies in marine systems.

Holocene hydrological conditions have shown significant, nonlinear response to gradually changing insolation, amplified by large climate systems like ENSO (Clement *et al.*, 1999; 2000; Ruter *et al.*, 2004). This study shows that ENSO-related changes are not confined to the tropics but are pronounced in the subtropics as well. Understanding and documenting these patterns of change better is a prime task for further research, because future climate warming will likely impact the global hydrological cycle to a large degree through nonlinear responses like ENSO.

Late Pleistocene and Holocene subtropical vegetation dynamics recorded in perched lake deposits on Fraser Island, Queensland, Australia

Abstract

The dune system of Fraser Island in subtropical Queensland, Australia, contains numerous perched lakes with organic-rich sediments. These lakes are located at the tropical - subtropical ecotone and are strongly influenced by precipitation and act as natural rainfall gauges, which makes them highly sensitive to environmental change.

Paleoecological and paleoclimatological investigations have been performed on sediment cores from Lake Allom, a small perched lake on central Fraser Island. A detailed chronology is based on a series of closely spaced AMS-radiocarbon data, supplemented with sedimentological information. Based on extrapolation, the chronology indicates an age range from ~56 ^{14}C ky BP to present, with a major hiatus occurring during the Last Glacial Maximum.

Pollen analysis of the Lake Allom sediment record reveals strong Glacial-Interglacial changes between rainforest and open woodland vegetation. The Holocene portion of the record shows a stepwise vegetation development, from dry conditions in the early Holocene, to high lake levels and forest succession between 5.5-3 cal ky BP. At 3-2 cal ky BP, a large diversification occurred towards the present-day heterogeneous sub-tropical rainforest vegetation, followed by a small rainforest decline at 0.45 cal ky BP. Furthermore, computer-aided charcoal analysis indicates changes in fire dynamics that occur contemporaneously with the major vegetation shifts.

Part of the reconstructed vegetation changes can be related to local and regional factors including forest succession, dune formation, sea-level rise and human impact. Comparison with paleoclimate records from tropical and temperate regions indicates that the temporal and spatial dynamics of vegetation changes in eastern Australia are primarily controlled by climate variability.

6.1. Introduction

Fraser Island, a large Pleistocene dune island off southeastern Queensland, lies at the transition between tropical and temperate Australia (Fig. 6.1A), near the southern limit of the Great Barrier Reef. The island's vegetation is characterized by a mosaic of mixed subtropical rainforest in moist patches, and dry sclerophyll forest, heath and coastal vegetation in drier areas. Eolian sand from the exposed shelf shaped the island during glacial periods when sea level was substantially lower (Walker, 1981). Within the resulting series of parabolic dune belts, a large number of perched lakes developed above impermeable layers known as coffee rock or B-horizon hardpans, which occur where leaf litter accumulations cemented together with the sandy substrate (Timms, 1986). The water-tables of the precipitation-fed lakes are positioned above the regional groundwater level and, sealed by the hardpans, act as very sensitive rainfall gauges, although some seepage does occur (Longmore, 1997a). The organic-rich sediments accumulating in the perched lake basins on Fraser Island provide an excellent natural archive for paleoenvironmental studies in this climate-sensitive area.

An initial palynological record from the Old Lake Coomboo Depression on Fraser Island revealed a distinct Glacial-Interglacial climatic control over vegetation succession (Longmore, 1997a), and confirmed the known pattern of increased aridity across Australia during the last Glacial (Dodson, 1994). A mid-Holocene dry period was documented on Fraser Island, which seemingly occurred in anti-phase with mid-Holocene moist conditions evident in records from southeastern and possibly northern Australia (Longmore, 1997b; Longmore and Heijnis, 1999). Holocene vegetation changes are well documented for the Atherton Tablelands in the Australian wet tropics (Kershaw, 1970; 1971; 1976; 1983; 1994; Moss and Kershaw, 2000; Turney *et al.*, 2004; Haberle, 2005) and coastal tropics (Genever *et al.*, 2003). The southern temperate regions have also been studied frequently, and detailed information on past vegetation dynamics from both inland (Dodson, 1986; Martin, 1986; Luly, 1993) and coastal sites (Dodson, 1974; D'Costa *et al.*, 1989, Edney *et al.*, 1990) is available. A comprehensive comparison of the contrasting areas, however, is hampered by the lack of well-dated high-resolution records from the transition zone between the northern tropical and southern temperate areas. The available data from subtropical Fraser Island focus primarily on long time-scales, and have insufficient temporal resolution to resolve the exact timing and duration of short-term changes during the Holocene. A detailed record of past environmental conditions is thus needed to corroborate or re-evaluate the previous findings. Moreover, the establishment of a high-resolution subtropical record will enable comprehensive comparisons between northern and southern regions. The accurate documentation of vegetation changes in the transitional zone between tropical and temperate eastern Australia will improve the understanding of the complex spatial and temporal evolution of environmental changes, as well as their driving mechanisms.

In this study, therefore, a high-resolution late Pleistocene-Holocene pollen record from a perched lake on Fraser Island is documented. Both pollen percentages and pollen influx data are provided. The age-assessment is based on a series of closely spaced AMS radiocarbon dates. Additionally, the sedimentary setting and past fire regimes have been studied to support the palynological data.

6.1.1. Locality

Fraser Island is the largest sand-dune island in the world with a length of 124 km and a maximum width of 24 km (Fig. 6.1B). At its highest point, it is 240 m above sea level (Whitehouse, 1968). It is situated between 24°40' and 25°50' South and 152°55' and 153°20' East. Annual rainfall varies between 1300 and1700 mm/year, and a moisture deficit occurs in the drier winter/spring season (Walker, 1981). Southeastern Queensland has as a warm subtropical slightly seasonal humid climate (Webb, 1994). Rainfall between seasons varies by about 40%, while temperatures range between 14 °C in winter and 29 °C in summer.

A perched basin named 'Lake Allom' (25°14'S, 153°10'E; 100 m a.m.s.l.) lies at the boundary between Pleistocene and Holocene parabolic dune systems, within the central rainforest belt on the island (Figs. 6.1C, D) (Grimes, 1987). Like most perched lakes, it is an oligotrophic acidic lake within a nutrient-poor catchment, but rich in dissolved tannins (Hadwen *et al.*, 2003). The lake measures approximately 300 x 80 m and is fringed by shore vegetation. Surrounding vegetation units are araucarian/notophyll vine forests and wet-sclerophyll tall forest on the Pleistocene units, and wet-sclerophyll to dry-sclerophyll open 'Blackbutt' forests with a grassy understorey on the Holocene units to the east (Fig. 6.1D). The relevant pollen source area of a medium-sized lake within patchy vegetation is estimated to be around 600-800 m in diameter (Sugita, 1994), which is covered by the detailed vegetation map in Fig. 6.1D. Due to this rather restricted catchment and the presence of regional perched water-tables, the lake level is most likely a good representation of the hydrological conditions prevailing for the local vegetation.

At glacial maxima the lowered sea level increased the degree of continentality and thus reduced effective precipitation in coastal areas of Australia (Dodson, 1994). The precipitation change was likely reflected in lakes by lowered water tables. The Fraser Island lakes and surrounding vegetation are expected to have adapted to these changes, as the perched water tables are primarily rainfall-dependent. To some degree, the perched water tables were influenced by the lowered regional water tables due to water seepage through the hardpans (Longmore, 1997a).

6.1.2. Soils and vegetation

The vegetation on the island is highly diverse, ranging from coastal shrubs and heaths on leached soils to inland layered rainforest and mixed sclerophyll vegetation on younger nutrient rich soils (Longmore, 1997a). The vegetation is laterally zoned and follows the contours of successive parabolic dune systems parallel to the coastline. Parabolic dunes occurring further east are generally younger (Grimes, 1987; Thompson, 1992). The central part of the island contains layered vine forest, mixed with wet-sclerophyll elements. Surrounding areas are nutrient-poor soils with dry-sclerophyll, heathland and shrub/grassland communities (Fig. 6.1C). Nutrient availability first increases with soil age and organic matter deposition, and subsequently declines due to soil leaching (Walker, 1987). Fire occurs naturally on the island, especially in the *Eucalyptus*-dominated sclerophyll belt around the rainforest. Since nutrient levels are low, fire represents an important recycling mechanism to sustain plant growth. Ultimately, however, soil formation processes and fire leads to loss of nutrients in old leached dune systems (Walker, 1987).

Figure 6.1 Location of Fraser Island (A,B). For the central section of the island a simplified vegetation map is given (C), based on 2001 surveys (Anon., 2003). Positions of the previously studied Lake Coomboo (Longmore, 1997a), and the present study site are indicated. A more detailed local vegetation map of the Lake Allom catchment is provided (D), in relation to Holocene and Pleistocene sand dune units (Grimes, 1987). Qpd_2 = mid- to late Pleistocene, Qd = latest Pleistocene, Qhd 3-4 = Holocene, all parabolic quartz dune fields.

The wet-sclerophyll tall open forest extends over a large range in Australia, primarily in mesic sites with rich understorey of herbs, shrubs and tree ferns. The forest type can develop in rainforest sites with appropriate fire regime. If rainfall is high enough and disturbance low, sclerophyll forest will be completely replaced by rainforest. A mix between wet-sclerophyll forest and rainforest can exist when fire frequency is low and severe burns occur only on a century scale.

Typical mesic elements on Fraser Island are:
Araucaria cunninghamii, A. bidwillii, Agathis robusta, Eucalyptus pilularis, E. grandis, E. cloeziana, E. microcorys, Syncarpia hillii, Casuarina torulosa, Elaeocarpus reticulatus, Cyathea spp. (more towards the south), Arecaceae (more towards the north). Rainforest species such as *Litsea reticulata* and *Argyrodendron* spp. grow in rainforest with eucalypt emergents that extend above the rainforest (closed) canopy (Ashton and Attiwill, 1994).

On the surrounding young Holocene dune systems, dry-sclerophyllous *E. pilulata* (blackbutt) with *Banksia serrata* understorey occur on incipient podsols. Pleistocene well-drained dunes are covered by woodland/forest consisting of *E. signata, Angophora costata, E. gummifera, E. intermedia* with a heath understorey. Furthermore, wet heaths with *Banksia oblongifolia* and *B. robur* (swamp banksias) occur. Hind-dunes support mesic *Acmena smithii* and *Cupianopsis anacardioides* and sheltered pockets of low closed rainforests (Clarke, 1994).

An ubiquitous element of the Fraser Island vegetation is *Casuarina,* which mostly occurs in (sub)tropical climates in open, coastal strand habitats, characterized by sand and shell beaches, rocky coasts, sand dunes, and sand bars. Because their roots are capable of producing nitrogen through microbial associations, *Casuarina* species can colonize nutrient-poor soils (Ng, 1987). Nitrogen-fixing ability seems to depend wholly on the availability of adequate soil moisture. The trees can grow on many different soil-types, ranging from dry, sandy beach ridges to wet lake margins. They tolerate average annual precipitation of 640 - 4300 mm yr^{-1}, average annual temperatures of 22.1 - 26.9 °C, and soil pH of 5.0 - 7.7 (Duke, 1979). *Casuarina* reaches maximum development in slightly depressional topography where adequate moisture is nearly always available, but withstands inundation only for short periods. The plants are resistant to salt spray and grows rapidly during hot weather. However, they are not well adapted to fire events (Clemens *et al.*, 1983).

6.1.3. Human impact
Aboriginal settlement likely influenced fire frequencies (Kershaw, 1986; Miller, 2005) and thereby impacted the natural vegetation. However, a tropical lowland pollen record relatively close to Fraser Island (Whitsunday Island, Genever *et al.*, 2003) reports little direct correlation between identified environmental change and cultural change in wet coastal sites. The pollen record and regional supporting data indicate major changes in vegetation at times when little or no change is seen in the archaeological record. A recent study of Aboriginal land and fire management ensured rainforest conservation to a high degree (Hill *et al.*, 2000). Potentially, European colonial impact on Fraser Island could have been more influential due to logging and sand mining activities (Young and

McDonald, 1987). However, remnant and pre-clearing vegetation maps (Anon., 2003) show little change for the areas studied, logging and mining industries being mainly restricted to the southern part of the Island.

6.2. Methods
6.2.1. Coring and sampling
Lake Allom was cored in July 2003 with an adapted Livingstone piston corer. At the time of coring, during the relatively dry Austral winter season, the central lake area had a water depth of 3.7 m. Three partly overlapping core sections were retrieved down to 3.2 m sediment depth, all consisting of dark, organic-rich sediments with some mixed sandy intervals and coarse charcoal particles (>0.5 mm^2) in the lower half of the core. Extensive areas with migrating sand dunes occur on the island today (Fig. 6.1C), which cause the presence of sand particles in the sediment. Before sub-sampling of the core, color reflectance was measured to identify the sandy intervals. A sediment interval around 180 cm depth showed increased compaction and was significantly drier compared to the rest of the core, which is indicative of an erosional surface. Volumetric sub-samples were taken for both palynological and macro-charcoal analysis.

6.2.2. Radiocarbon dating
Sixteen horizons were sampled for accelerator mass spectrometry (AMS) radiocarbon dating; sampled material mostly consisted of small leaf fragments, leaf-based organic detritus and charcoal particles. Samples were dried overnight at 60 °C and pre-treated according to an acid-alkali-acid procedure (Mook and Streurman, 1983). AMS radiocarbon dating was carried out at the AMS facility of Utrecht University. Holocene radiocarbon dates (<10 ky BP) were calibrated to calendar years with OxCal 3.10 calibration software (Bronk-Ramsey, 1995; 2001), using the SHCAL04 calibration dataset for the southern hemisphere (McCormac *et al.*, 2004). The δ^{13}C values were obtained from gas mass spectrometer analysis at the Earth Sciences Department, Utrecht University, The Netherlands.

6.2.3. Palynological analysis
Pollen and spores were isolated from samples following standard palynological peat processing techniques adapted from Faegri *et al.* (1989). Prior to processing, *Lycopodium clavatum* spore tablets were added in order to determine pollen concentration (pollen cm^{-3} sediment). Processing included carbonate and silicate removal with 30% HCl and 40% HF, respectively. Residues were sieved over 7 μm and 120 μm mesh to remove fine and coarse fractions. Organic compounds were removed with 10 % KOH, followed by acetolysis for removal of polysaccharides and staining of the pollen. Residues were mounted in silicon oil on microscopic slides for analysis by light-microscopy at 400x magnification.

Pollen and spores were identified to a minimum of 300 grains originating from land-based taxa. Reference collections of the Australian National University (Canberra, ACT, Australia), the Institute of Geological and Nuclear Sciences (Lower Hutt, New Zealand), and the online pollen database of Newcastle University (Newcastle, NSW, Australia, Shimeld *et al.*, 2000) were used for identification.

To delimit pollen assemblage zones (PAZ) in the record, samples were numerically zoned by applying optimal sum-of-squares partitioning of Birks and Gordon (1985) as implemented in the program ZONE (Lotter and Juggins, 1991), including only land-based taxa. The significant number of stratigraphic zones was assessed with the broken stick model (Bennett, 1996). Pollen diagrams were plotted with TGView 2.0.2. (Grimm, 1991-2004).

6.2.4. Charcoal analysis

To gain insight in abundance and source (local or regional) of charcoal particles, samples were analyzed at three different size fractions. Samples for macro-charcoal analysis (>120 μm) were soaked in 10% sodium pyrophosphate to dissociate the sediment matrix and bleached overnight in 4% sodium hypochlorite to remove organic fractions other than charcoal. Samples were subsequently sieved into two fractions of 120-250 μm and >250 μm respectively. Micro-charcoal particles (10-120 μm) were counted simultaneously with the pollen analyses, the macro-fractions were quantified by digital image analysis of photographs taken from each sample. The image analysis software 'AnalySIS 3.0' (Soft Imaging System GmbH, Germany) was used to measure and calculate both number and surface area of individual particles by selecting the appropriate color phase that represents the charcoal fraction in the samples. This method ensures high reproducibility and rapid objective analysis of large numbers of samples (Mooney and Black, 2003). For samples with little charcoal present, images were taken through a binocular microscope and results were corrected according to the magnification.

Table 6.1 Radiocarbon ages from Lake Allom, Fraser Island, Qld., Australia

Depth (cm)	UtC* #	^{14}C yr BP	± σ	δ ^{13}C (‰)	cal yr BP	± σ	Cal. curve
18	13485	623	32	-31.4	585	45	SHCAL04
37.5	13180	849	31	-31.6	707	28	SHCAL04
59	13486	1469	34	-31.6	1320	25	SHCAL04
79.5	13487	1770	60	-31.5	1625	75	SHCAL04
98	13488	2177	40	-31.2	2080	80	SHCAL04
107.5	13181	2477	31	-31.1	2510	160	SHCAL04
127.5	13182	3420	35	-31.4	3620	70	SHCAL04
142.5	13489	4213	42	-31.3	4725	105	SHCAL04
149	13490	4640	50	-31.4	5260	190	SHCAL04
161	13491	7620	60	-30.7	8375	55	SHCAL04
177	13492	9860	60	-31.2	11220	45	SHCAL04
201	13183	32500	400	-30.8	~36-40 ky[1]	n.a.	NotCal04
221	13184	35900	800	-30.2	~39-43 ky[1]	n.a.	NotCal04
264	13493	45200	1500	-30.8	~45-50 ky[1]	n.a.	NotCal04
304	13185	44600	2400	-30.8	n.a.	n.a.	n.a.
323	13494	45900	1900	-31.1	n.a.	n.a.	n.a.

* Laboratory code: R.J. Van de Graaff laboratorium, Utrecht University, the Netherlands.
[1] These ages are estimates only (Van der Plicht *et al.,* 2004)

Age-depth Lake Allom
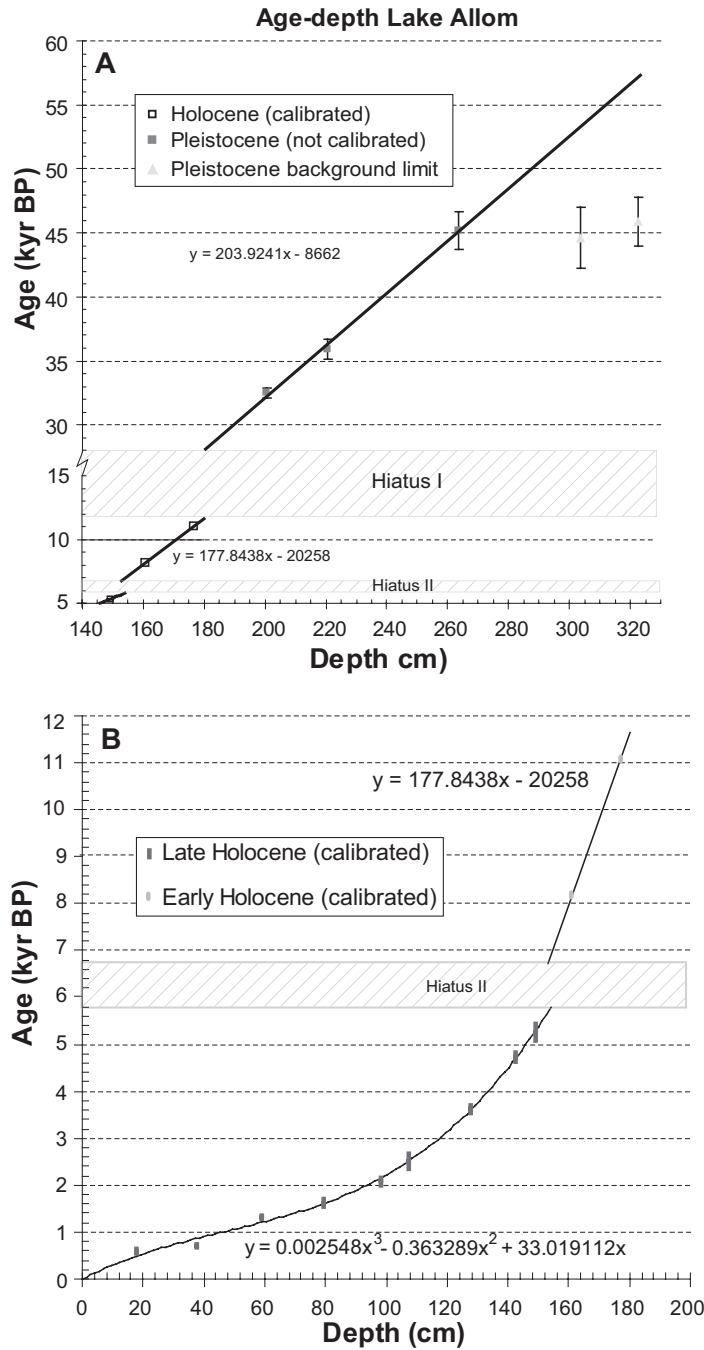
Figure 6.2 Radiocarbon data (1-sigma ranges) and age-depth model for the Lake Allom core. (A) Shows the Pleistocene section and Hiatus I & II, the Pleistocene section are non-calibrated data. (B) Shows the Holocene section and Hiatus II, with a prominent decline in compaction towards the top (note difference of y-axis scale between A and B).

6.3. Results

6.3.1. Chronology

Radiocarbon dating confirmed the presence of a hiatus in the sediment column at about 180 cm (Table 6.1). Below this level dates were older than 30 ^{14}C ky BP, reaching background values of >45 ^{14}C ky BP. Ages below 270 cm are based on extrapolation of the accumulation rate between 180 and 270 cm. Dates above 180 cm all correspond to the Holocene period and do not contain outliers or age-reversals.

An age-depth plot of the data revealed a second short unconformity, which lies within a relatively sandy sediment interval (Figs. 6.2, 6.4). The age-depth model therefore consists of three sections; a non-calibrated Pleistocene, an early Holocene and a late Holocene part. An estimation of the Pleistocene 'calibrated' age range was added based on the NotCal04 data comparison (Van der Plicht *et al.*, 2004); it should be emphasized that this is by no means a true calibration (Table 6.1). In the Holocene sections, the accumulation rates apparently increase towards the top, but this is largely due to taphonomic processes. The accumulation rates of the early Holocene and Pleistocene sections are highly comparable, even though the latter are based on uncalibrated radiocarbon data

6.3.2. Pollen and charcoal counts

Pollen assemblages show very distinct changes between the Pleistocene and Holocene parts of the section, and notably within the Holocene. A percentage diagram displaying all pollen types (single occurrences are omitted) shows a distinct succession of plant taxa through time (Fig. 6.3). The pollen is grouped according to functional types with a pollen sum based on land plants; also fern spores are included, as these are not over- represented and comprise an important part of the (understorey) ground cover. Based on ecological descriptions by Kershaw (1973), Groves (1994) and Longmore (1997a), a summary diagram

Table 6.2 Ecological grouping of pollen/spore types (see Figs. 6.4, 6.5), ranked to abundance.

Rainforest angiosperms	Rainforest gymnosperms	Cool ferns
Agyrodendron spp.	*Araucaria* spp.	*Dryopteris* type
Euodia type	*Agathis robusta* type	*Cyathea* spp.
Litsea reticulata	*Podocarpus elatus*	
Flindersia spp.	Araucariaceae undif.	**Other Ferns**
Rutaceae undif.		*Pteridium esculentum*
Cupianopsis anacarnoides	**Dry indicators**	*Polypodium* type
Euphorbiaceae undif.	*Amperea xiphoclada*	Monolete spores indet.
Palmae	Asteraceae Tubuliflorae	*Pteris* type
Sterculiaceae undif.	*Dodonea triquetra*	Trilete spores indet
Cunoniaceae undif.	*Dodonea tenuifolia*	*Botrychium* sp.
Eleocarpus type	*Banksia* spp.	*Todea* sp.
Low occurrences:	Asteraceae "short spine" type	*Pellaea* sp.
Ameyema sp.	Chenopodiaceae	
Balanops sp.	*Callitris* spp.	**Aquatics and shore**
Caesalpinaceae	Asteraceae Liguliflorae	*Restio* type
Celtis sp.	*Xanthorrhoea minor*	Poaceae
MacKinlaya sp.	*Plantago* sp.	Cyperaceae undif.
Melia type	Caryophyllaceae	*Myriophyllum implicatum*
Melicope sp.		*Typha/Sparganium* type
Melastomataceae		Juncaceae
Vitaceae		*Nuphar* sp.
Weinmannia sp.		*Eriocaulon* sp.

is composed by adding up indicator taxa into ecological groups (Fig. 6.4, Table 6.2). Taxa grouping in the absolute pollen diagram follows Table 6.2 as well (Fig. 6.5).

Seven separate pollen assemblage zones (PAZ) can be identified on the basis of the ZONE output and are described below. Within a small range, the PAZ boundaries coincide with both sedimentary hiatuses (±1 sample as indicated by the shaded PAZ boundaries in Figs 6.3-6.5). Whenever important differences occur between percentage and absolute pollen diagrams this is mentioned in the text, but the diagrams are not discussed separately.

Lake Allom 57-54 ^{14}C ky BP (~58-55 cal ky BP); PAZ Ple I, 323-307 cm)
Casuarinaceae and *Araucaria* spp. dominate Ple I, together with significant amounts of *Agathis robusta* type, *Podocarpus elatus*, *Callitris* sp. and various fern species. Virtually no rainforest angiosperms are present and, notably, Myrtaceae pollen is nearly absent in the lowermost samples. In the top of the zone Araucariaceae decline rapidly while Casuarinaceae pollen increases. Myrtaceae pollen increases slightly, and a peak in *Banksia* spp. occurs. The aquatic/shore taxa do not exceed ~15% of the pollen sum. Microscopic charcoal is relatively sparse, although the larger fractions are present in significant amounts, pointing to a nearby source of the fire.

Lake Allom 54-28 ^{14}C ky BP (~55-35 cal ky BP); PAZ Ple II, 307-182 cm)
Ple II represents the longest stable unit in the profile and is characterized by pollen types that are largely restricted to this zone. *Araucaria* spp. occurrence <10% is low, *Agathis* and *Podocarpus* remain constant around 5%. Shrub and herb communities (NAP, non-arboreal pollen), increase significantly to 20 % in the upper half of Ple II. *Amperea xiphoclada*, Asteraceae subf. Tubuliflorae, Chenopodiaceae, *Ixora* type, *Dodonaea triquetra*, *D. tenuifolia*, *Coprosoma* sp., and *Pteridium esculentum* dry-land *Xanthorrhoea minor* and Asteraceae subf. Liguliflorae occur nearly exclusively in Ple II, and are therefore of indicator value for Ple II.

Banksia spp., *Callitris* sp. and Myrtaceae tree pollen is continuously present, but never very abundant. *Amperea xiphoclada* and Myrtaceae group gradually increase within the zone, whereas the other main elements remain more stable. Casuarinaceae abundance is high, around 70%, but decreases slightly towards the top. However, the decrease is likely to be an artifact of the closed-percentage data, since the absolute values remain constant.

A prominent feature is the large increase in aquatic and shore-type pollen, reaching 60% (outside pollen sum). *Restio* type, *Myriophyllum implicatum*, *Typha/Sparganium* type, Poaceae and Cyperaceae are the main components. However, the total abundance of the aquatic/shore group fluctuates strongly, indicating dynamic local conditions. Charcoal particle values remain high. The microscopic fraction (<120 μm) even shows a clear increase, although the largest fraction (>250 μm) decreases towards the top of Ple II.

Hiatus I, 28-10 ^{14}C ky BP (~35-12 cal ky BP); ~182 cm
Radiocarbon dating indicates a hiatus of approximately 18 ^{14}C ky (Fig. 6.2A) at this level. Below the hiatus, ~5-cm of sediment is dry and compact.
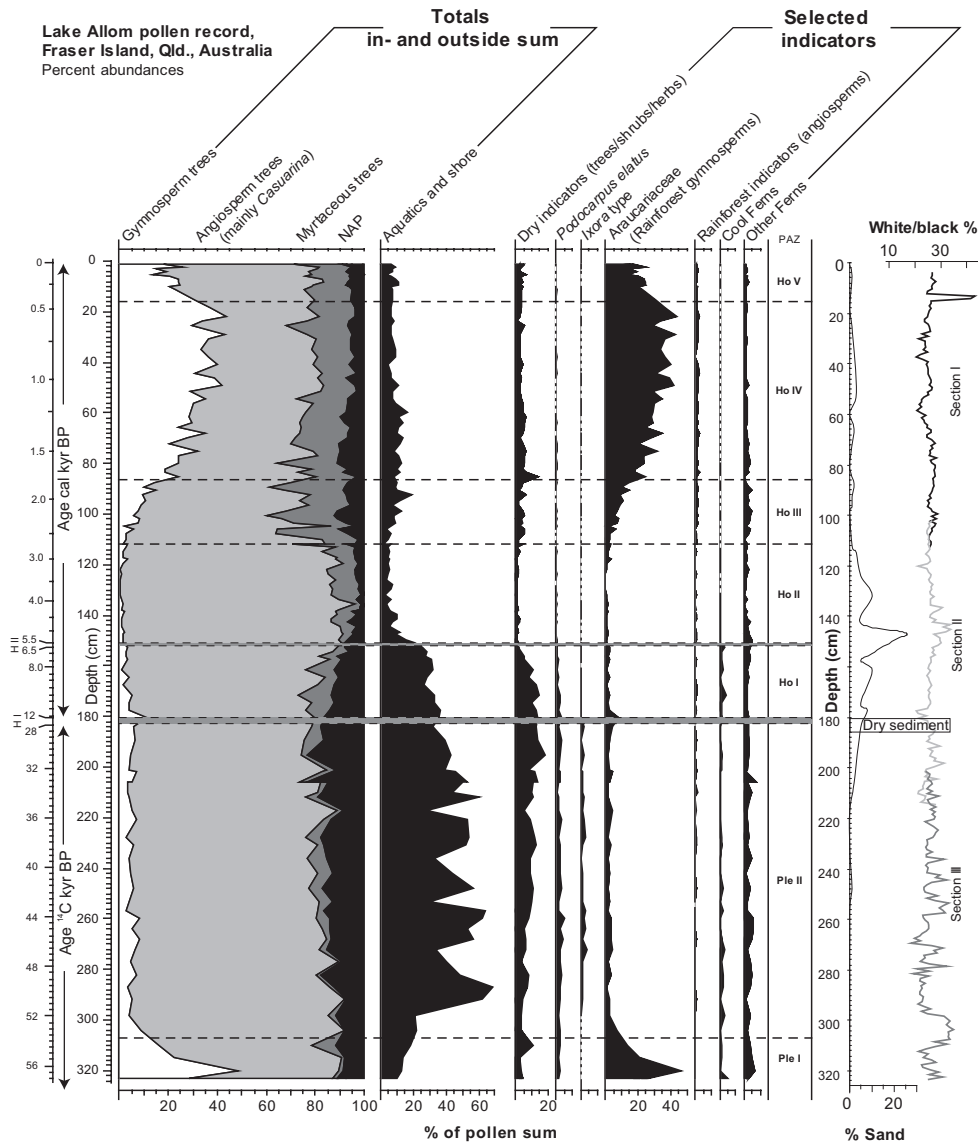
Figure 6.4 Summary percentage pollen diagram, with major ecological groups and groups with indicator value (see Table 6.2 and text). Sand content is given based on optical estimation, along with color reflectance data for each sediment section, expressed as % white. Note the high variability in the lowermost section of the core caused by the presence of large charcoal particles, and some sandy layers.

Figure 6.3 (see separate foldout sheet) Percentage pollen abundances from Lake Allom based on a terrestrial pollen sum, including ferns. Pollen types with a single occurrence are omitted. Pollen assemblage zones (PAZ) are based on relative-frequency changes of elements included in the pollen sum. The zones are described in the text and also used in Figs. 6.4 & 6.5.

Figure 6.5 (see separate foldout sheet) Absolute pollen and charcoal abundances (accumulation rates) from Lake Allom, with some grouping of pollen types (see Table 6.2). Primary y-axis is depth for purpose of comparison with other figures. Note different scale on high-abundance categories.

Lake Allom, 12-6.5 cal ky BP; PAZ Ho I, 185-151.5 cm

The composition of Ple II and Ho I is very similar, although some significant differences exist. Pollen of the herb communities decreases gradually, both in percentage and absolute terms, *Angophora* type and *Banksia* spp. tree pollen increases. Charcoal reaches maximum values in Ho I, while aquatics/shore taxa are less abundant. Rainforest angiosperms such as *Cupianopsis anarcanoides*, *Celtis* sp. and *Euodia* type have a first occurrence in Ho I, but in contrast to Ple I, no *Argydodendron* spp. occurs. *Epacris* type pollen forms a closed curve only in Ho I, indicating presence of heathland. Overall, Ho I represents a clear transition phase between Pleistocene and Holocene communities, incorporating important elements of both periods.

Hiatus II, 6.5-5.4 cal ky BP; ~ 151.5 cm

Radiocarbon dating and resulting age-depth modeling indicate a hiatus of approximately 0.9 cal ky (Fig. 6.2B) at this level. The hiatus occurs in a sandy sediment section (Fig. 6.4).

Lake Allom, 5.4-2.7 cal ky BP; PAZ Ho II, 151.5-112 cm

The base of Ho II follows Hiatus II and represents a distinctly different assemblage. Pollen of *Podocarpus elatus* and *Banksia* spp. tree communities only reach background levels, while Casuarinaceae strongly increase to maximum values of 90% and ~7000 grains cm^{-2} year^{-1}. Heathland expands with greater amounts of *Monotoca scoparia* and, particularly after ~4.0 cal ky BP, *Angophora* type increases. *Amperea xiphoclada* is absent from the base of Ho II upwards. *Coprosoma* sp., *Dodonaea triquetra*, *D. tenuifolia*, *Ixora*, type. and *Plantago* sp. reach minimum values in Ho II. A marked change occurs within the fern communities. *Cyathea* spp. have their last occurrences at the base of Ho II, and *Polypodium* type spores nearly disappear. However, absolute-abundance data show a significant increase of *Pteridium esculentum*. NAP reaches minimum values of ~5% in Ho II, also aquatic/shore elements and charcoal fragments are at their lowest level in this interval.

Lake Allom, 2.7-1.77 cal ky BP; PAZ Ho III, 112-86.5 cm

Within Ho III, Casuarinaceae decrease sharply, while pollen of several Myrtaceae taxa shows stepwise increase. In addition, *Agathis robusta* type gradually increases, followed towards the top of Ho III by *Araucaria* spp. Although reduced in absolute terms, rainforest angiosperms increase markedly (Table 6.2). Herbs, *Dodonaea triquetra*, *D. tenuifolia.* and *Banksia* spp. re-establish together with shore taxa, particularly *Restio* type, Poaceae and Cyperaceae.

Monotoca scoparia increases further, while other heathland types occur in low abundances. Charcoal counts increase slightly, particularly two prominent peaks occur within the larger fractions.

Lake Allom, 1.77-0.45 cal ky BP; PAZ Ho IV, 86.5-16 cm

The transition that started in Ho III is completed in the highly stable Ho IV. Araucariaceae values reach 40%, together with abundant Casuarinaceae and Myrtaceae. Ho IV is characterized by high diversity with no single element dominating the assemblage. Herb abundance is high in the lower half of Ho IV - but never as high as in Ple II/Ho I - and decreases slightly towards the top. The aquatic flora contains *Myriophyllum implicatum*

again, but *Typha*/S*parganium* type is not present. Charcoal counts remain relatively elevated as in Ho III.

Lake Allom, 0.45 ky BP - AD 2003; PAZ Ho V, 16-0 cm
The base of Ho V is characterized by the renewed increase of Casuarinaceae and an associated decline in Araucariaceae and several rainforest angiosperm types. Also *Callitris* spp*.,* which is present in the entire profile, is absent. However, the AP/NAP ratio remains constant, and aquatic and charcoal abundances remain constant. Ho II covers the period of European colonial settlement in Australia. Occurrence of *Pinus.* cf. *elliottii,* introduced on Fraser Island from North America, documents colonial influence in the uppermost levels.

6.4. Discussion
6.4.1. Quality and interpretation of the record
The presented pollen record provides detailed information on Glacial/Interglacial and Holocene vegetation dynamics. Despite the hiatus during the Last Glacial Maximum (LGM), the record does give insight in the broad patterns of vegetation development in subtropical Fraser Island during glacial conditions.

Preservation is generally good and pollen is abundant, but identification is occasionally complicated due to high diversity and many single occurrences. Although the Myrtaceae are abundant in the record, identification of different types is often problematic and therefore the group is not suitable for detailed ecological interpretation. As an alternative, specific indicator pollen types have been selected to interpret changes (Table 6.2). Since these are not very numerous in the assemblages, high counting sums (mostly >500 grains) are essential for obtaining a sufficient record of indicator pollen.

In the Holocene zones, clear differences exist between the percentage and accumulation-rate pollen diagrams. Notably Casuarinaceae have a dissimilar abundance in the two diagrams (Figs. 6.3, 6.5), thus biasing many elements in the closed-data percentage diagram. Accumulation rates provide a more realistic estimate of pollen abundances, but depend on added-exote counts, which introduces an additional error factor. An important complicating factor is imposed by the weakly consolidated sediments in the uppermost part of the core. The volumetric sampling method used compresses the sediment slightly, causing artificially increased influx values in the final reconstruction. Total accumulation rates and all individual curves are significantly higher within the upper third of the core (Fig. 6.5), although the main Casuarinaceae peak occurs earlier. Therefore, the pollen influx is most likely somewhat overestimated in Ho IV/V.

6.4.2. Pleistocene
The Pleistocene section of the Lake Allom record clearly represents a relatively dry and cool environment. Rainforest elements were reduced to background levels, but did not disappear completely. Most likely rainforest became restricted to local refugia in sheltered, moist valleys. The lowermost PAZ Ple I however, reflects intermediate conditions with the presence of drier rainforest, and likely represents a 4 ^{14}C ky-interstadial within the generally cool and arid Glacial period. The presence of araucarians in Ple I provides precise

paleoclimatic information as these trees are typical of rainforest margins (Kershaw and Wagstaff, 2001). According to the chronology and comparison with vegetation development in the Australian wet tropics reported by Kershaw (1986), the Ple I phase can thus be attributed to the first part of Marine Isotope Stage (MIS) 3. During the early MIS 3, conditions were clearly wetter and warmer than in the subsequent late MIS 3 and MIS 2. This cooling and increase in aridity in MIS 2 is evident from the strong reduction of rainforest conifers during Ple II in the Lake Allom record.

The sea level lowering of up to ~120 m during MIS 2 connected Fraser Island to the Australian mainland and repositioned the shoreline ~30 km eastwards at the north-side, and ~70 km at the south-side of the island (Longmore, 1999). The lowered sea level during Glacial periods increased the continentality, inducing a drawdown of regional water-tables and generally drier conditions. High abundance of NAP within Ple II indicates a semi-open landscape. The relatively high *Podocarpus elatus* values are in agreement with a larger and more open catchment, since bisaccate pollen can be dispersed over large distances. The local aquatic/swamp vegetation was very abundant within this period, and could grow close to the coring site fringing a strongly reduced lake basin. The significant increase in charcoal content during the Glacial, in both amount and size range (up to 0.8 cm²-sized particles), is also indicative for a low lake level. Most likely the lake was ephemeral in nature, which explains the low accumulation rates, the presence of large charcoal particles and growth of aquatic/shore plants within meters to the core locality.

The main Ple II zone is remarkably stable, and although sample resolution is relatively low, no rapid transitions are observed in the dry land taxa. More variability is present within the aquatic taxa but chronological control is not sufficient to relate shifts to known millennial-scale climate oscillations (i.e. Dansgaard-Oeschger cycles) during this period. The subsequent hiatus is probably caused by further reduction in available moisture, favoring erosion and near-zero sediment accumulation during the LGM in a nearly dried up or ephermeal lake. The time-span of the hiatus is concurrent with the maximum aridity phase between ~26 and 9 ¹⁴C ky BP reported for the Lynch Crater record in northern Queensland (Kershaw, 1986).

The Pleistocene-Holocene transition in Australia is characterized by a highly diverse spatial and temporal pattern resulting from large differences in geography, fire, soil, and moisture regimes, and human occupation across the continent (Dodson, 1994). In the Lake Allom record, vegetation response to the last Glacial-Interglacial transition was immediate, without any traceable time-lag caused by vegetation migration. Although in comparably low abundances, most present-day taxa are present throughout the entire record, and were able to re-expand from local refugia as soon as conditions improved during the early Holocene.

6.4.3. Early to middle Holocene
The Holocene PAZs in the record show prominent changes and reveal a much more dynamic vegetation development than during the Pleistocene (Fig. 6.3). Myrtaceous trees become very widespread within the Holocene units, and rainforest expanded significantly.

Above Hiatus I, *Banksia* spp. and Angophora type pollen, as well as charcoal particles occur more frequently. These changes document the development of fire promoting 'Blackbutt' forest, indicating a temperature increase. However, the local vegetation still reflects relatively dry conditions, comparable to the Pleistocene. Between 10 and 6 ky cal BP, sea level was still considerably below present levels (Bard *et al.*, 1996). Continentality also remained high compared to the present, reducing effective precipitation and drawing down regional water tables, which maintained the local dry conditions during the early Holocene.

High sand content during Ho I (Fig. 6.4) is indicative for the presence of migratory dunes in the vicinity of Lake Allom. The lake is located between Pleistocene and early Holocene sand units (Grimes, 1987), which points to active dune development during the LGM and early Holocene until ~6 ky BP when the sea level reached present-day levels and the shelf was no longer exposed (Ward and Grimes, 1987; Bard *et al.*, 1996).

A second, smaller Hiatus (II) marks the onset of distinctly different conditions after 5.5 ky BP. The sharp increase of sclerophyllous Casuarinaceae during Ho II can be explained by the ability of these trees to colonize the sandy low-nutrient soils on the early Holocene dunes. The capability of *Casuarina* to form symbiotic N_2-fixing associations with soil actinomycetes (Ng, 1987) allows them to grow on, and thus fix nutrient poor migratory dunes.

During Ho II, tree pollen increased, while the amount of pollen from aquatic plants was at a minimum. Presently, the lake only supports aquatic vegetation at the shores, and an increased distance between the coring location and lake margin results in a lower aquatic pollen sum. Compared to present-day conditions, lake size increased during Ho II. Minimum levels of dry indicator-taxa (Fig. 6.4) and charcoal deposition (Fig. 6.5) provide additional evidence of relatively mesic conditions. Although Casuarinaceae comprise sclerophyllous trees, they occur across a wide range of habitats (Groves, 1994) and may grow well under moist conditions (Kershaw, 1973). With further soil development, heath and Blackbutt forest successively increased while sand influx to the lake was lowered during the second half of Ho II.

6.4.4. Late Holocene changes
At the onset of Ho III, minor increases in dry indicators, aquatic taxa and charcoal particles show a return of overall slightly drier conditions (Figs. 6.4, 6.5). The increase in charcoal after 3 cal ky BP is small but significant. It occurs in the microscopic wind-blown fraction (<120 μm), which reflects regional-scale fire events. However, the subtropical rainforest expanded very significantly as well, documented by rises in the Araucariaceae and rainforest-angiosperm abundance in Fig. 6.4. Based on bioclimatic profiles from extant *Agathis* spp., *Litsea* sp. and *Flindersia* spp. (Kershaw and Nix, 1988), annual mean temperature must have exceeded 18 °C, and annual precipitation was at least 1200 mm/year. These taxa are also tolerant to strong seasonality, which characterizes the present climatic conditions in the area (Walker *et al.*, 1981).

During Ho III, some areas maintained moist conditions, while more exposed sites where precipitation could not be retained, became drier. Under increasingly heterogeneous conditions, forest development at an exposed or protected area resulted in differential vegetation types. The diversification is likely caused by increased variability or altered seasonality of the climate, causing more frequent exceptionally wet or exceptionally dry conditions due to variations in rainfall and/or temperature.

This heterogeneous forest composition is evident in the present-day vegetation cover (Fig. 6.1C, D) and explains an important difference between the Lake Allom and the Lake Coomboo (Longmore, 1997a) records. At Lake Allom, a prominent rise in araucarian rainforest occurs during the late Holocene, which persist to the present. The Lake Coomboo site is ephemeral and located in a slightly drier area just outside the present main rainforest zone, which explains low abundance of gymnosperm rainforest pollen during the Holocene in that record. It is therefore important to compare relative changes, and not correlate specific elements between records, since these small lakes represent restricted forest areas (Sugita, 1994).

6.4.5. Recent changes and human impact

The most recent phase in the Lake Allom record, Ho IV, shows a prominent drop in araucarian rainforest while most other parameters remain stable. Particularly fire and drought regime remain constant. Although logging affected the rainforest in the 20th century (Young and McDonald, 1987), the araucarian rainforest decrease in the pollen record occurs around 450 cal yr BP, which is clearly before European colonial impact, marked by the first *Pinus* occurrence. Since *Araucaria* spp. is typical for meso-thermal subtropical climates (Kershaw and Wagstaff, 1987), a temperature decrease might have created sub-optimal growth conditions.

This cooling might be related to the Little Ice Age (LIA), which is particularly known from Northern Hemisphere paleoclimate reconstructions as multiple, century-scale periods of anomalously cold, dry conditions between 450 and 130 cal yr BP. (Hendy *et al.*, 2002). However, a trend towards cooler unstable climate started already around 650 cal yr BP (Grove, 2001). Modeling results show that Northern Hemispere cooling impacts the Southern Hemisphere only after ~150 years due to the large heat storage capacity of the ocean (Goosse *et al.*, 2004). Therefore, the observed cooling at 450 cal yr BP in the Lake Allom record might be caused by a delayed impact of LIA cooling, but this has to be confirmed.

6.5. Concluding remarks

The presented record provides a high-resolution vegetation reconstruction with good time-control, documenting environmental conditions during the Late Pleistocene and, in particular, the Holocene. Combined pollen percentage and accumulation-rate results proved to be an effective approach, especially in the highly dynamic setting of Fraser Island. The large set of radiocarbon data enabled detection of unconformities in the perched lake sediments. Such unconformities are likely to be a common feature in sediments from ephemeral or shallow lakes on Fraser Island.

In broad terms, the record confirms Glacial-Interglacial dynamics reported earlier from Lake Coomboo on Fraser Island (Longmore, 1997a; Longmore and Heijnis, 1999). The early Holocene section indicates a dry setting and associated low accumulation rate, while fire intensity reaches maximum values. This dry phase is probably related to low sea-level during the early Holocene, rather than local climate. Conditions change after 5.5 cal ky BP with reduced fire regimes, rising lake levels and moist pioneer vegetation that settles migratory dunes. A further change to more variable and slightly drier conditions occurs after 3.0 cal ky BP.

These prominent dry-wet alterations refine previous reports of a mid-Holocene arid phase on Fraser Island revealed by changing sediment properties (Longmore, 1997b), and are not in contrast with Holocene changes from the northern tropics (e.g. Haberle, 2005) or temperate southeast (e.g. D'Costa, 1989). The regional environmental controls, such as precipitation, temperature and sea-level, are the same for individual perched lakes on Fraser Island, but sites have different initial conditions that need to be taken into account.

Holocene records from the Australian northern tropics show a slight increase in climate variability with more diverse taxa and araucarian forest expansion (McGlone *et al.*, 1992; Haberle, 2005). The Lake Allom record shows a more pronounced development of Holocene conditions than northern Queensland, particularly after 3 cal ky BP. Apparently, the tropical-subtropical ecotonal transition zone is more sensitive to small changes in climate than the northern tropical region.

Although edaphic factors exert an important control on the vegetation, climatic trends are considered to be the main factor for vegetation change in this region (Webb and Tracey, 1994; Longmore, 1997a). Since the perched lakes act as rainfall gauges, the observed changes in the Lake Allom record give evidence for past variations in the hydrological cycle. The modern climate on Fraser Island is seasonal with respect to rainfall (Walker *et al.*, 1981), and especially the dry austral winter season is affected by the strength of the El Niño - Southern Oscillation (ENSO), causing strongly variable conditions in water availability in eastern Australia (Van Oldenborgh and Burgers, 2005). Therefore the reconstructed hydrological changes are likely related to variations in past ENSO dynamics.

A detailed intercomparison of Holocene records is needed to determine whether past changes were concurrent across Australia, and consistent with climatic patterns that are associated with changes in ENSO dynamics (Gagan *et al.*, 2004). The Lake Allom high-resolution reconstruction provides a crucial link between available tropical and temperate records, and may therefore become an important focus point for record-intercomparison.

Transition of the eastern Australian climate system from the post-glacial to the present-day ENSO mode

Abstract

A review of Holocene climate patterns in eastern Australia is presented on the basis of a series of high-resolution pollen records across a North-to-South transect. Previously published radiocarbon data are calibrated into calendar years and fitted with an age-depth model. The resulting chronologies are used to compare past environmental changes and describe patterns of climate change on a calendar-age scale. Based on the present-day Australian climate patterns and impact of the El Niño – Southern Oscillation (ENSO), the palynological data are interpreted and the prevalent climate mode throughout the Holocene could be reconstructed. Results show that early Holocene changes are strongly divergent and asynchronous between sites, while middle to late Holocene conditions are characterized by more arid and variable conditions and greater coupling between northern and southern sites in agreement with increasing influence of ENSO.

7.1. Introduction

Australian vegetation and wildlife is well adapted to climate fluctuations imposed by the ENSO system (Nichols, 1992). The high adaptation capacity implies that this region is well suited for paleoclimatic studies related to the history of ENSO dynamics. Investigating Holocene ENSO variability is particularly important because in this time interval the effects of changes in background climate, caused by orbital precession, can be studied independently of large, long-term variations in global ice cover and sea level (Markgraf and Diaz, 2000).

Currently, ENSO causes significant interannual climate variability in Australia (Dodson, 2001). The early Holocene Australian environment was characterized by generally lower variability compared to the present situation. It is therefore unlikely, that the ENSO system has continuously operated in the present-day mode throughout the entire Holocene (McGlone *et al.*, 1992). More arid and variable conditions seen in Australian tropical monsoon-dominated areas after 4 ^{14}C ky BP (~3.7 cal ky BP) have been attributed to the establishment of modern-day ENSO dynamics (Shulmeister and Lees, 1995). Strongly ENSO-teleconnected regions in South-America (McGlone *et al.*, 1992) and the Southeastern United States (Chapter 5) have shown similar changes in past ENSO state.

Holocene ENSO variability has likely caused synchronous changes across large parts of Australia, since it presently impacts a wide area. Numerous high-resolution palynological records of Holocene vegetation cover in Australia are available, which have the potential to recognize temporal and spatial patterns of past climate dynamics. In order to accurately resolve the development and role of ENSO, these records must be compared on a calendar age-scale. However, available reviews of continental (Harrison, 1993; Hope *et al.*, 2004) or regional (Kershaw, 1994; Dodson, 1998; 2001; Dodson and Ono, 1997) vegetation and climate patterns ins Australian do not focus on the high-resolution detection of Holocene changes. Most published pollen records have been radiocarbon-dated, but especially pre-1993 records were not calibrated into calendar ages.

The present review provides a regional synthesis of environmental change documented in new and earlier published, high-resolution palynological records along a North-to-South transect in eastern Australia. Conversion to calendar ages of previously published radiocarbon data enables a more accurate comparison of the available records, allowing better assessment of both temporal and spatial patterns of environmental change. Re-evaluation of palynological records may reveal information on the differentiation of the climate system from the early Holocene mode to present-day ENSO forcing. Accurate timing further allows to test whether past changes in ENSO dynamics have resulted in synchronous vegetation changes are comparable with the recent impact pattern of ENSO.

7.1.1. Australian climate

The major patterns of the Australian climate are determined by a high-pressure belt positioned below the subtropical jet-stream across southern Australia. Anticyclonic activity moves eastward across the continent, causing arid conditions. During winter the high-pressure belt shifts northward to ~29-32 °S, allowing westerly winds to bring winter rainfall to the southern part of the continent. The developing northern monsoon during

Australian rainfall seasonality (After Magee *et al*., 2004)

1 Groote Eylandt, N.T. (Shulmeister, 1992; Shulmeister & Lees, 1995)
2 Lake Euramoo, Atherton Tablelands, Qld. (Kershaw, 1970; Haberle, 2005)
3 Quincan Crater, Atherton Tablelands, Qld. (Kershaw, 1971)
4 Whitehaven Swamp, Qld. (Genever *et al*., 2003)
5 Lake Allom, Fraser Island, Qld. (Chapter 6)
6 Barrington Tops, N.S.W. (Dodson *et al*., 1986)
7 Bega Swamp, N.S.W. (Green *et al*., 1988; Hope, in prep.)
8 Club Lake (Kosciuszko National Park), N.S.W. (Martin, 1986)
9 Sperm Whale Head, Vic. (Hooley *et al*., 1980)
10 Lake Frome, S.A. (Singh & Luly, 1991)
11 Middens, Flinders range, S.A. (McCarthy & Head, 2001)
12 Lake Tyrell, Vic. (Luly, 1993)
13 Fleurieu Peninsula, S.A. (Bickford & Gell, 2005)
14 Lake Leake, S.A. (Dodson, 1974)
15 Tower Hill, Vic. (D'Costa *et al*., 1989)
16 Lake Wangoom, Vic. (Edney *et al*., 1990)
17 Lake Johnston, Tas. (Anker *et al*., 2001)
18 Cynthia Bay, Tas. (Hopf *et al*., 2000)
19 Mt. Field (Eagle Tarn), Tas. (Macphail, 1979)

Figure 7.1 (Color version page 135) (A) Location of study sites and seasonality of annual rainfall (after Magee *et al*., 2004) across Australia.

(B-E) ENSO impact on Australian precipitation, expressed as a seasonally averaged correlation between gridded precipitation and the NINO3.4 index. Non-significant correlations are grey. Maps were made with KNMI Climate Explorer (Van Oldenborgh and Burgers, 2005).

SSS = Strongly seasonal, summer rain
WSS = Weakly seasonal, summer rain
UD = Uniform distribution
WSW = Weakly seasonal, winter rain
SSW = Strongly Seasonal, winter rain

Correlation NINO3.4 index with CRU precipitation (3-month averaged)

B) Jan-Mar (Sum)
C) Apr-Jun (Fall)
D) Jul-Sep (Win.)
E) Oct-Dec (Spr.)

-0.6 -0.5 -0.4 -0.3 -0.2
Correlation index

summer displaces the pressure belt southward to ~37-38 °S, thereby blocking westerly winds from southern Australia. Only western Tasmania receives precipitation all year round (Harrison, 1993; Dodson, 1998).

Winds developing on the equatorial side of anticyclonic spirals form the southeasterly trade winds (tropical easterlies), which are the dominant source of precipitation in the northeast. Occasional northwesterly monsoonal flows and associated tropical cyclones cause intensive but infrequent rainfall events during the austral summer when the intertropical convergence zone (ITCZ) is at its most southerly extent (Godfred-Spenning and Reason, 2002). The tropical cyclones are an important rainfall source for the arid interior and for general summer rainfall across the continent. Due to the monsoonal activity and migration of the high-pressure belt, southern areas experience a winter precipitation peak while northern areas mainly receive summer precipitation. The subtropical areas are intermediate and generally much less seasonal (Fig. 7.1A, after Magee *et al.*, 2004).

7.1.2. ENSO impact
At present, significant precipitation variability is generated by ENSO (Van Oldenborgh and Burgers, 2005), especially across the eastern side of the Australian continent (Dodson, 1998; 2001). During El Niño episodes, an Equator-ward movement of the ITCZ and a northeastward migration of the South Pacific convergence zone result in a significant decrease of summer precipitation in eastern Australia. In the northeastern tropics the deficit amounts to 150–300 mm below seasonal average (Dai and Wigley, 2000). Strong Walker circulation or La Niña conditions intensify moist monsoonal flow over the dry eastern interior, and to the north and east due to enhanced trade winds. Variations in ENSO dynamics affect the trade wind system and therefore influence the eastern Australian climate synchronously from North-to-South. Figs. 7.1B-E show the seasonal correlation between ENSO, expressed as the NINO3.4 index, and precipitation.

However, independent changes in the mean subtropical high-pressure belt position also significantly influence Australian climate (Pittcock, 1978; Harrison, 1993). In records of past climate, variation caused by changing ENSO dynamics can be distinguished from high-pressure belt migration since the latter causes non-synchronous changes from North-to-South (Dodson, 1998).

7.1.3. Last Glacial to early Holocene atmospheric circulation
The high-pressure belt and westerlies were displaced Southwards during Glacial periods, depriving coastal areas, including Tasmania, of moist winter conditions (Harrison, 1993). Glacial dune patterns in the arid interior indicate stronger circulation and reduced monsoonal flow (Hesse *et al.*, 2004). Conditions were more homogeneous and generally drier, while interior temperatures were strongly reduced (Hope *et al.*, 2004). Reduced evaporative water loss caused some arid regions to experience less severe drying (Harrison, 1993). Glacial/Interglacial changes in the Walker circulation, which would affect moisture transport by easterly trade winds, were obscured due to the general cooler and drier conditions.

7.1.4. Insolation during the Holocene

The dominant factor controlling Holocene climate variation is the orbital or Milankovitch forcing of insolation. Estimates of solar irradiance and seasonality for the past 15 ky BP in summer and winter are given in Fig. 7.2A for the Equator, 30 ° North and 30 ° South, based on the Laskar-90 solution (Laskar *et al.*, 1990). Fig. 7.2B shows the winter and summer gradient strength between 60 °S / 30 °S and the Equator. During the late Holocene the Southern Hemisphere experienced increased seasonality and summer warmth, but a reduced gradient between tropical and temperate areas, which implies a reduction of westerly airflow (Dodson, 1998). Northern winter insolation is an important control for the ITCZ position, which determines the Australian monsoon intensity (Magee *et al.*, 2004). Ocean-atmosphere modeling studies suggest that the seasonality changes caused by orbital precession are a major control over long-term ENSO variability through asymmetric heating of the Equatorial Pacific (Turney *et al.,* 2004).
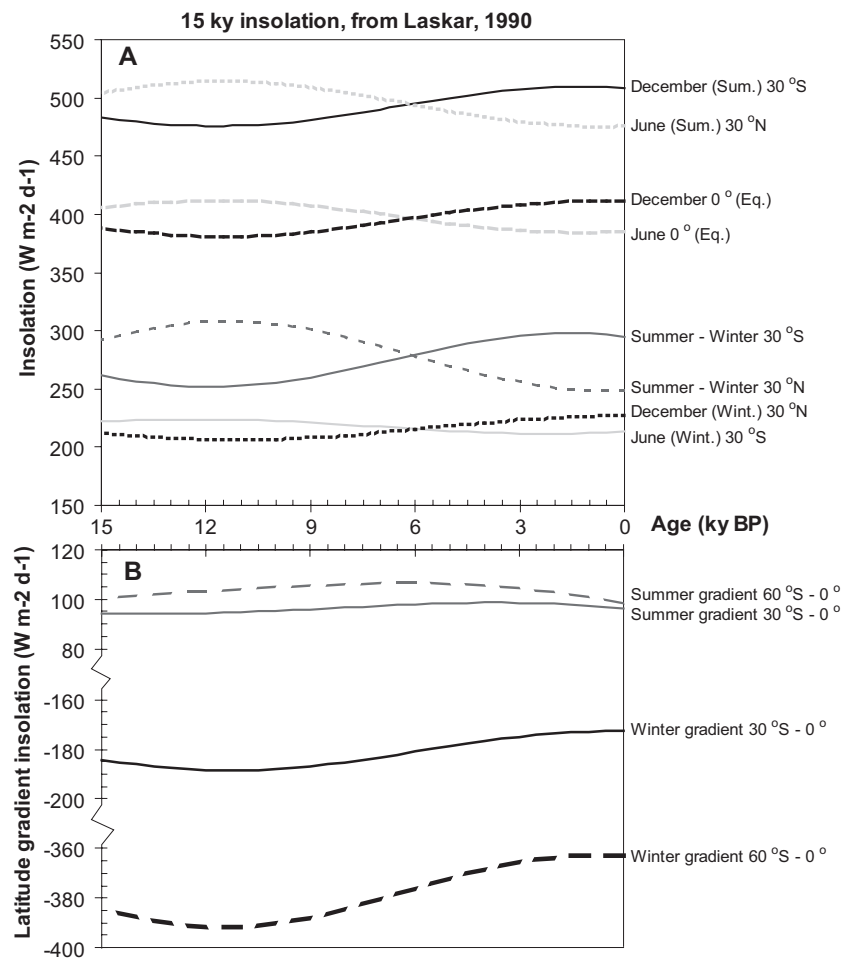
Figure 7.2 (A) December and June insolation values and seasonal amplitude for the equator, 30 °N and 30 °S during the last 15 ky based on the Laskar-90 orbital solution (Laskar, 1990). (B) Estimated mean insolation differences between the Equator and 30/60 °S for Summer and Winter.

7.2. Study sites

7.2.1. Data selection

Localities were selected on the basis of sample resolution (<500 yr/sample) and independent dating control (Table 7.1). In areas with abundant pollen records, such as Victoria and Tasmania, well-dated continuous records were preferred. Records are discussed per climate region as a) Monsoonal / Northern tropical, b) Subtropical, c) Temperate / eastern coast, d) Inland arid, e) Mediterranean-type and f) Southern temperate types. Records from the arid interior are important since they are particularly responsive to precipitation changes, and do not suffer from orographic effects that cause local rainfall anomalies (Shulmeister and Lees, 1995). Coastal records are more abundant and located in areas with strong ENSO control, but are often not independent of sea level changes.

Three high-resolution records, Lake Euramoo (Haberle, 2005), Lake Allom (Chapter 6) and Bega Swamp (Green *et al.*, 1988; Hope *et al.*, 2004), are used as a basis for the comparison. All three records are located in a highly ENSO-sensitive region (Fig. 7.1) and are well-dated, allowing detailed spatial and temporal comparison. The main trends of these records are represented by principal component analysis (PCA) output, based on major dry land taxa. The three key-sites are subsequently compared with newly calibrated records from other localities across eastern Australia to assess the patterning or consistency of climatic changes throughout the Holocene.

7.2.2. Chronology

Available radiocarbon data are calibrated into calendar ages for all sites (Table 7.1). For each previously un-calibrated record an age-depth curve is plotted (Fig. 7.3). Depending on the fit to the data, a linear or 2nd order model is used to describe the age-depth relationship. Published age-depth models based on calibrated ages (Anker *et al.*, 2001; Bickford and Gell, 2005; Haberle, 2005; Chapter 6) are applied unchanged (Fig. 7.3). Subsequently, the main conclusions and times of major vegetation change as described in the original publications were adjusted according to the new age-depth models. Although the calibrated records allow a much better comparison of temporal patterns than records on a ^{14}C-age base, significant differences in resolution and age model quality still exist.

Table 7.1 (right page) Pollen sites used in present study and radiocarbon data with calendar ages of previously uncalibrated records. Radiocarbon ages were calibrated with OxCal 3.10 (Bronk-Ramsey, 1995; 2001), using the SHCAL04 Southern Hemisphere calibration dataset (McCormack *et al.*, 2004). For ages older than 10 ^{14}C ky BP the INTCAL04 (Reimer *et al.*, 2004) dataset was used.

Radiocarbon age ranges of the Bega Swamp record are mostly duplicate samples. In the upper 150 cm they show little scatter and are assumed to be in chronological order. A Bayesian statistical function within OxCal combines duplicate samples and uses the prior assumption about sample order to reduce age ranges of overlapping radiocarbon data (Bronk-Ramsey, 2000). Subsequently, the reduced 1σ intervals were used for construction of the age-depth model.

#	Site & author	State	Lab code (ANU)	Depth cm	range cm	^{14}C age yr BP	sd yr	Method	Cal. age yr BP	sd yr	Calib.	Modeled yr BP	sd
1	Groote Eylandt Shulmeister, 1992	N.T.	7108	13	5	980	170	conv.	825	155	shcal04		
			7109	43	5	3960	170	conv.	4300	300	shcal04		
			7110	73	5	4200	100	conv.	4695	135	shcal04		
			7111	105	5	7450	90	conv.	8205	145	shcal04		
			7112	118	5	9250	230	conv.	10350	400	shcal04		
			7113	122	5	8690	200	conv.	9775	375	shcal04		
			AA 6460	150	5	10000	75	conv.	11425	185	shcal04		
2	Lake Euramoo Haberle, 2005	Qld.	See publication					210Pb			CIC		
			See publication					AMS			Intcal98		
3	Quincan Crater Kershaw, 1971	Qld.	See publication					conv.			n.a.		
4	Whitehaven Swamp Genever *et al.*, 2003	Qld.	WK 9389	500	10	6957	58	n.s.	7735	65	shcal04		
5	Lake Allom Chapter 6	Qld.	See publication					AMS			shcal04		
6	Barrington Tops Dodson *et al.*, 1986	N.S.W.	See publication					conv.			n.a.		
7	Bega Swamp Singh & Hope, unpublished	N.S.W.	5390B	17.5	0.5	109	3	conv.	135	145	shcal04	87	48
			5390A	17.5	0.5	100	2	conv.	135	145	shcal04		
			5391A	45	0.5	890	120	conv.	680	120	shcal04	779.5	120
			5391C	45	0.5	810	170	conv.	660	140	shcal04		
			5690A	61.8	0.5	2270	110	conv.	2225	235	shcal04	2255	105
			5690B	61.8	0.5	2430	120	conv.	2545	205	shcal04		
			5691A	68	0.5	2590	120	conv.	2625	275	shcal04	2615	125
			5691B	68	0.5	2540	110	conv.	2570	210	shcal04		
			5692A	73.8	0.5	3080	100	conv.	3455	185	shcal04	2840	70
			5692B	73.8	0.5	2730	100	conv.	2915	145	shcal04		
			5392A	79	0.5	2150	260	conv.	2150	600	shcal04	2885	75
			5392B	79	0.5	2530	160	conv.	2565	235	shcal04		
			5693A	91	0.5	3170	130	conv.	3615	215	shcal04	3220	150
			5693B	91	0.5	2970	170	conv.	3300	300	shcal04		
			5694A	102.2	0.5	3550	110	conv.	4195	215	shcal04	3725	115
			5694B	102.2	0.5	3440	150	conv.	3925	325	shcal04		
			5695A	111.5	0.5	3920	100	conv.	4900	400	shcal04	4020	130
			5695B	111.5	0.5	3210	150	conv.	3645	245	shcal04		
			5696A	122	0.5	4390	230	conv.	5700	650	shcal04	4725	145
			5696B	122	0.5	4270	100	conv.	5400	350	shcal04		
			5697A	132.4	0.5	4370	140	conv.	5725	275	shcal04	5055	215
			5697B	132.4	0.5	4470	140	conv.	5825	375	shcal04		
			5698A	144.8	0.5	4940	120	conv.	6475	165	shcal04	5525	195
			5698B	144.8	0.5	4710	230	conv.	6075	375	shcal04		
			5699A	156.4	0.5	6040	70	conv.	7685	105	shcal04	7627	43
			5699B	156.4	0.5	7960	100	conv.	9850	300	shcal04		
			5700A	167.9	0.5	5890	90	conv.	7545	125	shcal04	7810	110
			5700B	167.9	0.5	7960	100	conv.	9850	300	shcal04		
			5701A	170	0.5	8380	70	conv.	10550	140	shcal04	9070	80
			5701B	170	0.5	7250	150	conv.	8925	325	shcal04		
			5702A	181	0.5	7850	200	conv.	9825	375	shcal04	9250	160
			5702B	181	0.5	8500	210	conv.	10700	500	shcal04		
			5703A	203	0.5	6610	230	conv.	8215	205	shcal04	7425	245
			5704B	210	0.5	9440	70	conv.	10675	115	shcal04	10605	95
			5705	220	0.5	10910	130	conv.	12900	100	intcal04	12885	85
			5706A	230	0.5	11540	130	conv.	13400	150	intcal04	13115	115
			5706B	230	0.5	9940	220	conv.	11600	450	intcal04		
			5710A	267.5	0.5	12060	230	conv.	13950	350	intcal04		
			5710B	267.5	0.5	10920	480	conv.	12800	650	intcal04	13720	250

Table 1: continued

#	Site & author	State	Lab code	Depth	range	^{14}C age	sd	Method	Cal. age	sd	Calib
				cm	cm	yr BP	yr		yr BP	yr	
8	Kosciuszko Nat. Park	N.S.W.	GAK 2790	40	2.5	1180	100	conv.	1055	125	shcal
	Martin, 1986		GAK 3931	150	2.5	3260	90	conv.	3450	110	shcal
	(Club Lake I)		GAK 3932	205	5	3380	90	conv.	3570	120	shcal
			NZ 317	300	5	4400	90	conv.	5020	200	shcal
			W 770	310	5	4580	220	conv.	5175	325	shcal
			SUA 2250	455	5	6520	100	conv.	7365	95	shcal
			GAK 2791	530	5	6870	160	conv.	7670	160	shcal
			GAK 1192	625	5	6680	120	conv.	7515	95	shcal
9	Sperm Whale Head	Vic.	GX 5592	180	10	5080	180	conv.	5785	205	shcal
	(Hidden Swamp)		GX 5593	260	5	6840	150	conv.	7645	145	shcal
	(Loch Sport Swamp)		GX 4952	70	2	4430	150	conv.	5060	230	shcal
	Hooley *et al.*, 1980		GAK 1815	210	5	7200	320	conv.	8000	350	shcal
10	Lake Frome (Holocene part)	Vic.	ANU 3147	25	5	3180	100	conv.	3335	125	shcal
	Singh & Luly, 1991		ANU 3148	85	5	10850	320	conv.	12750	400	intcal
11	Flinders Range	S.A.	See publication					AMS			n.a.
	McCarthy & Head, 2001										
12	Lake Tyrell	Vic.	ANU 3066	46	2	3150	500	conv.	3350	700	shcal
	Luly, 1993		ANU 3070	64	2	5570	200	conv.	6250	250	shcal
			ANU 3071	78.5	2.5	4840	140	conv.	5490	170	shcal
			NZA 192	90	0.5	7215	270	AMS	7975	325	shcal
			NZA 193	90	0.5	7425	445	AMS	8150	500	shcal
			ANU 3067	112.5	2.5	7460	1030	conv.	8350	1200	shcal
			ANU 3068	132.5	2.5	10150	1650	conv.	11550	2100	intcal
13	Fleurieu Peninsula	S.A.	See publication					210Pb			CRS
	Bickford & Gell, 2005		See publication					conv.			intcal
14	Lake Leake	S.A.	ANU 1143	82.5	2.5	1360	140	conv.	1200	140	shcal
	Dodson, 1974		ANU 1143	172.5	2.5	2030	160	conv.	1925	205	shcal
	0-10 ky BP		ANU 1143	257.5	2.5	2960	80	conv.	3065	145	shcal
			ANU 1142	367.5	2.5	7860	110	conv.	8585	165	shcal
			ANU 1017	402.5	2.5	9470	120	conv.	10750	350	shcal
			ANU 1016	422.5	2.5	8530	110	conv.	9425	125	shcal
15	Tower Hill	Vic.	Beta 15096	525	10	5630	110	conv.	6385	115	shcal
	D'Costa, 1989		Wk 935	710	5	7730	130	conv.	8470	130	shcal
			Wk 926	985.5	2.5	11550	160	conv.	13420	170	intcal
	(North Core)		Wk 927	1115	10	15100	180	conv.	18400	300	intcal
	(Main Lake)		ARL 138	575	15	4660	170	conv.	5300	300	shcal
			Beta 9903	702.5	12.5	7400	90	conv.	8160	140	shcal
			ARL 159	957.5	12.5	11400	200	conv.	13265	195	shcal
16	Lake Wangoom	Vic.	Wk 789	202.5	2.5	5390	110	conv.	6130	140	shcal
	Edney *et al*, 1990		SUA 2427	297.5	2.5	7650	90	conv.	8430	110	shcal
	(Holocene section)		ARL 164	415.5	4.5	9160	200	conv.	10250	350	shcal
17	Lake Johnston	Tas.	See publication					n.s.			intcal
	Anker *et al.*, 2001										
18	Cynthia Bay	Tas.	OZD 693	55	0.5	4290	70	AMS	4745	125	shcal
	Hopf, 2000		Beta 108148	115	1	6420	50	AMS	7335	85	shcal
			OZD 694	155	0.5	8000	60	AMS	8810	170	shcal
			Beta 106999	229	1	11210	50	AMS	13130	60	intcal
			OZD 695	260	0.5	18450	100	AMS	22060	160	intcal
19	Mt. Field	Tas.	I 7585	245	15	5600	150	conv.	6325	205	shcal
	MacPhail, 1979		SUA 323	400	10	9960	300	conv.	11600	550	intcal
	(Eagle Tarn)		I 7684	454.5	9.5	11400	235	conv.	13275	225	intcal

n.a.: not applicable, see main text	intcal98: Stuiver *et al.*, 1998
n.s.: not specified in original publication	intcal04: Reimer *et al.*, 2004
N.T.: Northern Territory	shcal04: McCormack *et al.*, 2004
Qld.: Queensland	conv..: conventional radiocarbon date
N.S.W.: New South Wales	AMS: Accelerator mass spectrometry radiocarbon date
S.A.: South Australia	CRS: constant rate of supply model
Vic.: Victoria	CIC: constant initial concentration model
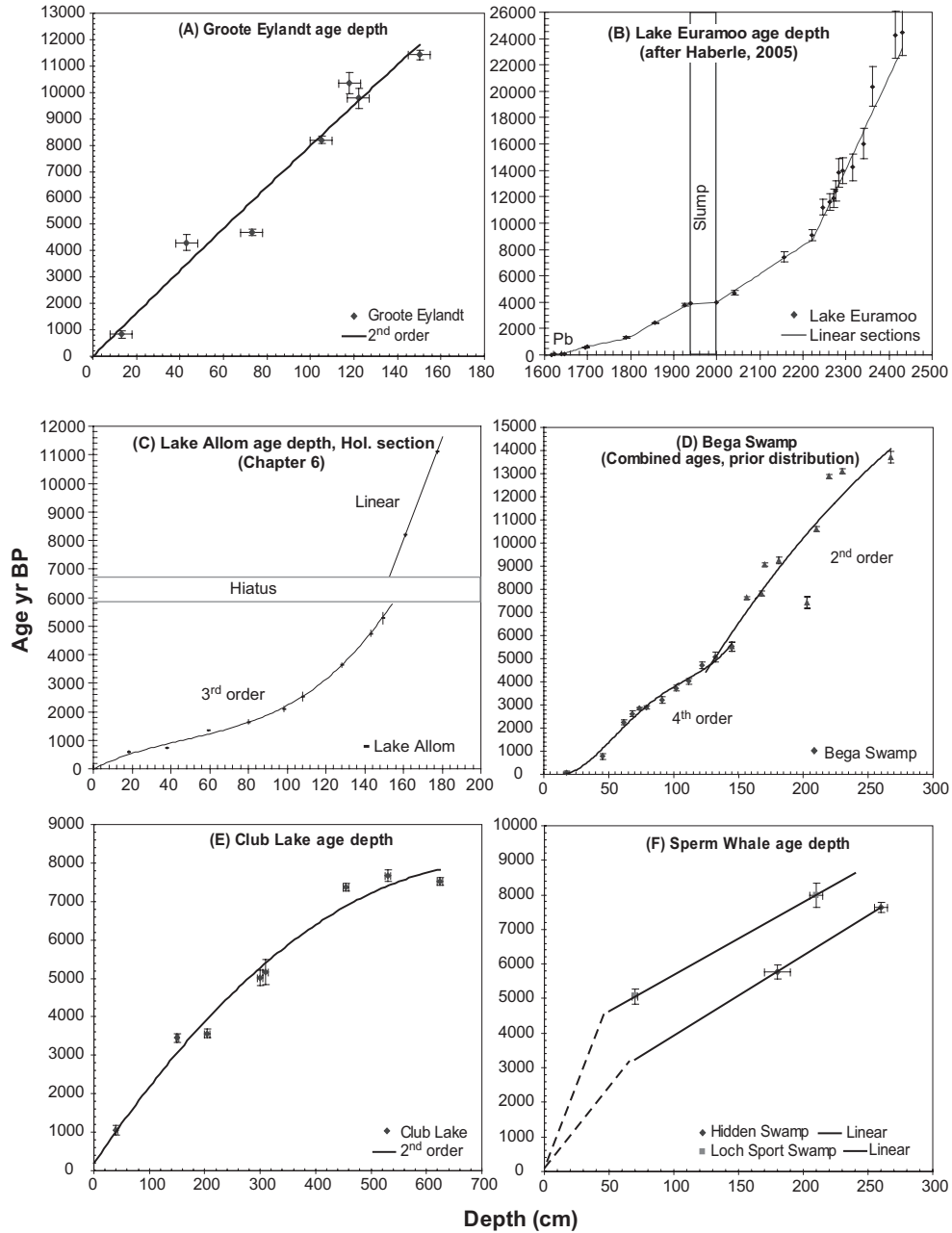
Figure 7.3 (continued on next page) Calibrated ages with 1σ ranges for age and sample depth (A-O). Age-depth models are based on linear or 2nd order fits to the data (top = present, except for the Sperm Whale Head site). Originally published 2σ ranges are given for the Fleurieu Peninsula (O), Lakes Euramoo (B) and Johnston (N) sites. The Bega Swamp (D) age-depth model below 150 cm is preliminary due to the high scatter. Note use of different axes scales between graphs.
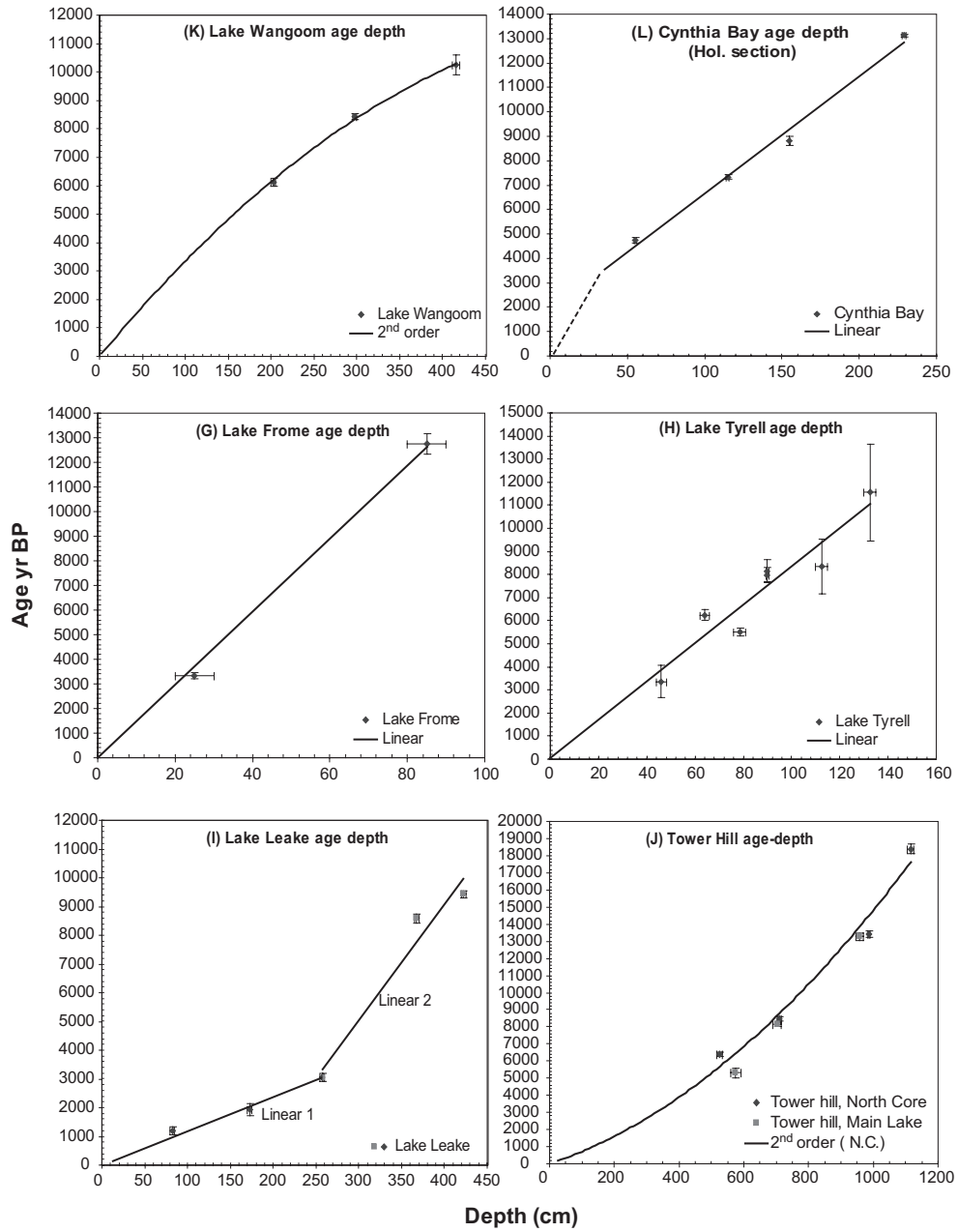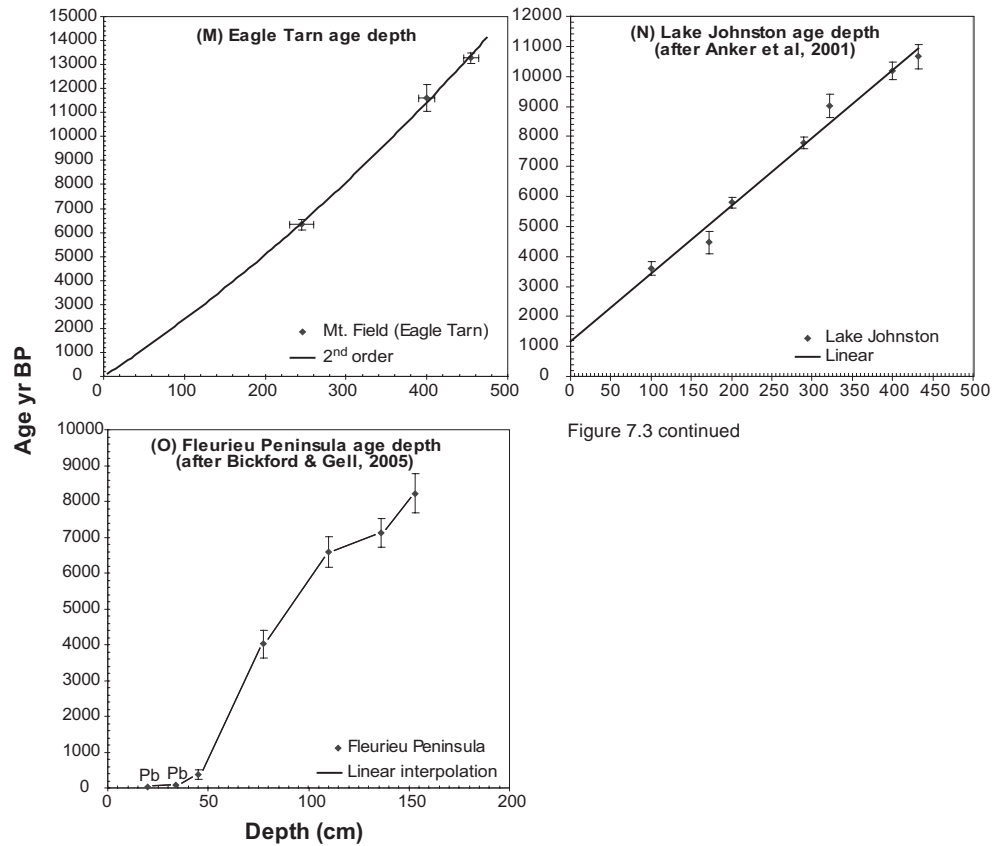
Figure 7.3 continued

(M) Eagle Tarn age depth

♦ Mt. Field (Eagle Tarn)
— 2nd order

(N) Lake Johnston age depth
(after Anker et al, 2001)

♦ Lake Johnston
— Linear

Figure 7.3 continued

(O) Fleurieu Peninsula age depth
(after Bickford & Gell, 2005)

♦ Fleurieu Peninsula
— Linear interpolation

Pb Pb

Age yr BP

Depth (cm)

7.3. High-resolution records of Holocene vegetation

The three principal detailed Holocene records from regions with high ENSO-impact are summarized individually. Figs. 7.4A-F shows the PCA output for the first and second axes of these records, indicating the main trends in the dry land taxa.

7.3.1. Northern tropics - Lake Euramoo (Atherton Tablelands)

The northern Queensland Atherton Tablelands have been studied extensively and yielded multi-proxy datasets that raise a picture of a highly dynamic landscape, sensitive to both climate change and human activity on timescales ranging from millennia to decades (Haberle, 2005). The area has a climate dominated by easterly tradewinds and a secondary monsoonal influence (Hope *et al.*, 2004). The tablelands, which uplifted during the Tertiary, support the most significant tropical rainforest area of Australia. Precipitation is ~1500 mm/yr with a distinctly dry austral winter season. Mean daily maximum and minimum temperatures are ~25.9 °C and ~14.4 °C and rare frosts occur during the austral winter months at times of weak trade winds and low cloud cover.

The most comprehensively studied site on the Atherton Tablelands is Lynch's Crater (e.g. Kershaw, 1986; Turney *et al.*, 2004.). However, the Holocene section in Lynch's Crater is

highly condensed, and does not allow detailed analysis (Kershaw, 1983). An alternative site, Lake Euramoo (2, Fig. 7.1A) is located in a double eruption crater, with a small catchment and no in- or outflows.

The first detailed pollen record from this lake reported a rainforest maximum at ~7.0 ^{14}C ky BP (~6.2 cal ky BP) (Kershaw, 1970), interpreted as the result of increased effective precipitation, with reduced seasonality relative to the present day (Kershaw and Nix, 1988). A recent, more detailed record, from Lake Euramoo (Fig. 7.1A) confirmed and extended the earlier findings (Haberle, 2005). It documents vegetation change and fire history from 23 cal ky BP to the present, with a high resolution of ~100 yr/sample during the last 9 ky BP. The Holocene chronology of the record is based on ^{210}Pb and 11 AMS ^{14}C measurements (Fig. 7.3B).

The main change at Euramoo occurs at 8.7 cal ky BP when dominance of sclerophyllous vegetation changed to rainforest, which reached maximum abundance and diversity at 7.3 cal ky BP. A concurrent charcoal influx minimum occurred between 7.3-6.3 cal ky BP. After 5.0 cal ky BP, rainforest changed into a more open and drought/disturbance-adapted vegetation type, characterized by increased *Agathis*, *Elaeocarpus* and *Mallotus/Macaranga*. Charcoal influx increased significantly after 2.7 cal ky BP (Fig. 7.4G). Effects of human occupation are evident from 120 cal yr BP, when forest clearing and burning caused rapid rainforest destruction.

The PCA results clearly show the attainment of modern rainforest (Figs. 7.4A, B). Axis 1 contrasts *Casuarina*/Poaceae with rainforest taxa, which is precipitation related. Axis 2 contrasts sub-montane/secondary rainforest species, related to increased disturbance or burning, with lower montane closed rainforest taxa as Cunoniaceae and Urticaceae/Moraceae (Haberle, 2005).

The trend toward increased disturbance or burning is very gradual and values become stable after 4.8 cal ky BP, although the main increase in fire-frequency is after 2.7 cal ky BP (Fig. 7.4G). The major Holocene shifts in the Lake Euramoo are rather subtle changes between different rainforest types, and are therefore not very pronounced in the PCA diagram. An additional record from Quincan Crater (3, Fig 7.1A, Kershaw, 1971) provides independent corroboration of the changes recorded at Lake Euramoo, although no detailed comparison is made here.

Figure 7.4 (right page) Principal component analysis (PCA) results of well-dated, high-resolution sites in Australia, showing the first 2 axes against time with the originally published pollen zonation. Bega Swamp and Lake Allom data was limited to dry land taxa exceeding 2% abundance at least once. *Eucalyptus* types were combined to omit multiple-person counting errors for Bega Swamp. Lake Euramoo data was limited to taxa exceeding 5% abundance at least once (Haberle, 2005). All data were square root transformed and PCA was performed with C[2] software (Juggins, 2003).

The Lake Euramoo PCA axis 1 (**A**) contrasts *Casuarina*/Poaceae with rainforest taxa, which is precipitation related. Axis 2 (**B**) contrasts sub-montane/secondary rainforest species, indicative of increased disturbance or burning, with lower montane closed rainforest taxa as Cunoniaceae and Urticaceae/Moraceae (Haberle, 2005). Lake Allom PCA axis 1 (**C**) contrasts *Casuarinaceae* with (araucarian) rainforest, while the axis 2 (**D**) shows disturbance related alterations between *Casuarinaceae/Araucaria* and *Eucalyptus/*heath-taxa. Bega Swamp PCA axis 1 (**E**) contrasts forest with open vegetation, while axis 2 (F) mostly contrasts dry Asteraceae/*Casuarina*/Chenopodiaceae with moist *Pomaderris*/heath and fern taxa. Charcoal accumulation rates for Lakes Allom and Euramoo (**G**) indicate fire frequency at the sites.
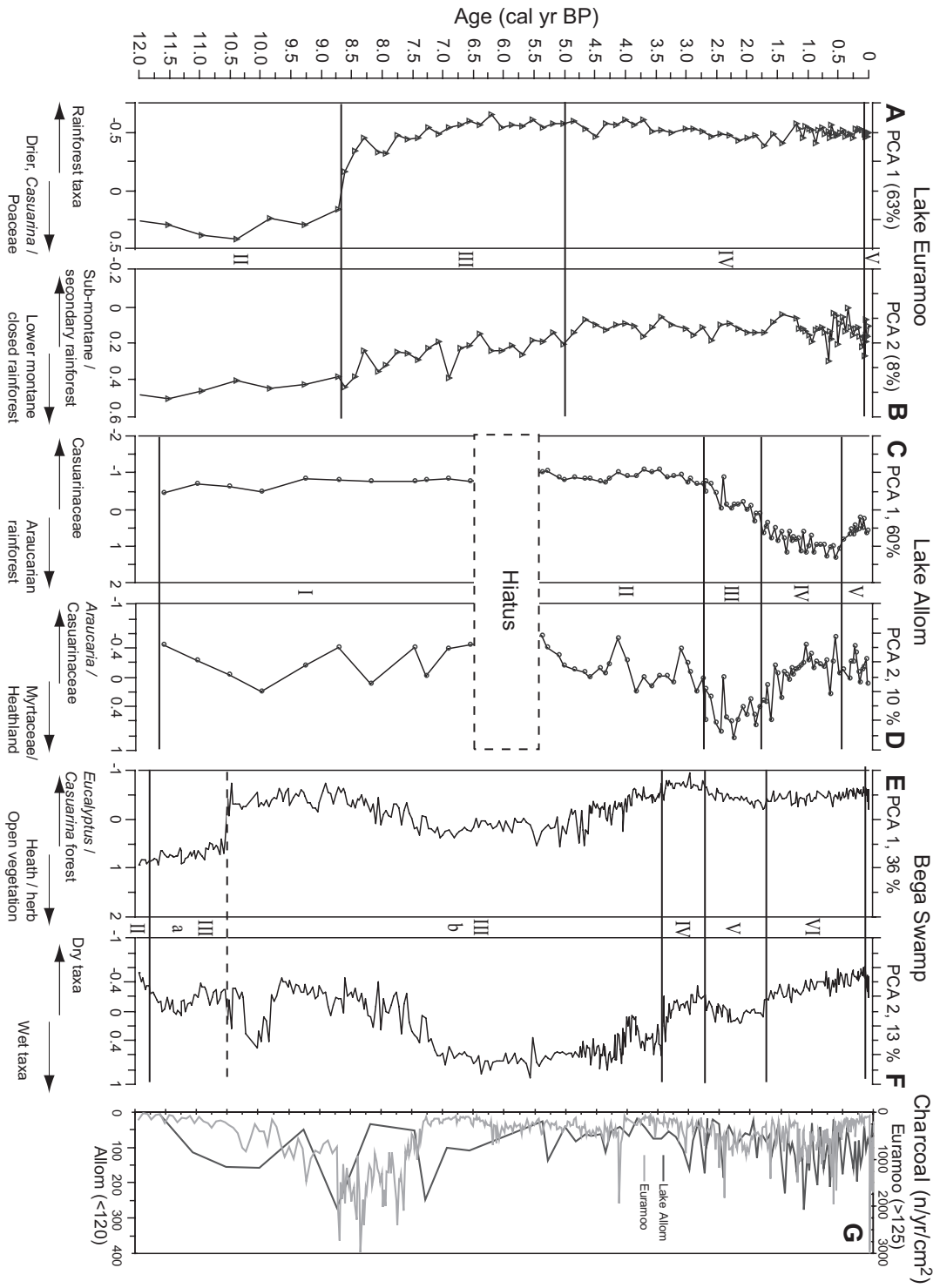
7.3.2. Subtropics - Lake Allom (Fraser Island)

A recent detailed pollen record from Lake Allom (5, Fig. 7.1A), Fraser Island reveals past vegetation changes in the tropical to temperate transition zone in Australia (Chapter 6). Fraser Island is a large Pleistocene dune system off the south-eastern Queensland coast characterized by numerous perched lakes, which act as very sensitive rainfall gauges (Longmore, 1997).

South-eastern Queensland has as a warm subtropical slightly seasonal humid climate (Webb, 1994), where temperatures range between ~14 °C in winter and ~29 °C in summer. Regional annual rainfall varies between 1300 to 1700 mm/year, and a moisture deficit occurs in the drier winter/spring season (Walker, 1981). Island vegetation is a mosaic of mixed subtropical rainforest in moist patches, to dry sclerophyll forest, heath and coastal vegetation in drier areas.

The Holocene section of the Lake Allom record is dated by 11 AMS ^{14}C ages and especially the upper half has a high temporal resolution of ~65 yr/sample. Low sea-levels during the early Holocene created dry continental conditions, with low accumulation rates, low lake levels, active dune formation and high fire frequencies (high charcoal influx, Fig. 7.4G). A short hiatus between 6.5 and 5.4 cal ky BP marks the onset of distinctly different conditions with high lake levels, forest succession and reduced fire frequency between 5.5 and 3 cal ky BP.

After 2.7 cal ky BP, a large diversification occurred towards the present-day heterogeneous subtropical rainforest vegetation. Lake level was slightly lower and fire frequency increased after ~2 cal ky BP (Chapter 6).

A small araucarian rainforest decline at 0.45 cal ky BP, well before European settlement of Australia, indicates sub-optimal growth conditions possibly caused by a temperature decrease (Chapter 6).

The Lake Allom PCA results (Figs. 7.4C, D) reflect the diversification in the pollen record. The first axis documents the shift to araucarian rainforest at ~2.7 cal ky BP, while the second axis shows disturbance related alterations between eucalypt forest and *Casuarina* from 5.5 cal yr BP onwards. These changes are accompanied by increased fire frequencies (Fig. 7.4G). Relatively stable conditions are attained after 1.5 cal ky BP.

7.3.3. Temperate – Bega Swamp

Bega Swamp (7, Fig. 7.1A) is a mire located 50 km inland, on the south-eastern edge of the Southern Tablelands in New South Wales and represents a more temperate record influenced by westerly winds. The catchment has low relief and gradient, favoring undisturbed accumulation. Annual rainfall is ~1000 mm/yr and limits plant growth in this region. Winter is relatively dry although seasonal variation is small. The swamp is surrounded by wet tall, open sclerophyll forest, with a rich shrub and herb understorey, containing elements as Asteraceae, *Acaena*, *Ranunculus*, *Hydrocotyle*, *Plantago*, *Wahlenbergia*, *Gonocarpus*, *Blechnum* and *Pteridium* (Green *et al.*, 1988).

A detailed study based on pollen traps and annual-resolution analyses of peat from the site focused on annual pollen production variability and in-wash in the mire. Results showed that pollen deposition and influx into the mire is controlled by spring and summer precipitation, respectively (Green *et al.*, 1988).

A 2.7 m peat profile from the mire has been analyzed at very high resolution, ~30 yr/sample during the last 15 ky BP, and has been dated by 39 conventional ^{14}C dates from 21 sample horizons (Hope *et al.*, 2004; Singh & Hope, unpublished results). A revised age-depth model is given in Fig. 7.3D, and is used in the interpretation of the record.

The main early Holocene forest expansion occurs around 10.5 cal ky BP, with increased *Eucalyptus*, *Casuarina*, *Pomaderris* and *Cyathea*. A mid-Holocene wet phase, characterized by expansion of wet heath and ferns, started around 7.5 cal ky BP, followed by Eucalypt expansion and drier conditions after 3.5 cal ky BP. Short centennial alterations between wet and dry taxa can be observed in the record (Fig. 7.4F). After 1.7 cal ky BP assemblages remained relatively stable until, around 100 cal yr BP, forest cover slightly declined caused by European settlement and deforestation.

PCA results provide a good summary of the pollen record (Figs. 7.4E, F). The first axis corresponds to changes between forest and open vegetation, while the second axis mostly represents the dry-wet alterations.

7.4. Regional comparison of Holocene vegetation changes
7.4.1. a) Monsoonal and northern wet tropics
Lowland tropical sites potentially provide the best sources of past climate change since upland areas, such as the Atherton Tablelands, are climatically somewhat a-typical. They receive orographic rain, which is susceptible to wind direction (Shulmeister and Lees, 1995). The only detailed Holocene record from the seasonally humid lowland tropics of Northern Australia is the Four Mile Billabong profile from Groote Eylandt (1, Fig. 7.1A), Northern Territory (Shulmeister, 1992). The site is a perennial lake within a dune field and is located within the strongly seasonal monsoonal tropics.

The pollen record reflects an early Holocene increase in effective precipitation during the post-Glacial sea-level rise, reaching a maximum between 8.4 and ~4.5 cal ky BP. A subsequent change to drier conditions during the late Holocene has previously been interpreted as indicative for the onset of present-day ENSO dynamics (Shulmeister and Lees, 1995). In the original study, the onset of dry conditions after 4 ^{14}C ky BP was based on a reconstructed decrease in pollen influx. This interpretation strongly depends on the accumulation rate that was used. Although the record has been dated by seven ^{14}C dates (Fig. 7.3A), the ages show a relatively high scatter. The reconstructed decrease in sedimentation rate was based on a single date, while organic content actually increases towards the core top (Shulmeister, 1992). Although, further dating would be needed to confirm the original conclusion, the record does show an expanse in swamp Restionaceae, higher charcoal and dry-land pollen during the late Holocene. Like at the Atherton Tableland sites (2, 3), these changes are indicative of more variable and/or drier conditions.

A lowland tropical record from Whitehaven Swamp (4, Fig. 7.1A), a semi-perched basin on Whitsunday Island, Queensland, confirms the general pattern of Holocene vegetation change in the Australian tropics (Genever *et al.*, 2003). The record has a fairly high resolution of ~140 yr/sample, but only a single basal ^{14}C date of 7735±65 cal yr BP. Similar to the Lake Allom record, early Holocene expansion of *Casuarina* is related to colonization of young dunes. The record reveals moister than present conditions between ~7.5 and 4.5 cal ky BP (based on a linear age-depth relation), followed by an increase in *Eucalyptus*. Although the site contains evidence of human presence, the vegetation shifts occur at the time of no substantial archeological change. Most likely the indigenous population did not significantly disrupt the vegetation, but adapted to dynamic ecosystem changes (Genever *et al.*, 2003).

Evidence for the ecosystem change in the Australian tropics is strong and while some chronologies could be improved, a consistent pattern emerges of increased disturbed and slightly drier conditions at 5 cal ky BP and further after 2.7 cal ky BP. Early Holocene changes are much more dissimilar and the attainment of the early to middle Holocene moisture maximum varies up to 1000 years between sites.

7.4.2. b) Subtropics

Apart from the recent Lake Allom (5) record (Chapter 6), few detailed subtropical Australian records exist. The only datasets available for comparison are from the inland Barrington Tops region (6, Fig. 7.1A, Dodson *et al.*, 1986). Eight upland sites between 1160 - 1530 m altitude provide a regional overview with a resolution of up to ~150 yr/sample. The site is located close to the present winter/summer rain boundary (Fig. 7.1A), and it is therefore sensitive to changes in moisture regime. Many of the records have a discontinuous accumulation and, although all have been radiocarbon dated, they are not discussed individually. The main conclusions of Dodson *et al.* (1986) were based on a radiocarbon age-scale, and have been adjusted according to the calendar age-scale in the present comparison.

Nothofagus moorei rainforest expanded on Barrington Tops from local refugia at 9 ky BP (10-10.2 cal ky BP). Between 6.5 and 3.5 ^{14}C ky BP (7.8-3.7 cal ky BP) cool temperate rainforest and wet-sclerophyll forest covered a larger area than present, likely caused by increased summer rainfall relative to today. Forest retreat began at 5 and lasted until 1.6 ^{14}C ky BP (5.6-1.4 cal ky BP). The changes were accompanied by increased fire intensity from 3.1 cal ky BP, while open lakes disappeared in favor of wetlands and bogs, which dramatically increased accumulation rates.

Similar to the tropical sites, there are some differences in the early Holocene records of between Barrington Tops and Lake Allom. The moisture optimum started significantly earlier at Barrington Tops, while both show higher fire intensity and slightly drier conditions after 3 cal ky BP. Conditions apparently stabilized after 1.5 cal ky BP at both sites, although some further small changes did occur.

7.4.3. c) Temperate - eastern coast

Bega Swamp (7) represents the most detailed pollen record available from temperate Australia. Other information is available from both coastal and alpine sites. Two records from a coastal lagoon system, Sperm Whale Head in eastern Victoria (9, Fig 7.1A), document a clear mid-Holocene moisture maximum (Hooley *et al.,* 1980). Although the barrier development is closely linked to sea-level changes, a late Holocene decrease in lake level and *Casuarina* abundance is in contrast with the effects of post-Glacial sea-level rise and likely results from changes in climate. Temporal resolution of the Hidden Swamp and Loch sport Swamp records is up to ~150 yr/sample but the chronologies do not agree (Fig. 7.3F). The Hidden Swamp radiocarbon data were obtained from a parallel core other than the one used for palynology, which might explain the temporal offset between both records.

The upland Club Lake site in Kosciuszko National Park, N.S.W. (8, Fig. 7.1A), has a better-constrained chronology (Fig. 7.3E). The site documents vegetation changes from the Late-Glacial to the present at 1950 m altitude in the Snowy Mountain range, which is an important climatic barrier between the westerlies and eastern tradewinds (Martin, 1986). A fen section adjacent to Club Lake is the best-dated and most detailed record from the site, ~200 yr/sample, and is used for the data comparison. Main tree expansion was before 7.5 cal ky BP, followed by a high moisture-related *Pomaderris* maximum between 7.5 and 6.5 cal ky BP. Different alpine taxa increase after 5.8 cal ky BP and alternate dominance after 3 ky. After 3.4 cal ky BP, *Pomaderris* is absent, *Pteridium* declined and the sedimentary regime indicates more variable conditions. However, this vegetation change was most likely not caused by a temperature decline since the position of the timberline was not negatively affected and even went upslope in the topmost samples (Martin, 1986).

Hence, temperature variability was likely small in the Holocene once modern conditions were reached. In accordance with late Holocene development at Bega Swamp, conditions became slightly drier after 6 cal ky BP and particularly drier and more variable after ~3.5 and 3 cal ky BP.

7.4.4. d) Arid interior

Two detailed Holocene records are available from the arid (eastern) interior of Australia, an area very sensitive to changes in precipitation and circulation patterns. Further data are available from stickrat (*Leporillus*) middens, but these records are not continuous. Lake Frome is close to the most arid center of Australia (10, Fig. 7.1A), at the summer-winter rainfall boundary (Singh and Luly, 1991). A Holocene pollen record from the lake indicates changes between arid Chenopodiaceae-Asteraceae shrub vegetation and grassland. Early Holocene grassland was more adapted to summer monsoon rain, which implies a persistent positive SOI or La Niña-like conditions (Singh and Luly, 1991). After 5.5-5 cal ky BP, the grass cover declined, followed by increases in *Acacia* and *Eucalyptus* and a decline in *Casuarina* after ~3 cal ky BP. However, the record has a low resolution, ~350 yr/sample, and is poorly dated (Fig. 7.2G), which precludes accurate comparisons.

The high-resolution Lake Tyrell site, with ~80 yr/sample, is located southeast of Lake Frome (12, Fig. 7.1A) and has a reasonably accurate chronology (Fig. 7.3H). Early Holocene

changes in Lake Tyrell are relatively small. Around 3.3 cal ky BP, *Casuarina* increase significantly in Lake Tyrell, in disagreement with the increase of *Acacia* and *Eucalyptus* seen at Lake Frome (Luly, 1993). This contradiction can be explained by the presence of extensive dunes around Lake Frome. Since *Casuarina* roots are capable of producing nitrogen through microbial associations, this genus can colonize nutrient-poor soils (Ng, 1987). Therefore, the late Holocene *Casuarina* increase likely reflects dune formation caused by slightly drier conditions, which is confirmed by the occurrence of evaporites in the sediment. Lake Tyrell is not located close to climatic boundaries, which likely explains the low variability in the record.

Pollen and macrofossil data from stickrat middens between Lakes Frome and Tyrell (11, Fig. 7.1A) confirm increased moisture relative to the present at 7-5 ^{14}C ky BP (~7.8-5.7 cal ky BP), and a more variable and drier climate at 4-2 ^{14}C ky BP (~4.4-1.9 cal ky BP) (McCarthy and Head, 2001).

7.4.5. e) Mediterranean climate – southern coast
The southern coast of eastern Australia is one of the best studied regions in Australia. Westerlies cause high precipitation during winter, while hot and dry summers are caused by southward expansion of the continental high-pressure system. Lake Leake, S.A.(14, Fig. 7.1A), is a volcanic crater lake perched by ash and clay with no long-distance water transport, which is highly sensitive to changes in precipitation regime (Dodson, 1974). A high-resolution pollen record from the lake, ~115 yr/sample, reveals a water table rise from dry swamp before 10 cal ky BP to maximum levels between 7.2 and 5.4 cal ky BP. Levels were higher than present between 7.2 and 3 cal ky BP (Dodson, 1974). The changes are mostly restricted to the aquatic vegetation, indicating that no environmental threshold was crossed for the regional forest vegetation.

The Tower Hill record in southwest Victoria (15, Fig. 7.1A) reveals changes that are concurrent with events at Lake Leake. Around 5 cal ky BP, *Casuarina* decreased and sclerophyllous vegetation expanded, followed by a slight reduction of the fern cover at 3 cal ky BP (D'Costa *et al.*, 1989). However, the onset of the early Holocene moisture maximum occurred earlier than at Lake Leake, around 8.4 cal ky BP. The temporal offset between the records is significant although the early Holocene chronology of Tower Hill is better constrained than at Lake Leake (Figs. 7.3I, J), despite lower sample resolution (~240 yr/sample).

Between 5 and 2 cal ky BP, *Casuarina* declined as well at Fleurieu Peninsula in eastern South Australia (13, Fig. 7.1A), favoring drier Myrtaceae, Chenopodiaceae and Asteraceae vegetation (Bickford and Gell, 2005). Although temporal resolution is low, ~400 yr/sample, the study further shows that Aboriginal burning affected the vegetation far less than the the impact of European settlement in the 19th century.

Similar to Lake Leake, Lake Wangoom is a closed crater lake sensitive to changes in precipitation (16, Fig. 7.1A). After the Late Glacial Maximum (LGM), sedimentation recommenced ~10.4 cal ky BP at Lake Wangoom. Pollen data from the site reveal a lake-level maximum between 8 and 5 cal ky BP, followed by decreasing and more variable

lake levels after ~3 cal ky BP (Edney *et al.*, 1990). The lake-level change was accompanied by a middle to late Holocene increase in fire occurrence.

The early Holocene dominance of *Casuarina* and the decline of the genus after 5 cal ky BP are consistent features in the southeastern pollen records, while most records indicate increased dry and variable conditions after 3 cal ky BP. However, the onset of early Holocene moist conditions is much more variable between records.

7.4.6. f) Southern temperate – Tasmania

Westerly winds influence Tasmania throughout the year since the island located south of the high-pressure belt, creating moist conditions and low seasonality mainly in western parts of the island (Harrison, 1993). *Nothofagus* rainforest characterizes the moist western side of the island, while *Eucalyptus* dominates the drier eastern side (MacPhail, 1979). Alpine vegetation in Tasmania is largely temperature dependent due to high altitudinal gradients (Anker *et al.*, 2001).

A detailed pollen profile from Lake Johnston, at 875 m altitude (17, Fig. 7.1A), provides one of the westernmost records from Tasmania. Maximum *Nothofagus* rainforest expansion was between 9.5 and 6.8 cal ky BP, with increased eucalypt and heath vegetation after 3.8 cal ky BP, suggesting colder and slightly drier conditions (Anker *et al.*, 2001).

Cynthia Bay lies halfway across the Tasmanian west-to-east vegetation gradient at 737 m altitude (18, Fig. 7.1A), and the site is more sensitive to precipitation variability than Lake Johnston. *Nothofagus* decreased at 4.9 cal ky BP at Cynthia Bay and *Eucalyptus*, Poaceae and Asteraceae expanded (Hopf *et al.*, 2000). However, little aquatic vegetation change occurred, indicating that Holocene precipitation variability was limited.

A central Tasmanian montane site close to the timberline, Eagle Tarn on Mt. Field (19, Fig. 7.1A), experienced rapid early Holocene warming and precipitation increase prior to 11 cal ky BP (MacPhail, 1979). The *Nothofagus* rainforest maximum was reached around 8.6 cal ky BP, increasing the timberline outside its present range, while *Pomaderris apetala* expanded into eastern Tasmania. The *Nothofagus/Eucalyptus* ratio increased until 5.4 cal ky BP, and subsequently decreased. *Nothofagus gunnii* disappeared after 3.4 cal ky BP with the development of more open forest (MacPhail, 1979).

The heterogeneous conditions in Tasmania complicate the correlation of climate patterns. Especially vegetation development at western sites differed from central or eastern Tasmanian sites and mainland Australia. However, more precipitation-limited sites do show changes concurrent with temperate sites on the Australian mainland, particularly during the late Holocene.

7.5. Discussion

The data comparison reveals significant Holocene variability at most, but not all, reviewed sites. Environmental changes, although considered to be relatively minor in the Holocene (Luly, 1993), are very pronounced at Lake Allom, due to its high rainfall dependence, heterogeneous setting and small catchment buffer capacity. At the other extreme, the arid interior Lake Tyrell record shows very little variability (Luly, 1993). It is likely that environmental changes throughout the Holocene are only clearly detectable at sites that are strongly dependent on precipitation, such as crater lakes, or at the transition between climatic regimes. Arid inland areas are potentially very sensitive to precipitation but a large part of the typical pollen types in arid records, such as Chenopodiaceae and Asteraceae, have broad environmental ranges and are thus less suited to detect relatively small changes in moisture balance.

Common to all records is a clear mid-Holocene moisture optimum, but especially the onset of the climate amelioration differs widely between records. The temporal offsets are most pronounced between upland sites like Lake Euramoo, where rainforest taxa occur from ~8.5 cal ky BP, and lowland sites like Lake Allom, which shows increasing moisture levels as much as 3 kyrs later.

The marginal seas apparently delayed the onset of moister conditions until the shelf areas had been inundated, so that the development of moist forests is significantly delayed (Hope *et al.*, 2004).

In temperate regions the early Holocene moisture maximum starts as early as 8.5 cal ky BP, further north around 7.5 cal ky BP, and in the subtropical regions the onset is evident only around 6 cal ky BP. However, tropical - monsoonal sites already show a moisture maximum around 8.5 cal ky BP. Likely the early Holocene warming caused shifts in the mean position of the high pressure belt, increasing moist westerly wind flow while easterly tradewinds remained fairly constant. The early Holocene moist conditions at tropical sites are related to increased monsoonal activity (Magee *et al.*, 2004), activated by high insolation across Asia (Fig. 7.2A), which displaced the ITCZ southward.

Subsequent changes occurred more synchronously over different climatic regions. At many sites the moisture optimum ends or starts to decrease at 5.5-5.0 cal ky BP, as in the high-resolution Lake Euramoo site. Especially Lake Allom and Bega Swamp show evidence of more synchronous changes indicating increased climatic coupling between northern and southern sites. The PCA axes for Lake Allom and Bega Swamp (Figs. 7.4D, F) reveal highly similar centennial-scale changes from 5 cal ky BP onwards, while rainforest at Lake Euramoo becomes more adapted to disturbance (Fig. 7.4B). Exceptions occur at the Lake Tyrell site and in Tasmania. Dune formation probably caused different vegetation development at Lake Tyrell, where a late Holocene *Casuarina* increase is reported (Luly, 1993), but this needs to be confirmed. As observed earlier (Anker *et al.* 2001), mid-Holocene changes within Tasmania are not synchronous. Especially western sites experience a very different climatic regime dominated by westerly airflow (Harrison, 1993), and are most likely not influenced by changes in tradewind or monsoon activity.

All the climatic regions, except Tasmania, show further changes around 3.0 cal yr BP. At the majority of sites conditions become slightly drier and more variable (adapted to disturbance). Both Lake Allom and Bega Swamp records have a pollen zone boundary at ~2.7 cal ky BP, concurrent with charcoal increases at Lake Euramoo and, to a lesser degree, Lake Allom (Fig. 7.4G). The increased fire frequencies are confirmed across eastern Australia at northern (Groote Eylandt), southern (Lake Wangoom) and upland (Barrington Tops) sites.

The nature and amplitude of environmental changes differ between sites but appear to be synchronous, within the uncertainties of the available age-depth models. Increased burning may be caused by Aboriginal practice but it cannot explain all variability. The environmental changes are highly synchronous, which is unlikely to be a consequence of human activities. In addition, available archeological data cannot be reconciled with periods of vegetation change (Genever *et al*, 2003; Bickford and Gell, 2005).

The observed changes after 3 cal ky BP could well reflect changing ENSO dynamics. Increasing variability is consistent with the effect of intensified ENSO, which causes wet/dry anomalies in Australia (Van Oldenborgh and Burgers, 2005). A gradual increase in ENSO frequency and intensity has been proposed on the basis of modeling exercises (Clement *et al*., 2000) and paleoclimatic evidence (McGlone *et al*., 1992; Shulmeister and Lees, 1995; Rodbell *et al*., 1999). Recent palynological evidence suggests a stepwise increase in ENSO activity (Chapter 5), around 5 and 3 cal ky BP. The late Holocene trend across Australia is in agreement with this scenario, since the main periods of change are confirmed. An intensification of the ENSO cycle would affect trade wind strength (Dodson, 1998) and ITCZ position (Haug *et al*., 2001). Trade wind variability in turn affects the entire East-Australian coast and creates moisture anomalies that are consistent with the reconstructions (Figs. 7.1B-E).

The changes across Australia are synchronous but not equally prominent. This may be partly explained by differences in climate sensitivity between sites, however, but also differences in seasonality may play a role. The major ENSO impact is during the southern winter/spring wet season, while it coincides with the Northern Australian dry season (Magee *et al*., 2004). Consequently, increased ENSO-related dry events are likely to affect the temperate to subtropical regions where ENSO has a high impact during the main period of moisture supply. These factors explain the pronounced changes observed in Lake Allom and Bega Swamp, which contrast with the relatively small shifts at Groote Eylandt and Lake Euramoo.

The late Holocene orbital forcing shows rising December insolation at the equator, which increased after 6 ky BP and reached about present-day levels at ~3 ky BP (Fig. 7.2A). Since El Niño warm events develop from the Indo-Pacific Warm Pool (IPWP) during austral summer (Diaz and Kiladis, 1992), the ENSO intensification is possibly caused by the increased equatorial IPWP warming, allowing warm events to develop more frequently (see: Chapter 8). Increased Southern Hemisphere seasonality (Fig. 7.2A) likely added to the occurrence of ENSO events after 5 cal ky BP (Markgraf, 1992). Effective Walker circulation requires significant upwelling along the Peru coast, (Shulmeister and Lees,

1995). Changing intensity of the Peru Current affects the upwelling of cold water, which increases the zonal SST gradient across the Pacific, allowing build-up of warm water in the IPWP needed for El Niño events or the 'cold-oscillating' mode (Rodbell *et al.*, 1999).

7.6. Conclusions

Recalibrated pollen records provide a more consistent view on Holocene climate patterns in eastern Australia. The new chronologies allow better comparison between terrestrial records, and will enable further integration of marine and terrestrial climate data.

The synchronicity of climatic events at 5 and 3 cal ky BP, contrary to the early Holocene moisture optimum, confirms earlier concepts about increased late Holocene ENSO activity (McGlone, *et al.*, 1992; Shulmeister and Lees, 1995; Clement *et al.*, 2000). A stepwise increase towards present-day ENSO dynamics provides the best explanation for the reconstructed changes in precipitation, and agrees in terms of temporal development with recent results from Florida, which is also strongly influenced by ENSO (Chapter 5). The Australian reconstructions are important for model-data comparisons, as well as correlations between marine and terrestrial records that reflect the Holocene dynamics of the coupled ocean/atmosphere ENSO system.

120

Integration of paleoclimatic and model scenarios for the Holocene onset of modern El Niño – Southern Oscillation variability

Abstract

An integrated overview of a variety of marine and terrestrial paleoclimatic data relevant for detecting ENSO variability is presented, focusing on two time-windows, 6-5 ky cal BP and 4.5-3.5 ky cal BP. Analysis of proxy climatic data indicate that, after a state-change at ~5 ky cal BP towards active ENSO cyclicity in the equatorial Pacific, ENSO-teleconnected regions are characterized by an increased amplitude of ENSO events around 3 ky cal BP. Comparison with climate model scenarios shows that ENSO intensification resulting from summer Pacific trade wind reduction cannot completely explain the observed Holocene changes. An additional mechanism is proposed, involving increased Indo-Pacific Warm Pool (IPWP) heat charging, which would have increased the ENSO amplitude.

8.1. Introduction

The El Niño – Southern Oscillation (ENSO) is the most potent source of inter-annual climate variability (Tudhope *et al.*, 2001). As a result of its widespread climatological and socio-economical impact, ENSO is presently one of the best-studied climate systems (Cane, 2005). Much effort is directed at improving prediction of El Niño events, as well as modeling the behavior of ENSO dynamics in a greenhouse world under increased radiative forcing. The past ENSO record provides important test cases for model simulations, and can contribute to the understanding of the forcing mechanisms by providing spatial and temporal patterns of past climate in regions influenced by ENSO.

Proxy records of past climate change show evidence for an active ENSO cycle at least 130,000 years ago (Tudhope *et al.*, 2001), while modeling studies indicate ENSO cyclicity as far back as the Eocene (Huber and Caballero, 2003). However, a growing body of evidence suggests that the intensity of the ENSO cycle has not been stable through time (McGlone *et al.*, 1992; Rodbell *et al.*, 1999; Koutavas *et al.*, 2002; Gagan *et al.*, 2004; McClymont and Rosel-Melé, 2005; Chapter 5). An intermediate-complexity model of equatorial Pacific climate (Zebiak and Cane, 1986) forced by orbital precession shows an early to middle Holocene reduction in ENSO intensity and frequency (Clement *et al.*, 2000). Reduced ENSO activity is confirmed by fully coupled model runs of selected time-intervals (Otto-Bliesner *et al.*, 2003). Available paleoclimatic evidence is largely in accordance with these model results, which are attributable to effects of increased insolation during the boreal summer season, creating easternly wind forcing that terminates the development of warm anomalies or El Niño events (Cane, 2005).

According to the model results, the subsequent middle to late Holocene ENSO intensification has been gradual, while many paleoclimatic records in reality show non-linear stepped changes centered around 5 and 3 ky BP (Koutavas *et al.*, 2002; Gagan *et al.*, 2004; Chapter 5; Chapter 7). Alternatively, some evidence indicates stability in the ENSO cycle throughout the Holocene (Nederbragt and Thurow, 2005).

Further controversy is related to the Holocene upwelling intensity in the Western Pacific, which is a crucial factor in the 'Bjerknes' feedback between SST (sea surface temperature) gradients and wind forcing for triggering ENSO warm events (Stute *et al.*, 2001; Cane, 2005). Reduced early Holocene ENSO activity was accompanied by mean warm conditions in the western Pacific according to some reconstructions (Sandweiss *et al.*, 1996; Rodbell *et al.*, 1999). These views are contrary to reconstructions of La Niña-like conditions between 8-5 ka BP with an increased zonal gradient and few warm events (Koutavas *et al.*, 2002). Recent views relate the warmer conditions to an absence of La Niña cold events rather than a permanent El Niño-warm state (Clement *et al.*, 2000; Cane, 2005).

These different interpretations illustrate the need for an improved examination of paleoclimatic evidence for changes in Holocene ENSO intensity. Although well-documented, evidence for Holocene environmental changes from the terrestrial realm is often inadequately cited in studies of past ENSO activity. A better integration of marine and terrestrial evidence can therefore provide a parsimonious view of Holocene ENSO

development and reveal whether changes were gradual or non-linear in relation to the insolation forcing.

The present paper compares marine and terrestrial proxy climatic information from two Holocene time windows with present-day climate conditions, characterized by an active ENSO cycle with pronounced warm and cold events. The first period, 6-5 ka BP (all ages are calendar ages), is thought to be characterized by reduced ENSO activity, while the second period, 4.5-3.5 ka BP, probably has an active but not a maximal ENSO oscillation. The validity of these assumptions can be tested by comparing insolation forcing, model results, marine and terrestrial proxy data and the present-day impact of ENSO (i.e. Ropelewski and Halpert, 1987; Markgraf and Diaz, 2000; Van Oldenborgh and Burgers, 2005). Furthermore, better insight may be obtained on the most likely mean state of the equatorial Pacific during the considered time windows, as well as in the exact timing and causation of ENSO development through the Holocene.

8.2. Data

A compilation of the available data relevant to paleo-ENSO reconstruction between 45 °N and 45 °S is given for 6-5 (Fig. 8.1) and 4.5-3.5 ka BP (Fig. 8.2). Both figures show the present-day contours of the Indo-Pacific Warm Pool (IPWP) (Gagan *et al.*, 2004) and region of Pacific inter-annual SST variability exceeding 1 °C (Deser and Wallace, 1990), indicative of the area where ENSO events are manifested.

The review includes circum-Pacific marine proxy data for reconstructing the mean zonal SST gradient and western Pacific upwelling regime, as well as varved sediments and fossil corals recording the actual intensity of ENSO events (Table 8.1). Terrestrial data originate from (sub)tropical regions bordering the equatorial Pacific, and strongly ENSO-teleconnected regions, such as Florida and eastern Australia. For the terrestrial data, either the mean moisture offset compared to the present-day condition or actual ENSO event strength is provided (Table 8.1).

Estimates of solar irradiance and seasonality for the past 12 ky BP in summer and winter are given in Fig. 8.3 for the Equator, 30 °N and 30 °S, based on the Laskar-90 dataset (Laskar *et al.*, 1990). Northern summer insolation is an important control for the ITCZ position (Haug *et al.*, 2001), which tends to lie over the warmest surface water and migrates towards the Equator during El Niño events.

8.3. Mid-Holocene ENSO patterns (6-5 ky BP)

Reconstructions of the mid-Holocene terrestrial environment indicate a climate state significantly different from today (Fig. 8.1, page 130). Indonesian charcoal (Haberle and Ledru, 2001) and pollen (Van der Kaars *et al.*, 2001) records show wetter and less variable conditions, a pattern also seen throughout eastern Australia (McGlone *et al.*, 1992; Gomez *et al.*, 2002; Chapter 7). This western Pacific pattern is contrasted by drier than present conditions at the equatorial eastern Pacific coast.

Table 8.1 Data sources, locations and proxies

Source	Region	Main proxy; environmental parameter
Marine records:		
Gagan et al., 1998	Great Barrier Reef & Indonesia	Coral (*Porites*) δ^{18}O & Sr/Ca; SST & salinity
McGregor and Gagan, 2004	Papua New Guinea	Coral (*Porites*) δ^{18}O; SST & salinity
Tudhope et al., 2001	Papua New Guinea	Coral (*Porites*) δ^{18}O; SST & salinity
McCulloch et al., 1996	Papua New Guinea	Coral (*Porites*) Sr/Ca; SST
Correge et al., 2000	Vanuatu	Coral (*Porites*) Sr/Ca; SST
Gagan et al., 2004 *	Indo-Pacific Warm Pool (IPWP)	Coral Sr/Ca & δ^{18}O & Alkenones & Foram Mg/Ca; SST & salinity
Brijker et al., in prep.	Central IPWP	Forminiferal δ^{18}O; SST & salinity
Koutavas et al., 2002	Galapagos	Foram Mg/Ca & alkenones; SST & salinity & upwelling
Sandweiss et al., 1996; 1997; 2001	Coastal Peru	Mollusk middens & Archeological remains; flooding history & SST
Nederbragt and Thurow, 2005	Santa Barbara Basin (USA)	Varve thickness; run-off
Marchant et al., 1999	Central Chile	Foram assemblages & δ^{18}O; productivity & SST
Friddell et al., 2003	Santa Barbara Basin (USA)	Foram δ^{18}O; SST & upwelling
Fontugne et al., 2004	Southern Peru	Reservoir ages in mollusk middens; upwelling
Martin et al., 1993	South-East Brazil	Beach ridges; current reversals
Barron et al., 2003	Northern California, ODP 1019	Pollen & alkenones; moisture & SST
Mohtadi et al., 2004	Northern Chile	Foraminiferal & diatom assemblages; productivity & upwelling
Terrestrial records:		
McGlone et al., 1992 *	Circum South Pacifc	Pollen & charcoal & sedimentology; moisture & temperature
Chapter 5	Southern Florida	Pollen; moisture
Chapter 7 *	Eastern Australia	Pollen & charcoal; moisture & temperature
Marchant and Hooghiemstra, 2004 *	African and South-American Tropics	Pollen & charcoal & sedimentology; moisture
Van der Kaars et al., 2001	West-Java	Pollen & diatoms; moisture & lake level
Haberle and Ledru, 2001 *	Indonesia & PNG, Central & South America	Charcoal; disturbance & moisture
Haberle, 1998	Central Papua New Guinea	Pollen & charcoal; moisture & disturbance
Ruter et al., 2004 *	Circum Carribean	Pollen & diatoms & sedimentology; moisture
Haug et al., 2001	Cariaco Basin (Venezuela)	Ti & Fe concentration; run-off
Riedinger et al., 2002	Galapagos	Sedimentology (clastic laminae); high rainfall events
Rodbell et al., 1999; Moy et al., 2002	South-West Ecuador	Sedimentology (clastic laminae); high rainfall events
Keefer et al., 2003	Southern coastal Peru	Sedimentology; flooding events
Kirkby et al., 2005	Southern California	LOI & magnetic susceptibility; moisture
Gomez et al., 2004	New Zealand North Island	Grain size; flooding and rainfall
Mancini et al., 2005 *	Southern South-America	Pollen; moisture
Hong et al., 2005	South & North-East China	Cellulose δ^{13}C; moisture (monsoon strength)

* = review study

Wet-dry patterns across the entire American continent are more complex. In the southern part of North America clearly dry anomalies occurred in Florida, the Southern High Planes, and California, but not in southwestern inland USA and northern Mexico (Barron *et al.*, 2003; Ruter *et al.*, 2004; Kirkby *et al.*, 2005; Chapter 5). South America was characterized by wetter conditions in regions south of ~30 ºS, in Venezuela and southern Panama, while Amazonia and central South America between ~15 ºN and 25 ºS were drier than present (Haug *et al.*, 2001; Haberle and Ledru, 2001; Marchant and Hooghiemstra, 2004; Mancini *et al.*, 2005).

These mid-Holocene conditions clearly differ from the present-day situation where the active ENSO cycle induces recurrent convective uplift increases in the western equatorial,

which bring rain to central South America (Ropelewski and Halpert, 1987) and, via enhanced Hadley circulation and storm-track intensification, to the southern USA (Vega *et al.*, 1998). Frequent warm anomalies in the eastern Pacific induce southward movement of the ITCZ, causing drier conditions in northern South America (Haug *et al.*, 2001). In the western Pacific, active El Niño creates reduced convective uplift and strong dry anomalies across Australasia (Dai and Wigley, 2000), as well as intensification of the Asian summer monsoon, while the Indian summer monsoon is reduced (Hong *et al.*, 2005).

The majority of the reconstructed mid-Holocene circum-Pacific moisture patterns is consistent with a reduced ENSO cycle, in which anomalies associated with present El Niño events are rare. Climate patterns from Central American pollen records are somewhat contradictory. However, present ENSO teleconnections in that region create opposite-sign moisture anomalies for winter and summer, explaining the divergent patterns. Inland southwestern USA also reveal a different climate pattern compared to other southern states, possibly due to the Sierra Nevada mountains that alter local rainfall patterns. These complex areas cause spatially variable climatic responses to ENSO events (Ruter *et al.*, 2004).

Important direct evidence for a reduced early to middle Holocene ENSO cyclicity comes from condensed and lower-frequency clastic laminae deposition in lake sediments from Ecuador (Rodbell *et al.*, 1999; Moy *et al.*, 2002) and the Galapagos Islands (Riedinger *et al.*, 2002) prior to 5 ky BP. These laminae are flood-induced and correlate with single El Niño events. A marine varve-thickness record from the Santa Barbara Basin off California fails to corroborate these results (Nederbragt and Thurow, 2005), although the ~5 year period typical of the ENSO spectrum seems not to be present during the early Holocene. The marine varve measurements are complicated by opposite responses to ENSO forcing of biogenic silica and organic matter layers within a single varve, thereby largely dampening the signal. Furthermore, a pair of high-resolution planktonic foraminiferal $\delta^{18}O$ records from the Santa Barbara Basin, correlated to ENSO activity, shows low early Holocene SST variability, with a gradual increase to maximal variability between 5.5 and 3.5 ka BP (Fridell *et al.*, 2003).

It may be expected that marine records from the tropical Pacific reflect any significant change in the ENSO cycle. Mg/Ca-based SST records off Galapagos indicate enhanced La Niña-like cool conditions and an increased zonal Pacific temperature gradient between 8 and 5 ky BP (Koutavas *et al.*, 2002). Large ^{14}C reservoir ages of mollusk middens confirm an altered ENSO state with intensive upwelling at the Peru margin before 4 ka BP. However, foraminiferal-assemblage and $\delta^{18}O$ records from the central Chilean coast reveal less intensive and unstable upwelling during the middle Holocene (Mohtadi *et al.*, 2004; Marchant *et al.*, 1999). These opposite trends likely result from a mid-Holocene northward shift rather than higher intensity of the main South-American upwelling area, which is consistent with the different dry/wet patterns between central and southern South America (Fig. 8.1). Confinement of increased SST cooling to the central-eastern Pacific is supported by model data of Liu *et al.* (1999).

Indications of an enhanced Pacific zonal SST gradient or 'La Niña-state' with a reduced ENSO cycle should coincide with enhanced Indo Pacific Warm Pool (IPWP) temperatures. The best estimates for IPWP paleo-temperatures are from combined $\delta^{18}O$ and Sr/Ca records of fossil corals, indicating a 0.5-1 °C higher annual mean SSTs (Gagan *et al.*, 1998; 2004) and reduced ENSO amplitude around 6 ky BP (Tudhope *et al.*, 2001; McGregor and Gagan, 2004). A decadal planktic foraminiferal $\delta^{18}O$ record, reflecting both temperature and salinity changes, from the center of the IPWP confirms the coral data and shows warm, wet and stable conditions before 5.3 ka BP (J.M. Brijker, pers. comm.).

Figures 8.1 & 8.2: see pages 130 & 131

8.4. Late Holocene ENSO patterns (4.5-3.5 ky BP)
Several records have indicated a timing of ~5 ky BP for the onset of present-day ENSO activity (Rodbell *et al.*, 1999; Koutavas *et al.*, 2002). A wide body of terrestrial and marine paleo-ENSO data shows that the ENSO cycle around 4 ky BP had indeed become more active with respect to the mid-Holocene (Fig. 8.2, page 131). However, circum-Pacific climate conditions were clearly not yet equivalent to today's climate. A more detailed analysis of clastic laminae in an Ecuadorian mountain lake, following the study of Rodbell *et al.* (1999), suggests that maximum ENSO variability only occurred between 3-1.2 ky BP (Moy *et al.*, 2002). The sub-maximal ENSO variability around 4 ky BP is reflected in the terrestrial ecosystems in Australasia and the Americas by reduced but still significant moisture anomalies compared to present (Fig. 8.2). Especially sites that are highly sensitive to moisture balance, such as the swamps of southern Florida and crater lakes and perched basins of eastern Australia, show changes at both 5 and 3 ky BP (McGlone *et al.*, 1992; Chapter 5; Chapter 7). Also the Holocene development of modern Asian and Indian summer monsoons was not a single transition, but rather a progressive strengthening of the Asian and a weakening of the Indian monsoon between 5-3 ky BP (Hong *et al.*, 2005). Although located central in the IPWP, most Indonesian charcoal records show no further changes at 3 ky BP. However, interpretation is complicated by effects of human influence (Haberle and Ledru, 2001).

Paleo-temperatures based on fossil corals generally indicate modern ENSO variability after 3 ky BP (Gagan *et al.*, 2004). One fossil coral from Vanuatu already recorded highly active ENSO around 4 ky BP (Corrège *et al.*, 2000). The coral data give accurate information on ENSO dynamics during short time windows but are not continuous and therefore difficult to interpret in terms of long-term trends.

Continuous marine paleo-SST data do indicate that the eastern-Pacific upwelling regime had changed by 4 ky BP towards the present-day variable state, caused by recurrent warm anomalies in the equatorial eastern Pacific (Fig. 8.2, Marchant *et al.*, 1999; Koutavas *et al.*, 2002; Fontugne *et al.*, 2004). Planktonic foraminiferal $\delta^{18}O$ data from the central IPWP reveal high-amplitude salinity variations from 5 ky BP, indicative of an active ENSO cycle. However, no changes are evident around 3 ky BP (J.M. Brijker, pers. comm.).

Records from various other sources show a difference between late and middle Holocene conditions (Fig. 8.2). Beach-ridge deposits along the Brazilian coast, which likely formed

during (phases of) enhanced ENSO activity due to current reversals, occurred from 5.1 ky BP onwards (Martin *et al.*, 1983). Further west, increased ice-accumulation interspersed with large dust events are found after ~4 ky BP in the tropical South-American mountain glaciers (Thompson *et al.*, 1984; 1995; 2000). In coastal Peru, the construction of monumental temples after 5.8 ky BP is considered to be a cultural response to increased flood occurrences. After ~3 ky BP the temple sites were abandoned (Sandweiss *et al.*, 2001). Composition of mollusk middens from the same region indicate active but lower than present ENSO dynamics between 5.8 and ~3 ky BP. (Sandweiss *et al.*, 2001).

8.5. Discussion

The data compilations of Figs. 8.1 and 8.2 provide an integrated overview of middle to late Holocene ENSO development. There is a clear distinction between development in the equatorial Pacific and subtropical regions. Marine and terrestrial paleoclimate records from the IPWP and eastern Pacific cold tongue indicate a state-change towards active ENSO cyclicity around 5 ky BP (e.g. Haberle and Ledru, 2001; Koutavas *et al.*, 2002). Strongly teleconnected areas however, such as continental South America, southern Florida, California, eastern Australia, and the Asian/Indian monsoon systems, still show significant offsets from the present climate conditions around 4 ky BP (Fig. 8.2). Higher-amplitude ENSO events after 3 ky BP (Moy *et al.*, 2002; Riedinger *et al.*, 2002) caused more variable conditions, exerting strong environmental pressure on vegetation, which is evident in pollen records from Australia and New Zealand (McGlone *et al.*, 1992; Chapter 7).

The model scenario of gradually increasing middle to late Holocene ENSO frequency and amplitude (Clement *et al.*, 1999; 2000) is not entirely reflected by the paleoclimate data, which indicate more abrupt changes. Boreal summer insolation (Fig. 8.3) is thought to control the ENSO dynamics by Northern Hemisphere warming (cooling) in summer/autumn and subsequent Pacific trade wind strengthening (weakening), thereby cooling (warming) the eastern Pacific, which inhibits (strengthens) El Niño build-up (Clement *et al.*, 2000; Cane, 2005).

However, insolation can provide further explanation for the increased ENSO amplitude after 3 ky BP. Modern observations indicate that westerly wind burst can initiate ENSO events only if enough heat has built up in the IPWP, and larger events require a longer recharge time than small events (McPhaden, 2003). Since warm water build-up leads ENSO events by 6 months (Wang and Picaut, 2004), boreal winter insolation is an important control for IPWP heat content. Boreal winter exceeded summer insolation since 6 ky BP, and reached maximum levels at ~3 ky BP (Fig. 8.3). Most probably, pronounced El Niño events were more likely to develop due to the enhanced IPWP heat build up, and since such El Niño's cause greater wave reflection, terminating the warm events and inducing strong La Niña conditions (Stute *et al.*, 2001), the entire ENSO cycle intensified to maximum variability around 3 ky BP. This mechanism can, apart from the increase of modern ENSO frequencies around 5 ky BP recorded in the equatorial Pacific, further explain the increase around 3 ky BP of ENSO strength and associated environmental change in strongly teleconnected areas as evident from paleoclimatic data.
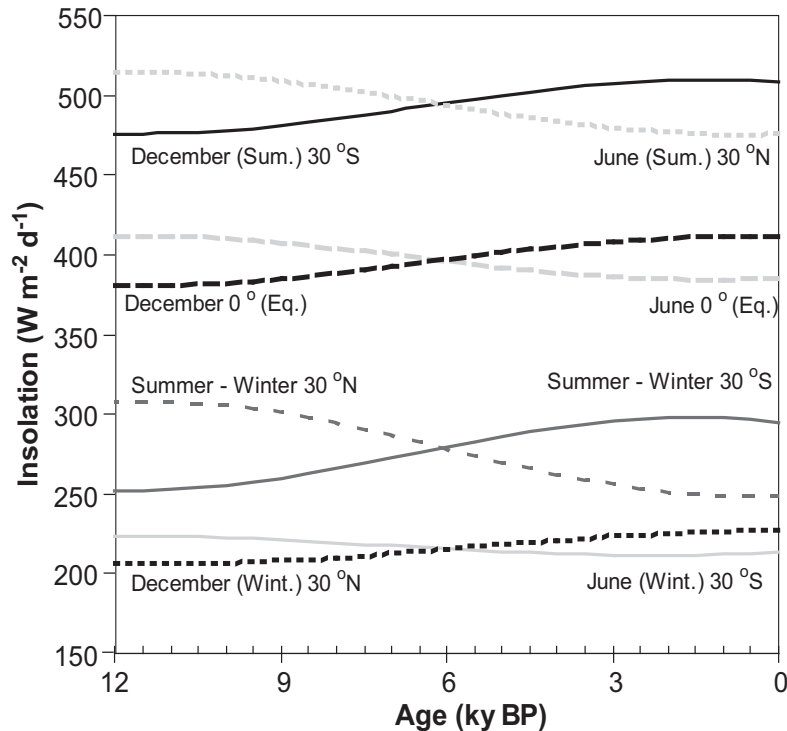
Figure 8.3 December and June insolation values and seasonal amplitude for the Equator, 30 ºN and 30 ºS during the last 12 ky based on the Laskar-90 orbital solution (Laskar, 1990).

8.6. Conclusions

On the basis of a comparison of marine and terrestrial proxy climatic data it is shown that an enhanced La Niña state with reduced variability is the most likely early to middle Holocene climatic condition in the equatorial Pacific. Around 5 ky BP, the modern ENSO recurrence and associated upwelling regimes developed, causing environmental change in the IPWP and present-day teleconnected areas. Subsequently, around 3 ky BP, the amplitude of ENSO events became larger, effectively causing further climatic change in teleconnected regions. Besides insolation-forced early termination of warm events, seasonal variation in IPWP heat charging is here proposed as an additional mechanism for changing ENSO dynamics.

Reconstruction of specific time-intervals provides an important test case for climate models needed to accurately predict future climate changes under greenhouse conditions. Further data-model comparisons are essential since radiative forcing changes have a large influence on ENSO dynamics, affecting global moisture distribution and oceanographic conditions. The role of the IPWP in triggering ENSO events under increased greenhouse conditions should be the main focus of model studies, while further high-resolution paleoclimatic data is needed to increase spatial and temporal resolution to resolve recent research issues like decadal modulation and volcanic forcing of ENSO intensity (Fedorov and Philander, 2000; Hoerling and Kumar, 2003; Cane, 2005).

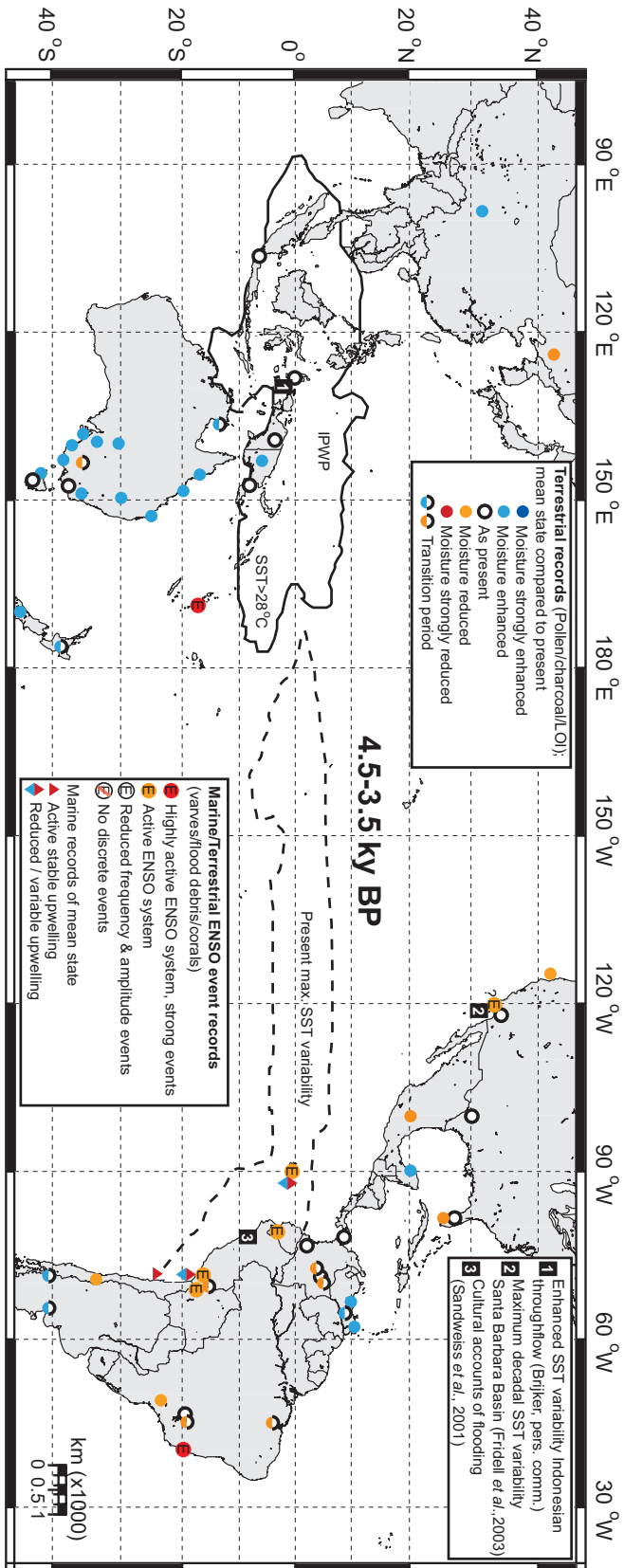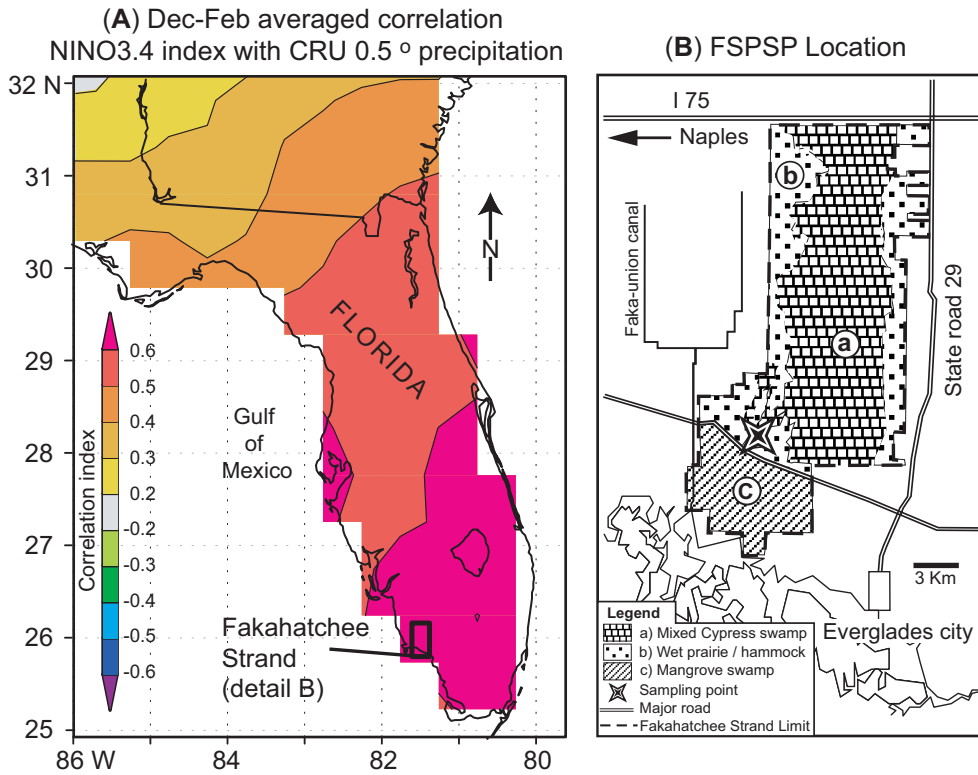Color figures
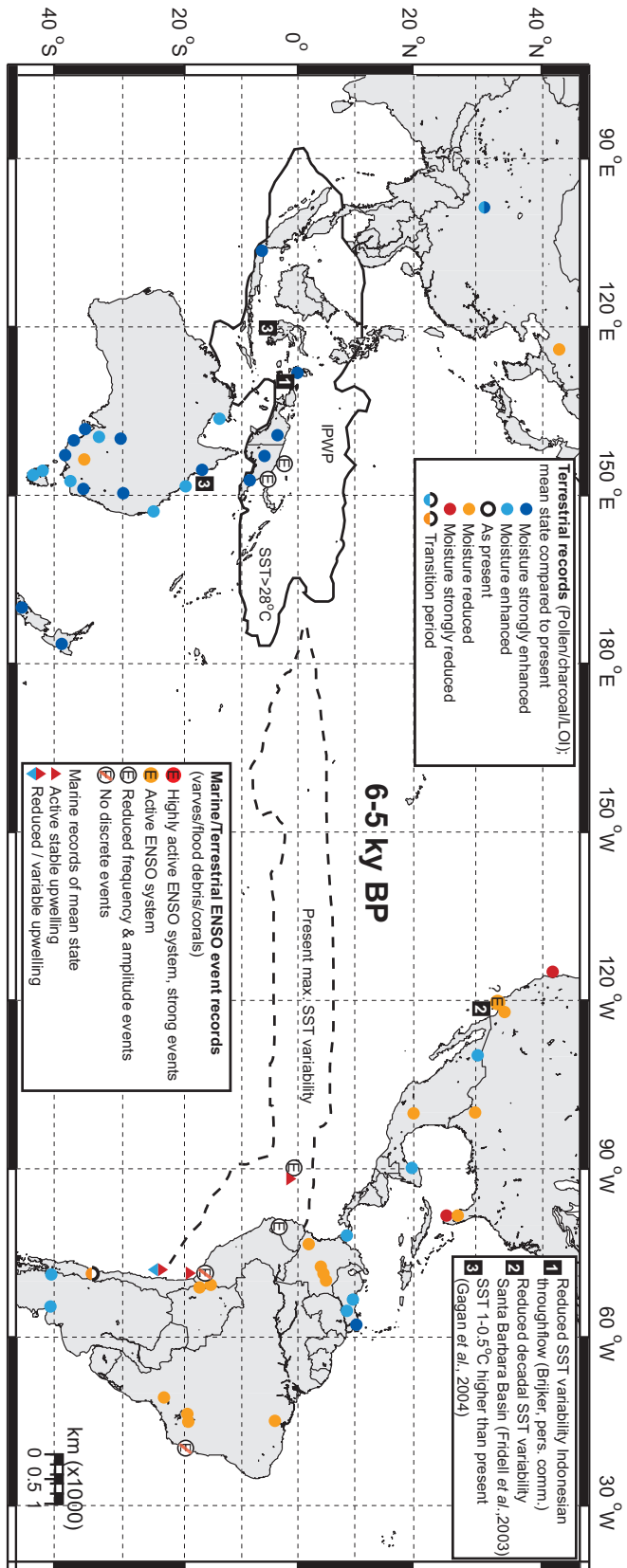
Figure 8.1 Paleo-environmental reconstructions of marine and terrestrial conditions in the circum-Pacific region in relation to ENSO for 6.0-5.0 ky BP. Data sources are listed in Table 8.1.

Figure 8.2 Paleo-environmental reconstructions of marine and terrestrial conditions in the circum-Pacific region in relation to ENSO for 4.5-3.5 ky BP. Data sources are listed in Table 8.1.

(A) Dec-Feb averaged correlation
NINO3.4 index with CRU 0.5 º precipitation

(B) FSPSP Location

Figure 4.1 (A) Location of the Fakahatchee Strand in Florida. Gridded overlay shows average winter (DJF) correlation between precipitation and the NINO3.4 index (performed by KNMI climate explorer, after Van Oldenborgh and Burgers, 2005), based on station data containing >50 years. Note the high correlation in southern Florida (r>0.6, P<0.0001), a region which contains extensive wetland ecosystems. (B) Coring location and the extent and composition of the Fakahatchee wetland.

Figure 5.3 (Right page) Pollen percentage diagram of FAK III98 displaying taxa with a minimum abundance of 2% and/or five occurrences. White bars represent exaggeration (factor 5) to visualize variations in low-abundance taxa.
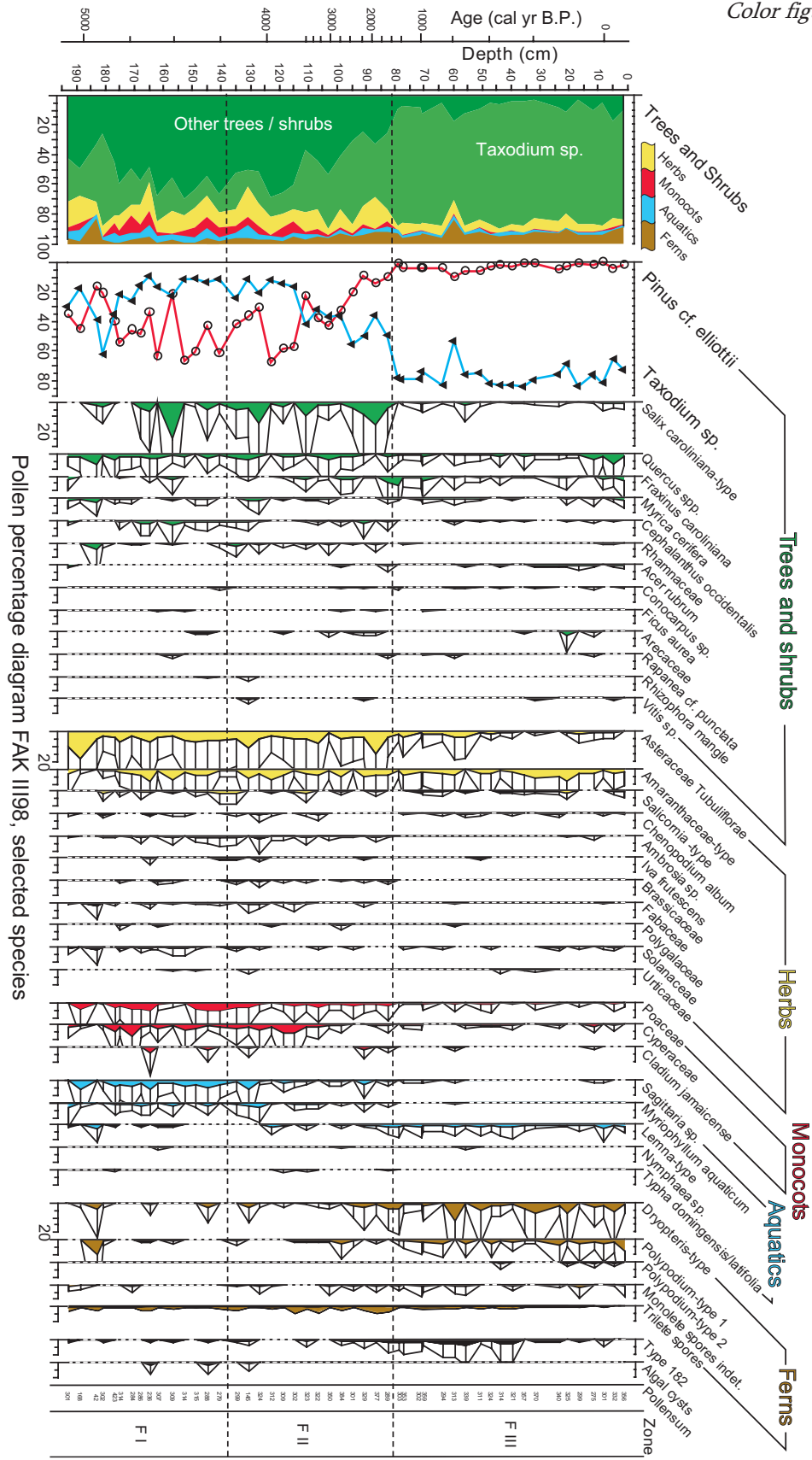
Pollen percentage diagram FAK III98, selected species
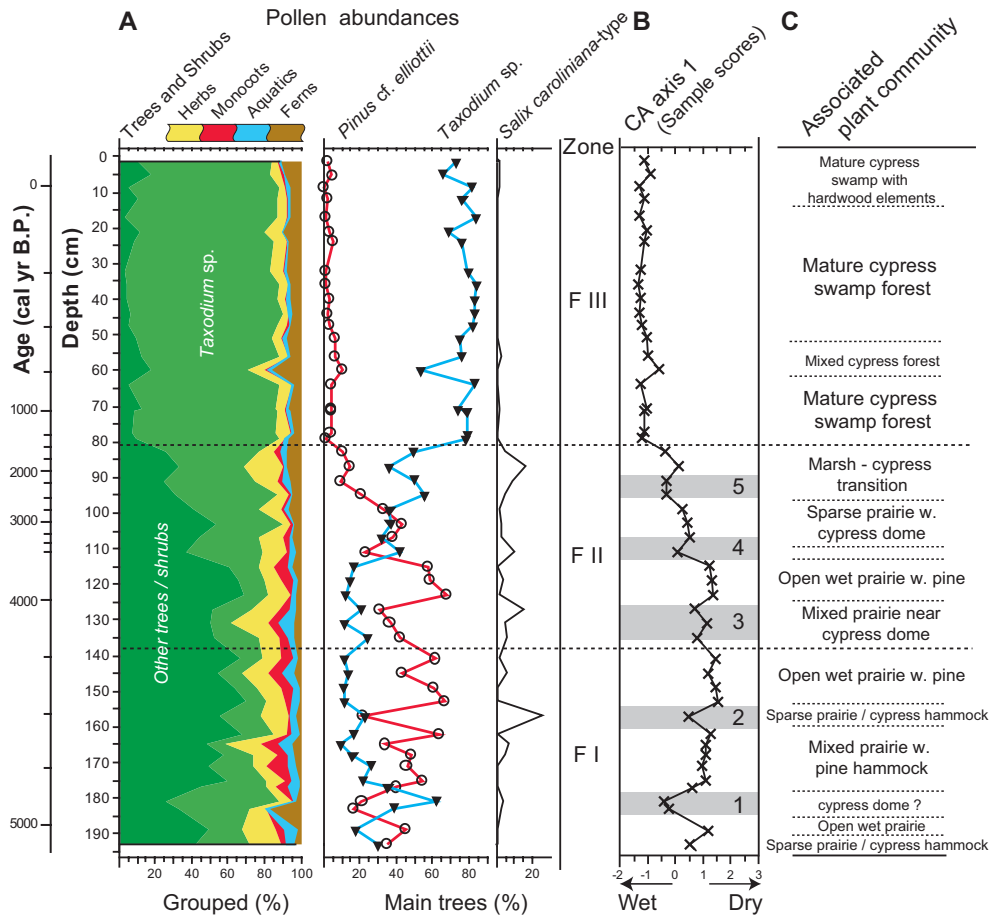
Figure 5.5 Summary pollen percentage diagram and reconstructed past vegetation from the FSPSP wetland in Florida. Major pollen curves (A) and general trend between dry and wet assemblages (B) and the associated vegetation units (C). *Pinus* represents relatively dry conditions in contrast to wet *Taxodium* phases. Numbers 1–5 represent short wet pulses characterized by high *Salix* and increased *Taxodium* as referred to in the text.

1 Groote Eylandt, N.T. (Shulmeister, 1992; Shulmeister & Lees, 1995)
2 Lake Euramoo, Atherton Tablelands, Qld. (Kershaw, 1970; Haberle, 2005)
3 Quincan Crater, Atherton Tablelands, Qld. (Kershaw, 1971)
4 Whitehaven Swamp, Qld. (Genever *et al.*, 2003)
5 Lake Allom, Fraser Island, Qld. (Chapter 6)
6 Barrington Tops, N.S.W. (Dodson *et al.*, 1986)
7 Bega Swamp, N.S.W. (Green *et al.*, 1988; Hope, in prep.)
8 Club Lake (Kosciuszko National Park), N.S.W. (Martin, 1986)
9 Sperm Whale Head, Vic. (Hooley *et al.*, 1980)
10 Lake Frome, S.A. (Singh & Luly, 1991)
11 Middens, Flinders range, S.A. (McCarthy & Head, 2001)
12 Lake Tyrell, Vic. (Luly, 1993)
13 Fleurieu Peninsula, S.A. (Bickford & Gell, 2005)
14 Lake Leake, S.A. (Dodson, 1974)
15 Tower Hill, Vic. (D'Costa *et al.*, 1989)
16 Lake Wangoom, Vic. (Edney *et al.*, 1990)
17 Lake Johnston, Tas. (Anker *et al.*, 2001)
18 Cynthia Bay, Tas. (Hopf *et al.*, 2000)
19 Mt. Field (Eagle Tarn), Tas. (Macphail, 1979)

Australian rainfall seasonality (After Magee *et al.*, 2004)

SSS = Strongly seasonal, summer rain
WSS = Weakly seasonal, summer rain
UD = Uniform distribution
WSW = Weakly seasonal, winter rain
SSW = Strongly Seasonal, winter rain

Correlation NINO3.4 index with CRU precipitation (3-month averaged)

B) Jan-Mar (Sum)
C) Apr-Jun (Fall)
D) Jul-Sep (Win.)
E) Oct-Dec (Spr.)

-0.6 -0.5 -0.4 -0.3 -0.2 0.2 0.3 0.4 0.5 0.6
Correlation index
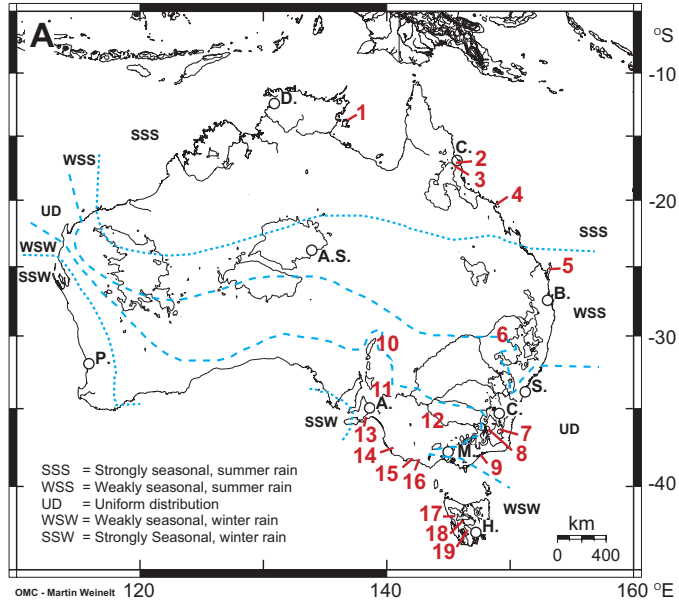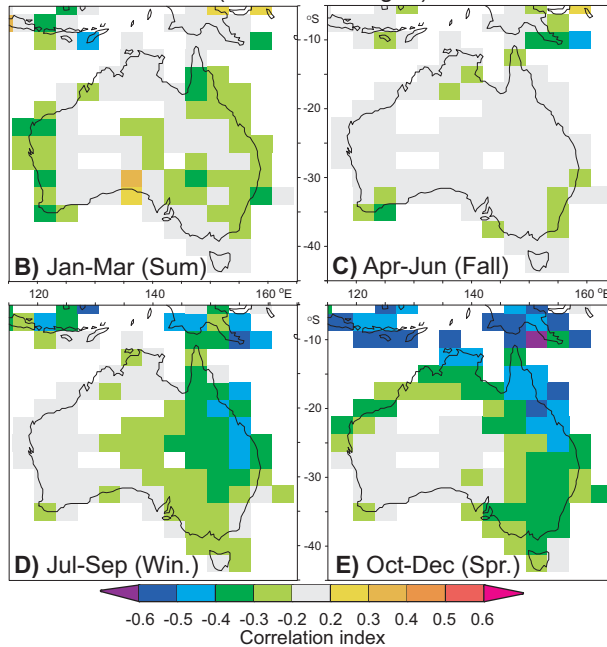
Figure 7.1 (A) Location of study sites and seasonality of annual rainfall (after Magee *et al.*, 2004) across Australia. (B-E) ENSO impact on Australian precipitation, expressed as a seasonally averaged correlation between gridded precipitation and the NINO3.4 index. Non-significant correlations are grey. Maps were made with KNMI Climate Explorer (Van Oldenborgh and Burgers, 2005).

Alexander, T.J. & Crook, A.G. (1974). Recent vegetational changes in Southern Florida. In *Environments of South Florida: present and past* (ed P.J. Gleason), Vol. 2, pp. 61-72. The Miami Geological Society, Miami.

Allan, R.J. (2000). ENSO and climatic variability in the past 150 years. In *El Niño and the Southern Oscillation: multiscale variability and global and regional impacts* (eds H.F. Diaz & V. Markgraf), pp. 3-55. Cambridge University Press, Cambridge.

Anker, S.A., Colhoun, E.A., Barton, C.E., Peterson, M., & Barbetti, M. (2001) Holocene vegetation and paleoclimatic and paleomagnetic history from Lake Johnston, Tasmania. *Quaternary Research*, **56**, 264-274.

Anonymous (2003) Survey and Mapping of Pre-clearing and 2001 Remnant Vegetation Communities and Regional Ecosystems of Queensland. Queensland Herbarium, Environmental Protection Agency, Brisbane, Queensland.

Appleby, P.G. (2001). Chronostratigraphic techniques in recent sediments. In *Basin analysis, coring and chronological techniques.* (eds W.M. Last & J.P. Smol), Vol. 1, pp. 171-203. Kluwer Academic, Dordrecht, the Netherlands.

Ashton, D.H. & Attiwill, P.M. (1994). Tall open-forests. In *Australian vegetation* (eds R.H. Groves). Cambridge University Press, Cambridge.

Austin, D.F., Jones, J.L., & Bennett, B.C. (1990) Vascular plants of the Fakahatchee Strand. *Florida Scientist*, **53**, 85-88.

Barber, K.E. & Charman, D.J. (2003). Holocene palaeoclimate records from peatlands. In *Global change in the Holocene* (eds A.W. Mackay, R.W. Battarbee & H.J.B. Birks), pp. 210-226. Arnold, London.

Bard, E., Hamelin, B., Arnold, M., Montaggioni, L., Cabioch, G., Faure, G., & Rougerie, F. (1996) Deglacial sea-level record from Tahiti corals and the timing of global meltwater discharge. *Nature*, **382**, 241-244.

Barron, J.A., Heusser, L., Herbert, T., & Lyle, M. (2003) High-resolution climatic evolution of coastal northern California during the past 16,000 years. *Paleoceanography*, **18**, 1020.

Bennett, K.D. (1996) Determination of the number of zones in a biostratigraphical sequence. *New Phytologist*, **132**, 155-170.

Bickford, S. & Gell, P. (2005) Holocene vegetation change, Aboriginal wetland use and the impact of European settlement on the Fleurieu Peninsula, South Australia. *The Holocene*, **15**, 200-215.

Birks, H.H. & Birks, H.J.B. (2003). Reconstructing Holocene climates from pollen and plant macrofossils. In *Global change in the Holocene* (eds A.W. Mackay, R.W. Battarbee, H.J.B. Birks & F. Oldfield), pp. 342-357. Arnold, London.

137

References

Birks, H.J.B. & Birks, H.H. (1980) *Quaternary Palaeoecology* Edward Arnold, London. pp. 289

Birks, H.J.B. & Gordon, A.D. (1985) *Numerical methods in Quaternary pollen analysis* Academic Press, London. pp. 317

Blaauw, M., Heuvelink, G.B.M., Mauquoy, D., Van der Plicht, J., & Van Geel, B. (2003) A numerical approach to ^{14}C wiggle-match dating of organic deposits: best fits and confidence intervals. *Quaternary Science Reviews*, **22**, 1485–1500.

Blaauw, M., Van Geel, B., Mauquoy, D., & Van der Plicht, J. (2004) Carbon-14 wiggle-match dating of peat deposits: advantages and limitations. *Journal of Quaternary Science*, **19**, 177-181.

Blackman, R.B. & Tukey, J.W. (1959) *The measurement of power spectra from the point of view of communication engineering* Dover Publications, New York. pp. 190

Blockley, S.P.E., Pyne-O'Donnell, S.D.F., Lowe, J.J., Matthews, I.P., Stone, A., Pollard, A.M., Turney, C.S.M., & Molyneux, E.G. (2005) A new and less destructive laboratory procedure for the physical separation of distal glass tephra shards from sediments. *Quaternary Science Reviews*, **24**, 1952-1960.

Blum, M.D., Carter, A.E., Zayac, T., & Goble, R. (2002) Middle Holocene sea-level and evolution of the Gulf of Mexico coast (USA). *Journal of Coastal Research, special issue*, **36**, 65-80.

Blum, M.D., Misner, T.J., Collins, E.S., Scott, D.B., Morton, R.A., & Aslan, A. (2001) Middle Holocene sea-level rise and highstand at +2 m, central Texas coast. *Journal of Sedimentary Research*, **71**, 581-588.

Bosabalidis, A.M. & Kofidis, G. (2002) Comparative effects of drought stress on leaf anatomy of two olive cultivars. *Plant Science*, **163**, 375-379.

Bronk Ramsey, C. (1995) Radiocarbon Calibration and Analysis of Stratigraphy: The OxCal Program. *Radiocarbon*, **37**, 425-430.

Bronk Ramsey, C. (2000) Comment on 'The Use of Bayesian Statistics for ^{14}C dates of chronologically ordered samples: a critical analysis'. *Radiocarbon*, **42**, 199-202.

Bronk Ramsey, C. (2001) Development of the Radiocarbon Program OxCal. *Radiocarbon*, **43**, 355-363.

Burns, L.A. (1984). Productivity and water relations in the Fakahatchee Strand of South Florida. In *Cypress Swamps* (eds K.C. Ewel & H.T. Odum), pp. 318-333. University Press of Florida, Gainesville.

Cain, W.F. & Suess, H.E. (1976) Carbon 14 in tree rings. *Journal of Geophysical Research*, **81**, 3688-3694.

Cane, M.A. (2005) The evolution of El Niño, past and future. *Earth and Planetary Science Letters*, **230**, 227-240.

Clarke, P.J. (1994). Quaternary dune systems. In *Australian vegetation* (eds R.H. Groves), pp. 501-521. Cambridge University Press, Cambridge.

Clemens, J., Cambell, L.C., & Nurisjah, S. (1983) Germination, growth and mineral ion concentrations of *Casuarina* species under saline conditions. *Australian Journal of Botany*, **31**, 1-9.

Clement, A.C., Seager, R., & Cane, M.A. (1999) Orbital controls on the El Niño/Southern Oscillation and the tropical climate. *Paleoceanography*, **14**, 441-456.

Clement, A.C., Seager, R., & Cane, M.A. (2000) Suppression of El Niño during the mid-Holocene by changes in the Earth's orbit. *Paleoceanography*, **15**, 731-737.

138

Clymo, R.S. (1988) A high resolution sampler of surface peat. *Functional ecology*, **2**, 425-431.

Cohen, A.D. (1975) Peats from the Okeefenokee swamp-marsh complex. *Geoscience and man*, **11**, 123-131.

Cohen, A.D., Gage, C.P., & Moore, W.S. (1999) Combining organic petrography and palynology to assess anthropogenic impacts on peatlands Part 1. An example from the northern Everglades of Florida. *International Journal of Coal Geology*, **39**, 3-45.

Colhoun, E.A. (2000) Vegetation and climate change during the Last Interglacial-Glacial cycle in western Tasmania, Australia. *Palaeogeography, Palaeoclimatology, Palaeoecology*, **155**, 195-209.

Cook, E.R., D'Arrigo, R.D., Cole, J.E., Stahle, D.W., & Villalba, R. (2000). Tree-ring records of past ENSO variability and forcing. In *El Niño and the Southern Oscillation: multiscale variability and global and regional impacts* (eds H.F. Diaz & V. Markgraf), pp. 297-323. Cambridge University Press, Cambridge.

Corrège, T., Delcroix, T., Récy, J., Beck, W., Cabioch, G., & Le Cornec, F. (2000) Evidence for stronger El Niño-Southern Oscillation (ENSO) events in a mid-Holocene massive coral. *Paleoceanography*, **15**, 465-470.

Cronin, T.M., Dwyer, G.S., Schwede, S.B., Vann, C.D., & Dowsett, H. (2002) Climate variability from the Florida Bay sedimentary record: possible teleconnections to ENSO, PNA and CNP. *Climate Research*, **19**, 233-245.

D'Costa, D., Edney, P., Kershaw, A.P., & De Deckker, P. (1989) Late Quaternary palaeoecology of Tower Hill, Victoria, Australia. *Journal of Biogeography*, **16**, 461-482.

Dai, A. & Wigley, T.M.L. (2000) Global patterns of ENSO-induced precipitation. *Geophysical Research Letters*, **27**, 1283-1286.

Davis, J.H. (1943) *The natural features of Southern Florida, especially the vegetation, and the Everglades* The Florida Geological Society, Tallahassee, Florida.

Dean, W.E. (1974) Determination of carbonate and organic matter in calcareous sediments and sedimentary rocks by loss on ignition: comparison with other methods. *Journal of Sedimentary Petrology*, **44**, 242-248.

Delcourt, H.R. & Delcourt, P.A. (1985). Quaternary Palynology and Vegetational History of the Southeastern United States. In *Pollen Records of Late Quaternary North American Sediments* (eds V.M. Bryant & R.G. Holloway), pp. 1-37. AASP Foundation.

Dennis, J.V. (1988) *The great cypress swamps* Louisiana State University Press.

Deser, C. & Wallace, J.M. (1990) Large-scale atmospheric circulation features of warm and cold episodes in the tropical Pacific. *Journal of Climate*, **3**, 1254-1281.

Diaz, H.F. & Kiladis, G.N. (1992). Atmospheric teleconnections associated with the extreme phases of the Southern Oscillation. In *El Niño: Historical and Paleoclimatic Aspects of the Southern Oscillation* (eds H.F. Diaz & V. Markgraf), pp. 7-28. Cambridge University Press, Cambridge.

Diaz, H.F. & Markgraf, V., eds. (1992) *El Niño: Historical and palaeoclimatic aspects of the Southern Oscillation*. Cambridge University Press, Cambridge.

Dodson, J.R. (1974) Vegetation history and water fluctuations at Lake Leake, south-eastern South Australia. I. 10, 000 B.P. to present. *Australian Journal of Botany*, **22**, 719-741.

Dodson, J.R. (1994). Quaternary vegetation history. In *Australian vegetation* (ed R.H. Groves), pp. 37-56. Cambridge University Press, Cambridge.

Dodson, J.R. (1998) Timing and response of vegetation change to Milankovitch forcing in temperate Australia and New Zealand. *Global And Planetary Change*, **18**, 161-174.

Dodson, J.R. (2001) Holocene vegetation change in the mediterranean-type climate regions of Australia. *The Holocene*, **11**, 673-680.

Duever, M.J., Carlson, J.E., Meeder, J.F., Duever, L.C., Gunderson, L.H., Riopelle, L.A., Alexander, T.R., Myers, R.L., & Spangler, D.P. (1986) *The Big Cypress National Preserve* National Audubon Society, New York. pp. 455

Edney, P., Kershaw, A.P., & De Deckker, P. (1990) A Late Pleistocene and Holocene vegetation and environmental record from Lake Wangoom, Western Plains of Victoria, Australia. *Palaeogeography, Palaeoclimatology, Palaeoecology*, **80**, 325-343.

Etheridge, D.M., Steele, L.P., Langenfels, R.L., Francey, R.J., Barnola, J.M., & Morgan, V.I. (1996) Natural and anthropogenic changes in atmospheric CO_2 over the last 1000 years from air in Antarctic ice and firn. *Journal of Geophysical Research*, **101**, 4115-4128.

Ewel, K.C. (1990). Freshwater wetlands and aquatic ecosystems: swamps. In *Ecosystems of Florida* (eds R.L. Myers & J.J. Ewel), pp. 281-323. University of Central Florida Press, Orlando.

Faegri, K., Kaland, P.E., & Krzywinski, K. (1989) *Textbook of pollen analysis*, 4th edn. John Wiley and Sons, Chichester. pp. 328

Fedorov, A.V. & Philander, S.G. (2000) Is El Niño changing? *Science*, **288**, 1997-2002.

Fontugne, M., Carré, M., Bentaleb, I., Julien, M., & Lavallee, D. (2004) Radiocarbon reservoir age variations in the south Peruvian upwelling during the Holocene. *Radiocarbon*, **46**, 531-537.

Ford, C.R. & Brooks, J.R. (2002) Detecting forest stress and decline in response to increasing river flow in southwest Florida, USA. *Forest ecology and management*, **160**, 45-64.

Fridell, J.E., Thunell, R.C., Guilderson, T.P., & Kashgarian, M. (2003) Increased northeast Pacific climatic variability during the warm middle Holocene. *Geophysical Research Letters*, **30**, 1560.

Gagan, M.K., Ayliffe, L.K., Hopley, D., Cali, J.A., Mortimer, G.E., Chapell, J., McCulloch, M.T., & Head, M.J. (1998) Temperature and surface-ocean water balance of the mid-Holocene tropical western Pacific. *Science*, **279**, 1014-1018.

Gagan, M.K., Hendy, E.J., Haberle, S.G., & Hantoro, W.S. (2004) Post-glacial evolution of the Indo-Pacific Warm Pool and El Niño-Southern Oscillation. *Quaternary International*, **118-119**, 127-143.

Genever, M., Grindrod, J., & Barker, B. (2003) Holocene palynology of Whitehaven Swamp, Whitsunday Island, Queensland, and implications for the regional archaeological record. *Palaeogeography, Palaeoclimatology, Palaeoecology*, **201**, 141-156.

Gleason, P.J. & Stone, P. (1994). Age, origin, and landscape evolution of the Everglades peatland. In *Everglades: the ecosystem and its restoration* (eds S.M. Davis & J.C. Ogden), pp. 149-197. St. Lucie Press, Delray Beach, Florida.

Godfred-Spenning, C.R. & Reason, C.J.C. (2002) Interannual variability of lower-tropospheric moisture transport during the Australian Monsoon. *International Journal of Climatology*, **22**, 509-532.

Gomez, B., Carter, L., Trustum, N.A., Palmer, N.A., & Roberts, A.P. (2004) El Niño-Southern Oscillation signal associated with middle Holocene climate change in intercorrelated terrestrial and marina sediment cores, North Island, New Zealand. *Geology*, **32**, 653-656.

Green, D., Singh, G., Polach, H., Moss, D., Banks, J., & Geissler, E.A. (1988) A fine-resolution palaeoecology and palaeoclimatology from South-Eastern Australia. *Journal of Ecology*, **76**, 790-806.

Grimes, K.G. (1987) Fraser Island, Sheet SG 56-3 (Part I). Department of Mines, Queensland.

Grimm, E.C. (1991-2001) Tilia, TiliaGraph and TGView software. Illinois State Museum, Springfield, Illinois, USA.

Grimm, E.C., Jacobson Jr., G.L., Watts, W.A., Hansen, B.C.S., & Maasch, K.A. (1993) A 50, 000-year record of climate oscillations from Florida and its temporal correlation with the Heinrich events. *Science*, **261**, 198-200.

Grove, J.M. (2001) The initiation of the "Little Ice Age" in regions around the North Atlantic. *Climatic Change*, **48**, 53-82.

Groves, R.H., ed. (1994) *Australian vegetation*, 2nd edn. Cambridge University Press, Cambridge. pp. 562

Haberle, S. (1998) Late Quaternary vegetation change in the Tari Basin, Papua New Guinea. *Palaeogeography Palaeoclimatology Palaeoecology*, **137**, 1-24.

Haberle, S.G. (2005) A 23ka pollen record from Lake Euramoo, Wet Tropics of NE Queensland, Australia. *Quaternary Research,* in press.

Haberle, S.G. & Ledru, M.P. (2001) Correlations among charcoal records of fires from the past 16,000 years in Indonesia, Papua New Guinea, and Central and South America. *Quaternary Research*, **55**, 97-104.

Hadwen, W.L., Arthington, A.H., & Mosisch, T.D. (2003) The impact of tourism on dune lakes on Fraser Island, Australia. *Lakes & Reservoirs: Research and Management*, **8**, 15-26.

Harrison, S.P. (1993) Late Quaternary lake-level changes and climates of Australia. *Quaternary Science Reviews*, **12**, 211-231.

Haug, G.H., Hughen, K.A., Sigman, D.M., Peterson, L.C., & Rohl, U. (2001) Southward migration of the intertropical convergence zone through the Holocene. *Science*, **293**, 1304-1308.

Hesse, P., Magee, J.W., & Van der Kaars, S. (2004) Late Quaternary climates of the Australian arid zone: a review. *Quaternary International*, **118-119**, 87-102.

Hicks, S. (2001) The use of annual arboreal pollen deposition values for delimiting tree-lines in the landscape and exploring models of pollen dispersal. *Review of Palaeobotany and Palynology*, **117**, 1-29.

Hill, R., Griggs, P., & Ngadimunku, B.B. (2000) Rainforests, agriculture and aborginal fire regimes in wet tropical Queensland, Australia. *Australian Geographical Studies*, **38**, 138-157.

Hoerling, M. & Kumar, A. (2003) The perfect ocean for drought. *Science*, **299**, 691-694.

Hong, Y.T., Hong, B., Lin, Q.H., Shibata, Y., Hirota, M., Zhu, Y.X., Leng, X.T., Wang, Y., Wang, H., & Yi, L. (2005) Inverse phase oscillations between the East Asian and Indian Ocean summer monsoons during the last 12 000 years and paleo-El Niño. *Earth and Planetary Science Letters*, **231**, 337-346.

Hooley, A.D., Southern, W., & Kershaw, A.P. (1980) Holocene vegetation and environments of Sperm Whale Head, Victoria, Australia. *Journal of Biogeography*, **7**, 349-362.

Hope, G., Kershaw, A.P., Van der Kaars, S., Xiangjun, S., Liew, P.-M., Heusser, L.E., Takahara, H., McGlone, M.S., Miyoshi, N., & Moss, P.T. (2004) History of vegetation and habitat change in the Austral-Asian region. *Quarternary International*, **118-119**, 103-126.

Hopf, F.V.L., Colhoun, E.A., & Barton, C.E. (2000) Late-glacial and Holocene record of vegetation and climate from Cynthia Bay, Lake St Clair, Tasmania. *Journal of Quaternary Science*, **15**, 725-732.

Huber, M. & Caballero, R. (2003) Eocene El Niño: evidence for robust Tropical dynamics in the "hothouse". *Science*, **299**, 877-881.

Indermühle, A., Joos, F., Fischer, H., Smith, H.J., Wahlen, M., Deck, B., Mastroianni, D., Tschumi, J., Blunier, T., Meyer, R., & Stauffer, B. (1999) Holocene carbon-cycle dynamics based on CO_2 trapped in ice at Taylor Dome, Antarctica. *Nature*, **398**, 121-126.

IPCC (2001) *Climate Change 2001: The Scientific Basis. Contribution of Working Group I to the Third Assessment Report of the Intergovernmental Panel on Climate Change.* Cambridge University Press, Cambridge, United Kingdom. pp. 944

Janssen, C.R. (1973). Local and regional pollen deposition. In *Quaternary plant ecology. 14th symposium of the British Ecological Society* (eds H.J.B. Birks & R.G. West), pp. 31-42. Blackwell, Oxford.

Jones, G.D., Bryant, V.M.J., Lieux, M.H., Jones, S.D., & Lingren, P.D. (1995) *Pollen of the Southeastern United States: with Emphasis on Melissopalynology and Entomopalynology.* AASP Foundation, Texas A&M University, College Station, Texas.

Jones, G.D., Lieux, M.H., Wilson, E.F., & Martin, J.A. (1999) *Light micrograph pollen identification reference, modern pollen poster.* AASP Foundation, Texas A&M University, College Station, Texas.

Juggins, S. (2003) C^2 Software for ecological and palaeoecological data analysis and visualisation. University of Newcastle, Newcasle upon Tyne.

Kaplan, A., Cane, M.A., Kushnir, Y., Clement, A.C., Blumenthal, M.B., & Rajagopalan, B. (1998) Analyses of global sea surface temperature 1856-1991. *Journal of Geophysical Research*, **103**, 18567-18589.

Kapp, R.O., Davis, O.K., & King, J.E. (2000) *Pollen and Spores*, 2nd edn. AASP Foundation, Texas A&M University, College Station, Texas. pp. 279

Keefer, D.K., Moseley, M.E., & deFrance, S.D. (2003) A 35,000-year record of floods and debris flows in the Ilo region of southern Peru and its relation to El Niño events

and great earthquakes. *Palaeogeography Palaeoclimatology Palaeoecology*, **194**, 41-77.

Keeland, B.D., Conner, W.H., & Sharitz, R.R. (1997) A comparison of wetland tree growth response to hydrologic regime in Louisiana and South Carolina. *Forest ecology and management*, **90**, 237-250.

Keeling, C.D. & Whorf, T.P.A.a.w. (2003) Atmospheric CO_2 concentrations-Mauna Loa observatory, Hawaii, 1958-2003 http://cdiac.esd.ornl.gov/ndp001.html.

Kerr, R.A. (2003) Climate change: A perfect ocean for four years of globe-girdling drought. *Science*, **299**, 636-636.

Kershaw, A.P. (1970) A pollen diagram from Lake Euramoo, north-east Queensland, Australia. *New Phytologist*, **69**, 785-805.

Kershaw, A.P. (1971) A pollen diagram from Quincan Crater, north-east Queensland, Australia. *New Phytologist*, **70**, 669-681.

Kershaw, A.P. (1973) Late Quaternary vegetation of the Atherton Tableland, north-east Queensland, Australia. *Phd Thesis*, Australian National University, Canberra.

Kershaw, A.P. (1976) A Late Pleistocene and Holocene pollen diagram from Lynch's Crater, north eastern Queensland, Australia. *New Phytologist*, **77**, 469-498.

Kershaw, A.P. (1983) A Holocene pollen diagram from Lynch's Crater, north-eastern Queensland, Australia. *New Phytologist*, **94**, 669-682.

Kershaw, A.P. (1986) Climatic change and Aboriginal burning in north-east Australia during the last two glacial/interglacial cycles. *Nature*, **322**, 47-49.

Kershaw, A.P. (1994) Pleistocene vegetation of the humid tropics of northeastern Queensland, Australia. *Palaeogeography, Palaeoclimatology, Palaeoecology*, **109**, 399-412.

Kershaw, A.P. & Hyland, B.P.M. (1975) Pollen transfer and periodicity in a rain-forest situation. *Review of Palaeobotany and Palynology*, **19**, 129-138.

Kershaw, A.P. & Nix, H.A. (1988) Quantitative palaeoclimate estimates from pollen data using bioclimatic profiles of extant taxa. *Journal of Biogeography*, **15**, 589-602.

Kershaw, A.P. & Wagstaff, B. (2001) The southern conifer family Araucariaceae: history, status, and value for palaeoenvironmental reconstruction. *Annual Review of Ecology and Systematics*, **32**, 397-414.

Kirkby, M.E., Lund, S.P., & Poulsen, C.J. (2005) Hydrologic variability and the onset of modern El Niño-Southern Oscillation: a 19250-year record from Lake Elsinore, southern California. *Journal of Quaternary Science*, **20**, 239-254.

Koutavas, A., Lynch-Stieglitz, J., Marchitto Jr., T.M., & Sachs, J.P. (2002) El Niño-like pattern in ice age tropical Pacific sea surface temperatures. *Science*, **297**, 226-230.

Kouwenberg, L., Wagner, F., Kürschner, W.M., & Visscher, H. (2005) Atmospheric CO_2 fluctuations during the last millennium reconstructed by stomatal frequency analysis of *Tsuga heterophylla* needles. *Geology*, **33**, 33-36.

Kürschner, W.M. (1997) The anatomical diversity of recent and fossil leaves of the durmast oak (*Quercus petraea* Lieblein *Q-pseudocastanea* Goeppert) implications for their use as biosensors of palaeoatmospheric CO_2 levels. *Review of Palaeobotany and Palynology*, **96**, 1-30.

Kürschner, W.M., Stulen, I., Wagner, F., & Kuiper, P.J.C. (1998) Comparison of palaeobotanical observations with experimental data on the leaf anatomy of

durmast oak [*Quercus petraea* (Fagaceae)] in response to environmental change. *Annals of Botany*, **81**, 657-664.

Kürschner, W.M., Van der Burgh, J., Visscher, H., & Dilcher, D.L. (1996) Oak leaves as biosensors of late Neogene and early Pleistocene paleoatmospheric CO_2 concentrations. *Marine Micropaleontology*, **27**, 299-312.

Kushlan, J.A. (1990). Freshwater wetlands and aquatic ecosystems: freshwater marshes. In *Ecosystems of Florida* (eds R.L. Myers & J.J. Ewel), pp. 324-363. University of Central Florida Press, Orlando.

Ladd, P.G., Orchiston, D.W., & Joyce, E.B. (1992) Holocene Vegetation History Of Flinders-Island. *New Phytologist*, **122**, 757-767.

Laskar, J. (1990) The chaotic motion of the solar system: A numerical estimate of the chaotic zones. *Icarus*, 266-291.

Levin, I., Kromer, B., Schoch-Fischer, H., Bruns, M., Munnich, M., Berdau, D., Vogel, J.C., & Munnich, K.O. (1994). Delta $^{14}CO_2$ records from two sites in Central Europe. In *Trends 93 - A compendium of data on global change: 203-222 and online updates (Online Trends).* (eds T.A. Boden, D.P. Kaiser, R.J. Sepanski & F.W. Stoss). Carbon Dioxide Information Analysis Centre. Oak Ridge National Laboratory, Oak Ridge.

Li, C. & Wang, K. (2003) Differences in drought responses of three contrasting *Eucalyptus* microtheca F. Muell. Populations. *Forest Ecology and Management*, **179**, 377-385.

Light, S.S. & Dineen, J.W. (1994). Water control in the Everglades: a historical perspective. In *Everglades: the ecosystem and its restoration* (eds S.M. Davis & J.C. Ogden), pp. 47-84. St. Lucie Press, Delray Beach.

Little, E.L., Jr. (1971) *Atlas of United States trees, volume 1, Conifers and important hardwoods* U.S. Department of Agriculture.

Liu, Z., Jacob, J., Kutzbach, S., Harrison, S., & Anderson, J. (1999) Monsoon impact on El Niño in the early Holocene. *PAGES newsletter*, **7**, 16-17.

Loader, N.J., Robertson, I., & McCarroll, D. (2003) Comparison of stable carbon isotope ratios in the whole wood, cellulose and lignin of oak tree-rings. *Palaeogeography, Palaeoclimatology, Palaeoecology*, **196**, 395-407.

Lockheart, M.J., Poole, I., Van Bergen, P.F., & Evershed, R.P. (1998) Leaf carbon isotope compositions and stomatal characters: important considerations for palaeoclimate reconstructions. *Organic Geochemistry*, **29**, 1003-1008.

Longmore, M.E. (1997a) Quaternary palynological records from perched lake sediments, Fraser Island, Queensland Australia: rainforest, forest history and climatic control. *Australian Journal of Botany*, **45**, 507-526.

Longmore, M.E. (1997b) The mid-Holocene "Dry" anomaly on the mid-eastern coast of Australia: Calibration of palaeowater depth as a surrogate for effective precipitation using sedimentary loss on ignition in the perched lake sediments of Fraser Island, Queensland. *Palaeoclimates*, **4**, 1-26.

Longmore, M.E. & Heijnis, H. (1999) Aridity in Australia: Pleistocene records of palaeohydrological and palaeoecological change from the perched lake sediments of Fraser Island, Queensland, Australia. *Quaternary International*, **57/58**, 35-47.

Lotter, A.F. & Juggins, S. (1991) POLPROF, TRAN and ZONE: programs for plotting, editing and zoning pollen and diatom data. *INQUA-Subcommission for the study*

of the Holocene Working Group on Data-Handling Methods, Newsletters, **4**, 4-6.

Luly, J.G. (1993) Holocene Paleoenvironments Near Lake Tyrrell, Semiarid Northwestern Victoria, Australia. *Journal of Biogeography*, **20**, 587-598.

Macphail, M. (1979) Vegetation and climates in southern Tasmania since the Last Glaciation. *Quaternary Research*, **11**, 306-341.

Magee, J.W., Miller, G.H., Spooner, N.A., & Questiaux, D. (2004) Continuous 150 ky monsoon record from Lake Eyre, Australia: Insolation-forcing implications and unexpected Holocene failure. *Geology*, **32**, 885-888.

Mancini, M.V., Paeza, M.M., Prietob, A.R., Stutza, S., Tonelloa, M., & Vilanovab, I. (2005) Mid-Holocene climatic variability reconstruction from pollen records (32 °-52 °S, Argentina). *Quaternary International*, **132**, 47-59.

Marchant, M., Hebbeln, D., & Wefer, G. (1999) High resolution planktic foraminiferal record of the last 13,300 years from the upwelling area of Chile. *Marine Geology*, **161**, 115-128.

Marchant, R. & Hooghiemstra, H. (2004) Rapid environmental change in African and South American tropics around 4000 years before present: a review. *Earth-Science Reviews*, **66**, 217-260.

Markgraf, V. & Diaz, H.F. (2000). The past ENSO record: a synthesis. In *El Niño and the Southern Oscillation: multiscale variability and global and regional impacts* (eds H.F. Diaz & V. Markgraf), pp. 465-488. Cambridge University Press, Cambridge.

Martin, A.R.H. (1986) Late Glacial and Holocene alpine pollen diagrams from the Kosciusko National Park, New South Wales, Australia. *Review of Palaeobotany and Palynology*, **47**, 367-409.

Martin, L., Fournier, M., Mourguiart, P., Sifeddine, A., & Turcq, B. (1993) Southern Oscillation signal in South American palaeoclimatic data of the last 7000 years. *Quaternary Research*, **39**, 338-346.

McCarthy, L. & Head, L. (2001) Holocene variability in semi-arid vegetation: new evidence from Leporillus middens from the Flinders Ranges, South Australia. *The Holocene*, **11**, 681-689.

McClymont, E.L. & Rosell-Melé, A. (2005) Links between the onset of modern Walker circulation and the mid-Pleistocene climate transition. *Geology*, **33**, 389-392.

McCormac, F.G., Hogg, A.G., Blackwell, P.G., Buck, C.E., Higham, T.F.G., & Reimer, P.J. (2004) ShCal04 Southern Hemisphere Calibration, 0-11.0 Cal Kyr BP. *Radiocarbon*, **46**, 1087-1092.

McGlone, M.S., Kershaw, A.P., & Markgraf, V. (1992). El Niño/Southern Oscillation climatic variability in Australasian and South American paleoenvironmental records. In *El Niño: Historical and Paleoclimatic Aspects of the Southern Oscillation* (eds H.F. Diaz & V. Markgraf), pp. 435-462. Cambridge University Press, Cambridge.

McGregor, H.V. & Gagan, M.K. (2004) Western Pacific coral $\delta^{18}O$ records of anomalous Holocene variability in the El Niño-Southern Oscillation. *Geophysical Research Letters*, **31**, L11204.

McPhaden, M.J. (2003) Tropical Pacific Ocean heat content variations and ENSO persistence barriers. *Geophysical Research Letters*, **30**,1480.

Megonigal, J.P. & Day, F.P. (1992) Effects of flooding on root and shoot production of Bald Cypress in large experimental enclosures. *Ecology*, **73**, 1182-1193.

Middeldorp, A.A. (1982) Pollen concentration as a basis for indirect dating and quantifying net organic and fungal production in a peat bog ecosystem. *Review of Palaeobotany and Palynology*, **37**, 225-282.

Mohtadi, M., Romero, O.E., & Hebbeln, D. (2004) Changing marine productivity off northern Chile during the past 19 000 years: a multivariable approach. *Journal of Quaternary Science*, **19**, 347-360.

Mook, W.G. & Streurman, H.J. (1983). Physical and chemical aspects of radiocarbon dating. In *Proceedings of the First International Symposium on ^{14}C and Archaeology* (eds W.G. Mook & H.T. Waterbolk), Vol. 8, pp. 31-55. PACT.

Mooney, S.D. & Black, M. (2003) A simple and fast method for calculating the area of macroscopic charcoal isolated from sediments. *Quaternary Australasia*, **21**, 18-21.

Morton, R.A., Paine, J.G., & Blum, M.D. (2000) Responses of stable bay-margin and barrier island systems to Holocene sea-level highstands, western Gulf of Mexico. *Journal of Sedimentary Research*, **70**, 478-490.

Moy, C.M., Seltzer, G.O., Rodbell, G.T., & Anderson, D.M. (2002) Variability of El Niño/Southern Oscillation activity at millennial timescales during the Holocene epoch. *Nature*, **420**, 162-165.

Myers, R.L. (1990). Upland ecosystems: scrub and high pine. In *Ecosystems of Florida* (eds R.L. Myers & J.J. Ewel), pp. 150-193. University of Central Florida Press, Orlando.

Nederbragt, A.J. & Thurow, J. (2005) Amplitude of ENSO cycles in the Santa Barbara Basin, off California, during the past 15000 years. *Journal of Quaternary Science*, **20**, 447-456.

Neftel, A., Friedli, H., Moor, E., Lötscher, H., Oeschger, H., Siegenthaler, U., & Stauffer, B. (1994). Historical CO_2 record from the Siple Station ice core. In *Trends: a compendium of data on global change* (eds T.A. Boden, D.A. Kaiser, R.J. Sepanski & F.W. Stoss), pp. 11-14. Carbon Dioxide Information Analysis Center, Oak Ridge National Laboratory, Oak Ridge, Tennessee, USA.

Nevo, E., Pavlíek, T., Beharav, A., Bolshakova, M.A., Martyn, G., Musatenko, L.I., & Sytnik, K.M. (2000) Drought and light anatomical adaptive leaf strategies in three woody species caused by microclimatic selection at "Evolution Canyon", Israel. *Israel Journal of Plant Science*, **48**, 33-46.

Ng, B.H. (1987) The effects of salinity on growth, nodulation and nitrogen fixation of *Casuarina equisetifolia*. *Plant and Soil*, **103**, 123-125.

Nichols, N. (1992). Historical El Niño/Southern Oscillation variability in the Australasian region. In *El Niño: Historical and Paleoclimatic Aspects of the Southern Oscillation* (eds H.F. Diaz & V. Markgraf), pp. 151-173. Cambridge University Press, Cambridge.

O'Neal, M.A., Tedesco, L.P., Sough, C., & Pachut, J.F. (2001) A pollen zonations of southwestern Florida using multivariate statistical methods and its application to two vertical sedimentary sequences. *Bulletins of American Paleontology*, **361**, 101-132.

Oppenheimer, H.R. (1960) Adaptation to drought: xerophytism. *Arid Zone Research*, **15**, 105-138.

Otto-Bliesner, B.L., Brady, E.C., Shin, S.-I., Liu, Z., & Shields, C. (2003) Modeling El Niño and its tropical teleconnections during the last glacial-interglacial cycle. *Geophysical Research Letters*, **30**, 2198.

Paillard, D., Labeyrie, L., & Yiou, P. (1996) Macintosh program performs time-series analysis. *Eos Transactions*, **77**, 379.

Penfound, W.T. (1931) Plant anatomy as conditioned by light intensity and soil moisture. *American Journal of Botany*, **18**, 558-572.

Pittock, A.B. (1978). Patterns of vairability in relation to the general circulation. In *Climatic change and variability: A southern perspective* (eds A.B. Pittock, L.A. Frakes, D. Jenssen, J.A. Peterson & J.W. Zillman), pp. 167-179. Cambridge University Press, Cambridge.

Reimer, P.J., Baillie, M.G.L., Bard, E., Bayliss, A., Beck, J.W., Bertrand, C.J.H., Blackwell, P.G., Buck, C.E., Burr, G.S., Cutler, K.B., Damon, P.E., Edwards, R.L., Fairbanks, R.G., Friedrich, M., Guilderson, T.P., Hogg, A.G., Hughen, K.A., Kromer, B., McCormac, G., Manning, S., Bronk-Ramsey, C., Reimer, R.W., Remmele, S., Southon, J.R., Stuiver, M., Talamo, S., Taylor, F.W., Van der Plicht, J., & Weyhenmeyer, C.E. (2004) IntCal04 terrestrial radiocarbon age calibration, 0-26 cal kyr BP. *Radiocarbon*, **46**, 1029-1058.

Riedinger, M.A., Steinitz-Kannan, M., Last, W.M., & Brenner, M. (2002) A ~6100 ^{14}C yr record of El Niño activity from the Galápagos Islands. *Journal of Paleolimnology*, **27**, 1-7.

Ristic, Z. & Cass, D.D. (1991) Leaf Anatomy of *Zea mays* L. in response to water shortage and high temperature: A comparison of drought-resistant and drought -sensitive lines. *Botanical Gazette*, **152**, 173-185.

Rodbell, D.T., Seltzer, G.O., Anderson, D.M., Abbott, M.B., Enfield, D.B., & Newman, J.H. (1999) An ~15,000-year record of El Niño-driven alluviation in southwestern Ecuador. *Science*, **283**, 516-520.

Ropelewski, C.F. & Halpert, M.S. (1987) Global and regional scale precipitation patterns associated with ENSO. *Monthly Weather Review*, **115**, 1589-1606.

Ruter, A., Arzt, J., Vavrus, S., Bryson, R.A., & Kutzbach, J.E. (2004) Climate and environment of the subtropical and tropical Americas (NH) in the mid-Holocene: comparison of observations with climate model simulations. *Quaternary Science Reviews*, **23**, 663-679.

Salisbury, E.J. (1927) On the causes and ecological significance of stomatal frequency with special reference to the woodland flora. *Philosophical Transactions of the Royal Society (London)*, B, **216**, 1-65.

Sandweiss, D.H., Maasch, K.A., Burger, R.L., Richardson, J.B.I., Rollins, H.B., & Clement, A.C. (2001) Variation in Holocene El Niño frequencies: Climate records and cultural consequences in ancient Peru. *Geology*, **29**, 603-606.

Sandweiss, D.H., Richardson, J.B., III, Reitz, E.J., Rollins, H.B., & Maasch, K.A. (1996) Geoarcheologial evidence from Peru for a 5000 years B.P. onset of El Niño. *Science*, **273**, 1531-1533.

Sandweiss, D.H., Richardson, J.B., III, Reitz, E.J., Rollins, H.B., & Maasch, K.A. (1997) Determining the early history of El Niño: Reply. *Science*, **276**, 966-967.

Schürmann, B. (1959) Über den Einfluß der Hydratur und des Lichtes auf die Ausbildung der Stomata-Initialen. *Flora*, **147**, 471-520.

Shimeld, P., Hopf, F., & Pearson, S. (2000) Pollen image management: the Newcastle digital collection initiative. *Quaternary Australasia*, **18**, 13-15.

Shulmeister, J. (1992) A Holocene pollen record from lowland tropical Australia. *The Holocene*, **2**, 107-116.

Shulmeister, J. & Lees, B.G. (1995) Pollen evidence from tropical Australia for the onset of and ENSO-dominated climate at *c.* 4000 BP. *The Holocene*, **5**, 10-18.

Singh, G. & Luly, J. (1991) Changes In Vegetation And Seasonal Climate Since The Last Full Glacial At Lake Frome, South-Australia. *Palaeogeography, Palaeoclimatology, Palaeoecology*, **84**, 75-86.

Smith, C.A. & Sardeshmukh, P. (2000) The Effect of ENSO on the Intraseasonal Variance of Surface Temperature in Winter. *International Journal of Climatology*, **20**, 1543-1557.

Spackman, W., Dolsen, C.P., & Riegel, W.L. (1966) Phytogenic organic sediments and sedimentary environments in the Everglades-Mangrove complex. Part I: Evidence of a transgressing sea and its effects on environments of the Shark River areas of southwestern Florida. *Palaeontographica abt. B*, **117**, 135-152.

Stuiver, M. & Quay, P.D. (1981) Atmospheric ^{14}C changes resulting from fossil fuel CO_2 release and cosmic ray flux variability. *Earth and Planetary Science Letters*, **53**, 349-362.

Stuiver, M., Reimer, P.J., & Braziunas, T.F. (1998) High-precision radiocarbon age calibration for terrestrial and marine samples. *Radiocarbon*, **40**, 1127-1151.

Stute, M., Clement, A.C., & Lohmann, G. (2001) Global climate models: past, present, and future. *Proceedings of the National Academy of Sciences*, **98**, 10529-10530.

Sugita, S. (1994) Pollen Representation of Vegetation in Quaternary Sediments - Theory and Method in Patchy Vegetation. *Journal of Ecology*, **82**, 881-897.

Sutula, M.A., Perez, B.C., Reyes, E., Childers, D.L., Davis, S., Day, J.W.J., Rudnick, D., & Sklar, F. (2003) Factors affecting spatial and temporal variability in material exchange between the Southern Everglades wetlands and Florida Bay (USA). *Estuarine, Coastal and Shelf Science*, **57**, 757-781.

Swayze, L.J. & McPherson, B.F. (1977). The effect of the Faka-union canal system on water levels in the Fakahatchee Strand, Collier County, Florida., Rep. No. WRI-77-61. US Geological Survey, Water Recources Division, Tallahassee. pp. 19

Ter Braak, C.J.F. & Smilauer, P. (1998) *Canoco reference manual and user's guide for Canoco for Windows. Software for Canonical Community Ordination (version 4)* Microcomputer Power, Ithaca, NY, USA.

Thomas, T.M. (1974). A detailed analysis of climatological and hydrological records of South Florida with reference to man's influence upon ecosystem evolution. In *Environments of South Florida: present and past* (eds P.J. Gleason), Vol. 2, pp. 82-122. Miami Geological Society, Miami.

Thompson, C.H. (1992) Genesis of podsols on coastal dunes in southern Queensland. I. Field relationships and profile morphology. *Australian Journal of Soil research*, **30**, 593-613.

Thompson, L.G., Mosely-Thompson, E., & Henderson, K.A. (2000) Ice-core palaeoclimate records in tropical South America since the Last Glacial Maximum. *Journal of Quaternary Science*, **15**, 377-394.

Thompson, L.G., Mosley-Thompson, E., Davis, M.E., Lin, P.E., Henderson, K.A., Cole-Dai, B., Bolzan, J.F., & Liu, K. (1995) Late Glacial stage and Holocene tropical ice core records from Huascarán, Peru. *Science*, **269**, 46-50.

Thompson, L.G., Mosley-Thompson, E., & Morales Arnao, B. (1984) Major El Niño Southern Oscillation events recorded in stratigraphy of the tropical Quelccaya ice cap. *Science*, **226**, 50-52.

Tichá, I. (1982) Photosynthetic characteristics during ontogenesis of leaves. 7. Stomata density and sizes. *Photosynthetica*, **16**, 375-471.

Timms, B.V. (1986). The coastal dune lakes of eastern Australia. In *Limnology in Australia* (eds P. De Deckker & W.D. Williams). CSIRO/DR W. Junk, Dordrecht.

Törnqvist, T.E., González, J.L., Newsom, L.A., Van der Borg, K., De Jong, A.F.M., & Kurnik, C.W. (2004) Deciphering Holocene sea-level history on the U.S. Gulf Coast: A high-resolution record from the Mississippi Delta. *Geological Society of America Bulletin*, **116**, 1026-1039.

Toscano, M.A. & Macintyre, I.G. (2003) Corrected western Atlantic sea-level curve for the last 11,000 years based on calibrated ^{14}C dates from *Acropora palmata* framework and intertidal mangrove peat. *Coral Reefs*, **22**, 257-270.

Tudhope, A.W., Chilcott, C.P., McCulloch, M.T., Cook, E.R., Chapell, J., Ellam, R.M., Lea, D.W., Lough, J.M., & Shimmeld, G.B. (2001) Variability in the El Niño - Southern Oscillation through a Glacial-Interglacial Cycle. *Science*, **291**, 1511-1517.

Turney, C.S.M., Kershaw, A.P., Clemens, S.C., Branch, N., Moss, P.T., & Fifield, L.K. (2004) Millennial and orbital variations of El Niño/Southern Oscillation and high-latitude climate in the last glacial period. *Nature*, **428**, 307-310.

Van der Borg, K., Alderliesten, C., De Jong, A.F.M., Van den Brink, A., De Haas, A.P., Kersemaekers, H.J.H., & Raaymakers, J.E.M.J. (1997) Precision and mass fractionation in ^{14}C analysis with AMS. *Nuclear Instruments and Methods in Physical Research Section B*, **123**, 97-101.

Van der Burgh, J., Visscher, H., Dilcher, D.L., & Kürschner, W.M. (1993) Paleoatmospheric signatures In Neogene fossil leaves. *Science*, **260**, 1788-1790.

Van der Kaars, S., Penny, D., Tibby, J., Fluin, J., Dam, R.A.C., & Suparan, P. (2001) Late Quaternary palaeoecology and palaeolimnology of a tropical lowland swamp: Rawa Danau, West-Java, Indonesia. *Palaeogeography Palaeoclimatology Palaeoecology*, **171**, 185-212.

Van der Plicht, J., Beck, J.W., Bard, E., Baillie, M.G.L., Blackwell, P.G., Buck, C.E., Friedrich, M., Guilderson, T.P., Hughen, K.A., Kromer, B., McCormac, F.G., Ramsey, C.B., Reimer, P.J., Reimer, R.W., Remmele, S., Richards, D.A., Southon, J.R., Stuiver, M., & Weyhenmeyer, C.E. (2004) NotCal04-Comparison/Calibration [14]C Records 26-50 Cal Kyr BP. *Radiocarbon*, **46**, 1225-1238.

Van Geel, B., Van Hallewas, D.P., & Pals, J.P. (1983) A late Holocene deposit under the Westfriese Zeedijk near Enkhuizen (Prov. of N-Holland, the Netherlands): palaeoecological and archaeological aspects. *Review of Palaeobotany and Palynology*, **38**, 269-335.

References

Van Hoof, T.B. (2004) Coupling between atmospheric CO_2 and temperature during the onset of the Little Ice Age. *PhD thesis,* Utrecht University, the Netherlands. LPP contribution series No. 18, pp. 125

Van Hoof, T.B., Kaspers, K.A., Wagner, F., Van de WAL, R.S.W., Kürschner, W.M., & Visscher, H. (2005a) Atmospheric CO_2 during the 13th century AD: reconciliation of data from ice core measurements and stomatal frequency analysis. *Tellus B*, **57**, 351-355.

Van Hoof, T.B., Kürschner, W.M., Wagner, F., & Visscher, H. (2005b) Stomatal index response of Quercus robur and Quercus petraea to the anthropogenic atmospheric CO_2 increase. *Plant Ecology*, **in press**.

Van Oldenborgh, G.J. & Burgers, G. (2005) Searching for decadal variations in ENSO precipitation teleconnections. *Geophysical Research Letters,* **32**, 15, L15701

Vega, A.J., Rohli, R.V., & Henderson, K.G. (1998) The Gulf of Mexico mid-tropospheric response to El Niño an La Niña forcing. *Climate Research*, **10**, 115-125.

Viles, H.A. & Goudie, A.S. (2003) Interannual, decadal and multidecadal scale climatic variability and geomorphology. *Earth-Science Reviews*, **61**, 105-131.

Vince, S.W., Humphrey, S.R., & Simons, R.W. (1989) The ecology of hydric hammocks: A community profile. *Biological report* **85**: 7.26, pp. 82. Fish and Wildlife Service, Research and Development, U.S. Department of the Interior, Washington, DC.

Visser, J.M. & Sasser, C.E. (1994) Changes in tree species composition, structure and growth in a bald cypress-water tupelo swamp forest, 1980-1990. *Forest ecology and management*, **72**, 119-129.

Wagner, F., Below, R., De Klerk, P., Dilcher, D.L., Joosten, H., Kürschner, W.M., & Visscher, H. (1996) A natural experiment on plant acclimation: Lifetime stomatal frequency response of an individual tree to annual atmospheric CO_2 increase. *Proceedings of the National Academy of Sciences of the United States of America*, **93**, 11705-11708.

Wagner, F., Dilcher, D.L., & Visscher, H. (2005) Stomatal frequency responses in hardwood-swamp vegetation from Florida during a 60-year continuous CO_2 increase. *American Journal of Botany*, **92**, 690-695.

Wagner, F., Kouwenberg, L.L.R., Van Hoof, T.B., & Visscher, H. (2004) Reproducibility of Holocene atmospheric CO_2 records based on stomatal frequency. *Quaternary Science Reviews*, **23**, 1947-1954.

Walker, J., Thompson, C.H., Fergus, I.F., & Tunstall, B.R. (1981). Plant succession and soil development in coastal sand dunes of subtropical eastern Australia. In *Forest succession, concepts and application* (eds D.C. West, H.H. Shugart & D.B. Botkin), pp. 107-131. Springer-Verlag, New York.

Wang, C. & Picaut, J. (2004). Understanding ENSO physics - a review. In *Ocean-Atmosphere Interaction and Climate Variability* (eds C. Wang, S.-P. Xie & J.A. Carton), pp. 1-54. American Geophysical Union.

Ward, W.T. & Grimes, K.G. (1987) History of coastal dunes at Triangle Cliff, Fraser Island, Queensland. *Australian Journal of Earth Sciences*, **34**, 325-333.

Watts, W.A. (1975) A late Quaternary record of vegetation from Lake Annie, south-central Florida. *Geology*, **3**, 344-346.

Watts, W.A. & Hansen, B.C.S. (1994) Pre-Holocene and Holocene pollen records of vegetation history from the Florida peninsula and their climatic implications. *Palaeogeography, Palaeoclimatology, Palaeoecology*, **109**, 163-176.

Webb, L.J. & Tracey, J.G. (1994). The rainforests of northern Australia. In *Australian vegetation* (ed R.H. Groves), pp. 87-130. Cambridge University Press, Cambridge.

Whitehouse, F.W. (1968) Fraser Island - geology and geomorphology. *Queensland Naturalist*, **19**, 4-9.

Willard, D.A., Cronin, T.M., & Verardo, S. (2003) Late Holocene climate and ecosystem history from Chesapeake Bay sediment cores. *The Holocene*, **13**, 201-214.

Willard, D.A., Holmes, C.W., & Weimer, L.M. (2001a) The Florida Everglades ecosystem: climatic and anthropogenic impacts over the last two millennia. *Bulletins of American Paleontology*, **361**, 41-55.

Willard, D.A., Weimer, L.M., & Riegel, W.L. (2001b) Pollen Assemblages as Paleoenvironmental Proxies in the Florida Everglades. *Review of Palaeobotany and Palynology*, **113**, 213-235.

Winkler, M.G., Sanford, P.R., & Kaplan, S.W. (2001) Hydrology, vegetation, and climate change in the southern Everglades during the Holocene. *Bulletins of American Paleontology*, **361**, 57-100.

Worbes, M. (2002) One hundred years of tree-ring research in the tropics - a brief history and an outlook to future challenges. *Dendrochronologia*, **20**, 217-231.

Zebiak, S.E. & Cane, M.A. (1987) A model El Niño-Southern Oscillation. *Monthly Weather Review*, **115**, 2262-2278.

ALGEMENE INLEIDING EN SAMENVATTING

De 'El Niño – Southern Oscillation' (El Niño – Zuidelijke Oscillatie, ENSO) in het tropische deel van de Stille Oceaan is de belangrijkste bron van wereldwijde klimaatvariabiliteit op een tijdschaal van enkele jaren. Het 'El Niño' verschijnsel is een periodieke verhoging van de temperatuur van het oppervlaktewater (SST) aan de westkust van Zuid-Amerika, waarbij er minder koud voedselrijk water aanwezig is dan gemiddeld. De 'Southern Oscillation', gemeten aan het luchtdrukverschil tussen Tahiti and Darwin, is de atmosferische component van het ENSO-systeem. De afwijkende watertemperaturen in de oostelijke Stille Oceaan versterken de thermiek langs de westkust van Zuid-Amerika, terwijl warme en vochtige lucht die normaliter opstijgt boven Indonesië zich verplaatst naar het midden van de Stille Oceaan. Als gevolg van deze verplaatsing veranderen de regenvalpatronen en vermindert de atmosferische circulatie van Oost naar West (zonale circulatie) in het tropische deel van de Stille Oceaan.

Veranderingen in de luchtcirculatie veroorzaken neerslagoverschotten en -tekorten in gebieden ver buiten de Stille Oceaan via zgn. teleconnecties in de atmosfeer. In veel gebieden van de wereld verstoort ENSO de weercondities om de 2 tot 7 jaar en heeft daardoor grote maatschappelijke en economische gevolgen. Om die reden is ENSO momenteel een van de best bestudeerde klimaatsystemen, waarbij veel aandacht uitgaat naar het verbeteren van voorspellingen van El Niño, en zijn tegenhanger, La Niña. Desondanks zijn de precieze mechanismen en oorzaken van El Niño's / La Niña's nog steeds onduidelijk. Er is vooral veel discussie over de vraag hoe ENSO zich zal gedragen in een toekomstig broeikasklimaat met meer stralingswarmte. Het is nog onduidelijk of een warmer wordend klimaat de frequentie, duur en intensiteit van El Niño's / La Niña's beïnvloedt en wat een dergelijke verandering wereldwijd voor gevolgen zou kunnen hebben.

Om de mechanismen en lange-termijn ontwikkeling van ENSO te begrijpen is het van belang het vroegere gedrag van dit grootschalige gekoppelde oceaan- / atmosfeersysteem te bestuderen. Een gedetailleerde reconstructie van ENSO-activiteit in het verleden kan inzicht bieden in de variatie die, zowel in tijd als in ruimte, wordt veroorzaakt door ENSO. Tegelijkertijd kan daarmee de invloed van de hoeveelheid stralingswarmte (door b.v. cyclische 'Milankovitch'-variaties van de positie en stand van de aarde ten opzichte van de zon) op ENSO worden bestudeerd. Het is van groot belang de oorzaken en gevolgen van ENSO-veranderingen te documenteren zodat de voorspelbaarheid van overstromingen en droogtes die met El Niño's / La Niña's gepaard gaan kan worden verbeterd.

Onderzoek in terrestrische systemen is essentieel aangezien de belangrijkste socio-economische gevolgen van ENSO op het land plaatsvinden. Milieu-indicatoren gebaseerd op preserveerbare resten van planten worden steeds vaker gebruikt voor het reconstrueren van het vroegere klimaat, aangezien planten zeer gevoelig zijn voor omgevingsfactoren en snel reageren op veranderingen in hun habitat als gevolg van droogte of wateroverschot. Plantenresten zoals pollen en bladeren die bewaard zijn gebleven in veen- en meersedimenten, bevatten nog steeds informatie over de aanpassing van het vroegere plantenleven aan specifieke milieucondities, zowel op niveau van de individuele soort als de ecologische plantengemeenschap. Deze natuurlijke archieven vormen belangrijk

uitgangsmateriaal voor het maken van klimaatreconstructies met behulp van biologische indicatoren.

In dit proefschrift worden botanische klimaatindicatoren geïntroduceerd, getest en toegepast bij de reconstructie van hydrologische veranderingen in sterk door ENSO beïnvloede gebieden. In het eerste deel ligt de nadruk op Florida. Het klimaat in dit gebied heeft een sterke, uitgebreid gedocumenteerde teleconnectie met ENSO zodat de reconstructiemethoden goed gekalibreerd kunnen worden.

Naast gedetailleerde klimaatsgegevens, zijn nauwkeurige chronologieën van de natuurlijke archieven een vereiste voor een succesvolle ontwikkeling en validatie van reconstructiemethoden. Verbeterde koolstof-14 chronologieën voor materiaal uit de 20ste eeuw worden ontwikkeld in **Hoofdstuk 1** en toegepast op twee jonge veenpakketten uit een subtropisch moerasgebied, het 'Fakahatchee Strand Preserve State Park' (FSPSP, Florida, VS). De ^{14}C-data worden gekalibreerd met behulp van een gecombineerde 'wiggle-match' en ^{14}C-atoombompiekmethode. De reproduceerbare resultaten laten zien dat de profielen zeer goed gedateerd kunnen worden met een nauwkeurigheid van 3 tot 5 jaar. Met deze methode is de korte FAK I98 kern gedateerd op AD 1912 terwijl de tweede, iets langere FAK I02 kern ongeveer 125 jaar omvat. Deze resultaten maken het mogelijk reconstructiemethoden te kalibreren aan de hand van meteorologische data en breiden het gebruik van ^{14}C-dateringen uit tot in de 20ste eeuw.

In **Hoofdstuk 2** wordt hoge-resolutie pollenanalyse gebruikt voor het bepalen van de recente hydrologische condities van de FSPSP middels de nauwkeurig gedateerde veenkern FAK I98. Gedurende de afgelopen 100 jaar veranderde de vegetatie in het moerasgebied geleidelijk van een vochtig tot een relatief droger type. De vegetatieverandering vond gelijktijdig plaats met droogleggingactiviteiten in het gebied. Een statistische vergelijking van subfossiele- en oppervlaktemonsters maakt het mogelijk het effect van de verstoringen van de waterhuishouding op de moerasvegetatie te bepalen. Dit maakt zowel de natuurlijke variatie alsook de mate van vegetatieverandering veroorzaakt door de mens zichtbaar. De dataset suggereert ook dat er een verband is tussen de jaarlijkse hoeveelheid winterneerslag en de hoeveelheid pollen dat wordt geproduceerd door de belangrijkste boomsoorten. De documentatie van de vegetatieveranderingen in de FSPSP, zowel veroorzaakt door jaarlijkse als langdurige verstoringen, biedt de mogelijkheid om hydrologische veranderingen te herkennen en te kwantificeren in oudere, soortgelijke afzettingen uit Zuidwest-Florida.

De invloed van de jaarlijkse variatie in winterneerslag op de vegetatie in Florida wordt verder onderzocht in **Hoofdstuk 3**. Hier wordt een nieuw ontwikkelde methode geïntroduceerd voor reconstructie van de hoeveelheid regenval. Deze is gebaseerd op de analyse van droogtestress-kenmerken in *Quercus laurifolia* bladeren. De dichtheid van epidermiscellen (ED) van zowel herbariummateriaal als accumulaties van jaarlijkse bladval in de FSPSP-kernen FAK I98 en FAK I02 laat een consistente inverse relatie met de hoeveelheid winterneerslag in Zuid-Florida zien. Gelijktijdige analyse van de hoeveelheid stomata op de subfossiele bladresten laat verder zien dat *Q. laurifolia* duidelijk gevoelig is voor veranderingen in de atmosferische CO_2 concentratie. Gecombineerde analyse van

155

CO_2 en droogtestress aan de hand van fossiel bladmateriaal uit Zuid-Florida biedt een unieke methode voor het documenteren van zowel atmosferische CO_2 concentraties als ENSO-afhankelijke regenval in periodes vóór het begin van instrumentele metingen.

De pollen- en ED-reconstructies van beschikbaarheid van water tijdens het groeiseizoen (Hoofdstuk 2 & 3) worden in **Hoofdstuk 4** getest op hun gevoeligheid voor ENSO. Hoogfrequente variatie in de pollendata (Hoofdstuk 2) wordt verder onderzocht in veenkern FAK I02. Spectraalanalyse laat zien dat de FAK I02 pollen- en ED-data significante variabiliteit binnen de 2-7 jaar bandbreedte bevat, die zeer goed vergelijkbaar is met de ENSO-periodiciteit. Een tijdsreeks van het gefilterde ENSO-signaal maakt duidelijk dat de ENSO-invloed de afgelopen 125 jaar steeds sterk aanwezig is geweest. De detectie van het ENSO-signaal in niet-gelamineerde sedimenten maakt het mogelijk de vroegere activiteit van ENSO direct te meten aan sedimentaire systemen met een hoge accumulatiesnelheid.

Een gedetailleerde pollenanalyse van midden- tot laat-Holocene veenpakketten uit Zuidwest-Florida in **Hoofdstuk 5** geeft aan dat de moerasvegetatie zich stapsgewijs heeft uitgebreid tijdens de afgelopen 5000 jaar. Dit duidt op een toename van de hoeveelheid zoet water die direct wordt bepaald door de regenval in het gebied. Zoals beschreven in Hoofdstuk 2, is de regenval gedurende de winter sterk afhankelijk van ENSO. Dit suggereert dat de hydrologische reconstructie een weergave is van de activiteit van het ENSO-systeem. Het subtropische ecosysteem reageerde 5000 jaar gelden op het ontstaan van een ENSO-variabiliteit die vergelijkbaar is met de huidige frequentie. Een verdere intensivering vond plaats vanaf 3500 jaar geleden. De stijging van het waterniveau werd mede in stand gehouden door een geleidelijke zeespiegelverhoging waardoor de drogere vegetatie niet meer kon terugkomen.

De concepten over Holocene ENSO-variabiliteit die zijn gebaseerd op de data uit Florida worden verder getest met behulp van materiaal uit oostelijk Australië. De sterke invloed van ENSO in deze regio is precies tegenovergesteld aan de effecten in Florida.

In het duingebied van Fraser Island in Queensland, komen veel meertjes voor die erg gevoelig zijn voor variaties in regenval, aangezien ze afgesloten en onafhankelijk zijn van de regionale grondwaterspiegel. In **Hoofdstuk 6** wordt belangrijke paleo-ecologische en paleoklimatologische data verkregen uit een gedetailleerde pollenanalyse van organische-rijke sedimenten van Lake Allom. Deze zijn geaccumuleerd in de afgelopen 56 duizend jaar, met een onderbreking gedurende het laatste ijstijdmaximum. Door de Glaciaal-Interglaciaal afwisselingen veranderde het open gematigde bos in een gemengde regenwoudvegetatie. In het Holoceen veranderde de plantengemeenschap rond 5500 jaar geleden van een relatief droog naar een vochtiger type en steeg het waterniveau van het meer. Tussen 3000 en 2000 jaar geleden werd het weer iets droger, nam de diversiteit in de omgeving van Lake Allom sterk toe en ontwikkelde zich het tegenwoordige lappendeken-vegetatiepatroon. Omstreeks AD 1500 nam het subtropische regenwoud iets in omvang af. Factoren als successie, duinontwikkeling, zeespiegelstijging en menselijke invloed zijn niet voldoende om deze veranderingen te verklaren en om die reden is klimaatvariabiliteit zeer waarschijnlijk een belangrijkste oorzaak geweest.

In **Hoofdstuk 7** worden de data van Fraser Island gebruikt bij een herziening van de Holocene klimaatsgeschiedenis van oostelijk Australië, gebaseerd op een reeks hoge-resolutie pollendiagrammen langs een Noord-Zuid transect. Een groot deel van de diagrammen wordt voor het eerst voorzien van een kalendertijdsschaal met gekalibreerde ^{14}C-dateringen. Aan de hand van deze chronologieën kunnen de vroegere milieu- en klimaatsveranderingen rechtstreeks met elkaar worden vergeleken. Op basis van de huidige klimaatssystemen in Australië kunnen uit de pollendata de belangrijkste klimaatsinvloeden gedurende het Holoceen worden gereconstrueerd. Hieruit blijkt dat verschillende regio's zich zeer verschillend ontwikkelden in het vroeg-Holoceen. Tijdens het midden- en laat-Holoceen werden de meeste gebieden in oostelijk Australië gelijktijdig droger en minder stabiel, hetgeen een patroon is dat overeenkomt met een toename van de ENSO-activiteit.

Tenslotte wordt in **Hoofdstuk 8** een geïntegreerd overzicht gegeven van zowel mariene als terrestrische data die relevant zijn voor het herkennen van ENSO-variabiliteit, met bijzondere aandacht voor de perioden van 6000 tot 5000 en van 4500 tot 3500 jaar geleden. Uit analyse van de verschillende klimaatreconstructies blijkt dat rond 5000 jaar geleden de ENSO-cyclus in de tropische Stille Oceaan actief werd. Gebieden met een sterke ENSO-teleconnectie werden vanaf ongeveer 3000 jaar geleden sterker beïnvloed door het voorkomen van heviger El Niño's / La Niña's. Een vergelijking met reconstructies uit klimaatmodellen laat zien dat de algemeen aanvaarde hypothese, waarin intensivering van ENSO wordt veroorzaakt door zwakkere passaatwinden in de zomer, de veranderingen in het Holoceen niet afdoende verklaart. Een aanvullende hypothese wordt gegeven waarbij het voorkomen van heviger El Niño's gedurende de afgelopen 3000 jaar wordt verklaard door een temperatuurstijging van de westelijke tropische Stille Oceaan.

Introduzione generale e riassunto

L'"El Niño – Southern Oscillation' (Oscillazione Meridionale di El Niño, ENSO) nell'Oceano Pacifico tropicale costituisce la più ampia fonte di variabilità climatica globale a scala interannuale. Il fenomeno di El Niño consiste in una riduzione periodica della risalita di acque profonde ed in un incremento di temperature delle acque superficiali (SSTs) lungo la costa occidentale del Sud America tropicale. La 'Southern Oscillation', definita dalla differenza di pressione fra Tahiti e Darwin, è la componente atmosferica del sistema ENSO. Le anomale SSTs nel Pacifico orientale aumentano la convezione atmosferica lungo la costa occidentale del Sud America, mentre la normale risalita di aria calda e umida viene dislocata dall'Indonesia al Pacifico centrale. Come risultato di questo spostamento i pattern di piovosità nel Pacifico tropicale vengono alterati e la forza della circolazione atmosferica zonale del Pacifico viene ridotta.

Una circolazione nel Pacifico alterata causa deficit e surplus di precipitazioni in aree geograficamente lontane attraverso una teleconnessione atmosferica. La modificazione climatica causata da ENSO ha ricorrenza di 2-7 anni ed ha un forte impatto sociale ed economico. Quindi l'ENSO è, al momento, uno dei più studiati sistemi climatici e molte attenzioni sono dirette a migliorare le previsioni di El Niño e della sua controparte, La Niña. Comunque, gli esatti meccanismi e le cause degli eventi di El Niño/La Niña sono ancora poco conosciuti e soprattutto il comportamento atteso di ENSO in un mondo caratterizzato dall'effetto serra, con un aumentato forzante radiativo, è ancora fortemente dibattuto. Non è chiaro se il previsto riscaldamento altererà la frequenza, durata e intensità degli eventi di El Niño/La Niña e quale sarà l'effetto globale di un possibile cambiamento nelle dinamiche di ENSO.

Per capire i meccanismi e le dinamiche di ENSO a lungo termine è importante studiare i comportamenti di questo sistema oceano/atmosfera di ampia scala. Una ricostruzione dettagliata della passata attività di ENSO può aiutare a fornire una profonda visione della variabilità climatica spaziale e temporale causata dal sistema ENSO in scale di tempo da centenaria a millenaria e, allo stesso tempo, può aiutare a valutare il potenziale ruolo dei cambiamenti nel forzante radiativo (e.g. insolazione di Milankovitch) come meccanismi guida per le dinamiche di ENSO. La documentazione delle cause e delle conseguenze delle diverse dinamiche di ENSO è di primaria importanza per migliorare la prevedibilità di estreme anomalie nelle precipitazioni associate con l'ENSO.

L'analisi dei sistemi terrestri è essenziale poiché gli impatti sociali ed economici di ENSO sono più prominenti sulla terra. Le registrazioni con indicatori botanici dei cambiamenti ambientali vengono sempre più usati poiché le piante sono altamente sensibili alle condizioni circostanti e rispondono immediatamente a cambiamenti del loro habitat come la siccità o un surplus di precipitazioni. I resti di piante, come foglie o pollini, che vengono sepolti nella torba o nei sedimenti lacustri conservano le modificazioni che le singole piante o le comunità ecologiche hanno attuato per adattamento ai segnali ambientali. Questi archivi naturali rappresentano la sorgente del materiale utilizzato nelle ricostruzioni climatiche basate sugli indicatori.

In questa tesi, indicatori basati sulle piante vengono introdotti, testati ed applicati per ricostruire le condizioni idrologiche passate in aree chiave per l'ENSO. La prima sezione di questa tesi è focalizzata sulla Florida meridionale, una regione dove una forte teleconnessione di ENSO è ben documentata da numerose e lunghe registrazioni strumentali che possono essere usate per la calibrazione degli indicatori ambientali.

In aggiunta a dettagliate serie di dati strumentali, un'accurata cronologia degli archivi naturali investigati sono un necessario prerequisito per lo sviluppo e la validazione degli indicatori. Datazioni al radiocarbonio (AMS ^{14}C) per un miglioramento della cronologia per materiale organico relativamente recente (XX secolo) sono oggetto del **Capitolo 1** e vengono applicate a due sequenze di torba derivate da una area umida della Florida subtropicale, la 'Fakahatchee Strand Preserve State Park' (FSPSP, Florida, USA). Datazioni al ^{14}C vengono calibrate usando una combinazione di approcci che include il 'wiggle-match' e il metodo del picco della bomba atomica. Sono stati ottenuti risultati riproducibili e una valutazione dei possibili errori inclusi fornisce un modello di età estremamente accurato con una precisione di 3-5 anni. Basandosi su questa strategia, la carota più corta FAK I98 risale al AD 1912, mentre la seconda, leggermente più lunga, FAK I02, rappresenta gli ultimi 125 anni. I risultati delle datazioni permettono una calibrazione diretta degli indicatori paleo-ambientali con dati meteorologici ed allargano la finestra temporale in cui il ^{14}C viene comunemente applicato al XX secolo.

Il **Capitolo 2** riguarda l'analisi di pollini e spore ad alta risoluzione per lo studio delle condizioni idrologiche in un profilo di torba accuratamente datato ricavato dalla carota FAK I98 prelevata nella FSPSP. La palude a cipressi gradualmente passa da una vegetazione umida ad un'associazione indice di condizioni secche negli ultimi 100 anni. Il momento dell'inizio delle attività di drenaggio nell'area viene perciò accuratamente riflessa dai cambiamenti di vegetazione nella palude. Un confronto statistico dei campioni (sub-)fossili con i sedimenti superficiali permette una determinazione delle variazioni nelle risposte della area umida della FSPSP ai disturbi idrologici, rivelando sia i cambiamenti naturali nella vegetazione che la risposta dell'area umida all'impatto dell'uomo.

Variazioni quasi-annuali nel record suggeriscono una correlazione positiva fra piovosità invernale e produttività dei pollini degli alberi dominanti. L'intervallo di risposte documentate dell'area umida FSPSP alle perturbazioni a scala sia annuale che decadale permette di riconoscere e quantificare i cambiamenti idrologici naturali in depositi più antichi della Florida.

L'impatto dei cambiamenti nelle precipitazioni annue invernali sulla vegetazione delle aree umide in Florida viene ulteriormente investigato nel **Capitolo 3**. Qui viene introdotto un nuovo indicatore per le precipitazioni sviluppato sulla base della morfologia delle foglie e basato sull'analisi delle caratteristiche strutturali xeromorfiche di *Quercus laurifolia*. Viene dimostrato che la densità delle cellule dell'epidermide (ED) sia di materiale prelevato dall'erbario sia di quello raccolto da sequenze di torba che contengono foglie accumulatesi annualmente nella FSPSP nelle carote FAK I98 e FAK I02 mostra una consistente relazione inversa con l'ammontare di precipitazioni invernali nella Florida meridionale. Analisi della frequenza degli stomi condotte in parallelo su foglie fossili di *Q. laurifolia* rivelano

inoltre una chiara sensibilità di questa specie alla CO_2. Analisi combinate di CO_2 e segnali di stress da siccità in resti di foglie fossili della Florida meridionale forniscono un metodo unico per documentare simultaneamente i cambiamenti nei pattern di precipitazione dovuti all'ENSO e le concentrazioni di CO_2 atmosferica oltre il limite delle registrazioni strumentali.

La ED ed i pollini introdotti nei Capitoli 2 e 3, indicatori della disponibilità di umidità durante la stagione di crescita delle piante, vengono testati per la sensibilità all'ENSO nel **Capitolo 4**. I cambiamenti ad alta frequenza registrati nel record pollinico della carota FAK I98 nel Capitolo 2 vengono investigati a più alta risoluzione nella carota FAK I02. L'analisi spettrale dello studio a risoluzione quasi-annuale dei pollini e della ED nella carota FAK I02 rivela una significativa variabilità nella banda 2-7 anni, altamente paragonabile con il tipico segnale di ENSO. Una serie temporale dei dati filtrati mostra una chiara impronta di ENSO nella carota FAK I02 durante gli ultimi 125 anni. Questi risultati dimostrano che l'impronta di ENSO può essere rilevata anche in sedimenti non laminati e che quindi è possibile verificare direttamente le dinamiche di ENSO nel passato in sequenze sedimentarie ad alto tasso di accumulo.

L'analisi ad alta risoluzione dei pollini in una carota di torba prelevata nella Florida sud-occidentale e datata medio-tardo Olocene è argomento del **Capitolo 5**. I risultati rivelano un andamento della vegetazione che indica un aumento nel flusso d'acqua dolce dovuto a maggiori precipitazioni durante gli ultimi 5000 anni. La stretta correlazione fra andamenti delle precipitazioni in inverno in Florida e l'intensità di ENSO descritta nel Capitolo 2 suggerisce che le registrazioni paleo-idrologiche riflettono cambiamenti nella passata attività di ENSO. Il record dell'area subtropicale indica l'inizio della risposta dell'ecosistema alla moderna periodicità di ENSO fra circa 7000 e 5000 anni BP. L'osservato aumento delle condizioni umide è confermato da un graduale aumento del livello del mare relativo che impedisce il ritorno naturale ad un tipo di vegetazione più secca.

I concetti riguardanti le dinamiche di ENSO durante l'Olocene presentati sulla base di studi effettuati in Florida, vengono valutati focalizzando l'attenzione sull'Australia orientale, una regione con una forte teleconnessione per ENSO, anticorrelata con gli impatti di ENSO in Florida.

I laghi sopraelevati e disconnessi dalle oscillazioni del livello del mare che si trovano nel sistema di dune della Fraser Island nell'Australia subtropicale (Queensland) sono fortemente influenzati dalle precipitazioni e pertanto rappresentano sonde naturali di misurazione delle precipitazioni. Essi sono quindi estremamente sensibili ai cambiamenti ambientali. Nel **Capitolo 6** vengono discusse rilevanti informazioni paleoecologiche e paleoclimatologiche sulla base di un record di pollini ad alta risoluzione ottenuto da sedimenti ricchi di materia organica che si sono accumulati nel Lago Allom negli ultimi 56000 anni (radiocarbonio), con un ampio iato durante l'ultimo massimo glaciale. Sono presenti pronunciati cambiamenti fra foresta pluviale e vegetazione boschiva più aperta durante le variazioni glaciale-interglaciale. La parte olocenica del record rivela un graduale sviluppo della vegetazione da condizioni secche all'inizio dell'Olocene ad una successione di foresta tra 5500 e 3000 anni cal. BP. Fra 3000 e 2000 anni cal. BP, si assiste ad un'ampia

diversificazione di vegetazione verso un tipo di foresta pluviale subtropicale eterogenea come quella attuale. In seguito, si assiste ad un lieve declino nella foresta pluviale a partire da 450 anni cal. BP.

Poiché la successione di foresta, la formazione delle dune, l'innalzamento del livello marino e l'impatto antropico non sono sufficienti per spiegare la variabilità osservata, le dinamiche del clima sono considerate essere le cause primarie dei cambiamenti di vegetazione nella Fraser Island.

Nel **Capitolo 7** i risultati ottenuti dal record di Fraser Island sono incorporati in un'ampia revisione degli andamenti climatici dell'Olocene nell'Australia orientale, basandosi su una serie di record di pollini ad alta risoluzione lungo un transetto nord-sud. Datazioni al radiocarbonio pubblicate in precedenza sono state calibrate in anni calendario e inserite in un modello profondità – età. Le risultanti cronologie sono state usate per paragonare i passati cambiamenti ambientali e descrivere gli andamenti dei cambiamenti climatici sulla base di una scala ad anni calendario. I dati palinologici sono stati interpretati sulla base degli attuali andamenti climatici in Australia e sugli impatti di ENSO, ed è stato quindi possibile ricostruire il clima dominante nell'Olocene. I risultati mostrano che i cambiamenti registrati all'inizio dell'Olocene sono fortemente divergenti e asincroni fra i diversi siti, mentre l'Olocene medio e recente è caratterizzato da condizioni più aride e variabili e da un maggior sincronia fra siti settentrionali e meridionali in accordo con un'aumentata influenza di ENSO.

Infine, nel **Capitolo 8,** viene presentato un riassunto integrato dei molteplici dati paleoclimatici sia terrestri che marini importanti per capire la variabilità di ENSO, concentrandosi su due finestre temporali, 6000-5000 anni BP e 4500-3500 anni BP. L'analisi degli indicatori climatici mostra che, dopo un cambiamento avvenuto a circa 5000 anni BP verso un'attiva ciclicità di ENSO nel Pacifico equatoriale, le regioni teleconnesse attraverso ENSO sono state caratterizzate da un'aumentata ampiezza degli eventi di ENSO a partire da circa 3000 anni BP. Un confronto con gli scenari scaturiti da modelli climatici mostra che la generalmente accettata teoria secondo la quale un'intensificazione di ENSO è il risultato di una riduzione degli Alisei durante l'estate nel Pacifico non può completamente spiegare gli osservati cambiamenti durante l'Olocene. Viene quindi proposto un meccanismo alternativo, che coinvolge un maggiore ricarico di calore nel Pacifico indonesiano (Indo-Pacific Warm Pool), come risultato di un aumento delle oscillazioni di ENSO.

ALLGEMEINE EINLEITUNG UND ZUSAMMENFASSUNG

Die stärkste natürliche Klimaschwankung auf Zeitskalen von einigen Monaten bis zu mehreren Jahren ist das El Niño - Südliche Oszillation (ENSO) System. Obwohl ENSO seinen Ursprung im tropischen Pazifik hat, beeinflusst es nicht nur das tropische, sondern auch das Weltklima.

Mit El Niño bezeichnet man eine großflächige Erwärmung der Oberflächenwässer des tropischen Pazifiks, während die Zufuhr nährstoffreicher Tiefenwässer entlang der Westküste Südamerikas stark reduziert ist. Die ozeanische El Niño Komponente des ENSO Systems ist eng mit der atmosphärischen Südlichen Oszillation verknüpft, welche die Luftdruckdifferenz zwischen Darwin (Nordaustralien) und Tahiti beschreibt.

Periodisch auftretende Anomalien des ENSO Systems, so genannte El Niño und La Niña Episoden, verursachen eine Verschiebung der normalerweise über dem West Pazifik situierten Niederschlagszentren in die zentralen Gebiete des Pazifiks (El Niño), oder verursachen eine Verstärkung der Normalsituation (La Niña).

Diese Verschiebungen der Luftdruckgebiete führen zu Niederschlagsextremen nicht nur im Pazifischen Bereich sondern auch über Fernwirkungen (Teleconnections) in Regionen weit außerhalb der tropischen Kernzone. Die mit einer Regelmäßigkeit von 2 – 7 Jahren auftretenden El Niño / La Niña Episoden haben schwerwiegende ökologische und ökonomische Konsequenzen für die direkt und indirekt betroffenen Länder.
Es ist deshalb nicht nur vom rein wissenschaftlichen, sondern auch vom wirtschaftlichen Standpunkt aus wichtig, die Dynamik des Systems Ozean-Atmosphäre im äquatorialen Pazifik zu verstehen um zu längerfristigen Vorhersagen kommen zu können.

Bis heute sind die exakten Mechanismen des ENSO Systems nur unzulänglich bekannt und dementsprechend sind die sehr wahrscheinlichen, zukünftigen Veränderungen in Häufigkeit und Intensität von El Niño / La Niña Episoden unter zunehmender Klimaerwärmung durch den anthropogenen Treibhauseffekt nur extrem schwer vorherzusagen.

Um die langfristige Entwicklung des ENSO Systems besser prognostizieren zu können, müssen die natürliche Dynamik und die Steuerungsmechanismen des ENSO Systems vollständig verstanden werden. Detaillierte Rekonstruktionen der ENSO Aktivität über den Zeitraum hinaus, für den instrumentelle Messungen vorliegen, können wichtige Daten über die maximale zeitliche und räumliche Variabilität des Systems liefern. Des weitern bieten Rekonstruktionen, die Zeiträume von Jahrhunderten bis Jahrtausenden umfassen, die Möglichkeit den potentiellen Einfluss sich ändernder Strahlungsregime (z.B. Insolation oder Melankovitchzyklen) zu evaluieren. Erst die genaue Dokumentation der Ursachen und Folgen der natürlichen Dynamik des ENSO Systems wird die Vorhersagbarkeit von El Niño Episoden verbessern und akkurate Langzeitsimulationen ermöglichen.

Die schwerwiegendsten Konsequenzen extremer El Niño / La Niña Niederschlagsanomalien wie Dürren und Überströmungen sind im terrestrischen Bereich zu verzeichnen, was die Bedeutung von Langzeitdokumentationen aus diesem Milieu verdeutlicht. Landpflanzen reagieren extrem empfindlich und schnell auf jegliche

Veränderungen in ihrem Habitat. Dementsprechend werden botanische Paläo-proxydaten in zunehmendem Maße zur Erforschung von Klima bedingten Veränderungen im terrestrischen Milieu hinzugezogen. In Seesedimenten oder Torfprofilen erhaltene Pflanzenreste wie Pollen, Sporen oder Blattfragmente dokumentieren Veränderungen im Niederschlagsregime, wobei Anpassungen auf dem Niveau von individuellen Pflanzen bis hin zu Verschiebungen ganzer Vegetationseinheiten archiviert sind.

In der vorliegenden Dissertation werden neue botanische Techniken entwickelt, getestet und in ENSO Schlüsselgebieten angewandt, um die hydrologische Vergangenheit in diesen Gebieten zu rekonstruieren. Der Schwerpunkt des ersten Teils der Arbeit liegt dabei auf Florida, USA. Für diese Region ist eine signifikante Kopplung des Winterniederschlags an das ENSO System aus zahlreichen, weit zurückreichenden Klimamessreihen bekannt. Diese instrumentellen Messdaten können gleichzeitig zur Kalibrierung der botanischen Proxies genutzt werden.

Neben der Verfügbarkeit detaillierter Klimadaten zu Kontrollzwecken, sind akkurate Chronologien der untersuchten sedimentären Archive eine Grundvorrausetzung für die erfolgreiche Entwicklung neuer Arbeitstechniken.

In **Kapitel 1** werden AMS Radiokarbon Chronologien dahingehend weiterentwickelt, dass genaue Altersbestimmungen für junge Torfprofile aus dem 20sten Jahrhundert möglich werden. Diese Technik wird auf Material aus dem Fakahatchee Strand Preserve State Park (FSPSP, Florida, USA) angewandt. ^{14}C Datenserien werden mit Hilfe der so genannten „Wiggle-match" Strategie gegen den „Bomb-Pulse" kalibriert. Dieses Verfahren ermöglicht extrem präzise Datierungen mit einer Genauigkeit der Altersmodelle von 3-5 Jahren. Die sich aus dieser Methode ergebenden Alter für die Torfprofile aus Florida sind 96 Jahre für Kern FAK I98 und 125 Jahre für Kern FAK I02. Die genaue Datierung der beiden Profile erlaubt die direkte Kalibrierung der paläoökologischen Daten mit meteorologischen Messreihen und erweitert den Einsatzbereich von ^{14}C Datierungen ins 20ste Jahrhundert.

Hochauflösende Pollen und Sporen Analysen werden zur Rekonstruktion der hydrologischen Verhältnisse in dem genau datierten Profil FAK I98 in **Kapitel 2** angewandt. Während der letzten 100 Jahre fand in dem Zypressen Sumpfgebiet ein gleitender Übergang von einem sehr feuchten zu einem eher trockenen Vegetationstypus statt. Die sichtbare Veränderung in der Vegetation steht in engem zeitlichem Zusammenhang mit den zunehmenden Drainageaktivitäten in Südwest Florida.
Der statistische Vergleich von rezenten Oberflächensedimentproben mit den subfossilen Proben aus FAK I098 ermöglicht den Anpassungsgrat der Vegetation an die hydrologischen Veränderungen in den FSPSP Sumpfgebieten zu bestimmen, und gibt Aufschluss über sowohl die natürlichen Vegetationsveränderungen, als auch über die Konsequenzen der sukzessiven Trockenlegung des Gebiets.

Den längerfristigen Trends sind jährliche Variationen überlagert, die des weiteren auf eine positive Korrelation zwischen Winterniederschlag und der Pollenproduktion der dominierenden Baumarten weisen. Die in FAK I98 beschriebenen Vegetationssignale auf

Zeitskalen von Jahren bis Jahrzehnten erlauben die Quantifizierung hydrologischer Veränderungen anhand pollenanalytischer Daten auch in älteren Ablagerungen in Südwest Florida.

In **Kapitel 3** wird ein neuer blattmorphologischer Proxy entwickelt und getestet, in dem das Auftreten struktureller xeromorphischer Merkmale in *Quercus laurifolia* (Laurel oak) Blättern an die jährliche Winterniederschlagsmenge gekoppelt wird. Untersuchungen der Epidermiszelldichten dieser Art an Herbarium Material zeigt eine deutliche Korrelation zwischen dem Größenwachstum der Epidermiszellen und der verfügbaren Niederschlagsmenge während der Wachstumsperiode. Diese Korrelation ist auch in den gut datierten Torfprofilen FAK I98 und FAK I02 zu erkennen, und ermöglicht die Rekonstruktion von Winterniederschlagsmengen über den instrumentell belegten Zeitraum von 100 Jahren hinaus.
Bestimmung der Spaltöffnungsdichten, einem weiteren botanischem Proxy für atmosphärische CO_2 Konzentrationen, deutet auf ein hohes Potential dieser Eichenart um paläoatmosphärische CO_2 Veränderungen zu rekonstruieren. Die parallele Analyse von Niederschlagsmengen und atmosphärischen CO_2 Konzentrationen macht erstmals eine synchrone Analyse dieser beiden Klimarelevanten Parameter möglich.

Nachdem in Kapiteln 2 und 3 der Nachweis erbracht worden ist, dass die Pollenproduktion und Blattwachstumsparameter Veränderungen im Winterniederschlag registrieren, wird in **Kapitel 4** mit Hilfe von Spektralanalysen gezeigt, dass die dokumentierte Variabilität in Epidermiszelldichten und Pollendaten den natürlichen 2-7 Jahre Zyklus des ENSO Systems folgen. Eine Zeitreihe der gefilterten Daten bestätigt die kontinuierliche Anwesenheit des ENSO Zyklus mit seinem deutlichen Einfluss auf den Winterniederschlag in Südwest Florida während der letzten 125 Jahre.

Die sukzessive Entwicklung der Sumpfgebiete während des Früh- bis mittleren Holozäns zeichnet sich in **Kapitel 5** in detaillierten Pollenanalysen an Torfprofilen ab, welche die letzten 5000 Jahre umfassen. Die hydrologischen Veränderungen, mit einer kontinuierlichen Zunahme des Süßwasseranteils aus Niederschlägen, folgen der allgemeinen Entwicklung des ENSO Systems. Das subtropische Ecosystem in Florida entwickelte sich vor 5000 Jahren, zu jener Zeit, in der das ENSO System des Pazifiks seine etwa heutige Variabilität erreichte, und sich ab 3500 Jahren v. H. auf dem gegenwärtigen Niveau stabilisierte. Die fortschreitende Vernässung der Sumpfgebiete in Florida lässt sich mit dem Zusammenspiel des deutlichen ENSO Signals und der Holozänen relativen Meeresspiegelerhöhung im Golf van Mexiko erklären, die einer Rückkehr der Vegetation zu den trockenen Stadien in der Sukzessionsreihe entgegenwirkt.

Die bis hierher erarbeiteten Konzepte zur Holozänen ENSO Dynamik werden im zweiten Teil der Dissertation auf Gebiete in Ostaustralien angewandt, einer Region in der der starke Einfluss des ENSO Systems in Antiphase zu den Effekten in Florida steht.

Die hydrologischen Verhältnisse isolierter Seen in den Dünengürteln auf Fraser Island (Queensland, Australien) sind weitestgehend von den jährlichen Niederschlagsmengen abhängig. Paläoökologische und paläoklimatologische Daten aus palynologischen

Analysen eines ~56.000 Jahre alten Sedimentkerns (Lake Allom) werden in **Kapitel 6** rekonstruiert. Obwohl während des Spätglazials ein Hiatus die Sedimentfolge unterbricht, sind deutliche Veränderungen von einer glazialen offenen Waldvegetation zu Regenwäldern im Interglazial zu erkennen. Währen des Holozäns selbst änderte sich die Vegetation von einer eher an trockene Verhältnisse angepasste Gemeinschaft zu einer, die feuchtere Verhältnisse anzeigt. Auch der Wasserspiegel im Lake Allom steigt deutlich an. Zwischen 3000 und 2000 v. H. wurde es wieder etwas trockener und entwickelte sich die sehr artenreiche subtropische Regenwaldvegetation, die auch heute noch Fraser Island charakterisiert. Ein um 1500 A.D. beobachteter Rückgang der Regenwaldflächen rund um Lake Allom ist mit Faktoren wie Florensukkzession, Dünenentwicklung, Meeresspiegelfluktuationen oder menschlicher Einfluss nicht ausreichend zu Erklären, und müssen Klimaschwankungen als mögliche Ursache in Betracht gezogen werden.

Die Holozäne Klimageschichte Ost-Australiens ist dann auch Schwerpunktthema in **Kapitel 7**. Ausgehend von den neuen Fraser Island Daten werden eine Reihe früher publizierter Pollendiagramme mit ähnlich guter zeitlicher Auflösung hier mit einer neu kalibrierten ^{14}C Chronologien versehen und mit einander verglichen. Die auf eine einheitliche Zeitskala gebrachten Pollendaten entlang eines Nord – Süd Profils durch Ostaustralien zeigen deutlich, das während des frühen Holozäns die Klimaverhältnisse zwischen den verschiedenen Gebieten stark voneinander abwichen und die Veränderungen zum Teil asynchron verliefen. Erst im mittleren Holozän ändert sich dieses Bild, wobei der zunehmende Einfluss des ENSO Systems für insgesamt trockenere, aber auch variablere Klimaverhältnisse in Nord- und Südaustralien sorgt.

Im abschließenden **Kapitel 8** wird für zwei Zeitfenster, von 6000 – 5000 v. H. und von 4500 – 3500 v. H., ein ausführlicher Vergleich der jeweils vorherrschenden ENSO Aktivität durchgeführt, wobei sowohl paläoklimatologische Daten aus dem marinen sowie terrestrischem Umweltbereich berücksichtigt werden. Aus dem Vergleich der Proxydaten wird deutlich, dass nach der Intensivierung der ENSO Zyklizität um 5000 v. H. auch die indirekt, über Teleconnections aneinander gekoppelte Gebiete verstärkt unter ENSO Einfluss geraten. Die gängige, auf Modelstudien beruhende, Theorie einer Intensivierung des ENSO Systems durch reduzierte Pazifische Windregime erklärt aber nur zum Teil die vorliegenden Daten zur Holozänen ENSO Dynamik. Eine zunehmende Erwärmung des Indo-Pazifischen Warm Pools (IPWP) wird hier als zusätzlicher Mechanismus postuliert, der zur weiteren Intensivierung des ENSO Systems im Verlauf des späten Holozäns führte.

After four years of dragging through swamps, flying across the globe, hours of sieving and peering through a microscope it's suddenly ready! This thesis is the result of a true group effort and therefore I need to thank many many people who helped me into putting this together. First of all, none of this would have happened if it wasn't for the great project Rike Wagner and Henk Visscher set up together. This was a true 'opportunity of a lifetime', where I could do research in the field of my choice with full support, traveling and working in places that were completely new to me. It has been a very fruitful cooperation and a great experience. Thanks very much to you both!

There is another reason why I owe much to the Laboratory of Palaeobotany and Palynology. In 1999 I was introduced to Francesca at the laboratory, the very person I married in July 2004! Not only did our work bring us together, but she also helped and inspired me and made me see that it was actually a good idea to start a PhD. And now it's ready ... but the next big project of our lives is already kicking at the door, and I am sure we will have a great and exciting new experience to raise our own "El Nino".

But the full story started earlier, I would have never ended up at LPP if Nol Duindam hadn't been such an inspiring high-school biology teacher. At the university, the field course" Flora and Landscape", taught at that time by Henk Brinkhuis and Han Leereveld, grabbed my attention and that was the point of no return. Little by little I was introduced into the world of "palaeo", a field where many people do highly inspired work discovering the past. Memories that come to mind immediately are the inspiring stories from Frans Bunnik on the impact of the Romans, Henk B's K-T disaster-lectures, the elegance of the "huidmondjes" work by Wolfram Kürschner and Rike Wagner.

Soon I found myself doing my master's research at LPP were I met many of my future fellow-AiO's. Together with Tom van Hoof (leve de WC-experience!), Appy Sluijs (In the grace of the almighty …), Lenny Kouwenberg (Nee, het is geen augurk), Merlijn Sprangers and Jeroen Warnaar and all the other students I started my LPP-life. Then the opportunity came to go abroad and work at David Dilcher's lab in Gainesville, Florida. I could not have made better choice. He and his wife Kathy and all the colleagues at the FLMNH made me feel at home straight away and I learned a lot about the area that later became the main research area of my PhD. Back home I finished the project with the enthusiastic support of Wolfram and before I knew it was time to start my PhD.

I had a great time sharing a room with Tom and our private zoo (hamster, snakes, mice, turtles, skink, and Nacho the indestructible fish).With the other colleagues and friends, Erica, Karin, Alice, Maaike, Welmoed, Oliver, Holger, Cindy, Anja, Hanneke and Marloes and all the other people at LPP is a unique and very good place to work. Thanks also to Andy Lotter who gave a fresh drive to the department and has helped with advice and support all along. Also our many guests from abroad make LPP a lively place, Nacho, Elisa, Gianluca, Walter, Verushka and Jörg are among the many that I have spent very good times with. Faruk, Stef, Claire and Barbara did a great job within the project during their master's research. It's good to see the work continued with the new "batch" of AiO's, Emiliya, Frederike, Peter, Nina and Micha good luck to you all!

Many thanks go to the people I have routinely bothered with questions, for help and advice; Ton, Natasja, Jan, Leonard, Marjolein and Zwier who keep the engine of LPP running. To Klaas van der Borg and Arie de Jong from the Utrecht AMS lab, Luc, Frits, Hayfaa, Ivo and Albert from "Strat & Pal" and Dan who popped up all across the world just when you needed him.

Special thanks go to the people who helped me doing my research and who were great hosts in the USA, Debra Willard from the USGS, Mike Owen and Ken Alvarez from the Florida State Park Service, all the Fakahatchee Strand and Rookery Bay staff, and Terry Lott at the FLMNH.

During my work in Australia and New Zealand I also met many great people who helped me along, particularly Simon Haberle, Geoff Hope and all people at RSPAS of the Australian National University in Canberra during my stay there. Important fieldwork support came from the Queensland department of Environmental Protection, Raphael Wust from James Cook University and the CSIRO Tropical Forest Research Centre in Atherton, Qld. I am very grateful for the legendary hospitality that I encountered both in Australia with Geoff and in New Zealand with Erica and John … I can recommend it to everybody! In New Zealand I spent a good and inspiring period at GNS in Wellington and at John Flenley's Laboratory at Massey University in Palmerston North.

Mille grazie a Giovanni Gabbianelli e il suo gruppo per l'ospitalitá presso il Laboratorio di Scienze della Terra del Centro Interdipartimentale di Ricerca per le Scienze Ambientali di Ravenna, Università di Bologna.

Last but by no means least I want to thank all my family and friends for supporting me, for keeping up with wherever on the earth I happened to be, and making sure that I still had touch with the 'real' world outside work, especially during the last writing months when all I saw was the computer screen in front of me. Jan en Margriet, Karen en Kees, Martijn, Lizette, Thijs en Isa, bedankt voor alle steun! Fulvia e Giampiero, e tutta la famiglia Sangiorgi e Missiroli, mille grazie anche a voi. Thanks for all the good times and nice company during busy times to Irene and Reinier, Wouter, Alvin, Jurgen and Ankie, Amanda and Kai, Stephanie, of course my great 'paranymfen' Karen and Appie (Aap), Sebastiaan for designing a 'keigave' cover, and all my friends and family in the Netherlands and Italy!

CURRICULUM VITAE

Timme Henrik Donders werd geboren op 18 september 1977 in Nieuwegein. In 1996 behaalde hij zijn VWO diploma op het Anna van Rijn College in Nieuwegein en begon datzelfde jaar met de studie Biologie aan de Universiteit Utrecht (UU). Hij volgde daar de afstudeerrichting Palaeo-ecologie en tijdens de specialisatiefase verrichte hij twee onderzoeksonderwerpen. Het eerste onderzoek bij de vakgroep Paleobotanie en Palynologie was gericht op de invloed van omgevingsfactoren op stomata dichtheden en stabiele koolstof isotopen van *Betula* bladeren en werd begeleid door Dr. Wolfram Kürschner. Voor het tweede onderwerp ging hij naar het Florida Museum of Natural History aan de University of Florida in Gainesville, USA, in samenwerking met het de vakgroep Palaeobotanie en Palynologie in Utrecht. Onder begeleiding van Prof. Dr. David Dilcher maakte hij daar, met behulp van pollenanalyse en historische luchtfoto's, een reconstructie van recente hydrologie veranderingen in een subtropisch moerasgebied. Hij rondde zijn studie af met een scriptie over de totstandkoming van de ijstijdtheorie bij Dr. Bert Theunissen van het Insituut voor de Geschiedenis en Grondslagen van de Wiskunde en Natuurwetenschappen aan de Universiteit Utrecht. Na het behalen van zijn doctoraaldiploma in 2001 trad hij in dienst als AiO bij de leerstoelgroep Palaeoecologie (Laboratorium voor Palaeobotanie en Palynologie). Daar ging hij werken binnen het NWO-IMPULS onderzoeksproject van Dr. Friederike Wagner op het gebied van ENSO variabiliteit in het verleden, onder toeziend oog van Prof. Dr. Henk Visscher. Sinds september 2005 is hij werkzaam als Post-Doc onderzoeker binnen dit project.